
PARTICLE SPIN DESCRIBED BY QUANTUM HAMILTON EQUATIONS

DISSERTATION

zur Erlangung des
Doktorgrades der Naturwissenschaften (Dr. rer. nat.)

der Naturwissenschaftlichen Fakultät II
Chemie, Physik und Mathematik

der
Martin-Luther-Universität
Halle-Wittenberg

vorgelegt von

Herr Michael Beyer, M.Sc.

Datum der Verteidigung: 06.12.2023

1. Gutachter: Prof. Dr. Wolfgang Paul
2. Gutachter: Prof. Dr. Steffen Trimper
3. Gutachter: Prof. Dr. Jean-Claude Zambrini

Halle (Saale), 12. Dezember 2023

Abstract

Quantum mechanics is currently the most extensively tested physical theory. However, the underlying principles of quantum mechanics continue to puzzle physicists, leading to various interpretations of quantum mechanics. One alternative perspective is Nelson's stochastic mechanics, which offers a stochastic quantization of classical mechanics to explain non-relativistic quantum phenomena. The quantum Hamilton equations (QHE) were derived recently by extending stochastic mechanics, offering a numerical approach to describe quantum systems without the need to solve the Schrödinger equation.

This thesis extends the QHE to describe quantum stochastic processes on manifolds, allowing for the study of systems in non-flat coordinates. The QHE provide a solvable framework for studying non-relativistic quantum phenomena without relying on the Schrödinger equation. Additionally, the thesis explores the Bopp-Haag-Dankel model, which treats spin within the framework of stochastic mechanics, providing a physical picture beyond the abstract representation of standard quantum theory. The coupling of spin to position is also investigated, offering insights into idealized spin measurements and correlations. Overall, this thesis aims to deepen our understanding of non-relativistic quantum mechanics by exploring alternative perspectives and expanding the toolbox of formalisms that describe quantum mechanics.

Zusammenfassung

Die Quantenmechanik ist derzeit die am umfassendsten getestete physikalische Theorie. Die zugrundeliegenden Prinzipien ebendieser geben jedoch weiterhin Rätsel auf, was zu verschiedenen Interpretationen der Quantentheorie geführt hat. Eine alternative Perspektive liefert die stochastische Mechanik von Nelson, die eine stochastische Quantisierung der klassischen Mechanik bietet, um nichtrelativistische Quantenphänomene zu erklären. Vor kurzem wurden die Quanten-Hamilton-Gleichungen (QHE) abgeleitet, die die stochastische Mechanik erweitern. Sie bieten einen numerischen Ansatz zur Beschreibung von Quantensystemen ohne Lösung der Schrödinger-Gleichung.

Diese Arbeit erweitert die QHE, um stochastische Prozesse auf Mannigfaltigkeiten zu beschreiben, was die Untersuchung von Systemen in krummlinigen Koordinaten ermöglicht. Die QHE bieten einen lösbaren Rahmen für die Untersuchung nichtrelativistischer Quantenphänomene, ohne auf die Schrödinger-Gleichung zurückzugreifen. Darüber hinaus wird in dieser Arbeit das Bopp-Haag-Dankel-Modell untersucht, das den Spin im Rahmen der stochastischen Mechanik behandelt und ein physikalisches Bild liefert, das über die abstrakte Darstellung der Standard-Theorie der Quantenmechanik hinausgeht. Desweiteren wird die Kopplung von Spin und Position untersucht und bietet damit Einblicke in idealisierte Spinmessungen und Korrelationen. Insgesamt zielt diese Arbeit darauf ab, das Verständnis der nichtrelativistischen Quantenmechanik zu vertiefen, indem alternative Perspektiven untersucht werden womit der Werkzeugkasten zur Beschreibung der Quantenmechanik erweitert wird.

Contents

1	Introduction	3
2	Stochastic processes in quantum mechanics	9
2.1	Overview	9
2.2	Stochastic processes and stochastic calculus	11
2.3	Nelson's stochastic mechanics	19
2.4	Connection to other interpretations of quantum mechanics	28
2.4.1	Hydrodynamic model	28
2.4.2	De Broglie-Bohm mechanics	29
2.4.3	Optimal transport theory	30
2.5	Criticism on/Controversies in stochastic mechanics	31
3	Quantum Hamilton equations	35
3.1	Variational principles in stochastic mechanics	35
3.2	Quantum Hamilton equations	38
3.2.1	Deterministic optimal control: Pontryagin principle	38
3.2.2	Stochastic optimal control	39
3.3	Examples	45
3.3.1	Harmonic oscillator	45
3.3.2	Two-body problem	47
3.3.3	Tunneling	48
4	Quantum Hamilton equations on manifolds	51
4.1	Stochastic differential equations on a manifold	51
4.2	Classical dynamics on manifolds	54
4.3	Quantum Hamilton equations on manifolds	54
4.4	Example: Hydrogen atom	57
5	Rotating bodies in quantum Hamilton equations	65
5.1	The model of a rotating particle in stochastic mechanics	66
5.1.1	Spin in quantum mechanics	66
5.1.2	Spin in stochastic mechanics	67
5.1.3	Construction of the stochastic process	68
5.2	Spinning bodies in classical mechanics	70
5.3	Quantum Hamilton equations of spinning particles	73
5.4	Freely spinning particle	77
5.4.1	Numerical solution	78
5.4.2	Results	79
5.4.3	Quantization of the spin states	83
5.4.4	Relation to the Pauli equation	86

6	Spinning particles moving in space	89
6.1	Hamilton equations of motion	90
6.2	Quantum Hamilton equations	91
6.3	Anomalous Zeeman effect	94
6.4	Stern-Gerlach experiment	96
6.4.1	Experimental setup	96
6.4.2	Stochastic description	98
6.5	Einstein-Podolsky-Rosen-Bohm experiment	111
6.5.1	The EPR, Bell's inequality, and Bell separability	111
6.5.2	Stochastic description of a non-interacting particle pair	115
6.5.3	Bell separable particle pairs	117
6.5.4	Entangled spin states	122
7	Conclusion	133
A	Basic definitions of probability theory	135
B	Numerical solution of stationary quantum Hamilton equations	137
C	Basics of geometry	141
D	The rotation group $SO(3)$	143
D.1	Relation of $SO(3)$ to $SU(2)$	143
D.2	Parametrizations of $SO(3)$	144
E	The role of the osmotic kinetic energy terms	147
F	Superposition of solutions	149
G	Extension to multiple spins	151
H	Spin orbit coupling in the hydrogen atom	153

List of Abbreviations

QHE	Quantum Hamilton equations
QM	Quantum mechanics
SDE	Stochastic differential equation
FBSDE	Forward-backward stochastic differential equation
PDE	Partial differential equation
COM	Center of mass
SUSY	Supersymmetry
BHD	Bopp-Haag-Dankel
SG	Stern-Gerlach
EPR(B)	Einstein-Podolsky-Rosen(-Bohm)
CHSH	Clauser-Horne-Shimony-Holt

Chapter 1

Introduction

One should examine closely even the elementary and the satisfactory features of our Quantum Mechanics and criticize them and try to modify them, because there may still be faults in them. The only way in which one can hope to proceed on those lines is by looking at the basic features of our present Quantum Theory from all possible points of view. Two points of view may be mathematically equivalent and you may think for that reason if you understand one of them you need not bother about the other and can neglect it. But it may be that one point of view may suggest a future development which another point does not suggest, and although in their present state the two points of view are equivalent they may lead to different possibilities for the future. Therefore, I think that we cannot afford to neglect any possible point of view for looking at Quantum Mechanics and in particular its relation to Classical Mechanics. Dirac, 1951 [Dir51]

For various reasons, the word “quantum” has gained significant attention over the last century. Firstly, quantum physics and its fundamental principles have paved the way for groundbreaking advances in various scientific fields and technology and still evolve rapidly. In this context, the term “quantum” is frequently associated with materials, sensing, computing, cryptography, or communication, where especially the last three have captured the attention of researchers, and the general public. This is evidenced by the recent Nobel Prize in Physics [nob22], highlighting the significance and impact of the contributions in these domains. Secondly, quantum physics has made its way into popular culture. Concepts like quantum teleportation, parallel universes, and quantum superposition have become intriguing subjects that captivate artists and authors. These concepts allow the artists and authors to draw inspiration from quantum theory’s mysterious and mind-bending aspects to create thought-provoking works.

The mystery surrounding quantum physics arises from its seeming departure from classical theories. Basic phenomena of QM such as energy quantization, tunneling, spin, decoherence, and superposition contribute to this mystique. For the latter, e.g., see figure 1.1 concerning the famous double-slit experiment which reveals wave-like behavior of quantum particles. These phenomena baffle many people, as the fundamental concepts are difficult to grasp from a single interpretation. This has led to the formulation of memorable quotations by famous physicists, with Richard Feynman’s statement that “nobody understands quantum mechanics” being one of the most prominent examples.

In the historical context, the development of mathematical formalisms in quantum mechanics can be traced back to the contributions of Planck, Einstein, Bohr, Schrödinger, Heisenberg, Dirac, Born, von Neumann, Weyl, and others at the end of the 19th and beginning of the 20th century. These advancements were a response to experimental observations related to atomic spectra, the radiation emitted by hot objects, the photoelectric effect, as well as the stability of atoms and radioactivity. Nowadays, orthodox quantum mechanics typically refers to interpretations emerging from that era that utilize the wave function as the fundamental quantity of the system. For instance, in the non-relativistic regime, the wave function follows the Schrödinger equation, and its description proves to be highly power-

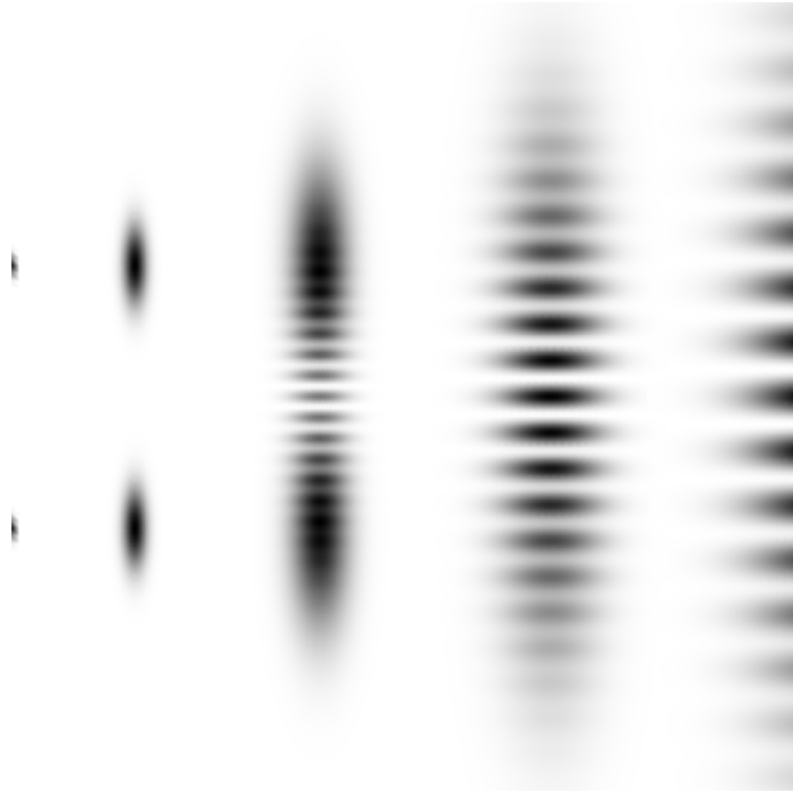


Figure 1.1: The plot shows snapshots of the probability amplitudes in two dimensions for 5 different times for an idealized double slit experiment associated with the wave function satisfying the Schrödinger equation.

ful in explaining phenomena on a microscopic scale. On the other hand, in the relativistic regime, the standard approach is quantum field theory, which incorporates the creation and annihilation of particles.

There is no doubt that the standard quantum theory has proven to be very successful in the prediction of measurement outcomes. Empirically, it is one of the most extensively tested theories. However, despite the overwhelming success of the existing theory, quantum physics still puzzled many physicists in the last 100 years. This is manifested in a very active field of research on quantum foundations which deals with the underlying questions regarding reality, ontology, or the relationship between quantum theory and other branches of physics, such as general relativity.

Compared to fields like statistical mechanics, classical mechanics, or general relativity, quantum mechanics surely has an extraordinary standing due to the multitude of interpretations connected to it. For instance, the wave function is usually accompanied by a physical interpretation, the so-called Copenhagen interpretation. The wave function is a state vector in the Hilbert space that describes the physical system completely. In a closed system, it evolves unitarily¹ in time according to the Schrödinger equation. The state vector generally describes a superposition of all possible measurement outcomes before the measurement. After a measurement, however, we find the system to be in one specific state. As a result, the evolution equation no longer describes the change of the state vector. Instead, the transformation of the state vector is governed by the projection postulate, commonly referred to as the collapse of the wave function. This collapse, characterized by its non-unitary and discontinuous nature, exclusively occurs when the quantum system is under observation.

Consequently, a multitude of questions arise regarding the mechanics of measurement, e.g., what exactly causes the state to collapse? Is it an objective process? What is the role of

¹A unitary transformation preserves the inner product of two state vectors in the Hilbert space.

the observer? Does the state vector change instantaneously, and if so, when does it happen? Are there hidden variables that explain the randomness of the measurements? These questions are related to the measurement problem in quantum mechanics, and it is one of the driving forces in the pursuit of a comprehensive interpretation of the subject.

Due to the empirical success of quantum theory, it is plausible to disregard these questions and come to a slightly provocative conclusion:

Without wasting time and effort on philosophical justifications and implications, we write down the conditions for the Hamiltonian of a quantum system for rendering it mathematically equivalent to a deterministic system. t’Hooft, 2020 [tH20]

Or, alternatively, following Mermin’s famous quote:

If I were forced to sum up in one sentence what the Copenhagen interpretation says to me, it would be ‘Shut up and calculate!’ Mermin, 1989 [DM89]

While it is possible to accept the effectiveness of the theory, there remains a desire to understand the underlying physics on a fundamental level to deepen our understanding of quantum physics. Some even argue that an excessive focus on the mathematical framework has hindered progress in physics in general [Hos18].

Given the seemingly non-classical nature and puzzling phenomena, quantum mechanics has continuously challenged physicists to seek alternative perspectives based on a physically satisfying interpretation of its underlying principles. One such perspective is Nelson’s stochastic mechanics [Nel66, Nel85], which offers a stochastic generalization of classical mechanics. Stochastic mechanics proposes a framework for understanding non-relativistic quantum phenomena by introducing Markov processes representing the coordinates of the system. The considered stochastic process is governed by stochastic differential equations featuring two velocity fields as the fundamental quantities. These equations describe a conservative Brownian motion with drift, extending the Newtonian mechanics.

The interest in studying quantum mechanics through the lens of stochastic processes lies in the possible extension of fundamental classical concepts. This includes the notion of trajectories and the treatment of the probabilities associated with stochastic processes.² It, thus, provides an alternative perspective on the behavior of quantum systems, offering resolutions to certain peculiar properties associated with the traditional formulation of quantum mechanics, such as the collapse of the wave function and quantum tunneling. For example, the measurement of a quantum system can be simply described as the current state of the stochastic process at the time of observation. Its subsequent evolution is then conditional on the measurement outcome. Hence, there is no need for an additional measurement postulate.

The stochastic representation of quantum mechanics is certainly not among the popular interpretations of quantum systems, which is due to some misconceptions connected to the theory, and, more prominently, due to the limitations of applicability. In most cases, it is easier to use the common operator representation and then using the wave function to deduce the velocity fields, for example. Recently, however, a generalization of the classical Hamilton equations of motion was established by Köppe [KGP17], which is built on Nelson’s stochastic mechanics. This generalization is derived from the quantum version of Hamilton’s principle [Pav95b], reformulated as a stochastic optimal control problem. As a result, kinematic and dynamic stochastic differential equations for the quantum process, known as quantum Hamilton equations (QHE), are obtained.

A key advantage of the quantum Hamilton equations lies in their solvability for quantum systems through numerical methods [Köp18, BPGP19], which allows us to describe the

²However, it is worth noting that the reality of the paths suggested by Markov processes is questioned due to the ambiguity in defining the stochastic mean acceleration, and the velocity fields may not necessarily describe the mean velocity of the particle, particularly in discussions involving entangled states in the last chapter of the thesis.

behavior of quantum systems, including their dynamics and properties, without solving the Schrödinger equation or variants thereof. In recent years, it has been shown that some of the foundational examples of quantum phenomena can be described by QHE, including tunneling phenomena, the hydrogen atom, or energy quantization [KPGP18, KPB⁺20, BPGP19].

It is important to emphasize that the establishment of the quantum Hamilton equations should not be viewed as a competitor to ordinary non-relativistic quantum theory. Instead, it should be regarded as an extension of the toolbox of quantum mechanics, analogous to the various formalisms employed in classical mechanics. For instance, in classical mechanics, depending on the problem at hand, one may utilize the Lagrange formalism to handle motion constraints, or we could describe the problem in phase space with Hamilton's equations, or employ the Hamilton-Jacobi equation. Each of these classical descriptions provide a distinct viewpoint of the same physics, with corresponding counterparts in quantum mechanics. For example, Feynman's path integral formulation corresponds to the action principle in classical mechanics, the Schrödinger equation corresponds to the Hamilton-Jacobi equation, the Madelung equation corresponds to the dynamics of a classical fluid, and Nelson's stochastic mechanics corresponds to Newton's equation of motion. Thus, the QHE establish an additional correspondence between quantum and classical mechanics, broadening our understanding of the field.

This thesis focuses on an extension of the QHE by exploring further fundamental aspects of non-relativistic quantum mechanics. Specifically, the QHE are extended to describe quantum stochastic processes on (Riemannian) manifolds. This extension allows for studying systems in non-flat coordinates, providing a broader framework for investigating quantum phenomena in various physical contexts. A notable application of the extension considered in this thesis is the description of a stochastically spinning particle in Nelson's mechanics, which is in contrast to the usual treatment of spin in quantum mechanics.

A concept of a magnetic moment in standard quantum mechanics was needed to describe effects that the Schrödinger equation alone could not account for, such as the anomalous Zeeman splitting in the atomic spectra and, more famously, the quantized nature of the Stern-Gerlach experiment. In quantum mechanics, the spin is an intrinsic property added as a label to the particle itself. Classically motivated models have been proposed to explain spin based on extended particles, but they were dismissed due to conflicts with special relativity. These models would require superluminal rotation velocities, e.g., of the electron's shell, to match its spin angular momentum magnitude. The stochastic theory, however, avoids these conflicts by employing non-differentiable trajectories and undefined instantaneous velocities. Revisiting these models could be valuable as they offer a physical picture beyond the abstract perspective of standard quantum theory. With open questions about the fundamental nature of spin, exploring these models can enhance our quantum mechanics toolbox and provide further insights.

The thesis, in particular, focuses on the classical model introduced in the work of Bopp, Haag [BH50] and Dankel [Dan70], which provides a non-relativistic treatment of spin within the framework of stochastic mechanics. In this model, particles have an assigned orientation and inertia, such as an extended rigid rotor with a radius. The associated angular velocities lead to spin fields, driving the change in orientation, as illustrated in figure 1.2.

It was shown that:

- 1) their expectations agree with quantum mechanics,
- 2) the time-averaged spins are quantized, and

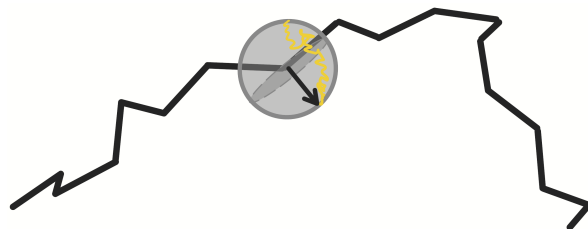


Figure 1.2: The figure illustrates a stochastic process regarding position and orientation.

- 3) the associated partial differential equations to the orientational Markov process are associated with the Pauli equation in the limit of vanishing inertia.

The first two points, however, relied on the use of eigenfunctions to the Laplace-Beltrami operator. Dankel took these eigenfunctions, calculated the corresponding velocity fields, and finally the state's expectation values. The Bopp-Haag-Dankel (BHD) model is revisited within the formalism of the QHE. Here, the stochastic velocity and spin fields are considered as critical points of a stochastic optimal control problem. It is shown that the QHE for a spinning symmetric top lead to the same results as discussed by Dankel in the free case without referencing the Schrödinger equation on the considered manifold.

In a subsequent step, the coupling of spin to position is included, allowing for the discussion of idealized spin measurements and correlations. In orthodox quantum mechanics, the coupling to the position is introduced by the superposition of the different spin states represented as a spinor. If the beam of particles is sent into a field gradient, it splits into distinct channels such that only one spinor component is apparent after observation of the object. The measurement leads to a collapse of the quantum state where the ensemble of particles produces probability amplitudes related to the wave function at the preparation stage.

Thus, in the BHD model, the spins act as if they have an undefined direction until a measurement is performed. This is fundamentally different in the context of a stochastically spinning particle, where the spins and their expectation values have well-defined directions that continuously change with time according to their dynamics. In the case of measurement, the spins undergo a continuous but stochastic change during and after the magnetic field gradient. Eventually, the expectation values of the spins become quantized after the measurement. The thesis demonstrates that this behavior can be explained using the QHE, which include additional torque terms to account for spin alignment.

In the final step, the thesis considers two-particle pairs entering two different Stern-Gerlach (SG) devices based on the analysis of the QHE for a single SG experiment. This allows us to discuss the famous Gedankenexperiment by Einstein, Podolsky, Rosen, and Bohm [EPR35, Boh51], where a pair of particles that interacted in the past passes through two space-like separated SG devices. By recording the coincidences of the resulting deflections of the particles for different measurement settings, the correlations of the spins can be stronger for certain spin pair states in quantum mechanics that are not describable by any 'classical' probabilistic theory. Such correlations are only possible if the state is entangled, where the 'non-classical' correlations can be quantified with Bell's inequality [Bel64, CHSH69]. The thesis discusses such a system using the QHE for a two-particle system, examining the detailed behavior of the spins and highlighting the differences from the standard approach with hidden variables, where the spins are quantized and not continuous as in stochastic mechanics.

The thesis is organized as follows: We begin by establishing the basics of stochastic mechanics. Next, we investigate variational principles in stochastic mechanics and derive the quantum Hamilton equations. We then extend these equations to (Riemannian) manifolds, enabling the study of quantum systems in curvilinear coordinates. Finally, as an illustrative example, we apply the equations to the hydrogen atom using the system's symmetry in spherical coordinates. After that, we examine the model of a freely spinning particle. This model allows us to study the implications of spin within the framework of the quantum Hamilton equations. Moreover, we discuss the different nuances to spin measurements, using these equations to gain a deeper understanding of the behavior and dynamics of spinning particles.

In conclusion, this thesis seeks to contribute to our understanding of quantum mechanics by considering the alternative viewpoint of Nelson's stochastic interpretation. Furthermore, by revisiting the fundamental properties of spin and investigating spin measurements within the framework of the quantum Hamilton equations, we aim to deepen our comprehension of quantum phenomena.

Chapter 2

Quantum mechanics in terms of stochastic processes: Nelson's stochastic mechanics

2.1 Overview

The behavior of matter on a microscopic scale, such as atoms and subatomic particles, is described by quantum mechanics, a fundamental theory in physics. This theory is typically discussed within the context of the Hilbert space, which permits the depiction of quantum states and their evolution over time using operators. Since its inception, one of the main challenges in quantum theory was the problem of explaining the measurement process, e.g., for a state which is in a superposition of all measurable outcomes. This is due to the instantaneous localization of a quantum state to a state associated with the measured outcome in an experiment.

In the standard theory, no (physical) description explains the abrupt change of the state. It is argued that the Copenhagen interpretation was favored over others in the early years, like de-Broglie's interpretation [DB27], since the measurement outcomes could be described by a "simple" collapse of the state without the treatment of the measurement process [BV09]. To address this problem, the Born rule was introduced ad hoc, which gives a probabilistic interpretation of the quantum states in terms of probability amplitudes (instead of distributions), which successfully describe quantum measurements.¹

The acceptance of the interpretations related to the Schrödinger equation [Sch26b, Sch26a, Sch26c], Heisenberg's matrix mechanics [Hei25] and variants thereof [Dir26, Dir81] grew rapidly since they could successfully describe most of the (non-relativistic) experiments. However, due to the unintuitive nature of quantum systems, the attempt to combine an inherently probabilistic description of quantum mechanics began with the establishment of standard quantum theory. Schrödinger himself was puzzled by the (not yet understood) relationship between the wave mechanical equation and the Fokker-Planck equation of diffusion [Sch31]. Whereas in classical systems, we deal with the probability density, the wave function describes the quantum state in the Schrödinger equation. One may argue that it seems to be a mathematical auxiliary function rather than a real physical quantity because, on the one hand, the Schrödinger equation is not a wave function due to the first-order time derivative. On the other hand, it is not directly connected to a diffusion due to the occurrence of an imaginary time.

Notable steps towards a probabilistic interpretation were taken by Fürth's uncertainty relation for a diffusion process [Für33] and by Fényes [Fén52] later on. Nelson established a rigorous mathematical formulation of quantum stochastic processes in 1966 [Nel66]. He

¹It should be noted that quantum physics is more generally described by density matrices which allow the description of mixed states, including preparation, transmission, and measurement. See e.g., [Adl21] for a recent overview on quantum foundations. The thesis focuses on pure states in non-relativistic quantum mechanics.

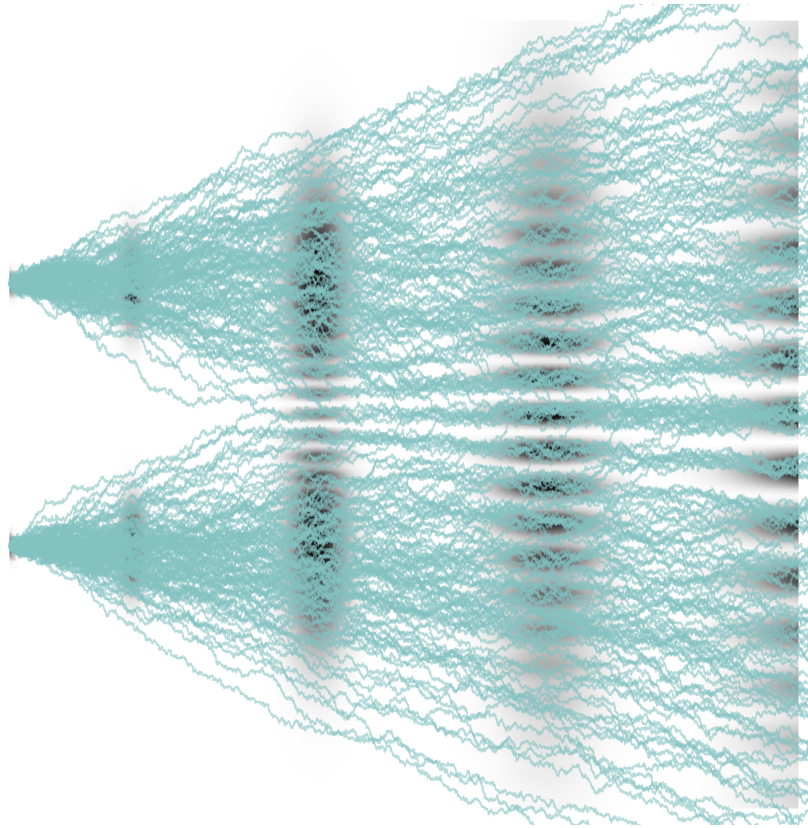


Figure 2.1: The figure depicts the same plot as figure 1.1 with an overlay of an ensemble of 200 stochastic paths generated according to Nelson's stochastic mechanics.

considered massive particles in an open system which are subject to a stochastic Newton-law and an unspecified background field that is in permanent contact with the particles. The resulting Brownian motion is non-dissipative, which is required for a time-reversible stochastic process.

In Nelson's stochastic mechanics, the wave function is replaced by two velocity fields governing the motion of a stochastic process. Furthermore, the stochastic process evolves in time according to stochastic differential equations such that the random realizations of the process apparently result in a physical picture of the quantum fluctuations on small scales. The noise is caused by the interaction of particles with a background field. Aside from the physically satisfying elegance of the stochastic theory, it enables the definition of real observables as stochastic processes, which include tunneling times or first hitting times, as opposed to the operator theory. This is due to the sample paths and their corresponding observables. Figure 2.1 depicts a number of stochastic realizations of a Nelson process (right plot) moving from a double-slit on the left to a detection screen on the right. Apparently, the paths avoid certain areas and agree with the probability amplitudes following Born's rule for the double-slit wave function on the left.

The measurement problem in the Copenhagen interpretation is not apparent in stochastic mechanics since the stochastic process replaces the wave function. Thus, the collapse of the wave function corresponds just to a measurement of the stochastic process' current state. In terms of the probability density associated to the quantum process, the measurement leads to an update about the knowledge of the system, i.e., the further development has to be described by a stochastic process conditioned on the measurement outcome.

It was shown by a variety of authors [Yas81b, Yas81a, Yas83, GM83, Zam85] that the postulated Nelson-Newton-law can be derived from variational principles in analogy to classical mechanics. Recently, the variational principles were reformulated as a stochastic optimal control problem, which will be discussed in section 3. Attempts were also made

regarding a generalization to field theories [Nel85, Nel73, Gue81]. Furthermore, stochastic mechanics was extended to particles moving on a manifold [Nel85, DG79], which includes the main topic of this thesis, the spin [Dan70, Dan77, Far82, Gar90].

Constructing a relativistic counterpart of stochastic mechanics on the Lorentzian manifold poses challenges, as the creation of a relativistic Markov process is not a simple task due to the existence of “no-go” theorems [Dud66, Lop53], which is elaborated on shortly. They imply that the usual interpretation of the non-relativistic diffusion equation

$$(\partial_t - \frac{\sigma^2}{2} \Delta) \rho(t, x) = 0 \quad (2.1)$$

for the distribution ρ depending on t and position x has to be adjusted since time and position should be put on an equal footing. One way to deal with this is by giving up Markovianity which allows to consider the telegrapher’s equation [Kac74]

$$(\tau_v \partial_t^2 + \partial_t - \frac{\sigma^2}{2} \Delta) \rho(t, x) = 0 \quad (2.2)$$

with a relaxation time τ_v . This, in turn, is related to the Dirac equation [GJKS84], for example. See also [DH09] for a good overview. Relativistic extensions of stochastic mechanics, including stochastic field theory, were put forward by Guerra [GR73, GR78, Gue81] and later rather sparsely by others [MV95, Pav01]. Recent work on a relativistic stochastic quantization reformulates stochastic quantization in terms of a relativistic diffusion process on a pseudo-Riemannian manifold [Kui21b, Kui21a, Kui22]. It is based on a complexified Wiener process with complex velocity $v_q = v - iu$ and *position* $Z = X + iY$, which may be of interest in the field of quantum gravity [Erl18].

In summary, stochastic mechanics is a valid description of non-relativistic quantum mechanics and has the ability to provide an intuitive explanation for quantum phenomena. As with all interpretations and formulations of quantum mechanics, however, there are some challenges to this approach, such as the unclear nature of the background field, the inequivalence to the Schrödinger equation² and the non-locality of the velocity fields. The latter will be addressed in the thesis in more detail. Finally, it should be mentioned that Nelson himself had problems with the theory [Nel12], although some of his arguments have been resolved. Nonetheless, the stochastic theory can still inspire seminal work by offering different perspectives on certain quantum phenomena, making it a worthwhile consideration.

In the following subsection, some introductory information on stochastic processes will be provided before delving into the details of Nelson’s postulates.

2.2 Stochastic processes and stochastic calculus

Nelson’s stochastic mechanics is a conservative Brownian motion characterized by forward-backward stochastic differential equations (FBSDEs) that govern a stochastic process. Readers familiar with these terms may proceed to Section 2.3.

This section mostly follows the notations in Øksendal [Øks03]. Additional literature on stochastic processes and stochastic differential equations (SDEs) can be found in various books, including [Pav14]. For important mathematical definitions related to probability, please refer to Appendix A.

²The inequivalence between Nelson’s stochastic mechanics and the Schrödinger equation lies in the fact that not every Nelson process, with its associated velocity fields, is a solution to the Schrödinger equation. However, every wave function has a stochastic counterpart in Nelson’s theory, allowing for a wider range of solutions compared to the Schrödinger equation [Wal94]. This property is also shared with the Madelung equations in quantum hydrodynamics [Mad27, Tak52].

Random variables

Random variables, or measurable functions, are given on a probability space denoted by a tuple of a sample space, a σ -Algebra and a probability measure (Ω, \mathcal{F}, P) . The sample space Ω is the set of all possible outcomes of an event while the σ -algebra \mathcal{F} is a certain collection of subsets of the sample space depending on the interest of what is to be studied. For example, consider a four-sided die with a focus on the outcome of 2. In this case, $\Omega = \{1, 2, 3, 4\}$ and $\mathcal{F} = \{\emptyset, \{2\}, \{1, 3, 4\}, \Omega\}$. Assigning probabilities, represented by real numbers in the interval $[0, 1]$, to the possible outcomes in \mathcal{F} gives rise to the definition of a probability measure $P : \mathcal{F} \rightarrow [0, 1]$ on the measurable space (Ω, \mathcal{F}) . For the chosen example, we have $P(\emptyset) = 0$, $P(\Omega) = 1$, $P(\{2\}) = 1/4$, and for the complement, $P(\{1, 3, 4\}) = 3/4$.

A real random variable $X : \Omega \rightarrow \mathbb{R}^n$ induces a probability measure, also denoted as distribution $\mu_X(B) = P(B)$ such that the expectation of X is

$$E[X] = \int_{\Omega} X(\omega) dP(\omega) = \int_{\mathbb{R}^n} x d\mu_X(x). \quad (2.3)$$

X is said to be integrable if $E[|X|] < \infty$. The variance is defined as

$$\text{Var}[X] = E[(X - E[X])^2]. \quad (2.4)$$

Likewise, if f is an appropriate function with $E[|f(X)|] < \infty$, then

$$E[f(X)] = \int_{\mathbb{R}^n} f(x) d\mu_X(x). \quad (2.5)$$

In the remainder of the thesis the distribution associated with X will be denoted by $\rho(x) = \mu_X(x)$.

Stochastic processes

In general, a stochastic process $\{X_t, t \in I\}$ is defined as a set of random variables on a given probability space that takes values in a measurable space $(\tilde{\Omega}, \tilde{\mathcal{F}})$, i.e. $X_t : \Omega \rightarrow \tilde{\Omega}$ for $t \in I$. For each $t \in I$, the function $X_t(\omega)$ is a random variable, i.e., each ω may refer to a particle or a measurement, while t plays the role of time. In this thesis the index set I denotes (continuous or discrete) time, $\tilde{\Omega} = \mathbb{R}^n$ ($n \in \mathbb{N}$) and $\mathcal{F} = \mathcal{B}(\mathbb{R}^n)$ with the corresponding Borel σ -algebra $\mathcal{B}(\mathbb{R}^n)$.

A path or stochastic realization is described for fixed $\omega \in \Omega$ with the varying parameter $t \in I$. The considered processes in the thesis have (almost surely)³ continuous trajectories. I.e., if we have an outcome ω in the given set of possible events Ω , the corresponding sample path $X_t(\omega)$ is continuous in t . Note that for brevity, the shorthand notation X_t or X will be used over $(X_t)_{t>0}$ at some points for a stochastic process. $X(t)$, $X_t(\omega)$ or $X(t, \omega)$ are different notations used in the literature.

Depending on the accessible information about a process, it is useful to define sets of σ -Algebras (subsets of \mathcal{F}) for a stochastic process X_t at time t ,

- \mathcal{P}_t as the information generated in the past by X_s , $s < t$,
- \mathcal{F}_t as the information generated in the future by X_s , $s > t$
- and \mathcal{C}_t as the current information given by X_t .

E.g., if the future is unknown to the stochastic process, i.e., only the past \mathcal{P}_t is accessible, the process X_t is said to be non-anticipative with respect to \mathcal{P}_t . Depending on the information available on the stochastic process at a given instant, the predictability could be increased.

³If $P(A \in \Omega) = 1$, then the outcome A is said to occur almost surely (a.s.). For convenience, this may not be written throughout the thesis.

Consider $(\mathcal{P}_t)_{t \geq 0}$ as a set of increasing sub- σ algebras $\mathcal{P}_s \subset \mathcal{P}_t \subset \mathcal{F}$ for all $s < t$. Then $(\mathcal{P}_t)_{t \geq 0}$ is called a *filtration*. Filtrations are fundamental for the definition of adapted processes: a stochastic process $(X_t)_{t \geq 0}$ is adapted to a filtration $(\mathcal{P}_t)_{t \geq 0}$ if X_t is a \mathcal{P}_t -measurable random variable for each time $t \geq 0$. This simply states that the value X_t is observable at time t . Furthermore, if we assume that for every $t \in [0, T]$ the σ -algebra \mathcal{P}_t is defined as the smallest σ -algebra that contains the set $(X_s)_{s \leq t}$, then, $(\mathcal{P}_t)_{t \geq 0}$ is called a natural filtration of $(X_t)_{t \geq 0}$ inheriting information that increases in time ($\mathcal{P}_t \subset \mathcal{P}_s \subset \mathcal{P}$, $\forall t \leq s$) and can be viewed as a representation of all events that may be observed at a given time. There is no future information available about the stochastic process under the assumption that the stochastic process is forward-in-time. $(\mathcal{F}_t)_{t > 0}$ accordingly describes a set of decreasing sub- σ algebras which can be viewed as a time-reversed filtration.

To reduce the uncertainty about the outcome of X_t at time $t > s$ one can make use of the accessible information at time s and calculate the expectation value conditional on this information in terms of a σ -algebra $\mathcal{P}_s \subset \mathcal{F}$. This leads to the *conditional expectation* $E[X_t | \mathcal{P}_s]$ which is defined for $E[|X_t|] < \infty$ such that

- (i) $E[X_t | \mathcal{P}_s]$ is \mathcal{P}_s -measurable and
- (ii) $\int_{\mathcal{A}} X_t dP = \int E[X_t | \mathcal{P}_s] dP$, $\forall \mathcal{A} \in \mathcal{P}_t$.

Point (ii) shows that the conditional expectation is a random variable in contrast to the expectation value. The advantage is that if, e.g., the information stored in \mathcal{P}_s and X_t are coupled, we can expect a better prediction about the values of X_t at $t > s$ in comparison to the expectation value that has “no” information. Roughly speaking, it is the best estimate of the random variable X_t given the information stored in \mathcal{P}_s at time $s < t$.

One of the most important stochastic processes is the Wiener process $(W_t)_{t > 0}$ [Wie23]. It is the first mathematical description of Brownian motion, which is a random process describing the erratic movement of particles suspended in a fluid. It is characterized by the continuous and irregular movement of particles, with their position changing in a random and unpredictable manner. Einstein explained Brownian motion in 1905 [Ein05] as a result of the random collisions between the particles and the fluid molecules.

The Wiener process is a continuous-time stochastic process that is defined by its mean and variance, and has the property that the increment between any two points in time is Gaussian distributed with mean zero and variance proportional to the time interval. Mathematically, the Wiener process $(W_t)_{t > 0}$ defined on the interval $[0, T]$ is defined as follows:

- (i) $\forall s, t \in [0, T]$, with $s < t$ the increments $W_t - W_s$ are independent and homogeneous,
- (ii) the increments are Gaussian distributed with mean 0 and variance $|t - s|$,
i.e., $W_t - W_s \sim \mathcal{N}(0, |t - s|) \forall t, s \in [0, T]$,
- (iii) $W_0 = 0$ almost surely, and
- (iv) $(W_t)_{t \geq 0}$ is continuous in t with probability 1.

It follows that the Wiener process has zero expectation $E[W_t] = 0$ for all $t > 0$. From the independence⁴ (i) we have $E[W_t W_s] = E[W_t] E[W_s] = 0$ for $t \neq s$.

Furthermore [Øks03],

$$E[W_t - W_r | \mathcal{P}_r] = 0, \quad E[(W_t - W_r)^2 | \mathcal{P}_r] = t - r \quad \text{for } 0 \leq r < t \leq T \quad (2.6)$$

with $(\mathcal{P}_t)_{t \geq 0}$ as the filtration generated by the Wiener process. This definition results also in other interesting properties of the Wiener process. E.g., the trajectories of $(W_t)_{t \geq 0}$ are by definition continuous, whereas they are nowhere differentiable [Doo53], which may seem

⁴If events $\{X \in A\}$ and $\{Y \in B\}$ are independent, the joint probability distribution of X and Y factors into the product of their marginal distributions.

odd later when stochastic processes for continuous paths of particles are stated which are not differentiable.⁵

To give an idea why the Wiener process is not differentiable, consider that the increments $W_{t+\Delta t} - W_t$ are Gaussian distributed with mean 0 and variance Δt . Thus the process increment is of order $\sqrt{\Delta t}$, so that informally

$$\lim_{\Delta t \rightarrow 0} \frac{W_{t+\Delta t} - W_t}{\Delta t} \sim \lim_{\Delta t \rightarrow 0} \frac{1}{\sqrt{\Delta t}}.$$

This leads to the fact that from the physical point of view, there exists no “classical” velocity that can be related to the Wiener process, i.e., the particle is subjected to a sudden change of its velocity at all times.

Stochastic calculus

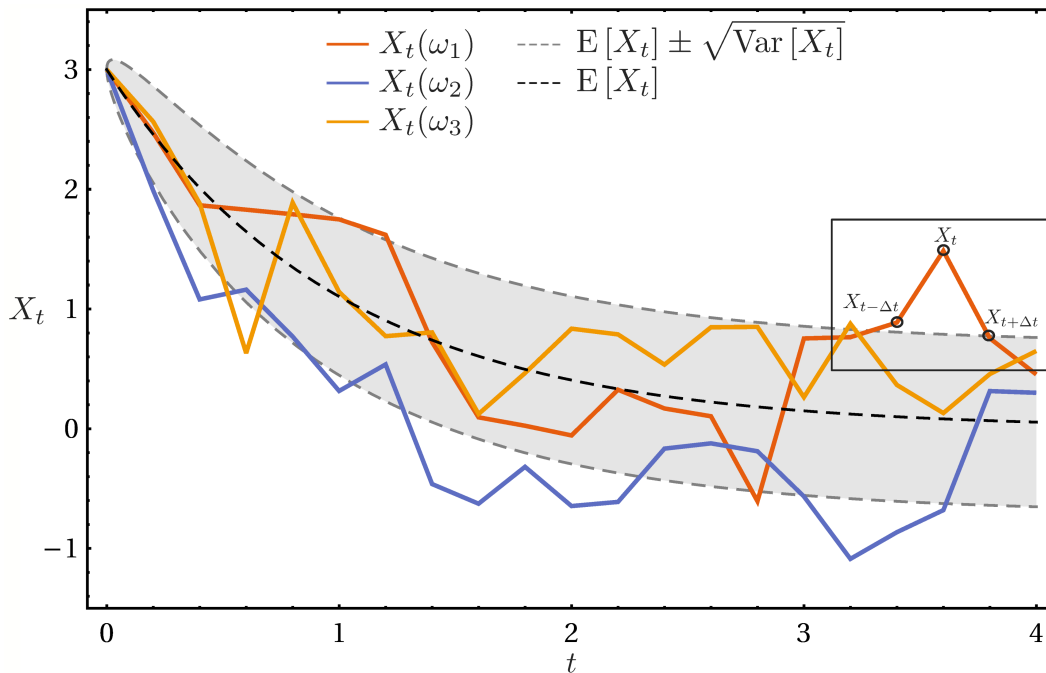


Figure 2.2: The plot illustrates a stochastic process $(X_t)_{t>0}$ governed by the SDE $dX_t = -X_t dt + dW_t$. Three sample paths $X_t(\omega_k)$ with solid lines, starting from $X_0 = 3$, are numerically integrated and displayed. The ensemble average $E[X_t]$ is depicted with a black dashed line, while the gray band represents the standard deviation. The rectangle on the right highlights the non-differentiability caused by the noise, which becomes more apparent as $\Delta t \rightarrow 0$.

The development of stochastic calculus was motivated by the need to provide a rigorous mathematical framework for analyzing and modeling random processes such as the Brownian motion with possible drift. A simple extension from ordinary differential equations could look like

$$\frac{dX_t}{dt} = b(t, X_t) + \sigma(t, X_t) \frac{dW_t}{dt} \quad (2.7)$$

where the additional term in the differential equation can be viewed as the product of a diffusion coefficient σ that may depend on t and x and the random perturbation dW_t/dt , which should mimic a white noise. However, the differential equation above is ill-defined due to

⁵Note that when speaking about properties like continuity of stochastic processes one has to add that this is only valid w. r. t. the probability measure. Therefore, one should add ‘with probability 1’ or P-almost surely. However, this will be omitted here for the sake of simplicity.

the non-differentiability of the Wiener process, i.e., dW_t/dt does not exist. More generally, the problem with any other comparable definition is that one runs into trouble because no such process exists [Øks03]. That is the case where SDEs and, more precisely, stochastic integrals come into play.

Itô [Itô51] introduced the concept of stochastic integration and stochastic differential equations. If we rewrite (2.7) in differential notation, this yields the SDE with initial value x_0 (\mathcal{F} -measurable)

$$dX_t = b(t, X_t)dt + \sigma(t, X_t)dW_t, \quad X_0 = x_0. \quad (2.8)$$

To make sense of (2.8) it has to be reformulated as an integral equation

$$X_t = X_0 + \int_0^t b(s, X_s)ds + \int_0^t \sigma(s, X_s)dW_s. \quad (2.9)$$

The first integral is defined as a common integral on the paths, e.g., the Lebesgue-Stieltjes integral. The second integral $\int_0^t \sigma(s, X_s)dW_s$ has to be treated differently from the usual integral. Namely, it has to be interpreted as a stochastic integral.

The concept of stochastic integrals can be defined in different ways. First, one has to admit a certain class of functions $\sigma(t, X_t)$ [Øks03]. Then, by dividing a time interval $[0, T] = \bigcup_{i \in I} [T_i^n, T_{i+1}^n)$ into 2^n equal sub-intervals, the integral is defined as

$$\int_0^T \sigma(s, X_s)dW_s = \lim_{n \rightarrow \infty} \sum_{i=0}^{2^n} \sigma(t_i^n, X_{t_i^n}) [W_{T_{i+1}^n} - W_{T_i^n}] \quad (2.10)$$

with $t_i^n \in [T_i^n, T_{i+1}^n)$. The mid-point average $t_i^n = 1/2(T_i^n + T_{i+1}^n)$ gives the *Stratonovich* integral while the *Itô* integral is defined for $t_i^n = T_i^n$, i.e., the left edge of the interval. The latter definition is non-anticipating and is easier to solve numerically in (2.8). The Stratonovich integral, on the other hand, is neither anticipating nor non-anticipating. It is very useful in stochastic calculus, especially on manifolds, since it preserves the rules of ordinary calculus, i.e., no second-order terms for a differential change of the process.

These two commonly used stochastic integral definitions possess different analytical properties, and the choice between them depends on the specific problem being studied. In most cases, the Itô integral is used herein. When used, the Stratonovich integral and differential will be indicated with “ \circ ”, e.g., $X_t \circ dY_t$.

Some useful properties of Itô’s calculus for measurable functions $f, g: [0, T] \times \Omega \rightarrow \mathbb{R}^n$ adapted to the natural filtration generated by W_t and $E[\int_0^T f^2 dt] < \infty$ are [Øks03]

- (i) $E[\int_0^T f dW_s] = 0$,
- (ii) $E[(\int_0^t f dW_s)(\int_0^t g dW_s)] = E[\int_0^t f g ds]$,
- (iii) $E[M_t | \mathcal{P}_s] = M_s, \forall s, t \in [0, T], s \leq t$.

Property (iii) refers to the definition of martingales stating that the expectation of the random process M_t is determined by the information \mathcal{P}_s . The interesting thing is that one can turn this around and state that every martingale w.r.t. \mathcal{P}_t can be represented as an Itô integral.

With the help of these properties, it is possible to state a chain-rule-like version for the Itô integral and rewrite this in differential notation. Consider a stochastic process X_t fulfilling (2.8). If $f(t, X_t)$ is a sufficiently smooth function then $Y_t = f(t, X_t)$ is a stochastic process

and fulfills a SDE

$$dY_t = \partial_t f(t, X_t)dt + \partial_{X_t} f(t, X_t)dX_t + \frac{1}{2}dX_t^T (\partial_{X_t}^2 f(t, X_t))dX_t \quad (2.11)$$

$$= \left[\partial_t f(t, X_t) + b(t, X_t) \cdot \partial_{X_t} f(t, X_t) \right. \quad (2.12)$$

$$\left. + \frac{1}{2}\text{Tr} \left[\sigma^T(t, X_t) (\partial_{X_t}^2 f(t, X_t)) \sigma(t, X_t) \right] \right] dt + dW_t \cdot \partial_{X_t} f(t, X_t). \quad (2.13)$$

This is Itô's Lemma for a multidimensional drift-diffusion process. Informally speaking this is simply a Taylor expansion of f where all terms of higher order $\mathcal{O}(dt^{3/2})$ are neglected. The differential form in (2.13) is a shorthand notation and can only be understood again in form of stochastic integrals. In this context it makes use of stochastic quadratic variations

$$[X, Y]_t = X_t Y_t - X_0 Y_0 - \int_0^t X_s dY_s - \int_0^t Y_s dX_s. \quad (2.14)$$

Here the product of two stochastic differentials has to be read as $dX_t dY_t = d[X, Y]_t = [X, Y]_{t+dt} - [X, Y]_t$. The quadratic variation of the d -dimensional forward (backward) Wiener processes follows property (iii) above

$$[W^i, W^j]_t = \delta^{ij} dt. \quad (2.15)$$

Hence, $dW_t \cdot dW_t = dt$ and $dW^i dt = \mathcal{O}(dt^{3/2}) \forall i \in 1, \dots, d$. These shorthand expressions have to be read in the integral sense. They are of big importance because they state that in Itô's integral formulation, second order effects are not negligible when dealing with Brownian motion. These additional terms are a consequence of the non-anticipating choice of the Itô integral defined above.

Stochastic processes that solve (2.8) are called Itô diffusions. These processes satisfy the Markov property

$$\mathbb{E}[X_t | \mathcal{P}_s] = \mathbb{E}[X_t | X_s] \forall s < t, \quad (2.16)$$

where the conditional probability for a Markov process may be written as $\mathbb{E}[f(X_t) | X_s] = \int dx' f(x') p(t', x' | s, x)$ with the transition probability $p(t, x' | s, x)$ going from x at s to x' at t . Equation (2.16) states that the history of $(X_t)_{t \geq 0}$ w.r.t. the information stream \mathcal{P}_s up to time $s < t$ is irrelevant; it only depends on the state of the process at time s . Here, $(\mathcal{P}_t)_{t \geq 0}$ is the filtration generated by $(W_t)_{t > 0}$ up to time t .

Backward stochastic differential equation

In the context of stochastic processes, it is also useful to consider the evolution backwards in time depending on a condition in the future. For example, this approach is frequently employed in finance, where one might seek to attain a particular value X_T and wishes to determine the necessary investment at time X_0 .

In deterministic theories the time-reversal is easily done since the configuration is determined. The stochastic integral in Itô's sense may be defined following (2.10) by evaluation at the end of the time interval $t_i^n = T_{i+1}^n$. It describes a process that does not know anything about the past. In terms of stochastic integrals the time direction is reversed

$$X_t = X_T - \int_t^T b_-(s, X_s) ds - \int_t^T \sigma(s, X_s) d_- W_s^-, \quad X_T = x_T \quad (2.17)$$

and the backward Wiener process $W_t^- := W_{T-t}^+$ is introduced. It has the same properties as the forward Wiener process where t is replaced by $T - t$. The d_- indicates that the integral has to be interpreted backward-in-time. The backward Itô integral with respect to a Wiener

process W_t^- is an anticipating integral because the argument of the considered function $f(X_t)$ has to be evaluated at the end of a partition interval $T_{k+1} \in [T_k, T_{k+1}]$.

For such processes, the above definitions should be adapted to going backward in time, e.g., a backward Wiener process that is non-anticipative w.r.t. the past. The shorthand notation for the backward SDE to (2.17) reads

$$dX_t = b_-(t, X_t)dt + \sigma(t, X_t)d_-W_t^- \quad (2.18)$$

with $dt > 0$. The backward Itô formula for $Y_t = f(t, X_t)$ then yields a backward SDE

$$dY_t = \left[\partial_t f(t, X_t) + b_-^T(t, X_t) \partial_{X_t} f(t, X_t) \right. \quad (2.19)$$

$$\left. - \frac{1}{2} \text{Tr} \left[\sigma^T(t, X_t) (\partial_{X_t}^2 f(t, X_t)) \sigma_t(X_t) \right] \right] dt + dW_t^- \cdot \partial_{X_t} f(t, X_t). \quad (2.20)$$

where $dW_t^{-,k} dW_t^{-,j} = -\delta^{kj} dt$. In most cases, the distinction of the backward integrals and differentials from the ones forward in time is clear from the context, e.g., as in dW_t and $d_-W_t^-$. Hence, the index “-” is dropped, i.e., $d = d_-$, in the remainder of the thesis.

Mean velocity

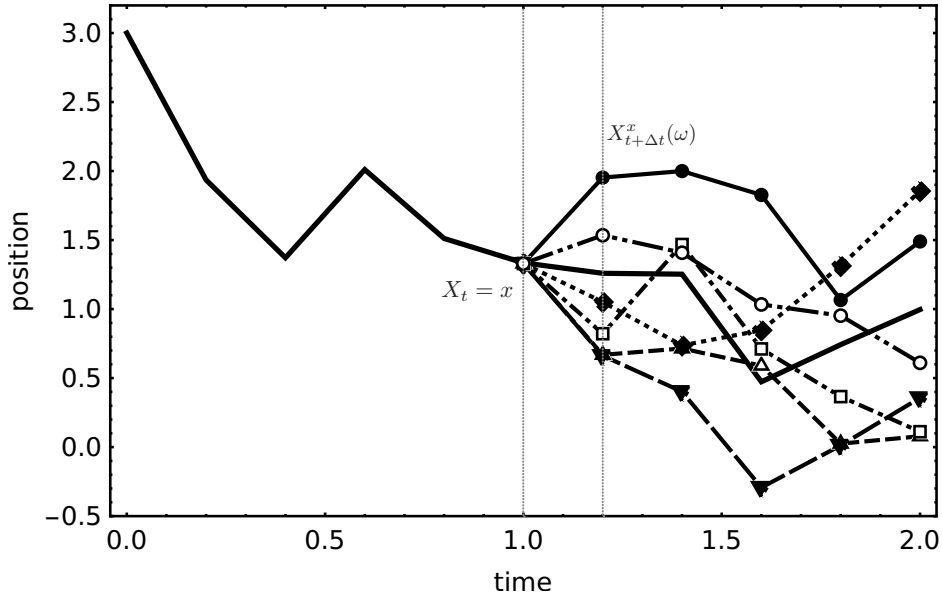


Figure 2.3: The plot displays the numerically integrated sample path of a stochastic process $(X_s)_{[0,t]}$ starting from $X_0 = 3$ and governed by $dX_s = -X_s ds + dW_s$ until time $t = 1$. Seven possible future realizations are shown starting from $X_{t=1} = x$. Since the path is not differentiable, a (forward) velocity for a particle at $X_t = x$ can only be defined as a mean of all possible future positions $X_{t+\Delta t}^x$ depending on the initial position x . Hence, the mean velocity at t depends on (t, x) .

Consider a stochastic process $(X_t)_{t>0}$ at time t with $X_t = x$. A time change by $\Delta t > 0$ forward (or backward) in time according to (2.8) ((2.18)) leads to $X_{t\pm\Delta t}(\omega)$. Due to the noise, there are infinitely many possibilities for the new position as schematically shown in figure 2.3 for the integration forward-in-time. From the information of the current position it is possible to calculate the expected velocity conditional on $X_t = x$

$$D_+ X_t = \lim_{\Delta t \rightarrow 0} \frac{1}{\Delta t} E[X_{t+\Delta t} - X_t | X_t = x]. \quad (2.21)$$

Nelson defined the rhs of this equation as a forward mean derivative of the stochastic pro-

cess $D_+X_t = b_+(t, X_t)$ by using the martingale property of the Wiener process. The backward mean derivative is defined accordingly

$$D_-X_t = \lim_{\Delta t \rightarrow 0} \frac{1}{\Delta t} \mathbb{E}[X_t - X_{t-\Delta t} | X_t = x] = b_-(t, X_t). \quad (2.22)$$

This allows us to make sense of (mean) velocities associated to non-differentiable processes. These velocities, thus, allow an estimation of the new position forward or backward in time.

Relation to the Fokker-Planck equation

As already stated, we are dealing with stochastic processes $(X_t)_{t \geq 0}$ characterized via SDEs describing so called Itô processes. They are also called Itô diffusion because with them one is capable to describe diffusions. That in turn is usually connected to probability distributions. Therefore, the probability distribution $\rho(t, x)$ associated with X_t at time t is governed by a PDE as well, namely the *Fokker-Planck equation*. The Itô formula (2.13) bridges the path between a SDE and a partial differential equation (PDE). Consider a smooth function $f(X_t)$ and the expectation conditional on the value $X_t = x$ in shorthand notation $\mathbb{E}^x[\cdot] = \mathbb{E}[\cdot | X_t = x]$. This yields

$$\mathbb{E}^{x_t}[f(X_t + h)] = f(x_t) + \mathbb{E}^{x_t} \left[\int_t^{t+h} b^T(s, X_s) \partial_x f(X_s) ds \right. \quad (2.23)$$

$$\left. + \frac{1}{2} \int_t^{t+h} \text{Tr} \left[\sigma^T(s, X_s) (\partial_x^2 f(X_s)) \sigma(s, X_s) \right] ds \right]. \quad (2.24)$$

Rearranging (2.24) and taking the limit $h \rightarrow 0$ the dominated convergence theorem gives

$$\mathcal{A}f(x) := \lim_{h \rightarrow 0^+} \frac{1}{h} (\mathbb{E}^x[f(X_t + h)] - f(x)) . \quad (2.25)$$

where \mathcal{A} is the so-called generator of the time-homogeneous diffusion process $(X_t)_{t \geq 0}$. With $p(x, t | y, 0)$ as the transition probability density and

$$u(s, y) = \mathbb{E}^{x_s}[f(X_t)] = \int f(x) p(t, x | s, y) dx \quad (2.26)$$

for $s < t$ we get a backward-in-time differential equation for p with final state as Dirac delta distribution in space. This allows to derive PDEs concerning the probability density $\rho(s, x) = \int p(s, x | T, y) \rho(T, y) dy$, namely the Kolmogorov backward equation

$$-\partial_t \rho(s, x) = b_i(s, x) \partial_i [\rho(s, x)] + \frac{1}{2} \sigma_{ik}(s, x) \sigma_{jk}(s, x) \partial_{ij} [\rho(s, x)] . \quad (2.27)$$

Its counterpart forward-in-time is referred to as Fokker-Planck-equation;

$$\partial_t \rho(t, x) = -\partial_i [b_i(t, x) \rho(t, x)] + \frac{1}{2} \partial_{ij} [\sigma_{ik}(t, x) \sigma_{jk}(t, x) \rho(t, x)] . \quad (2.28)$$

This PDE describes the evolution of the probability density starting from the initial value $\rho(0, x) = \rho_0(x)$. The backward-in-time Fokker-Planck equation

$$\partial_t \rho(t, x) = -\partial_i [b_i(t, x) \rho(t, x)] - \frac{1}{2} \partial_{ij} [\sigma_{ik}(t, x) \sigma_{jk}(t, x) \rho(t, x)] \quad (2.29)$$

carries a minus sign in front of the diffusion coefficient, which is due to the time reversal.

Numerical solution of SDEs

In theory, there are two approaches for solving SDEs. One is based on the solution of associated PDEs, and the other based on the direct evaluation of the SDEs through numerical integration. This report uses the latter approach, where a partition $\pi = 0, t_1, \dots, t_{n_T} = T$ of the time axis with $0 < t_1 < \dots < T$ is defined to approximate the stochastic process $(X_t)_{t>0}$ solving the SDEs. The approximated stochastic process $(X_t^\pi)_{t>0}$ with respect to the partition π is said to have a strong order of convergence α if

$$\mathbb{E}[|X_T^\pi - X_T|] \leq c|\pi|^\alpha, \quad (2.30)$$

where $|\pi| = \max_i |t_{i+1} - t_i|$ and c is a constant. For instance, the simplest approximation method, the Euler-Maruyama scheme, has a strong convergence order of $1/2$, which is the stochastic counterpart to the Euler method for ordinary differential equations. A more precise approximation is the stochastic Heun method, a two-step scheme that already has a strong convergence order of 1. Depending on the required accuracy, either method was used in this thesis.

These are some of the mathematical basics that are needed in the following chapters. For a more detailed insight, e.g., including solvability of SDEs and uniqueness of solutions, the reader may have a look at books on stochastic differential equations, e.g., [Øks03, GS69].

2.3 Nelson's stochastic mechanics

In the usual practice of modeling natural phenomena, we begin by identifying a system, described by its Hamiltonian as well as its environment and interaction. It is typically assumed that the system's interaction with its environment is small compared to the effects of the system's internal dynamics and, therefore, can be treated as a perturbation. This enables us to simplify the model by reducing it to the system's Hamiltonian and gain a better understanding of the problem's main characteristics.

Nelson's 1966 paper departs from the conventional approach to modeling quantum phenomena. According to Nelson, the traditional assumption that the interaction between a quantum particle and its environment can be treated as a small perturbation does not hold in the quantum world. Instead, Nelson proposes a model of conservative Brownian motion, which posits that the interaction between a quantum particle and the universally present background field is fundamental to the quantum system's behavior. This assumption is phenomenological in that the specific details of the background noise are unknown, but only its statistical properties are relevant, as is typical in Brownian motion.⁶

Three physical assumptions define the theory:

1. The quantum particle is driven by a Brownian motion where the coupling to the stochastic background field is given by the diffusion coefficient $D = \sigma^2/2$. For macroscopic objects, the diffusion coefficient is expected to be negligible. Thus, for a particle with mass, one can assume that it is inversely proportional to the particle's mass such that $\sigma^2 = \hbar/m$.
2. A properly defined stochastic acceleration of the particle is proportional to the classical force F . This is a stochastic Newton law, also called the Nelson-Newton law, which leads to a Brownian motion with drift.
3. The diffusion is non-dissipative and may be described by a time-reversible stochastic process.

⁶One may think of some sort of background field permanently influencing the particle and, consequently, the impossibility of isolating the particle from that. If we think of this background field as a summation of infinitely unpredictable, minor disturbances, this leads to a summation of random variables. Due to the central limit theorem, this leads to a Gaussian distributed perturbation leading to the diffusive motion of the particle.

These assumptions are depicted in figure 2.4. Let us elaborate on the three points in more detail.

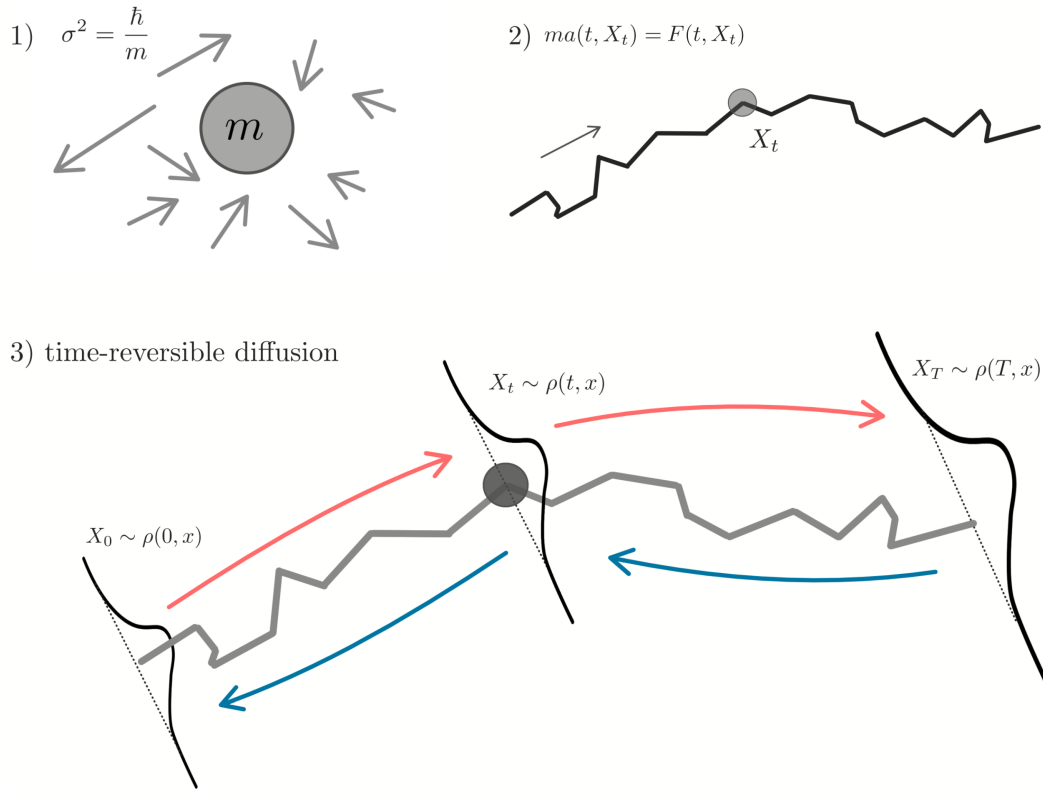


Figure 2.4: The figure illustrates the fundamental principles of stochastic mechanics. A quantum object, represented in position space with mass m , is subjected to random perturbations with a diffusion constant of $\sigma^2 = \hbar/m$ as shown in the upper left. The stochastic motion follows a modified version of Newton's law (upper right). The time reversibility of the probability density is demonstrated in the bottom of the figure.

The first point states that the particle moves randomly. The configuration variable, e.g., the particle's position, is then described by a stochastic process $(X_t)_{t>0} \subset \mathbb{R}^n$. A forward Itô SDE governs its kinematics

$$dX_t = b_+(t, X_t)dt + \sigma dW_t, \quad X_0 = x_0, \quad (2.31)$$

where $b_+(t, x)$ is the forward drift depending on the current configuration $x = X_t$, $(W_t)_{t>0}$ is a n -dimensional Wiener process forward in time, σ is the square root of the diffusion coefficient $\sigma^2 = 2D$ and x_0 is a (\mathcal{F}_0 measurable) initial value distributed according to the distribution $\rho(t = 0, x)$.⁷ Taking the conditional expectation according to equation (2.21) leads to $D_+X_t = b_+(t, X_t)$ where the velocity $(b_+(t, X_t))_{t \geq 0}$ itself is a stochastic process.

The Itô SDE (2.31) is to be read forward in time. I.e., as time moves forward the process starting at $X_0 \sim \rho(0, x)$ will be at $X_t \sim \rho(t, x)$. Most of the stochastic processes described by SDE (2.31), like the Ornstein-Uhlenbeck or the Black-Scholes process, are dissipative diffusions, where energy is transferred between the system and its environment. The density distribution will expand with time, and mathematically this is manifested by a parabolic differential equation, e.g., in the case of a Brownian motion, the probability density evolves according to the heat equation. The same applies to physical systems, where a diffusion is usually associated with a dissipative process. For example, the Einstein-Smoluchowski [Ein05, VS06] diffusion describes a steady loss of the particle's energy due

⁷Note that in this case, σ does not depend on the position or the time as it is generally possible for Itô processes. This is if we consider the quantum SDE on manifolds, as discussed later.

to constant friction in a fluid.

However, standard quantum mechanics requires the energy transfer between the system and its environment to be zero on average, i.e., it is a closed system. Additionally, the distribution in quantum mechanics has to be reversible in time with given distributions at initial and final times. Regarding stochastic mechanics, the system is open, but the system's expected energy loss is zero.

For that, Nelson introduced a time-reversed evolution equation depending on the future. Consider the example of the double slit shown in figure 2.1 problem again: the forward-in-time propagation of the stochastic process leads to a spreading of the density with its wave-like interference. When moving backward in time, it is necessary to ensure that the process ultimately leads from the observed interference pattern back to the initial configuration of the two slits. Thus, in general, the backward drift $b_-(t, x) \neq b_+(t, x)$.

Consider a backward SDE for the same stochastic process $(X_t)_{t>0}$,

$$dX_t = b_-(t, X_t)dt + \sigma dW_t^-, \quad X_T = x_T \sim \rho(T, x) \quad (2.32)$$

with increments dW_t^- , which are independent of the past, i.e., all $X_s, s < t$.⁸ The diffusion coefficient is the same as in the forward SDE due to the invariance of fluctuations with respect to t . A backward-in-time process with x_T distributed according to a marginal distribution $\rho(T, x)$ at $t = T$ should properly describe the transition to the initial distribution $\rho(0, x)$ at $t = 0$.⁹ The backward velocity is, again, the mean derivative D_- (2.22) of the stochastic process $D_-X_t = b_-(t, X_t)$.

On the level of probability distributions ρ , the forward and backward SDEs are equivalent to the two Fokker-Planck equations given by (2.28) and (2.29). The sum of the two Fokker-Planck equations gives the continuity equation

$$\partial_t \rho(t, x) + \nabla [v(t, x)\rho(t, x)] = 0, \quad (2.33)$$

with the definition

$$v(t, x) = (b_+(t, x) + b_-(t, x))/2. \quad (2.34)$$

The field $v(t, x)$ is called the *current velocity* and represents the particle's mean velocity. Furthermore, for a smooth function $f(t, x)$ we have

$$D_{\pm}f(t, X_t) = \left[\partial_t + b_{\pm}\nabla + \frac{\sigma^2}{2}\Delta \right] f(t, X_t). \quad (2.35)$$

If we set $f(t, X_t) = X_t$, use the product rule $E[gD_+f] + E[fD_-g] = D[fg]$ and integrate by parts this results in [Nel66]

$$b_- = D_-x = b_+ - \sigma^2 \frac{\nabla \rho}{\rho}. \quad (2.36)$$

Hence, it is reasonable to define a second velocity, namely the *osmotic velocity* $u(t, x)$

$$u := \frac{1}{2}(b_+ - b_-). \quad (2.37)$$

The osmotic velocity appears whenever the forward and backward equation drift velocities do not coincide. It is related to the gradient of the probability distribution by

$$u(t, x) = \frac{\sigma^2}{2} \frac{\nabla \rho(t, x)}{\rho(t, x)} = \sigma^2 \nabla R(t, x), \quad (2.38)$$

⁸Note that $\sigma dW_t^- = \sigma d_-W_t^-$ has to be read as backward Itô integral.

⁹Note that the stochastic process for *one* realization, i.e., $\omega \in \Omega$, has to describe the same path.

where we wrote the probability as $\rho(t, x) = \exp\{2R(t, x)\}$. The osmotic velocity of a particle subjected to an external force balances the osmotic force $\propto \nabla\rho$ in equilibrium [Nel66]. Equation (2.38) can also be derived by subtracting the two Fokker-Planck equations (2.28), (2.29).

The two coupled forward-backward stochastic differential equations for the position process thus read

$$dX_t = [v(t, X_t) + u(t, X_t)] dt + \sigma dW_t, \quad (2.39)$$

$$dX_t = [v(t, X_t) - u(t, X_t)] dt + \sigma dW_t^-. \quad (2.40)$$

These equations are Nelson's coupled FBSDEs and describe the kinetics of a time reversible diffusion process with two unknown velocities v and u .¹⁰ Note that this formulation describes Markov processes. Up to now, they are coupled solely through the continuity equation; therefore, some additional constraint is needed to fix them.

For that, Nelson proposed a definition of the mean acceleration (postulate 2)

$$ma(t, X_t) := \frac{m}{2} (D_+ D_- + D_- D_+) X_t = F(t, X_t). \quad (2.41)$$

which is proportional to the force F acting on the particle. The definitions of the two velocity fields v, u together with Nelson-Newton law (2.41) equation leads with

$$(D_+ D_- + D_- D_+) X_t = D_+ b_- + D_- b_+$$

to the partial differential equation

$$\partial_t v + (v \cdot \nabla)v - (u \cdot \nabla)u - \frac{\sigma^2}{2} \nabla^2 u = F(t, X_t). \quad (2.42)$$

The set of partial differential equations (2.33) and (2.42) is a system of nonlinear coupled differential equations that characterize the two needed velocity fields v and u and can be referred to as conservative Brownian motion. If we know the initial values $X_0, v(0, x)$ and $u(0, x)$ of the Markov process, the system of (2.40) and (2.33), (2.42) determines the complete process and of course its state at time t_0 . Hence, the two velocity fields are at the core of the description of stochastic mechanics.

The acceleration may be rewritten in terms of [dlPCVH15]

$$a = D_c v - D_s u \quad (2.43)$$

with a classical $D_c = \partial_t + v \cdot \nabla$ and a stochastic contribution $D_s = u \cdot \nabla + \sigma^2/2 \nabla^2$ to the derivative w.r.t. time. These definitions are used in stochastic mechanics emerging from a zero-point field [dlPCVH15] with $D_c = 1/2 (D_+ + D_-)$ as a time-symmetric average and $D_s = 1/2 (D_+ - D_-)$ as the subtraction of Nelson's mean derivatives such that

$$v = D_c X_t, \quad \text{and} \quad u = D_s X_t. \quad (2.44)$$

A similar form for the acceleration was also used by Faris [Far82].

Recovering the Schrödinger equation

The derived equations (2.33), (2.42) can be linked to quantum theory by a proper choice of σ (postulate 1). Assume that we can define another scalar field $S(t, x)$ so that

$$v(t, x) = \frac{1}{m} \nabla S(t, x). \quad (2.45)$$

¹⁰For differentiable curves as in classical mechanics we have $D_+ X_t = D_- X_t = \dot{x}(t) = v(t)$ so that the equations reduce to $\dot{X}_t = v(t, X_t)$.

The analogy to classical analytical mechanics suggests the prefactor and identifies $S(t, x)$ as the action. Note that this demands no closed flows for the two velocities when dealing with multidimensional problems.

Using the Itô formula (2.13) for $R(t, X_t)$ and $S(t, X_t)$, we obtain

$$\begin{aligned}\partial_t S &= \frac{m\sigma^4}{2}\nabla^2 R + \frac{m\sigma^4}{2}(\nabla R)^2 - \frac{1}{2m}(\nabla S)^2 - V \\ \partial_t R &= -\frac{1}{2m}\nabla^2 S - \frac{1}{m}(\nabla R) \cdot (\nabla S)\end{aligned}\tag{2.46}$$

For a more detailed account see [Nel85, PB13]. These equations recover the Madelung equations [Mad27] if the diffusion coefficient is defined as

$$\sigma^2 = \frac{\hbar}{m}.\tag{2.47}$$

The diffusion coefficient should vanish for macroscopic objects, so one can assume that it is inversely proportional to the mass of the particle.¹¹

Equations (2.46) are so-called Nelson-Madelung equations since they are the stochastic generalization of the hydrodynamic equations of classical mechanics. The quantum terms depending on the strength \hbar/m can be seen as additional stochastic forces, where for $\hbar/m \rightarrow 0$, the classical Hamilton-Jacobi equations are recovered. The first of these two equations is associated with the momentum balance, while the second corresponds to the conservation of probability.

Finally, let $\psi(t, x) = \exp\{R(t, x) + \frac{i}{\hbar}S(t, x)\}$. This definition allows us to recover the Schrödinger equation for solutions R and S of the Madelung equations [Mad27]. However, it should be noted that the Madelung equations allow for a broader range of solutions [Tak52, Wal94], and thus the transformation does not guarantee complete equivalence between the two theories. The true equivalence is only guaranteed in the case of node-free $\psi(t, x)$, which is valid for the ground state of a stationary system. Section 3.2.2 will discuss the variational principles to understand how this limitation to the ground state arises. The limited equivalence between the Madelung equations and the Schrödinger equation raises questions about the existence of Nelson diffusions for excited states and their behavior around nodes. Carlen [Car84] demonstrated that such diffusion processes exist for excited states and called them singular diffusions.

Nelson's stochastic processes are related to the Madelung equations, which can be transformed into a Schrödinger equation. It is also possible to go the other way, where the Schrödinger equation implies a system of differential equations characterizing the velocity fields and the Markov process according to (2.40). That is, Nelson's ansatz recovers a quantum mechanical system described by the Schrödinger equation but, in his case, as a generalization of classical mechanics. That this is done without referencing the Schrödinger equation is intriguing. It should be noted that the velocity fields v and u can be determined for any solution of the Schrödinger equation by

$$v = \frac{\hbar}{m}\nabla [\Im\{\ln \psi(t, x)\}]\tag{2.48}$$

$$u = \frac{\hbar}{m}\nabla [\Re\{\ln \psi(t, x)\}].\tag{2.49}$$

¹¹The definition of σ is ambiguous depending on the definition of the stochastic acceleration as shown in [Dav79]. We will stick here to the proposed definition of Nelson.

Hence, for the momentum operator, we have

$$\hat{p}\psi(t, x) = m(v - iu)\psi(t, x) \quad (2.50)$$

$$\begin{aligned} \hat{p}^2\psi(t, x) &= \hat{p}(m(v(t, x) - iu(t, x))\psi(t, x)) \\ &= [m^2(v^2(t, x) - u^2(t, x)) - \hbar m \nabla \cdot (u(t, x) - iv(t, x))] \psi(t, x). \end{aligned} \quad (2.51)$$

If the wave function has nodes, this leads to singularities in the osmotic velocity resulting in a set of points in configuration space that is never reachable for the quantum particle within finite time.

Conservative diffusion

Carlen [Car84] shows that in a given potential $V(x)$ with a corresponding finite energy solution to the Schrödinger equation, there exists a corresponding *non-dissipative* or frictionless diffusion. Hence, these are called *conservative* diffusions. This also includes singular velocity fields, which arise due to zeros in the wave function. Thus, the diffusion generator is singular in general. In terms of constant of motion, this refers to the expectation of the sum of kinetic and potential energy

$$\frac{d}{dt} \mathbb{E} [T(t, X_t) + V(t, X_t)] = 0. \quad (2.52)$$

The finite energy condition on a time interval $[0, T]$ reads

$$\int_0^T \int (u^2 + v^2) \rho(t, x) dx dt = \int_0^T |\nabla \psi(t, x)|^2 dt < \infty \quad (2.53)$$

which requires the time integral of the quantum mechanical energy to be finite.

Observables

Every (physical) theory has to comply with the outcomes in an experiment, e.g., the position $x(t)$ measurement of an object at time t . As is well-known, the wave function satisfying the Schrödinger equation is not measured itself, it is rather a tool needed to calculate an expectation of the observable, i.e., in the example above, the outcome is predicted as

$$\langle \hat{x} \rangle_{\psi(t)} = \langle \psi(t) | \hat{x} | \psi(t) \rangle \quad (2.54)$$

where we used the bracket notation. The time evolution of a particle's position $x(t)$ can be seen as a random path and is subsequently a random variable X_t for every t . It has an associated probability distribution $\rho(t, x)$ for all t . Since the wave function ψ satisfying the Schrödinger equation and ρ are related,

$$\rho(t, x) = |\psi(t, x)|^2, \quad (2.55)$$

it follows that Born's probability interpretation of the wave function is intrinsic to the picture of stochastic mechanics.

In Nelson's formalism, observables A are typically linked to position measurements, meaning that $A(X_t)$ are also stochastic variables. As a result, the measurement at time t produces an outcome associated with the probability distribution. This is also true in the Schrödinger picture, although it is described differently. In the Copenhagen interpretation, the measurement problem arises due to the localization of the wave function.

Coming back to observables in general the outcomes are not predictable in both cases,

the expected values however, coincide if $\langle \psi | \hat{A} | \psi \rangle = \langle \psi | A(x) | \psi \rangle$,

$$E[A(x)] = \int dx A(x) \rho(t, x) = \int dx A(x) |\psi(t, x)|^2 = \langle \psi | \hat{A} | \psi \rangle. \quad (2.56)$$

This is not true for all operators, in general. E.g., for the square of the momentum operator \hat{p} , we have (e.g., see [PB13])

$$\langle \psi | \hat{p} | \psi \rangle = mE[v - iu] = mE[v] \quad (2.57)$$

with $E[u] = 0$. If we define the stochastic analog of the momentum operator as $p = m(v - iu)$, we get $E[p] = E[m(v - iu)] = \langle \hat{p} \rangle_\psi$. Considering the second moment, however, one can show that

$$\langle \psi | \hat{p}^2 | \psi \rangle = m^2 E[u^2] + m^2 E[v^2], \quad (2.58)$$

where $E[p^2] = m^2 E[v^2 - u^2] \neq m^2 E[v^2 + u^2]$. Here we used that $E[v \cdot u] = 0$. The correct second moment is recovered if the momentum is defined as the real momentum $p_R = m(v + u)$, such that $E[p_R^2] = \langle \hat{p}^2 \rangle_\psi$.

Furthermore, the Schwarz inequality leads to

$$\text{Var}[X_t] \text{Var}[mu] \geq \text{Cov}^2[X_t, u] = |E[(X_t - E[X_t])(mu - E[mu])]|^2 = \hbar^2 \quad (2.59)$$

since

$$E[X_t u] = \frac{\hbar}{m} \int x \nabla \rho dx = -\frac{\hbar}{m}. \quad (2.60)$$

Hence [Gol85],

$$\text{Var}[X_t] \text{Var}[mu] \geq \frac{\hbar^2}{4}. \quad (2.61)$$

This is exactly Heisenberg's uncertainty relation which in the stochastic picture originates from the variance of the osmotic velocity that vanishes in the limit of classical systems. In addition, we see that u contributes to the total energy

$$E(t, x) = \frac{m}{2} (v^2(t, x) + u^2(t, x)) + V(t, x) \quad (2.62)$$

which can be defined by analogy to the classical energy of a particle. The average energy

$$\bar{E} = E \left[\frac{m}{2} (v^2 + u^2) + V \right] = \int dx \rho(t, x) \left[\frac{m}{2} (v^2(t, x) + u^2(t, x)) + V(x) \right] \quad (2.63)$$

is conserved in the sense that [Nel85]

$$\frac{d\bar{E}}{dt} = (\partial_t + v \cdot \nabla) \bar{E} = 0. \quad (2.64)$$

The latter equation is another form of the Hamilton-Jacobi-like equation in (2.42). Note that $\bar{E} = \langle \hat{H} \rangle_\psi$.

The stochastic energy $E(t, X_t)$ given in (2.62) along two sample paths and the numerically calculated ensemble expectation $\bar{E} = E[E(t, X_t)]$ for 10^5 realizations are shown in figure 2.5 for the harmonic oscillator in the ground state. The energy $E(t, X_t)$ along sample paths is not constant, but its expectation is. It is important to note that for a node-free probability distribution, the ensemble average $E[E]$ of the energy agrees with the time-averaged energy $\langle E \rangle_T = \lim_{T \rightarrow \infty} T^{-1} \int_0^T E(t, X_t) dt$ for one sample path. This does not hold, however, if the probability distribution has nodes. In those cases, the velocity fields are singular such

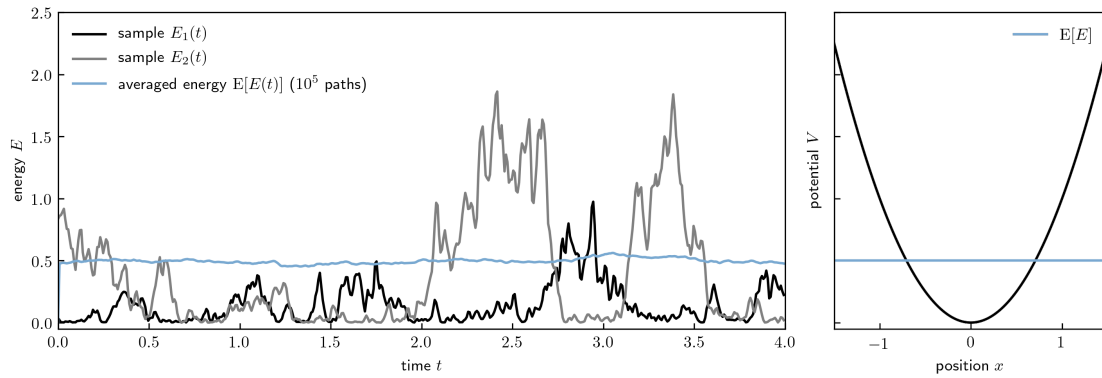


Figure 2.5: The left plot shows the energy calculated along two sample paths (grey and black) of a particle in the ground state of the Harmonic oscillator. The blue line is the numerically calculated ensemble average as a function of time. The plot on the right depicts the ground state's potential and energy expectation.

that the process cannot access the whole configuration space in general.

Equation (2.64) together with (2.38) leads to an average energy that depends on the probability density non-linearly. This contrasts classical particles described in statistical descriptions with only one velocity v . Here the term with the gradient of the probability may be seen as the additional energy needed to localize the particle [Smo86].

The expectation value of the energy is conserved, although the system is not isolated like in ordinary quantum mechanics. E.g., there it is possible to have particles bound in a potential fixed at a certain energy value with non-vanishing wave functions in regions where the particle's energy is lower than the external potential. These regions are considered (classically) forbidden since the energy law is violated. In the stochastic picture, conversely, a definition of a forbidden region is not reasonable. Due to the fluctuations - represented by the Gaussian white noise in the SDEs - the particles can overcome any finite potential barrier with a certain probability. This formalism does not contradict the description in the Hilbert space since the expectation value of the energy over time in Nelson's stochastic mechanics corresponds to the quantized values for the energy.

The role of the velocity fields

The forward (backward) velocity field gives the best possible prediction on how the configuration will change (was changing), conditional on the information of the past (future) at the current time t . In the context of Nelson, the properties of interest are the velocity fields $v(t, x)$ and $u(t, x)$. Hence, their combination in the SDE as drift terms $v \pm u$ is crucial for the movement of the considered quantum object. It is important to recall that these velocity fields are not instantaneous velocities of the stochastic process X_t . They are defined as conditional expectations, i.e., averages over the configuration variable x .

The velocities in a system with conservative diffusion can be derived from the stochastic Newton law expressed in equation (2.41), where the classical force F acts on the particle's mean acceleration. The current velocity corresponds to the expected (semiclassical) velocity, while the osmotic velocity is proportional to the gradient of the probability distribution and localizes the particle. This phenomenon is illustrated in figure 2.6, which depicts the double-slit experiment. In this experiment, the current velocity steers the particle towards the screen. The osmotic velocity is mostly perpendicular to the particle's average motion from the slits to the screen and aims to keep the particle at positions of higher likelihood. This is manifested by their expectations $E[u] = 0$ and $E[v] \neq 0$ and $E[v \cdot u] = 0$.

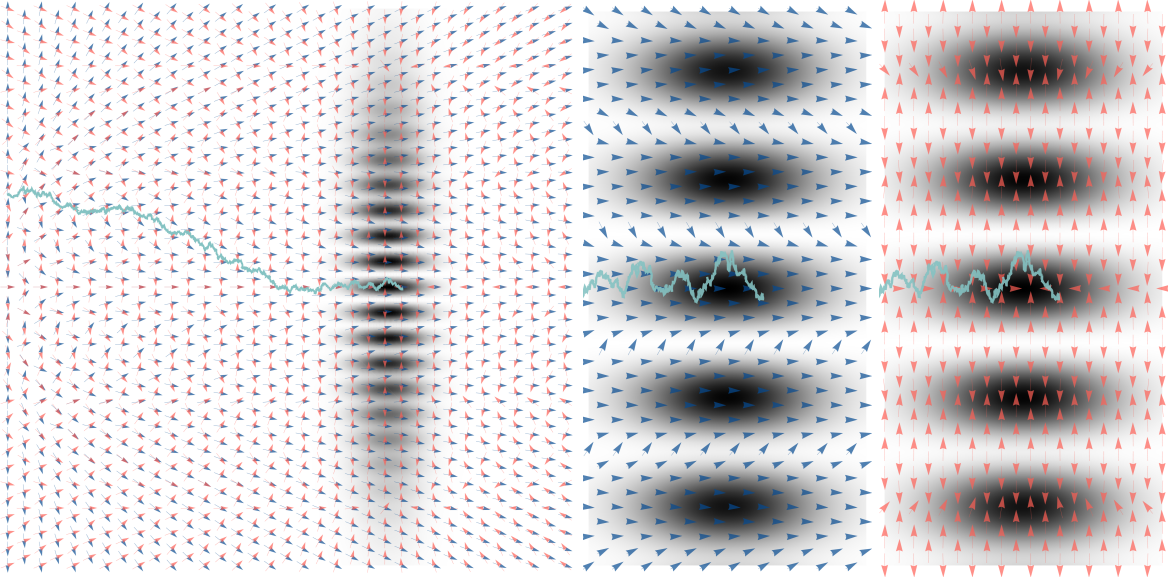


Figure 2.6: A stochastic realization (turquoise) is shown at a time $t > 0$ after passing the double slit in the big figure to the left. It is accompanied by the $2d$ vector field of v (blue arrows) and u (red arrows), as well as the current probability distribution (gray) associated with the stochastic process. The two plots on the rhs depict a detailed view of the same figure for each velocity field.

The osmotic velocity is a consequence of the diffusive motion and vanishes in the classical limit and under expectation since it is the gradient of the probability distribution. Hence, it does not contribute to the expectation value of the stochastic momentum $p = m(v + u)$. Regarding the second moments, however, the osmotic velocity is crucial for the uncertainty relations and the discrete values as given from ordinary quantum mechanics, e.g., the energy expectations as shown in figure 2.5 or the spin expectations values as discussed in section 5.3.

Furthermore, there is a subtle but important difference between $v(t, x), u(t, x)$ and $v(t, X_t), u(t, X_t)$ from a physical point of view. Consider, e.g., the current velocity v . Then $v(t, x)$ gives an estimate of the velocity, which is described for the whole configuration space x at t . It is, thus, a global field, i.e., non-local, which describes current knowledge about the particle from which predictions are made. The velocity described by $v(t, X_t)$, on the other hand, describes the mean velocity given by a conditional expectation along the stochastic trajectory X_t at t . One may argue that if, at least, only $v(t, X_t)$ has a physical meaning [Kui23] since it describes the (average) velocity of a quantum particle. The fields $v(t, x), u(t, x)$, however, can be seen as mathematical fields, e.g., comparable to the action $S(t, x)$ in the classical Hamilton-Jacobi theory, which do not represent physical properties. The same applies to the wave function $\psi(t, x)$, which is non-local and represents the best knowledge about the non-relativistic quantum system until measurement.

Applications of stochastic mechanics

The formalism of stochastic mechanics usually involves solving the Schrödinger equation and using the principles of stochastic mechanics to compute additional properties. This approach has been applied to generate and analyze sample paths of conservative diffusions described by the wave function, resulting in intriguing numerical applications as described in references such as [Zam85, MR88, NK07, NK08, KN13, Pau12]. One particularly valuable application is determining the time required for certain quantum processes. Since quantum mechanics does not have a time operator, it is impossible to directly compute the duration of a process using the expectation value of a self-adjoint operator. However, it is natural to inquire about the time it takes for a diffusion process to cross a barrier [IOY95] or move from the plane of a double-slit to the measurement screen [NK08, DDKS22]. In Section 3.2.2, we

will revisit the issue of barrier traversal, also known as tunneling times.

Multiple particles in stochastic mechanics

The theory of stochastic mechanics may be extended to include electromagnetic interaction [Nel66] and to many particles [Nel85]. For a system of multiple particles with position $x_j \in \mathbb{R}^3$ for the j th particle, the velocity fields may be defined for each particle individually so that for the j th particle, there is v_j and u_j . The probability distribution $\rho(t, x_1, x_2, \dots)$ depends on the position of all particles and fulfills the continuity equation. The relation of the osmotic velocity in (2.38) of particle j to the distribution is defined as

$$u_j = \frac{\hbar}{2m_j \rho} \nabla_j \rho. \quad (2.65)$$

If one assumes that the general probability distribution is not factorizable

$$\rho(t, x_1, x_2, \dots) \not\approx \prod_{j=1}^n \rho_j(t, x_j), \quad (2.66)$$

it follows that $u_j(t, x_1, x_2, \dots)$, i.e., the osmotic velocities of different are interdependent. This may be true even in the case of space-like separated particles. Consider, for example, the correspondence to the Hilbert space formulation of quantum mechanics. Since there is a stochastic process to each wave function ψ solving the Schrödinger equation with $\rho = |\psi|^2$, the immediate reduction of ψ in a measurement of particle j leads to an instantaneous change of the (osmotic) velocities of all other particles independent of their distances. This fact is revisited in the context of criticism on stochastic mechanics in section 2.5 and in the paradox put forward by Einstein, Podolsky, Rosen [EPR35] and Bohm [Boh51] discussed in section 6.5.

2.4 Connection to other interpretations of quantum mechanics

Stochastic mechanics is often compared to other interpretations and formalisms of quantum mechanics due to possible similarities. E.g., Pavon [Pav00] studied the relation of the stochastic trajectories to the sample paths in Feynman's path integral formulation. The following considers three other closely related formalisms in more detail.¹²

2.4.1 Hydrodynamic model

The Madelung equations occur on the path to show the correspondence of the Schrödinger equation and the conservative diffusion defined by Nelson in both ways. They are a hydrodynamical description of quantum mechanics and follow from the Schrödinger equation by the polar substitution of the wave function [Mad27] $\psi = \sqrt{\rho} e^{\frac{i}{\hbar} S}$ with amplitude $\sqrt{\rho(t, x)} = \sqrt{\psi^*(t, x)\psi(t, x)}$ and argument $1/\hbar S(t, x)$.

The Schrödinger equation then decomposes into two separate but coupled partial differential equations, its real part,

$$\partial_t S + \frac{1}{2m} (\nabla S)^2 + V - \frac{\hbar^2}{2m} \frac{\nabla^2 \sqrt{\rho}}{\sqrt{\rho}} = 0 \quad (2.67)$$

¹²Note that the stochastic quantization due to Parisi and Wu [PW81] on the other hand is a stochastic field theory that differs from the field theories suggested in the framework of stochastic mechanics, e.g., see [Nel85].

and its imaginary part

$$\partial_t \rho + \frac{1}{m} \nabla \cdot (\rho \nabla S) = 0. \quad (2.68)$$

Equation (2.68) is similar to a continuity equation, whereas (2.67) is a Hamilton-Jacobi-like equation with an additional term

$$V_Q = -\frac{\hbar^2}{2m} \frac{\nabla^2 \sqrt{\rho}}{\sqrt{\rho}} \quad (2.69)$$

depending on the inhomogeneity of the probability density distribution. This term disappears in the classical limit because of the \hbar coupling. Thus, in some theories like Bohmian mechanics, it is called the quantum potential.

The Madelung equations are considered as a hydrodynamical description of quantum mechanics where the particles are subject to a fluid [Tak55]. The velocity field is the gradient of a flow S in continuum mechanics.

2.4.2 De Broglie-Bohm mechanics

De Broglie-Bohm's theory [DB27, Boh52a, Boh52b] is often referred to as *causal interpretation* of quantum mechanics. This is because it describes a deterministic time development of a quantum object where a *local* velocity v is driving the system. This also allows for the calculation of paths of quantum systems. In contrast, however, the wave function Ψ , governed by the Schrödinger equation, is essential to the theory and serves as a *guiding wave*. Since the guiding wave is known at all times and all places, the system's dynamics may change with any change of distant other particles. Thus, the Bohm theory is also non-local.

The main difference to the Schrödinger formalism is the particle-like picture. Here, the quantum configuration may be described by some variable $x(t)$, e.g., the position, that is governed by the dynamical law

$$v(t, x(t)) = \frac{dx(t)}{dt} = \frac{\hbar}{m} \Im \left\{ \left. \frac{\nabla \Psi(t, x)}{\Psi(t, x)} \right|_{x=x(t)} \right\}. \quad (2.70)$$

The deterministic trajectories follow a path in a potential which is a combination of the classical potential V and a so-called quantum potential

$$V_Q = -\frac{\hbar^2}{2m} \frac{\nabla^2 |\psi|}{|\psi|}. \quad (2.71)$$

This quantum potential vanishes in the classical limit, i.e., it is crucial for the non-classical behavior that accounts for the quantum phenomena. The uncertainty of the measurements is then solely due to the system's initial (or final) conditions: if a particle's position is measured at the end of an experiment, its trajectory can be determined exactly, hence "causal interpretation".

The de Broglie-Bohm formalism is often thrown into one pot with Nelson's stochastic mechanics, since the velocity v in (2.70) may be rewritten as $v = \frac{1}{m} \nabla S$ for $\psi = e^{R+i/\hbar S}$. I.e., it is the same as the current velocity in stochastic mechanics. The definition of the velocity and the momentum here are motivated from the hydrodynamic formulation as in section 2.4.1 by neglecting the \hbar^2 terms in the Madelung equations (2.67) in a WKB approximation of the Schrödinger equation [BH89]. The crucial difference in stochastic mechanics is that quantum systems are represented by diffusion processes where the wave function has no fundamental role. This is established by the osmotic velocity u added to the current velocity v in stochastic mechanics. It is the quantity that makes the process "quantum", and it has a

direct connection to the quantum potential in De Broglie-Bohm's theory through

$$V_Q = -\frac{m}{2}u^2 - \frac{\hbar}{2}\nabla \cdot u. \quad (2.72)$$

Under expectation, there is

$$E[V_Q] = E\left[\frac{m}{2}u^2\right]. \quad (2.73)$$

Hence, it is related to the osmotic part of the kinetic energy which is of significance for the various Lagrangians used in the variational principles in stochastic mechanics. This is also reflected in the case of a spinning particle where the osmotic part leads to a quantum torque that causes the splitting of particle trajectories depending on their spin in a Stern-Gerlach experiment.

A more unsatisfactory interpretation in pilot-wave theory follows in the case of stationary bound eigenstates, where the argument S of the wave function is constant for some states like the eigenstates of the harmonic oscillator or the s states of the hydrogen atom. It follows that $v \propto \nabla S = 0$, and with that, the particle is at rest. This is explained by the quantum force balancing the classical force on the particle. However, this static behavior does not occur in stochastic mechanics due to the osmotic velocity. The example of the hydrogen atom is discussed in sections 3.3.2 and 4.4, including visualizations of orbitals in the stochastic interpretation.

2.4.3 Optimal transport theory

Nelson's approach is associated with the field of optimal transport theory [vR12, CGP16]. It can be seen as a transport problem with an addition of potential energy and the Fisher information. The stochastic variational problem

$$\inf_b \left\{ \int_0^T E \left[\frac{m}{2} \dot{X}_t^2 - V(X_t) \right] dt : dX_t = b_+(t, X_t)dt + \sigma dW_t, \right. \\ \left. X_0 \sim \rho(x, 0), X_T \sim \rho(x, T) \right\} \quad (2.74)$$

may be used to derive the Schrödinger equation. Here X_t is a stochastic process with fixed initial and final probability densities, $b_+(t, x)$ is the usual forward drift, W_t is a standard Brownian motion, and σ determines the strength of the noise. It is possible to show that

$$\int_0^T E \left[\frac{\dot{X}_t^2}{2} - V(X_t) \right] dt = \int_0^T E \left[\frac{m}{2} b_+(t, X_t)^2 + \sigma^2 \nabla \cdot b_+(t, X_t) - V(X_t) \right] dt. \quad (2.75)$$

The expectation in terms of the probability density function allows rewriting (2.75) into a variational problem of deterministic nature

$$\inf_{b_+} \left\{ \int_0^T \int_{\mathbb{R}^n} \left[\frac{m}{2} b_+^2 \rho + \frac{\sigma^2}{2} \nabla \cdot b_+ \rho - V \rho \right] dx dt \right\} = \\ \inf_v \left\{ \int_0^T \int_{\mathbb{R}^n} \left[\frac{m}{2} v^2 \rho - \frac{\sigma^4}{8} (\nabla \ln \rho)^2 \rho - V \rho \right] dx dt \right\} \quad (2.76)$$

with respect to the current velocity $v(t, x) = b_+(t, x) - \frac{\sigma^2}{2} \nabla \ln \rho(t, x)$ in the latter equation. The probability density function satisfies the (forward) Fokker-Planck equation with drift b or rewritten with v the continuity equation

$$\partial_t \rho + \nabla(\rho v) = 0 \quad (2.77)$$

with fixed initial and final densities given. The second term in (2.76) is also referred to as Fisher information

$$\mathbb{I} = \int_{\mathbb{R}^n} (\nabla \ln \rho)^2 \rho dx. \quad (2.78)$$

A closely related deterministic variational problem was proposed by Guerra and Morato [GM83, Mor22], where the critical point satisfies the Madelung equations, which in turn can be recast via the complex Hopf-Cole transformation $\psi = \sqrt{\rho} e^{i/\hbar S}$ into the Schrödinger equation.

2.5 Criticism on/Controversies in stochastic mechanics

The stochastic interpretation of quantum mechanics in terms of conservative diffusions is not very popular and was even considered dead by Nelson [Nel12] himself. This is mainly due to some controversies and open questions based on the underlying classical picture of stochastic mechanics, e.g., non-locality, or the formal inequivalence to the excited states predicted by the Schrödinger equation. This subsection tries to address the most prominent among them.

Non-locality

Non-locality arises in Nelson's theory, e.g., for multi-particle systems where the change of position of one particle changes the velocity fields of all other particles. Those velocity fields contain information at every point x for each time t in the form of averaged quantities defined through conditional expectations. I.e., those statistical averages cover the whole space in this model, which is resembled via the velocity fields.

Starting from wave mechanics, this is clearly visible for the connection of the drift term to the wave function, see also chapter 8 in [dlPCVH15]. E.g., for two particles, the forward velocity of particle 1 derived from the Schrödinger equation reads

$$b_1(t, x_1, x_2) = \frac{\hbar}{m} \left(\Im \left\{ \frac{\nabla_1 \Psi(t, x_1, x_2)}{\Psi(t, x_1, x_2)} \right\} \right). \quad (2.79)$$

In general, the drift term may depend on the position of the other particle. In that case, particles that are no longer interacting locally are subjected to a change in the velocity field. Non-locality is also apparent in the case of spin as will be shown later in chapter 6.4. Nelson himself [Nel85] argued that this might be due to the Markovian nature. However, in a review in 2012 [Nel12], he considered this point as a flaw in his model since the motivation of a classically motivated theory that describes quantum phenomena surely is thought to accept local interaction only.

Correlated measurements

Related to the non-locality is the controversy around successive measurements of a quantum system. As argued by Grabert [GHT79] or Nelson [Nel85] the example of two dynamically uncoupled harmonic oscillators with frequency ω_0 was considered to show that the correlation in stochastic mechanics differs from standard quantum mechanics in general. This would stand in contrast to the claim that the stochastic mechanics and standard quantum mechanics lead to the same measurement outcomes, since correlations are generally measurable.

The considered oscillators are assumed to have the same frequency ω_0 . Thus, it is easier to solve for one oscillator only. The stationary ground state of the harmonic oscillator can be

derived from the wave function

$$\Psi_0 = N \exp\left(-i\omega_0 t + \frac{\omega_0 m x^2}{2\hbar}\right), \quad (2.80)$$

and the corresponding forward (backward) SDE from Nelson read

$$dX_t = \mp\omega_0 X_t dt + \sqrt{\frac{\hbar}{m}} dW_t^\pm. \quad (2.81)$$

The solution to the forward SDE in (2.81) is known as the Ornstein-Uhlenbeck process which may be found by multiplying with $e^{-\omega_0 t}$ and integrating over time

$$X_t = \exp^{-\omega_0 t} X_0 + \sqrt{\frac{\hbar}{m}} \int_0^t e^{-\omega_0(t-s)} dW_s^+. \quad (2.82)$$

The first term in (2.82) mimics the exponential decay from the initial condition to 0 while the second part describes the randomness of the process in terms of a Brownian motion that depends on past values¹³.

The expectation value of X_t shows the exponential loss of information regarding the starting configuration $E[X_t] = e^{-\omega_0 t} E[X_0]$ with increasing t . Its correlation is

$$E[X_t X_0] = e^{-\omega_0 t} E[X_0^2]. \quad (2.83)$$

According to this example, the correlation in stochastic mechanics is exponentially decaying, which contrasts the quantum mechanical prediction from the Heisenberg picture. In the case of the two-time correlation of the quantum system, the position measurement $x(0)$ at time 0 and a successive measurement of the system's position at time $t > 0$, $x(t)$ leads to an expectation

$$\langle \hat{x}(0)\hat{x}(t) \rangle_{\psi(t)} = \langle \psi(t) | \hat{x}(0)\hat{x}(t) | \psi(t) \rangle \quad (2.84)$$

in the Heisenberg model which is periodic in time. This follows from the commutator

$$[\hat{x}(0), \hat{x}(t)] = i\hbar \frac{\sin \omega_0 t}{m\omega_0} \quad (2.85)$$

where $\hat{x}(t) = \exp(\frac{i}{\hbar}\hat{H}t)\hat{x}(0)\exp(-\frac{i}{\hbar}\hat{H}t)$. For times t as multiples of $\frac{\pi}{\omega_0}$ the commutator (2.85) vanishes and thus $\langle \hat{x}(0)\hat{x}(t) \rangle_{\psi(t)}$ is alternating between $\pm \frac{\omega_0 m}{2\hbar}$.

These results seem to be in contradiction with each other. However, in stochastic mechanics, the velocity fields depend on all the information known about the system at a certain time. This includes particularly any kind of measurement. Hence, one has to take into account the update of the knowledge about the system. In standard QM this is described by the collapse of the wave function at time $t = 0$ in form of a delta distribution. The measurement of the starting position $x_0 = X_0$ at $t = 0$ thus leads to a change of the wave function, or in terms of stochastic mechanics, to the change of the velocity field. A new process has to be considered depending on the positional measurement $X_t^{x_0}$ with new drift depending on x_0 as demonstrated in [BGS86] or [PM00]

$$\frac{x}{\tan \omega t} - \frac{x_0}{\sin \omega t}. \quad (2.86)$$

The related stochastic drift after the “exact” measurement is clearly different from the ground state solution. It finally gives the same correlation predictions as given in the Heisenberg picture above.

¹³If one wishes to solve the backward SDE of (2.81) the fluctuation term would depend on future values of the stochastic process.

The key point to consider is the non-locality of quantum mechanics and the implications of the stochastic formalism when applying the single harmonic oscillator correlation to two locally separated and uncoupled harmonic oscillators. In such cases, measuring one oscillator results in a reduction of the wave function, which in turn changes the knowledge about the second oscillator. This change in knowledge must be reflected in the stochastic mechanical distribution, as it contains the updated information on the system. This aspect differs from standard diffusions, where conditioning the probability density yields the same result for all starting distributions before a measurement. The non-local nature of the theory, as exemplified by the osmotic velocity, plays a crucial role in this process, as it changes with the measurement, implicitly altering the probability density. For a more detailed description, refer to [PM00]. A similar problem arises in the Einstein-Podolsky-Rosen-Bohm Gedankenexperiment discussed in Section 6.5, where a system of two entangled spins is considered.

Quantization and inequivalence to the Schrödinger equation

As shown by Wallström [Wal94], stochastic mechanics is not necessarily equivalent to the Schrödinger equation. This is especially true for excited states with non-vanishing angular momentum. Here the stochastic approach seems to allow for any real values, whereas the wave function requires the momentum to be quantized in order to be single valued. The constraint of single valuedness of the wave function is lost and has to be restored ad-hoc in the Madelung equations or stochastic mechanics, respectively. The first mention of this fact in the context of a hydrodynamical picture was given by Takabayashi [Tak52]. There are several proposals that solve this issue by including the Zitterbewegung of a particle [Der17] or the inclusion of the singular term in the stochastic Lagrangian of the variational principle [Kui22].

Origin of the background field

The underlying physical nature of the fluctuations is not fully understood in the picture of stochastic mechanics. Nelson's conjecture is based on the electromagnetic background field that interacts with any quantum particle [Nel85]. This is possible within this formalism since the considered systems are open as opposed to the Schrödinger picture. Other possible explanations include an interaction with a stochastic zero-point field, e.g., see [dlPCVH15]. The possible underlying picture of the fluctuations, however, will not be discussed in further detail in this thesis.

Especially the wave function has proven to be very convenient in describing quantum phenomena since it seems to comprise all information needed to describe a system. However, other mathematical structures may be used to describe quantum systems depending on the field of application. In the remainder of the thesis, we will focus on a recently derived theory of the quantum Hamilton equations.

Chapter 3

Quantum Hamilton equations

The quantum Hamilton equations are a set of coupled Forward-Backward Stochastic Differential Equations, which were derived by Köppe [KGP17] as a generalized version of the Hamilton equations of motion for quantum systems. These equations are derived using the calculus of stochastic optimal control theory and enable the description of a quantum system through kinematic and dynamic equations. Moreover, their derivation and numerical solution are independent of the Schrödinger equation, making them a valuable tool to investigate quantum systems from a different perspective.

Stochastic control theory and optimal feedback controls have been extensively studied in recent decades, which enabled the development of the stochastic Hamilton equations by drawing an analogy to the deterministic optimal control problem. To illustrate the similarities between the two approaches, the derivation of Hamilton's equation of motion from Hamilton's principle is discussed. The variational principles in stochastic mechanics are also covered. This chapter's last part is dedicated to the derivation and application of the QHE in Euclidean space.

This section follows in parts review [BP21]. An in-depth description of the maximum principles used to derive the Quantum Hamilton equations can be found in the following publications [KGP17, Köp18, BPGP19].

3.1 Variational principles in stochastic mechanics

Nelson's stochastic formalism is built upon a generalized Newton law for the mean acceleration of a particle, as expressed in equation (2.41). The expectation term becomes irrelevant in the classical limit, and Newton's second law is restored. From classical mechanics, it is known that these dynamic differential equations can be reformulated in different ways, including integral equations based on Hamilton's principle. According to this principle of stationary action, the system's dynamics are determined by the extremization of a functional known as the action,

$$S[x] = \int_0^T \mathcal{L}(x, \dot{x}, t) dt. \quad (3.1)$$

It is stationary with respect to a critical path $x = (x(t))_{t \in [0, T]}$ with fixed end points $x(0)$, $x(T)$, where the Lagrangian $\mathcal{L}(x, \dot{x}, t) = \frac{m}{2} \dot{x}^2 - V(t, x)$ contains the physical information of the system.

Short notations such as $x = x(t)$, $\dot{x} = \dot{x}(t)$, and $X = X_t$ may be used throughout this section for brevity. A functional derivative of the action with respect to x is denoted as $\delta_x S[x]$, and a vanishing functional derivative evaluated at $x = x^*$ is represented as $\delta_x S[x]|_{x=x^*} = 0$. This condition leads to the Euler-Lagrange equations:

$$\frac{\partial \mathcal{L}}{\partial x^*} - \frac{d}{dt} \frac{\partial \mathcal{L}}{\partial \dot{x}^*} = 0. \quad (3.2)$$

Variational principles and optimal control problems in the stochastic framework generally involve searching for criticality among non-differentiable paths. These principles should include classical variational principles as special cases. While a cost functional's criticality cannot control the path itself due to the noise term, it is possible to adjust the mean of the stochastic behavior, i.e., the expectation value.

In the 1980s, suggestions were made in the framework of stochastic mechanics by Yasue [Yas80, Yas81a, Yas83, Zam85] and Guerra and Morato [GM83]. The time-reversibility of the diffusion and the smoothed mean forward and backward derivatives introduced by Nelson are two important aspects here. Yasue's "Lagrangian approach" considers a cost functional of the form

$$S[X] = \mathbb{E} \left[\int_0^T \mathcal{L}(X_t, b_+, b_-, t) dt \right], \quad (3.3)$$

The suitably defined Lagrangian \mathcal{L} involves the two conditional smooth velocities $D_+X_t = b_+(t, X_t)$ and $D_-X_t = b_-(t, X_t)$ with respect to the present. Due to the stochasticity, the functional tries to extremize an expectation value w.r.t. the probability density $\rho(t, x)$ associated to $(X_t)_{t \geq 0}$ denoted by \mathbb{E} .

When considering a critical process X^* for which the action functional S is minimized, any variation of the functional around X^* by a stochastic process Z must satisfy the condition $S[X^* + Z] - S[X^*] = \mathcal{O}(|Z|)$ with fixed endpoints X_0 and X_T . This condition leads to the stochastic Euler-Lagrange equations

$$\frac{\partial \mathcal{L}}{\partial X} - D_+ \left(\frac{\partial \mathcal{L}}{\partial D_- X} \right) - D_- \left(\frac{\partial \mathcal{L}}{\partial D_+ X} \right) = 0. \quad (3.4)$$

These stochastic Euler-Lagrange equations resemble their deterministic counterparts, where $D_+X_t = D_-X_t = \dot{x}(t)$. The choice of $\mathcal{L} = \mathcal{L}_Y = \frac{1}{4}((D_+X_t)^2 + (D_-X_t)^2) - V$ for the Lagrangian leads to the Nelson-Newton law (2.41) for (3.4). Written in terms of the current and osmotic velocities, the Lagrangian, in that case, is similar to the classical one

$$\mathcal{L}_Y = T - V = \frac{m}{2}(v^2 + u^2) - V \quad (3.5)$$

with an additional kinetic energy due to the osmotic velocity.

Unlike the Yasue approach, which uses stochastic calculus, Guerra and Morato [GM83] utilized stochastic control theory. In this approach, the goal is to optimize the cost functional with respect to the smoothed forward velocity $b_+(t, X_t) = D_+X_t$ (this works similarly for D_-X_t), subject to the control equation $dX_t = b_+(t, X_t)dt + \sigma dW_t^+$, and fixed initial probability density $\rho(\cdot, 0)$ and final probability density $\rho(\cdot, T)$. Thus, this approach is based on the fluid dynamics picture. Their Lagrangian is defined as

$$\mathcal{L}_G = \mathcal{L}(X_t, D_+X_t, D_-X_t) = \frac{m}{2}D_+X_t \cdot D_-X_t - V(t, X_t), \quad (3.6)$$

where the variation of the cost functional w.r.t. a deviation from the critical velocity corresponds here to a variation of the critical drift b_+^* by a stochastic process Z . Note that although Guerra's [GM83] approach is a control problem, it still seeks to find critical points of the action, i.e., $\delta S = 0$. The quantum Hamilton-Jacobi-like Equation (2.46) for the velocities $v = \frac{1}{2}(D_+X_t + D_-X_t)$ and $u = \frac{1}{2}(D_+X_t - D_-X_t)$ is derived once again. Their derivation also states that both velocity fields are gradients of scalar functions.

It is worth noting that the Lagrangians \mathcal{L}_G and \mathcal{L}_Y differ by a sign in front of the osmotic energy when comparing their definitions,

$$\mathcal{L}_G = \frac{m}{2}(v^2 - u^2) - V. \quad (3.7)$$

The special role of this additional (kinetic) term can be explained by taking the expectation

$$E \left[\frac{m}{2} u^2(t, x) \right] = \int \left(\frac{\hbar}{2m} \frac{\nabla^2 \rho(t, x)}{\rho(t, x)} \right) \rho(t, x) dx = E[V_Q], \quad (3.8)$$

where we used equation (2.38). Thus, taking the expectation shows the equivalence between the osmotic energy and Bohm's postulated quantum potential V_Q in the pilot-wave theory [BST55]. This implies that the fluctuation of the kinetic energy with the minus sign $-\frac{m}{2}u^2$ in (3.7) can be interpreted as an additional contribution to the potential V , without the need to postulate an additional potential. Furthermore, in (3.8), the gradient of the Fisher information (functional) appears, which is used in the theory of optimal mass transport. It has been shown that the nonrelativistic evolution of quantum systems, namely the Madelung fluid equations, can be derived from the optimal interpolation of flows in the so-called Wasserstein space between fixed initial and final measures [vR12], see also Section 2.4.3. The sign of the dissipation term and the sign of the osmotic energy in the Lagrangian is explained by the underlying particle formulation. The particle formulation proposed by Yasue $T_U = mu^2/2$ describes the osmotic kinetic energy. In contrast, the formulation proposed by Guerra can be interpreted to describe fluid dynamics since $-T_U$ represents the interaction of the particle with an effective potential in the fluid [CP18].

Many of the suggested variational principles recover the Hamilton-Jacobi-like equation, including the quantum correction terms, which is one of the Madelung equations. In addition, the continuity equation is satisfied due to the assumption of time-reversibility. The quantum Hamilton equations, however, are built on two variational principles introduced by Pavon [Pav95b].

He introduced the so-called quantum Hamilton principle, which is based on two variational principles that recover both Madelung equations. The proposed method involves searching for saddle-points for the current and osmotic velocity, i.e., two controls, with the help of Lagrangian functionals. As shown in Equation (3.7), the Lagrangian is convex in v and concave in u . Pavon suggests using this Lagrangian and considers it as a zero-sum stochastic differential game for two players, where the player controlling the current velocity aims to minimize the cost, while the one controlling the osmotic part tries to maximize it. Thus, the cost functional can be written as follows

$$J_1[X^*, u^*, v^*] = \max_X \min_v \max_u E \left[\int_0^T \mathcal{L}_G(X, u, v, t) dt + S_1(X_T) \right]. \quad (3.9)$$

The stochastic controls v_t and u_t are denoted by small letters, and a given continuous function $S_1(\cdot)$ is used as a final constraint. It is worth noting that initial conditions could also be used instead of final conditions. In addition, a second variational principle based on the system's entropy is proposed. This principle relies on the configurational entropy of the system, which is defined as $S_E(t) = -\int \rho(t, x) \ln \rho(t, x) dx$. This principle aims to increase the entropy in the diffusion process,

$$J_2[X^*, u^*, v^*] = \max_X \max_v \min_u E \left[\int_0^T [-\sigma^{-2} v \cdot u] dt + R_1(X_T) \right], \quad (3.10)$$

where $R_1(\cdot)$ is a continuous given function. The saddle-point entropy production principle is related to the continuity equation and leads to a time-reversible diffusion. In the zero-sum case we have $J_1[X^*, u^*, v^*] + J_2[X^*, u^*, v^*] = 0$.

Recently, these variational principles have been reformulated as stochastic optimal control problems using the mathematical theory developed over the past few decades, including optimal feedback controls for Nelson's diffusion processes [KGP17, BPGP19, KPB⁺20, ØS14, BG10]. By analogy to the deterministic optimal control problem, where a stochas-

tic Hamiltonian is pointwise extremized, this approach allows the derivation of stochastic Hamilton equations. Additionally, these variational principles can be combined into a single principle using complex numbers, known as the quantum Hamilton principle, which Pavon introduced. This reformulation provides an elegant way to represent the quantum process more concisely, as discussed in subsection 3.2.2.

3.2 Quantum Hamilton equations

3.2.1 Deterministic optimal control: Pontryagin principle

Hamilton's principle given in (3.1) is expressed through the action functional, denoted as $S[x]$, which is defined as the integral of the Lagrangian, $\mathcal{L}(x, \dot{x}, t)$, over time from 0 to T , where the Lagrangian contains the physical information of the system. To link this to a stochastic optimal control problem, Hamilton's principle can be reformulated as a deterministic optimal control problem. This is achieved by introducing a new quantity, $v(t)$, called the control, which has the same dimension as $\dot{x}(t)$ and is restricted to a set of physically reasonable admissible controls. The action is then a functional with respect to v . The optimal control problem can be expressed as minimizing the action functional over the admissible set of controls subject to a set of differential equations that relate v and x . The optimal control problem can be written as

$$S[v] = \int_0^T \mathcal{L}(x, v, t) dt + \phi(x(T)), \quad (3.11)$$

$$\dot{x}(t) = v(t), \quad x(0) = x_0 \quad (3.12)$$

Here, the control v replaces \dot{x} in the functional, and the controlled equation relates v and x . The objective is to find the optimal control v that minimizes the action.

The control Hamiltonian \mathcal{H} is constructed similarly to the introduction of Lagrange multipliers for constraints as

$$\mathcal{H}(x, v, p, t) = p \cdot v - \mathcal{L}(x, v, t), \quad (3.13)$$

where $p(t)$ is the costate variable and the canonical momentum in Hamiltonian mechanics. Pontryagin's maximum principle states that the optimal state trajectory x^* , the optimal control v^* , and the associated costate p^* have to pointwise maximize this Hamiltonian. In other words,

$$\mathcal{H}(x^*(t), v^*(t), p^*(t), t) \geq \mathcal{H}(x^*(t), v(t), p^*(t), t) \quad (3.14)$$

for all $t \in [0, T]$ and all admissible controls v . This implies that

$$\partial_v \mathcal{H}(x^*(t), v(t), p^*(t), t) = 0. \quad (3.15)$$

In addition, there is an ordinary differential equation that has to be satisfied:

$$\dot{p} = -\partial_x \mathcal{H}(x^*, v^*, p, t) \quad p(T) = \partial_x \phi(x(T)), \quad (3.16)$$

where ϕ is a scalar function that encodes the desired terminal state. If we set $\phi(x(T)) = 0$, we obtain the case of the 'classical' Hamilton principle, where the final state is fixed, and there is no terminal condition on the costate vector. Using

$$\dot{x} = \partial_p \mathcal{H}(x, v, p, t), \quad (3.17)$$

we obtain Hamilton's equations of motion for the optimal pair of canonical coordinates

(x^*, p^*)

$$\dot{p}^* = -\partial_x \mathcal{H}|_{x=x^*} \quad (3.18)$$

$$\dot{x}^* = \partial_p \mathcal{H}|_{p=p^*}. \quad (3.19)$$

The stochastic generalization of the deterministic control problem is discussed in the following subsection.

3.2.2 Stochastic optimal control

Stochastic optimal control theory has a broad area of applications, mainly focused on finance and engineering. The connection to quantum mechanics has been outlined in a few publications recently, e.g., [BSS21, CPV17, Ohs19, LL19], and it also gained interest in theories focused on quantum gravity [Erl18, Ans22]. The quantum Hamilton equations originally derived by Köppe [KGP17] fit into the development in the last years.

Assume that we are concerned with a particle moving in d dimensions characterized by the position X_t at time $t \in [0, T]$ where $X = (X_t)_{0 \leq t \leq T}$ is a stochastic process in \mathbb{R}^d in a probability space. The stochastic process X follows Nelson's FBSDEs (2.40) with the current and osmotic velocity acting as optimal controls $v = (v_t)_{t>0}$ and $u = (u_t)_{t>0}$, respectively. At this point, there is no assumption of the Nelson-Newton law. These kinematic equations serve as constraints in the optimization problem of the quantum Hamilton principle, which combines two saddle-point principles in stochastic optimal control theory. The goal is to derive an equivalent to the Schrödinger equation using this principle.

The idea is to find the saddle-point of two functionals within optimal control theory. The first cost function

$$J_1[u^*, v^*] = \min_v \max_u \mathbb{E} \left[\int_0^T \mathcal{L}(X_t, u_t, v_t, t) dt + S(X_T) \right] \quad (3.20)$$

is based on (3.9). It is subject to Nelson's FBSDEs (2.40) for the path X_t . We seek to find solutions for the velocities u_t, v_t which are optimal feedback controls to X_t denoted by v, u , i.e.,

$$u_t = u(t, X_t), \quad v_t = v(t, X_t). \quad (3.21)$$

It is important to note that only square integrable velocities over the time interval $[0, T]$ are considered admissible controls. Because if the square of the velocity were not integrable, the functional and subsequent functionals will not be well-defined. More specifically, if the integral of the square of a velocity does not exist over the finite time interval, the optimal path would either reach a repulsive singularity, which is a contradiction, or an attractive one with an indefinitely increasing absolute value of velocity. Therefore, from a physical standpoint, this constraint ensures that only finite-energy diffusions are admissible as optimal controls [Pav95b]. This is also reflected in the Lagrange function

$$\mathcal{L}(t, X_t, u_t, v_t) = \mathcal{L}_G(t, X_t, D_+ X_t, D_- X_t) = \frac{m}{2} (v_t^2 - u_t^2) - V(t, X_t) \quad (3.22)$$

suggested by Pavon where m represents the mass of the particle. Note that the choice of the Lagrangian is related to Guerra's $\mathcal{L} = \mathcal{L}_G$, see subsection 3.1. The second variational principle

$$J_2[u^*, v^*] = \max_v \min_u \mathbb{E} \left[\int_0^T [-\sigma^{-2} v_t \cdot u_t] dt + R(X_T) \right] \quad (3.23)$$

represents a saddle-point entropy production principle. It tries to maximize the configurational entropy of the system. There are two approaches to tackling the saddle-point principles. One option is to solve both principles simultaneously by identifying a Nash equilibrium, as suggested in [ØS14]. This method requires the use of Lagrangian multipliers in problem-solving [Köp18].

Another option, as proposed by Pavon [Pav95b], is to utilize the complex quantum Hamilton principle. This approach combines the two stochastic optimal controls into a single control. The problem is reformulated using a complex velocity known as the *quantum velocity*, represented as $v^q = v - iu$, resulting in a dense formulation of the problem. The stochastic optimal control problem can then be rewritten with the cost functional

$$J[v^q] = \mathbb{E} \left[\int_0^T \mathcal{L}(t, X_t, v_t^q) dt + \Phi_T(X_T) \right] \quad (3.24)$$

which is to be extremized w.r.t. v^q [KGP17, BPGP19]. Here, the terminal value of the cost function is represented by $\Phi_T(X_T) = -i\hbar R(T, X_T) + S(T, X_T)$, where $R(\cdot, x(\cdot))$ and $S(\cdot, x(\cdot))$ are differentiable functions in x . With $\mathcal{L} = \frac{m}{2}(v_t^q)^2 - V$, the real and imaginary parts of the functional refer to J_1 and J_2 . The functional $J[v_t^q]$ is subject to the controlled stochastic differential equation

$$dX_t = v_t^q dt + \frac{1}{2}\sigma((1-i)dW_t^+ + (1+i)dW_t^-), \quad X_0 = x_0, \quad (3.25)$$

where the quantum velocity is eventually considered as feedback control (3.21). This complex SDE is obtained by combining the FBSDEs of Nelson [Pav95b]. It is called a doubly backward SDE because it involves a forward and a time-reversed Wiener process, denoted by $W_t^+, W_t^- \subset \mathbb{R}^d$, respectively. Pavon defined the quantum noise

$$dW_t^q := 1/2((1-i)dW_t^+ + (1+i)dW_t^-) \quad (3.26)$$

which has a complex covariance $dW_t^q dW_t^q = -idt$ so that the complex Itô formula for a smooth function $f(t, X_t)$ w.r.t. to SDE (3.25) reads [Pav95b]

$$df = \left[\partial_t + v_t^q \cdot \nabla - i\frac{\sigma^2}{2}\Delta \right] f dt + \partial_x f \cdot dW_t^q. \quad (3.27)$$

The corresponding integral notation to (3.25) includes both, forward and backward Itô integrals, as follows

$$X_t = x_0 + \int_0^t v_s^q ds + \frac{\sigma}{2} \int_0^t ((1-i)dW_s^+ + (1+i)dW_s^-). \quad (3.28)$$

The cost functional has a structure similar to that of Hamilton's principle, which can be rewritten as an optimal control problem. Therefore, one can proceed by analogy to the classical problem. In the deterministic case, one can use Pontryagin's maximum principle. This principle states that the control should be selected such that the associated Hamiltonian is minimized, which is necessary for the solution of the optimal control problem.

However, since we are dealing with complex numbers, we are not trying to minimize the Hamiltonian but rather find its critical points. This corresponds to finding the roots of the complex functional. Hence, it is necessary to identify an associated stochastic optimal control Hamiltonian to (3.24). E.g., from [BG10] we get

$$\mathcal{H}(t, X_t, v_t^q, P_t, \Pi_t) = -\mathcal{L}(t, X_t, v_t^q) + P_t \cdot v_t^q - \frac{1+i}{2}\sigma \text{Tr}[\Pi_t]. \quad (3.29)$$

In this particular problem, the stochastic costate variables $P_t \in \mathbb{C}^d$ and $\Pi_t \in \mathbb{C}^{d \times d}$ are intro-

duced to account for the randomness of the terms in the cost functional. These stochastic processes play the role of the costate variables or Lagrange multipliers in the deterministic case and are necessary to find the optimal trade-off considering the uncertainty of the system. The SDEs describing the evolution of P_t and Π_t can be derived based on Peng's maximum principle in stochastic control theory [Pen90] and are provided in the paper by Bahlali [BG10] for backward doubly SDEs as follows

$$dP_t = -\partial_x \mathcal{H} dt + \Pi_t dW_t^-, \quad P_T = \partial_x \Phi_T(X_T), \quad (3.30)$$

where the derivatives are taken along the optimal paths $X_t = X_t^*$, for example, $\partial_x \mathcal{H} = \partial_x \mathcal{H}(t, X_t^*, v_t^{q*}, P_t, \Pi_t)|_{x=X_t^*}$.

Equation (3.30) represents the adjoint equation, which is solved backwards in time to the constraint (3.25). It is worth noting that (1) for a non-euclidean metric space, typically a (pseudo-)Riemannian manifold, the value of σ depends on the metric and can be a function of generalized coordinates, and (2) that the SDE for P_t is backward in time according to the Hamilton function's definition and the given final conditions. One could also define a costate process $\underline{P}(t)$, which satisfies a forward SDE, depending on initial conditions given by $\Phi_0(X_0)$ in the cost function (3.24). This is in accordance with the derivation from the Nash equilibrium, where forward and backward SDEs for the costate process appear [Köp18].

The critical points of the Hamiltonian correspond to finding the roots of the complex functional with respect to v_t^q , leading to the equation

$$P_t = mv_t^q, \quad (3.31)$$

such that P_t may be associated with the quantum canonical momentum to the quantum velocity. Hence, for critical v^{q*} , we have $P_t^* = mv_t^{q*}$. From here, $P_t = P_t^*$, $v_t^q = v_t^{q*}$ and $X_t = X_t^*$ denote critical processes for brevity.

In summary, the Quantum Hamilton equations in terms of the stochastic processes X_t, P_t, Π_t are given by (3.25) and (3.30) as follows

$$\begin{aligned} dX_t &= \frac{1}{m} P_t dt + \sigma dW_t^q, \quad X_0 = x_0 \\ dP_t &= -\partial_x \mathcal{H} dt + \Pi_t dW_t^-, \quad P_T = \partial_x \Phi_T(X_T), \end{aligned} \quad (3.32)$$

where X_t denotes the stochastic process regarding the position, P_t is the costate process which can be identified with the canonical momentum and Π_t is a stochastic matrix needed to balance the noise for the pointwise extremization of the Hamiltonian. Equations (3.32) are generalized Hamilton equations of motion since in the classical limit ($\sigma, |u| \rightarrow 0$), we have a real momentum $P_t = mv_t$ with equations

$$\dot{x} = \partial_p \mathcal{H} = v, \quad \dot{P}_t = m\dot{v} = -\partial_x \mathcal{H}. \quad (3.33)$$

As we seek for a solution of the form $v_t^q = v(t, X_t)$, the identification (3.31) allows to write (3.32) with the feedback velocities (3.21) as

$$dX_t = [v(t, X_t) - iu(t, X_t)]dt + \sigma dW_t^q, \quad (3.34)$$

$$d[v(t, X_t) - iu(t, X_t)] = -\frac{1}{m} \partial_x \mathcal{H} dt + \sigma \partial_x [v(t, X_t) - iu(t, X_t)] dW_t^-, \quad (3.35)$$

with $X_0 = x_0$ and $m[v(T, X_T) - iu(T, X_T)] = \partial_x (S_T(X_T) - i\hbar R_T(X_T))$. The term for the stochastic process Π_t is identified with

$$\Pi_t = m\sigma \partial_x v_q(t, X_t) \quad (3.36)$$

following the complex Itô's formula (3.27) applied to $v_q(t, X_t)$ and comparing the terms in

front of the noise. The comparison of the drift terms in (3.35) lead to

$$\left[\partial_t + v_q \cdot \nabla - \frac{i\sigma^2}{2} \Delta \right] v_q = -\frac{1}{m} \nabla \mathcal{H} \quad (3.37)$$

where $\nabla = \partial_x$ and $v_q = v_q(t, x)$. If the potential on \mathcal{H} does not depend on the velocity, we have $\nabla \mathcal{H} = \nabla V$. Separating real and imaginary parts leads to

$$\begin{aligned} \partial_t v + (v \cdot \nabla)v - (u \cdot \nabla)u - \frac{\sigma^2}{2} \Delta u &= -\frac{1}{m} \nabla V \\ \partial_t u + (v \cdot \nabla)u + (u \cdot \nabla)v + \frac{\sigma^2}{2} \Delta v &= 0. \end{aligned} \quad (3.38)$$

The first equation is the Nelson-Newton law (2.41), while the second equation refers to the gradient of the continuity equation. Hence, the same partial differential equations for the velocities v and u can be derived by applying Itô's formula to $P(t, X_t) = mv_q(t, X_t) = P_t$ in (3.32) and comparing the drift terms.

This means that the quantum Hamilton equations (3.34)-(3.35) recover

- 1) Nelson's forward backward SDEs, and
- 2) the postulate of the mean acceleration (2.41).

In other words, the formalism allows to derive a set of kinematic and dynamical equations in terms of SDEs describing quantum systems that is equivalent to the Schrödinger equation, at least in the case of node-free functions, i.e., the ground state for stationary problems.

The QHE can also be written as real FBSDEs. The separation of the real and imaginary parts of equations (3.35) leads to

$$\begin{aligned} dX_t &= [v(t, X_t) + u(t, X_t)]dt + \sigma dW_t^+ \\ dX_t &= [v(t, X_t) - u(t, X_t)]dt + \sigma dW_t^- \\ m dv(t, X_t) &= -\partial_x V(t, X_t)dt + \sigma \partial_x [v(t, X_t)]dW_t^- \\ m du(t, X_t) &= \sigma \partial_x [u(t, X_t)]dW_t^- . \end{aligned} \quad (3.39)$$

If we add the latter two stochastic differential equations we get a backward SDE for the (real) physical momentum defined by $p(t, X_t) = m[v(t, X_t) + u(t, X_t)]$

$$dp(t, X_t) = -\partial_x V(t, X_t)dt + \sigma \partial_x p(t, X_t)dW_t^- . \quad (3.40)$$

Note that the expectations of the real momentum $p(t, x)$ agrees with the expectations in standard quantum mechanics $\mathbb{E}[p] = \langle \hat{p} \rangle$ and $\mathbb{E}[p^2] = \langle \hat{p}^2 \rangle$.

The first two equations in (3.39) are Nelson's FBSDEs that were used to derive the constraint for the control problem (3.25). The last two equations have been discussed in [KGP17, BPGP19] in more detail. However, the problem with these real equations is that they do not lead to (3.38) in the non-stationary case by a straightforward application of the Itô formula.

At this point, it should be mentioned that in a follow-up paper [Pav95a] to the quantum Hamilton principle [Pav95b], Pavon derived a set of SDEs, including one for the quantum velocity v_q by using his variational approach as follows

$$\begin{aligned} dX_t &= v_q(t, X_t)dt + \sigma dW_t^q \\ m dv_q(t, X_t) &= -\partial_x V dt + m \sigma \nabla v_q(t, X_t) dW_t^q . \end{aligned} \quad (3.41)$$

These equations are similar to (3.35) with another backward doubly SDE for the quantum velocity, i.e., forward- and backward-in-time Wiener processes occur in one SDE. Opposite to that, in Köpffe's original derivation, there is a backward Wiener process only. The difference to the present formalism is not yet fully understood.

Interestingly equations (3.41) can be derived from the same stochastic optimal control problem considered here with initial conditions $\psi_0(X_0)$ if we allow for two costate processes P_t, \underline{P}_t and two corresponding matrices $\Pi_t, \underline{\Pi}_t$ with a stochastic control Hamiltonian

$$\begin{aligned} \underline{\mathcal{H}}(t, X_t, v_t^q, P_t, \Pi_t, \underline{P}_t, \underline{\Pi}_t) = & -\mathcal{L}(t, X_t, v_t^q) + (P_t + \underline{P}_t) \cdot v_t^q \\ & - \frac{1+i}{2} \sigma \text{Tr}[\Pi_t] + \frac{1-i}{2} \sigma \text{Tr}[\underline{\Pi}_t]. \end{aligned} \quad (3.42)$$

Then we get equations (3.32) together with an additional forward SDE for

$$dP_t = -\partial_x \underline{\mathcal{H}} dt + \underline{\Pi}_t dW_t^+, \quad \underline{P}_0 = \partial_x \phi_0(X_0). \quad (3.43)$$

The SDE for P_t, \underline{P}_t can then be combined to give (3.41), which also shares similarities with finding the Nash equilibrium for the real processes [Köp18]. Hence, there are several versions of quantum Hamilton equations.

In the thesis, we will mostly refer to the version with the feedback controls (3.35). The numerical schemes based on conditional expectation [KGP17, Köp18] that solve the SDE usually consider both the stochastic processes, e.g., P_t, u_t , etc., in combination with their feedback fields $P(t, x), u(t, x)$. See also appendix B for more details on the numerical treatment. The important point here is to distinguish between the stochastic process u_t and the feedback control $u(x)$ in the numerical simulation.

Energy in the QHE

The quantum Hamilton equations describe a conservative motion. Hence, the energy expectation should match the quantized energies given in Schrödinger's theory. The Hamilton operator determines the energy of a normalized quantum state as $E_Q = \langle \psi | \hat{H} | \psi \rangle$. In contrast, the stochastic analog is described by the stochastic Hamiltonian \mathcal{H} , as shown in equation (3.42). In the optimal control problem, the Hamiltonian should be extremized pointwise. Therefore, for an optimal control v_t^q , \mathcal{H} should correspond to E_Q . In fact, if we express \mathcal{H} in terms of the feedback controls, we obtain

$$\mathcal{H} = \frac{m}{2} v_q^2(t, x) + V(t, x) + i \frac{\hbar}{2} \nabla \cdot v_q(t, x) \quad (3.44)$$

The gradient term with respect to the quantum velocity is derived from the stochastic matrices, which are given in equation (3.36).

Now, consider an eigenstate of the Hamilton operator, i.e., $\hat{H}\psi = E_Q\psi$. The phase S of the wavefunction $\psi = e^{R+iS/\hbar}$ is constant with $S = -E_Q t$ and the Hamilton-Jacobi-like equation in the Madelung equations (2.46) reduces to an equation for the system's energy

$$E_Q = -\frac{\hbar^2}{2m} \nabla^2 R(x) - \frac{\hbar^2}{2m} (\nabla R(x))^2 + V(x). \quad (3.45)$$

Consider this eigenstate ψ in stochastic mechanics. It corresponds to a stationary process with $v = 0$ such that the stochastic Hamiltonian (3.44) is real with

$$\mathcal{H} = -\frac{m}{2} u^2(x) + V(x) - \frac{\hbar}{2} \nabla \cdot u(x). \quad (3.46)$$

Using $u = \hbar \nabla R / m$ we end up with (3.45). Hence, the stochastic optimal control Hamiltonian is constant for a critical process $(X_t, u(X_t))$ if the corresponding quantum state is an eigenstate of the Hamilton operator. Then, we have $E_Q = \mathcal{H}$. It should be noted that along any stochastic realization $X_t(\omega)$, equation (3.46) is constant. This is different from the general case where the stochastic theory provides equality for the classical Hamiltonian $H_c = m/2[v^2(t, x) + u^2(t, x)] + V(t, x)$ such that under expectation, we have $E_Q = \mathbb{E}[H_c]$. The difference is due to the sign in front of the osmotic kinetic energy and the additional

gradient term of the osmotic velocity.

Semiclassical limit

At first glance, the drift terms in the momentum equations of (3.35) or (3.32) appear to depict the motion of a classical point particle in a force field. Hence, one may be tempted to conclude that these equations only contain classical motion with some added noise, whereas in hydrodynamics (Section 2.4.1) or in the theory of Bohm (Section 2.4.2), a quantum potential occurs. So the question is: What makes these QHE “quantum”?

To understand the quantum nature of these equations, one can examine the stochastic optimal control problem where the classical Lagrangian is modified to include the osmotic velocity. The diffusive part of the kinetic energy in this formulation corresponds to the quantum potential (2.71) under expectation. The QHE (3.32) with the Itô formula lead to (3.37), where the real part obeys

$$(\partial_t + (v \cdot \nabla))v - (u \cdot \nabla + \frac{\sigma^2}{2} \nabla^2)u = -\frac{1}{m} \nabla V. \quad (3.47)$$

Note that the equation above is $D_c v - D_s u = -1/m \nabla V$. Rearranging leads to

$$(\partial_t + (v \cdot \nabla))v = -\frac{1}{m} \nabla V + (u \cdot \nabla + \frac{\sigma^2}{2} \nabla^2)u \quad (3.48)$$

Thus, using the classical definition of the total time derivative $d_{cl}/dt = \partial_t + v \cdot \nabla$ with the current velocity v , we can define an effective potential

$$V_{\text{eff}} = V - \frac{m}{2} u^2 - \frac{\hbar}{2} \nabla \cdot u \quad (3.49)$$

so that equation (3.48) may be written as

$$m \frac{d_{cl} v}{dt} = -\frac{1}{m} \nabla V_{\text{eff}}. \quad (3.50)$$

This effective potential incorporates the osmotic velocity and is analogous to the potential in the pilot-wave theory proposed by Bohm, $V_{\text{eff}} = V + V_Q$. Hence, the osmotic velocity implicitly accounts for the quantum behavior in the QHE as in (3.35). Since the osmotic velocity is the gradient of the probability, any non-trivial initial distribution leads to quantum effects that are driven by the osmotic velocity.

Stationary systems

Stationary systems refer to time-independent distributions $\rho(x)$. Hence, one of the two FB-SDEs for X_t can be omitted since it inherits no additional information on the process. The quantum Hamilton equations can be derived from the saddle point principle J_1 since $v = 0$ for the ground state [KGP17] and reduce to

$$dX_t = u(t, X_t)dt + \sigma dW_t^+ \quad (3.51)$$

$$m du(t, X_t) = -\partial_x V(t, X_t)dt + \sigma \partial_x [u(t, X_t)] dW_t^- . \quad (3.52)$$

They are easier to solve and can be used to numerically determine the ground state of a quantum state. As already stated, the ground state wave functions are node-free; thus, the corresponding diffusions are non-singular. The excited states can be determined with the help of partner potentials calculated from the node-free states [Gri91, KGP18]. For example, consider a ground state solution $u_0(x)$ to a given potential $V_0(x)$. The first partner potential reads $V_1(x) = V_0(x) - \hbar \partial_x u_0(x)$. The solution $u_1(x)$ w.r.t. to potential $V_1(x)$ is again a ground state to $V_1(x)$ with expected energy E_1 matching the energy of the first excited

state when using the Schrödinger equation.¹ The following excited energy states can then be determined iteratively to the potentials $V_{n+1}(x) = V_n(x) - \hbar \partial_x u_n(x)$. This scheme is valid for unidimensional problems and can be extended to multiple dimensions [BPGP19]. This can be used to calculate excited states, e.g., for the hydrogen atom (see section 4.4) or the spin eigenstates (see section 5.3).

Concluding remarks

The QHE equations offer a direct method for describing quantum systems in phase space without resorting to non-linear partial differential equations like (2.41). Equation (3.33) confirms that the generalization of Hamilton's equations of motion to stochastic mechanics holds for the QHE. While classical mechanics predicts the same outcomes as, for example, Hamilton-Jacobi theory, it does so from a different perspective. Given the analogy between the derivation of QHE and classical Hamilton equations, we can argue that the latter can be regarded as a special case of (3.32). Notably, we can draw conceptual parallels between classical and quantum mechanics based on their mathematical formulations. For instance, while the Hamilton-Jacobi equation corresponds to the Schrödinger equation, the classical action principle corresponds to Pavon's quantum Hamilton principle. Consequently, the quantum Hamilton equations represent the stochastic generalization of their classical counterparts. Each set of equations can be independently solved within their respective frameworks, while being associated with one another.

The departure of the stochastic formalism from the standard theory in quantum mechanics allows to consider systems from a different perspective [NK08, IOY95, Pau12], especially in areas such as tunneling times, dynamics of quantum systems, and non-equilibrium systems. The theory of QHE enhances the formalisms in the stochastic picture. They have been applied to some systems, including the harmonic oscillator [KGP17, KPB⁺20], the double-well potential [KPGP18] or the two-body problem [BPGP19]. It was shown that the QHE can be solved by directly evaluating the SDE without taking a detour to the Schrödinger equation. The results have been used to analyze tunneling time distributions [KPGP18], e.g., and the theory was also extended to include the determination of excited states [BPGP19]. Currently, a disadvantage of the formalism is rooted in the complexity of the numerical formalism used to solve high dimensional quantum systems and the lack of a reliable algorithm for non-stationary systems. Additionally, the theory in its current form can only be applied to pure quantum states, i.e., an extension to mixed states is needed [GL81, JP84]. This is still a work in progress.

3.3 Examples

3.3.1 Harmonic oscillator

The problem of the stationary one-dimensional harmonic oscillator with potential $V_0(x) = \frac{m\omega^2}{2}x^2$ leads to QHE for the stochastic processes X_t and u_t , which are described by the coupled FBSDEs given by

$$\begin{aligned} dX_t &= u(X_t)dt + \sigma dW_t^+ \\ du_t &= -\omega^2 X_t dt + \Pi_t dW_t^- . \end{aligned} \tag{3.53}$$

Here, the current velocity v_t is zero. Taking the expectation values of (3.53), the averages $X_t^{\text{cl}} = E[X_t]$ and $u_t^{\text{cl}} = E[u_t]$ follow classical paths. In other words, if (X_t, u_t) is a solution, then $(X_t + X_t^{\text{cl}}, u_t + u_t^{\text{cl}})$ is also a solution. This is similar to the coherent states for the quantum harmonic oscillator. The coupled FBSDEs can be solved numerically using an

¹The actual excited state which corresponds to a singular diffusion is calculated by application of an operator [KPGP18].

iterative scheme to determine $u(x)$. This scheme includes a forward-backward integration of (3.53) such that each X_t has an associated u_t . The solution can also be found analytically using the Itô formula. Both methods lead to the ground state solution $u_0(x) = -\omega x$, denoted by index 0. To plot the feedback control over all realizations and time steps w.r.t. x , we use

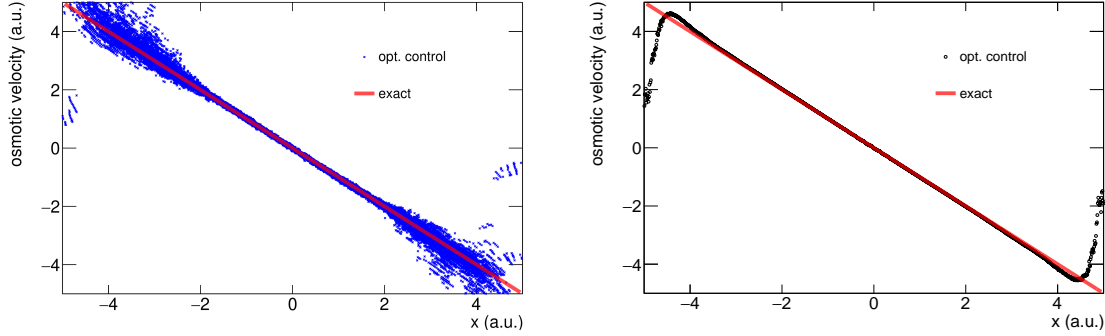


Figure 3.1: The plot displays the numerical solution for the ground state of the harmonic oscillator, using a solution scheme for a backward SDE [BD07], see appendix B. In the left plot, the stochastic control $u_{0,t}$ associated with the current position $X_{0,t}$ is depicted in blue, which is calculated from the stochastic backward integration for an iteration close to convergence. The right plot shows the averaged osmotic velocity as a feedback control $u_0(x)$ of position x . The exact solution is depicted in red in both plots.

the iterative solution of the QHE (3.53). This yields stochastic processes for each realization ω_i at time t in the form of a pair of values $(X_t(\omega_i), u_t(\omega_i))$. We plot these values with blue crosses for 10^3 realizations over 100 time steps. After an iteration run, we average all the blue points with respect to a bin size Δx to obtain a step function for the feedback control $u(x)$. The left plot in figure 3.1 shows the iterative solution of (3.53), while the right plot shows the averaged feedback control over all realizations and time steps depending on x .

The stochastic process $X_{0,t}$ associated with $u_0(x)$ represents the ground state process, with a stationary distribution of $\rho_0(x) = Ne^{-\frac{m\omega}{\hbar}x^2}$, where N is the normalization constant. Therefore, according to Born's rule, it corresponds to the Gaussian ground state probability, which is determined by the wave function for the harmonic oscillator. The energy is calculated from the stochastic Hamiltonian for the ground state \mathcal{H}_0 given in equation (3.46) as follows,

$$E_0 = \mathcal{H}_0 = -\frac{m}{2}u_0^2 + V_0 - \frac{\hbar}{2}\nabla u_0 = \frac{\hbar}{2}\omega. \quad (3.54)$$

This result is identical to the energy expectation value of the classical Hamiltonian, i.e., $E_0 = \mathbb{E} \left[\frac{m}{2}u_0^2(x) + V_0(x) \right] = \frac{1}{2}\hbar\omega$.

In the stationary case, the excited states cannot be obtained directly from the optimal control formulation as the ground state produces the optimal control for the energy in Equation (3.46). However, it is possible to determine the complete bound spectrum using the supersymmetric construction. This well-known formalism dates back to a mathematical concept for a special type of differential equations. This construction involves adjusting the potentials to obtain partner Hamiltonians, which leads to quantized raising or lowering of the mean energy. In stochastic mechanics, this adjustment is made iteratively by modifying the partner potential V_n , which is obtained from V_{n-1} by subtracting $\hbar\partial_x u_{n-1}^0$, where u_{n-1}^0 is the ground state of the $(n-1)$ -th partner potential. For example, the first partner potential obtained from the ground state $u_0^0 = u_0 = -\omega x$ is shifted by a constant $\hbar\omega$, i.e., $V_1 = V_0 + \hbar\omega$, resulting in an averaged energy shift of $\hbar\omega$. Furthermore, the ground state solution to V_1 equals the ground state solution of V_0 as shown in Equation (3.53). The n -th

partner potential is $V_n = V_0 + n\hbar\omega$, and the corresponding mean energy is given by

$$E_n = \mathcal{H}_n = -\frac{m}{2}(u_n^0(x))^2 + V_n(x) - \frac{\hbar}{2}\partial_x u_n^0(x) = \left(\frac{1}{2} + n\right)\hbar\omega. \quad (3.55)$$

Note that the ground state solutions to the partner potential do not correspond to excited states, as they are node-free. To calculate the actual excited states of the harmonic oscillator, including nodes in the probability distribution, one can use an iterative method based on the osmotic velocities without using the wave function. The method is described in [BPGP19] from what follows

$$u_0^n(x) = u_0^{n-1}(x) + \frac{\hbar}{m} \frac{\partial_x [u_0^0(x) + u_0^{n-1}(x)]}{u_0^0(x) + u_0^{n-1}(x)}, \quad (3.56)$$

For instance, the first excited state of the original partner potential is given by

$$u_0^1(x) = -\omega x + \frac{2\hbar\omega}{m x}. \quad (3.57)$$

This drift field has a singularity at $x = 0$, which corresponds to the node of the antisymmetric wave function of the first excited state of the harmonic oscillator. Thus, by using the quantum Hamilton equations, it is possible to determine the energy spectrum and the bound states of the system in their entirety.

3.3.2 Two-body problem

Consider a quantum mechanical two-body system consisting of a proton and an electron with masses m_n and m_e and opposite charges e and $-e$. They interact through the Coulomb potential $V(r) = -\frac{e_0^2}{|r_n - r_e|}$, where r_n, r_e are the position of the nucleus and the electron and $e_0^2 = \frac{e^2}{4\pi\epsilon_0}$. In the stochastic picture, the positions of the particles are subject to random fluctuations with diffusion coefficients $\sigma_n^2 = \hbar/m_n, \sigma_e^2 = \hbar/m_e$ such that we are dealing with stochastic processes denoted by R_t^n, R_t^e .

Analogous to the Kepler problem in classical mechanics, this system possesses two Galilean symmetries: (1) translational and (2) rotational symmetry.² In terms of QHE, the first symmetry leads to the conservation of the center of mass momentum $R_t^{cm} = \frac{m_n R_t^n + m_e R_t^e}{m_n + m_e}$, i.e., $E[dR_t^{cm}] = 0$, which results in a free 3d Brownian motion with constant drift [BPGP19]. The relative coordinate $R_t = R_t^n - R_t^e$ between the nucleus and the electron, on the other hand, can be treated separately from the center of mass. This leads to stationary stochastic differential equations [BPGP19].

$$\begin{aligned} dR_t &= v_q(R_t)dt + \sqrt{\frac{\hbar}{\mu}} dW_t^+ \\ \mu dv_q(R_t) &= \frac{e^2}{4\pi\epsilon_0 |R_t|^3} R_t dt + \sqrt{\frac{\hbar}{\mu}} \nabla_R v_q(R_t) dW_t^-, \end{aligned} \quad (3.58)$$

where μ is the reduced mass and the diffusion coefficient $\sigma^2 = \hbar/\mu$. This is a quantum-mechanical version of the Kepler problem. Under expectation, the equations of motion for the relative coordinate R_t and velocity v_q are given by

$$\begin{aligned} dE[R_t] &= E[v_t^q] dt \\ \mu dE[v_t^q] &= E\left[\frac{e_0^2}{|R_t|^3} R_t\right] dt, \end{aligned} \quad (3.59)$$

which are analogous to the classical equations of motion for the Kepler problem. This cor-

²There is one more symmetry due to the Lenz-Runge vector.

response manifests Ehrenfest's theorem, which states that the time derivative of the expectation values of the position and momentum operators obey the corresponding classical equations of motion. In classical mechanics, the proton would trap the electron for zero angular momentum. However, in the quantum-mechanical version, the $3d$ fluctuations are crucial in "stabilizing" the system.

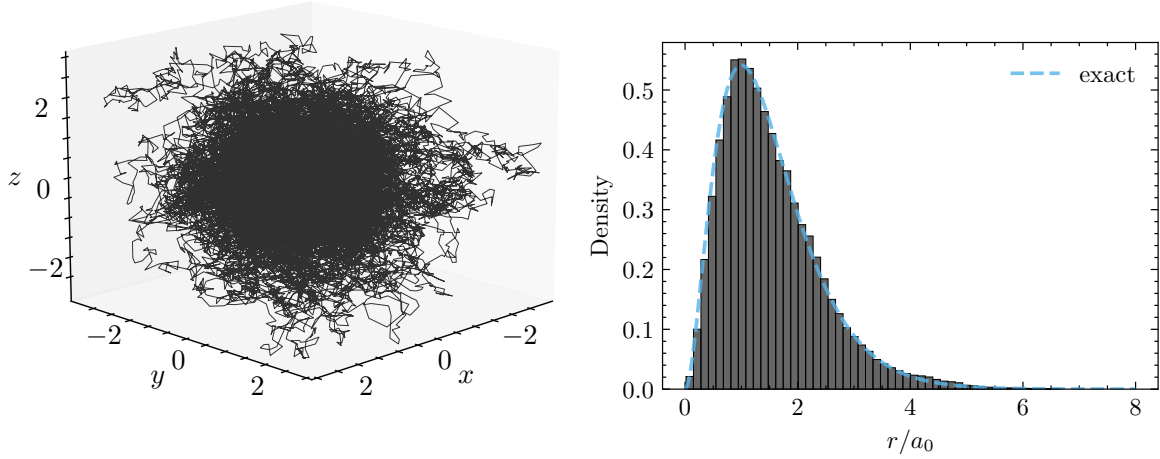


Figure 3.2: The plot on the left shows a sample path obtained from the solution to the QHE for the hydrogen atom. The corresponding normalized visiting histogram as a function of the radial distance of this path is presented on the right, depicted by gray columns. Additionally, the blue dashed line in the same graph shows the exact radial probability density that corresponds to the ground state of the Schrödinger equation.

The QHE (in Rydberg units) for the relative coordinate can be discretized according to the numerical scheme in the appendix B

$$R_{t_{i+1}}^\pi = R_{t_i}^\pi u_{t_i} \Delta t + \sqrt{2} \Delta W_{t_i}^+ \quad (3.60)$$

$$u_{t_i}^\pi = \mathbb{E}[u_{t_{i+1}}^\pi | R^\pi(t_i)] - \frac{4}{|R_{t_i}^\pi|^3} R_{t_i}^\pi \Delta t. \quad (3.61)$$

The numerical solution to equation (3.61) yields a ground state with zero angular momentum, given by the feedback control $u(R) = -\frac{\hbar}{a_0 \mu} \frac{R}{|R|}$. The corresponding average energy can be calculated from the stochastic Hamiltonian \mathcal{H}_0 given in equation (3.46) $E_0 = \mathcal{H}_0 = -\frac{\mu e_0^4}{2\hbar^2}$, or similarly from $E_0 = \mathbb{E} \left[\frac{m}{2} u_0^2(R) + V(R) \right] = -\frac{\mu e_0^4}{2\hbar^2}$. This is in agreement with the ground state following the Schrödinger theory.

The osmotic velocity allows us to visualize a sample path of the hydrogen atom in the ground state, as shown in figure 3.2. In this state, the electron moves diffusively in the ground state around the proton, corresponding to the s orbital. The most probable distance between the electron and proton is the Bohr radius a_0 . However, unlike in the Bohr model, there is no Kepler-like elliptic motion of the electron due to the lack of an angular velocity in the mean.

3.3.3 Tunneling

Quantum tunneling is the phenomenon where a particle can cross an energy barrier, despite having an energy lower than the height of the barrier. In terms of the wave function, the wave can propagate through the barrier, resulting in a probability of finding the particle inside the barrier, which is classically forbidden. However, in the stochastic description,

the concept of tunneling is not required since the system is driven by noise. For instance, consider a stationary state in a double-well potential with energy lower than the barrier height. In this case, the trajectories of the system are expected to remain most of the time within one of the two wells. Eventually, the system will hop from one well to the other, depending on the strength of the noise. The minimum amount of energy required for the state X_t to overcome the energy deficit concerning the potential barrier is provided by the noise.

One can calculate mean hopping or mean first passage times, which measure the average time required for a process to end up on the other side of the barrier. The mathematical theory involved in this calculation works with the definition of a stopping time

$$\tau_A^x = \inf\{t \geq t_0 : X_t^x \notin A\} \quad (3.62)$$

where X_t^x is the process X_t starting at $X_0 = x$ in a domain A . Note that τ_A^x is a stochastic process. The mean first passage time can be calculated as the conditional expectation, depending on the starting point of the process x [Pav14]

$$t_m(x) = E[\inf\{t \geq t_0 : X_t^x \notin A\} | X_0 = x]. \quad (3.63)$$

If one is interested in an ensemble of starting points leaving the domain A with respect to a probability distribution $\rho_0(x)$, the expected ensemble exit time is given by

$$\langle t_m(x) \rangle = \int_A t_m(x) \rho(x) dx. \quad (3.64)$$

Tunneling times are a long-standing issue in quantum mechanics and concern the time spent by particles in classically forbidden regions [Mac32]. This problem has gained new relevance with the advent of attosecond experiments in recent years. Various papers have proposed different tunneling times, which range from instantaneous tunneling [SXW⁺19] to finite time tunneling [RSRS20]. The lack of a time operator in standard quantum mechanics and the non-local behavior of the wave function allow for multiple interpretations of tunneling times, as suggested by different studies [Wig55, BL82, Baz66]. As an example, let us con-

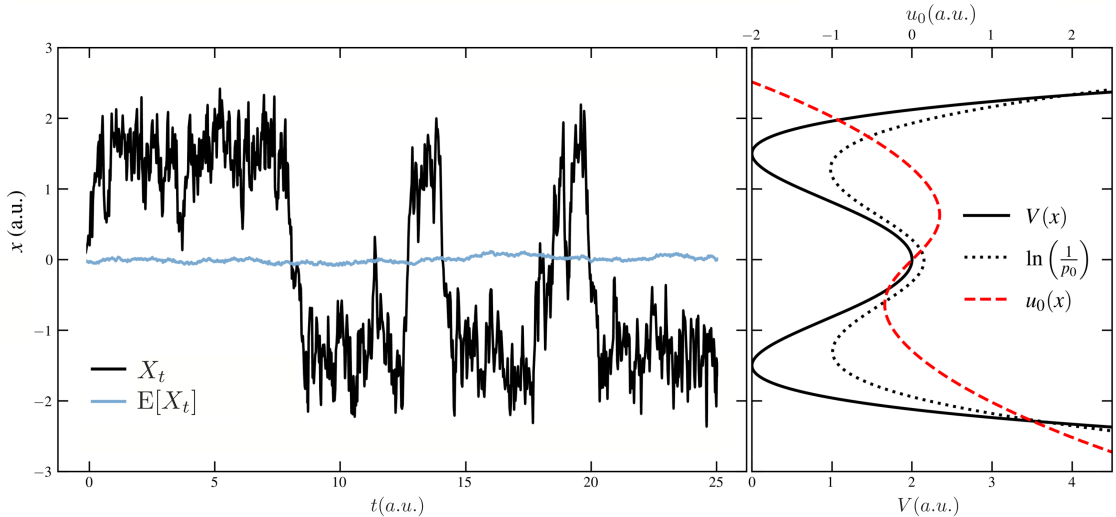


Figure 3.3: The left figure shows a sample path of the stochastic process X in the ground state of the double-well potential driven by fluctuations, while the blue line represents the ensemble mean of 10^4 paths. The graphic on the right shows the corresponding double-well potential $V(x)$ (solid black) with parameters $V_0 = 2$ and $a = 1.5$ and the osmotic velocity $u_0(x)$ (dashed red). The dotted black line depicts the 'diffusive potential' according to Kramers' theory $\ln \frac{1}{\rho_0(x)} \propto V_K(x)$ (dotted black) based on the ground state probability $\rho_0(x)$ of the system.

sider a stationary system with a quartic double-well potential given by $V(x) = \frac{V_0}{a^4}(x^2 - a^2)^2$, where V_0 is the barrier height and $\pm a$ denote the locations of the potential minima [KPGP18]. Using the quantum Hamilton equations, one can obtain the ground state osmotic velocity $u_0(x)$ and excited states numerically in analogy to the subsection 3.3.1- 3.3.2. This enables simulation of the time required for a particle starting from a position x in a well to reach a defined exit point x_t after crossing the barrier. Figure 3.3 shows a sample path for the stationary ground state of the double-well potential with $V_0 = 2$ and $a = 1.5$, exhibiting diffusive motion and transition between the two wells.

The diffusive motion observed in this system is similar to the thermally activated crossing of a barrier in Kramer's theory, where $\ln \frac{1}{\rho_0(x)}$ acts as the diffusion potential and $u_0(x) \propto -\nabla \ln \frac{1}{\rho_0(x)}$ is proportional to the negative gradient of the diffusion potential, as shown on the right-hand side of figure 3.3.

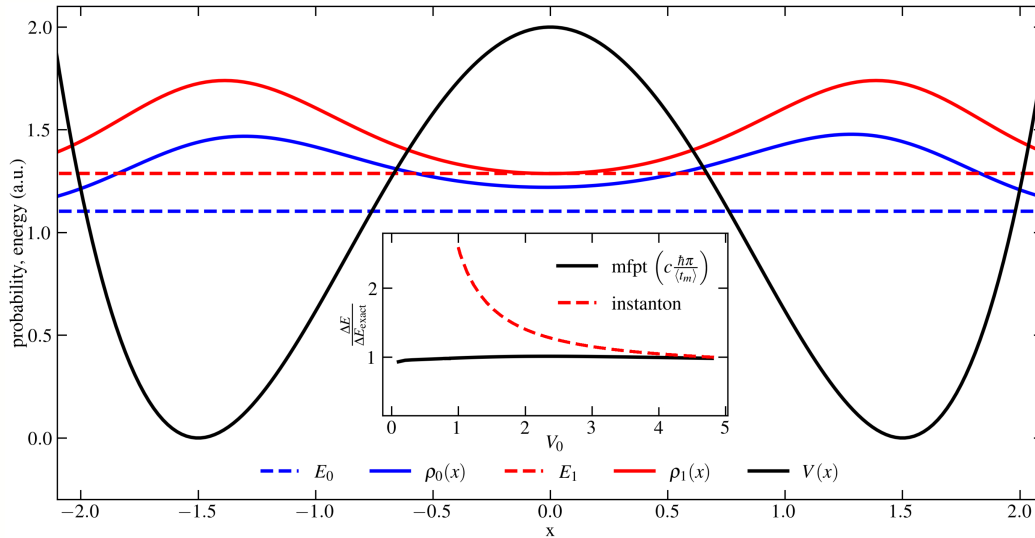


Figure 3.4: The big figure shows the ground state ρ_0 (solid blue) first excited state ρ_1 (solid red) probability, the corresponding first two mean energies E_0 (dashed black) and E_1 (dashed red) and the potential V (solid black). The inset compares the ratio of predicted and exact energy splitting $\Delta E = E_1 - E_0$ of the mean first passage time (solid black) and an instanton approximation (dashed red) depending on the barrier height V_0 .

The mean first passage time t_m for a stationary problem can be expressed in terms of probability densities only as [PB13]

$$t_m(x) = \frac{2m}{\hbar} \int_x^{x_t} \frac{dx'}{\rho_0(x')} \int_{-\infty}^{x'} \rho_0(x'') dx'', \quad (3.65)$$

where m is the particle mass, \hbar is the reduced Planck constant, and x_t is the exit point. The average $\langle t_m(x) \rangle$ can predict the energy splitting, denoted by $\Delta E := E_1 - E_0$, between the ground and first excited state, as noted by Koppe [KPGP18], where

$$\Delta E = c \frac{\hbar \pi}{\langle t_m \rangle}, \quad (3.66)$$

with $c \approx \frac{2}{\pi}$ being a constant independent of the barrier parameters. Here, E_0 and E_1 are the expected energies of the ground and first excited state, respectively. Figure 3.4 shows the energy splitting for $V_0 = 2$, $a = 1.5$, along with numerical results. The inset demonstrates that the stochastic approach provides better agreement with the exact solution than the instanton method proposed in [VZNS82], where the energy splitting due to tunneling effects is approximated starting from the harmonic ground state.

Chapter 4

Quantum Hamilton equations on manifolds

The upcoming sections focus on the extension of the Markovian stochastic process characterized by the QHE from the previous section to include a rotation degree of freedom in configuration space. The aim is to analyze the conservative diffusion as introduced by Dankel [Dan70], which results in a continuously changing random variable for the canonical angular velocities denoted by s_t , the spin of the particle. The values of the spin components are quantized in the stochastic sense, which can be measured as expectation values of the angular velocities.

Consequently, the model of a rigid rotating particle in space in the target manifold M is expanded to describe translations together with rotations in space in $\mathbb{R}^3 \times SO(3)$. This approach requires familiarity with stochastic processes on the relevant manifold to ensure that the configuration remains on the manifold. The following sections provide the necessary geometrical background to describe stochastic processes and stochastic differential equations on a manifold and derive Quantum Hamilton equations on manifolds.

This chapter primarily focuses on the mathematical background rather than physics and is, therefore, intentionally kept short. It should be seen as a preparation for the two following chapters regarding a freely spinning particle in chapter 5 and its measurements in chapter 6.

The first section provides a rough overview of stochastic processes on manifolds. Afterward, a stochastic optimal control problem on the manifold is proposed, which allows us to derive the QHE on a manifold. Finally, we apply these equations to the hydrogen atom in curvilinear coordinates in Section 3.3.2.

4.1 Stochastic differential equations on a manifold

The construction of a stochastic process on a manifold needs some intermediate steps. A few fundamental basics of differential geometry are covered in appendix C. For more details, one may see, e.g., [Éme12, Kui21b].

Nelson's FBSDEs on manifolds

A manifold M can be covered by a collection of charts. E.g., the earth is often represented in the form of flat maps where the sphere is projected onto Euclidean space via the charts. A stochastic process on M is a random variable for each t on the measurable space $(M, \mathcal{B}(M))$, and it is adapted to the (forward) filtration $(\mathcal{P}_t)_{t>0}$. If $(Z_t)_{t>0} \subset M$, one has to make sense of a stochastic differential dZ_t . Especially in the case of numerical calculations of (stochastic) processes on manifolds according to the SDE, the state is in danger of leaving the manifold.

The desired stochastic process $(Z_t)_{t>0}$ is assumed to take values in the d -dimensional manifold $M \subset \mathbb{R}^n$. In other words, we consider submanifolds M embedded in Euclidean space \mathbb{R}^n . Formally a process $(Z_t)_{t>0}$ on the manifold may be defined through a stochastic

differential equation, for example, see the construction of Elworthy [Elw82], Émery [Éme12] or Hsu [Hsu02],

$$dZ_t = B_s(t, Z_t)dt + H_i(t, Z_t) \circ dW_t^i, \quad (4.1)$$

with $B_s(t, z) \in T_zM, z \in M$ as a vector field on M , the n -dimensional Wiener process $(W_t)_{t>0} \in \mathbb{R}^n$ with increments independent of the future, \circ denoting the Stratonovich integral and the map $H_i(t, z) : \mathbb{R}^d \rightarrow T_zM$ taking the Wiener process to the tangent space of the manifold. The Stratonovich integral has the advantage of preserving an analogy to standard geometric calculus since the mid-point average ensures that the process does not “fall off” the manifold. E.g., for a smooth vector-valued function $f : M \rightarrow \mathbb{R}^k$ with drift $B_s = 0$ the projected process obeys similarly to geometric calculus

$$df(Z_t) = df[H_i(t, Z_t)] \circ dW_t^i \quad (4.2)$$

with $df[H_i(t, x)]$ as directional derivative of f at point $x \in M$ in the direction $H_i(t, x)$.

In the context of Nelson’s stochastic mechanics on a manifold, equation (4.1) refers to the forward SDE, i.e., $dZ_t = Z_{t+dt} - Z_t$, with the drift field B_s being composed of the current and osmotic velocity on M , denoted by $V_s(t, z)$ and $U_s(t, z)$ [Nel85], respectively. Consider, e.g., the current and osmotic angular velocity fields in the tangent space $\mathfrak{so}(3) = T_eSO(3)$ of the rotation group $SO(3)$. They are the key components to describe the change in orientation and may be represented as a vector $\omega_{u,v} \in \mathbb{R}^3$ acting on $a \in \mathbb{R}^3$ as $\omega_{v,u} \times a$, see, e.g., appendix D.

The problem with the extension to manifolds is that the Stratonovich form leads to $E[H_i(t, Z_t) \circ dW_t^i] \neq 0$. If we define the (forward) mean velocity $B(t, Z_t)$ of Z_t according to Nelson’s conditional expectation, it follows that

$$B(t, Z_t) = D_+Z_t = \lim_{\Delta t \rightarrow 0} \frac{1}{\Delta t} E[Z_{t+\Delta t} - Z_t | Z_t] \quad (4.3)$$

does not transform as a vector under coordinate changes. Hence, $B(t, Z_t) = D_+Z_t \neq B_s(t, Z_t)$ in equation (4.1). In the context of stochastic mechanics, this problem was encountered by Dankel [Dan70], where it was shown that the first-order definition of the stochastic mean derivative on a field does not suffice to describe a stochastic process on the manifold. The first-order derivative essentially describes parallel transport along the stochastic path. Dohrn and Guerra [DG79] later added a second-order correction to the parallel transport, which includes the notion of geodesic deviation. A more detailed introduction to the mathematical details, especially related to the stochastic processes by Nelson, can be found in the book by Nelson [Nel85], or more recently in the work by Kuipers [Kui21b].

This exemplifies that stochastic calculus on manifolds, in general, needs an extension that includes some kind of second-order geometry, see [Éme12, Hsu02]. Consider a (Riemannian) manifold M with a chart at point $z \in M$. The (first-order) velocity fields on the tangent space T_zM are denoted by v^i w.r.t. to basis vectors e_i and on the cotangent space T_z^*M by v_i w.r.t. to e^i .¹ One can define second order velocity fields on the second order (co-)tangent spaces $\tilde{T}_z^{(*)}M$. This leads to additional contributions to the velocities in the form of $v^i e_i + v^{ij} e_{ij}$ and $v_i e^i + v_{ij} e^{ij}$ with additional second-order contributions to the bases e_{ij}, e^{ij} . In Euclidean space, these second-order terms appear in the Itô formulation of SDE (4.1). For that, the SDE (4.1) and its corresponding Brownian motion defined on M will be transferred to an SDE on d -dimensional Euclidean space.

This thesis considers Riemannian manifolds, which consist of smooth manifolds M and a smooth metric tensor g . Consider a local coordinate chart with local or generalized coordinates $x = (x^1, \dots, x^d)$ where points on the manifold are represented as $z = \tilde{z}(x) \in M$. By embedding the manifold in Euclidean space, the metric tensor g in local coordinates denoted by g_{ij} is the induced positive definite metric with the corresponding Christoffel symbols of

¹The basis vectors are usually defined as $e_i = \partial_i = \partial_{x^i}$ and $e^i = dx^i$. This gives $v = v^i \partial_i \in T_zM$ and $\tilde{v} = v_i dx^i \in T_z^*M$ such that $v \cdot \tilde{v} = v^i v_i = g^{ij} v_i v_j = g_{ij} v^i v^j$.

the second kind Γ_{jk}^i . The forward Itô SDE for the corresponding stochastic process of the component X_t^i in Euclidean space then reads (cf. [Éme12])

$$dX_t^i = \left[b^i(t, X_t) - \frac{1}{2} \Gamma_{jk}^i(t, X_t) h_l^j(t, X_t) h_l^k(t, X_t) \right] dt + h_k^i(t, X_t) dW_t^k. \quad (4.4)$$

Here $b^i(t, x)$ and $h_k^i(t, x)$ are the forward drift and the diffusion tensor, respectively, in terms of the generalized coordinates. Moreover, $(W_t)_{t>0} \subset \mathbb{R}^d$ is the forward Wiener process. It is important to note that the treatment in local coordinates is only valid until the process leaves the local coordinate chart, which is relevant to the numerical investigation of these SDEs.

The additional drift term $w^i = -1/2 \Gamma_{jk}^i h_l^j h_l^k$ in equation (4.4) follows from the construction of a Brownian motion on the manifold. Here, the infinitesimal generator of the Brownian motion is half the Laplace-Beltrami operator on M as $\frac{1}{2} \Delta_M$. Defining the map h_k^i in equation (4.4) as the symmetric square root of the inverse metric times the diffusion coefficient, $h_l^j h_l^k = \sigma^2 g^{jk}$ [Ito62], yields

$$w^i = -\frac{\sigma^2}{2} \Gamma_{jk}^i g^{jk}, \quad (4.5)$$

which agrees with the additional second-order term in the Laplace-Beltrami operator C.9

$$\Delta_M f = g^{ij} \partial_{ij} f - g^{ij} \Gamma_{ij}^k \partial_k f. \quad (4.6)$$

As explained above, the terms w^i do not transform as a vector under change of coordinates [DG79, DG85] and are of second order due to the non-anticipating definition of the Itô integral. They are necessary to keep the stochastic process (or Brownian motion) on the manifold. However, they lead to non-covariant drift fields.

Consequently, they also follow by taking the expectation of the Stratonovich integral with the Wiener process. In local coordinates, there is

$$E[h_j^k(t, Z_t) \circ dW_t^j] = -\frac{1}{2} g^{ij} \Gamma_{ij}^k. \quad (4.7)$$

In general, the diffusion matrix h_k^i does not have to be related to the metric g_{ij} , especially for gravitational or relativistic Brownian motions where the metric g_{ij} may not be positive semi-definite [DG85]. In this thesis, however, the metric is always chosen such that $h_l^i h_l^j = \sigma^2 g^{ij}$. E.g., in the flat case $g^{ij} = \delta^{ij}$ in \mathbb{R}^3 leads to $\Gamma_{ij}^k = 0$ and thus to the known FBSDEs established by Nelson [Nel66].

Note that Nelson's stochastic mechanics is postulated as conservative Brownian motion, which manifests in Z_t also obeying a backward SDE [Nel85]

$$Z_t - Z_{t-dt} = dZ_t = B_s^-(t, Z_t) dt + H_i^-(t, Z_t) \circ dW_t^{-,i}, \quad (4.8)$$

with a backward drift $B_s^- (\neq B_s$ in general), a map H_i^- and a time-reversed Wiener process $W_t^- \in \mathbb{R}^d$ with increments independent of the past. Notice that the index “-” is used in the context of backward SDE, and “+” or no index is used for the SDE forward in time. The backward SDE for the generalized coordinates reads accordingly

$$dX_t^i = \left[b_-^i(t, X_t) + \frac{\sigma^2}{2} \Gamma_{jk}^i(t, X_t) g^{jk}(t, X_t) \right] dt + h_k^i(t, X_t) dW_t^{-,k}. \quad (4.9)$$

With this, one may define a second-order osmotic velocity as

$$\tilde{u}^i = u^i - \frac{\sigma^2}{2} g^{jk} \Gamma_{jk}^i \quad (4.10)$$

in addition to the usual definition of current and osmotic velocity $v^i = \frac{1}{2}(b_+^i + b_-^i)$ and $u^i = \frac{1}{2}(b_+^i - b_-^i)$. These second-order terms enter the quantum stochastic control principle where the quantum velocity $v^q = v - iu$ is replaced by $\tilde{v}^q = v - i\tilde{u}$. This is discussed in section 4.3. The following section is a refresher on Lagrangian mechanics in curvilinear coordinates in classical mechanics.

4.2 Classical dynamics on manifolds

Consider a classical particle moving on a manifold M with mass m and charge q . The particle's position is described by local coordinates $x = (x^1, \dots, x^d)$ and we seek a solution to its trajectory $(x(t))_{0 \leq t \leq T} \subset M$ with given initial and final endpoints.

In a variational treatment, the classical Lagrangian \mathcal{L} is defined on $M \times T_x M \times [0, T] \rightarrow \mathbb{R}$ and given by

$$\mathcal{L} = T - V = \frac{1}{2}g_{ij}(x)v^i v^j + qv^i A_i(t, x) - V(t, x), \quad (4.11)$$

where T is the kinetic energy, V is the scalar potential, g_{ij} is the metric tensor, v^i are the (contravariant) components of the velocity, A_i are the covariant components of the vector potential. The control problem corresponding to the action integral is given by $S[x] = \int_0^T \mathcal{L}(x, v, t) dt$. The canonical momentum is defined as

$$p_j = \frac{\partial \mathcal{L}}{\partial v^j} = g_{ij}v^i + qA_j, \quad (4.12)$$

and the velocities in terms of the momenta are given by

$$v^j = g^{ij}(p_i - qA_i). \quad (4.13)$$

Then, the classical Hamiltonian is obtained as

$$\mathcal{H}_c = v^i p_i - \mathcal{L} \quad (4.14)$$

$$= \frac{1}{2}g^{ij}(x)p_i p_j - qg^{ij}(x)p_i A_j(t, x) + \frac{q^2}{2}g^{ij}(x)A_i(t, x)A_j(t, x) + V(t, x). \quad (4.15)$$

Finally, the equations of motion are given by

$$\dot{x}^j = \frac{\partial \mathcal{H}_c}{\partial p_j} = g^{jk}(p_k - qA_k) = v^j \quad (4.16)$$

$$\dot{p}_j = -\frac{\partial \mathcal{H}_c}{\partial x^j} = -\frac{1}{2}\partial_j(g^{kl})(p_k - qA_k)(p_l - qA_l) - g^{kl}\partial_j A_k(p_l - qA_l) - \partial_j V$$

with initial conditions $x_j(0) = x_{j,0}$ and $p_j(0) = g_{ij}(x_0)v_0^i + qA_j(0, x_0)$ and where $\partial_j = \frac{\partial}{\partial x^j}$. All the derivatives should be taken with respect to $x = x(t)$ and $p = p(t)$, i.e., along the paths. The second equation rewritten in terms of the velocity ($A = 0$)

$$m\dot{v}^j + \Gamma_{kl}^j(x)v^k v^l = -\partial_j V \quad (4.17)$$

includes the fictitious forces due to the curvilinear coordinates. It should be noted that the derivative with respect to spatial variables includes curvature terms due to the metric.

4.3 Quantum Hamilton equations on manifolds

A stochastic variation approach is needed to obtain the quantum Hamilton equations for a Riemannian manifold. Among the several principles suggested in the literature, e.g., see sec-

tion 3.1, we use the straightforward generalization to manifolds based on the complex cost functional suggested by Pavon [Pav95b]. This is in analogy to the presentation in section 3. The main difference is the occurrence of the metric g_{ij} in local coordinates and the introduction of the vector field $A_j(t, x)$. Note that the charge q is included in the vector potential A_j for brevity and to avoid confusion with the quantum velocity index in this section.

The cost function of the quantum Hamilton principle established in [Pav95b] may be generalized to a manifold (in analogy to [ADG92])

$$J[v_{q,t}] = \mathbb{E} \left[\int_0^T \left(\frac{1}{2} g_{ij} v_{q,t}^i v_{q,t}^j + v_{q,t}^j A_j - V \right) dt + \Phi_T(X_T) \right]. \quad (4.18)$$

Here, $\mathbb{E}[\cdot]$ denotes, again, the ensemble average with respect to the probability distribution of the stochastic process X_t , and $\Phi_T(x)$ is a terminal cost function. The Lagrangian in the cost function is the classical one given in (4.11) with v^i replaced by the complex velocity composed of current and osmotic velocity $v_{q,t}^i = v_t^i - iu_t^i$. The quantum Hamilton principle then states that (4.18) is to be extremized with respect to the so-called quantum velocity $v_{q,t}^i$ while equation

$$dX_t^i = \left[v_{q,t}^i + i \frac{\sigma^2}{2} \Gamma_{jk}^i(X_t) g^{jk}(X_t) \right] dt + \frac{1}{2} h_k^i(X_t) \left((1-i) dW_t^{+,k} + (1+i) dW_t^{-,k} \right) \quad (4.19)$$

serves as the control equation with X_T^i distributed according to $|\Phi_T|$. The quantum velocity serves as optimal feedback control $v_{q,t} = v_q(t, X_t)$. Thus, the real components v_t^i and u_t^i are the optimal controls representing the generalized velocities associated with the stochastic process X_t in local coordinates. Note that $dX_t^i dX_t^j = -i\sigma^2 g^{ij} dt$.

For this problem, a stochastic Hamiltonian $\mathcal{H} = \mathcal{H}(t, X_t, v_{q,t}, P_t, \Pi_t)$ [Bis78, BG10] can be defined as

$$\mathcal{H} = -\frac{g_{kj}}{2} v_{q,t}^k v_{q,t}^j - A_j v_{q,t}^j + V + P_{t,j} \left(v_{q,t}^j + \frac{i}{2} \sigma^2 g^{kl} \Gamma_{kl}^j \right) - \frac{(1+i)}{2} \text{Tr}\{\Pi_t H^T\} \quad (4.20)$$

where shorthand notation is used and the matrix $H = (h_j^i)$ is introduced.² The stochastic Hamiltonian has to be extremized point-wise. In comparison to the classical equations, we see that in addition to the trace term in equation (4.20), there is

$$i P_{t,j} \sigma^2 g^{kl} \Gamma_{kl}^j / 2. \quad (4.21)$$

The term (4.21) follows from the second-order correction to the Brownian motion on a manifold and is zero in the flat case.

The stochastic processes $P_{t,j} \in \mathbb{C}^d$ and $\Pi_t \in \mathbb{C}^{d \times d}$ introduced in this study, again, satisfy corresponding backward SDEs similar to the classical Pontryagin principle for the costate. Specifically, we have

$$dP_{t,j} = -\partial_j \mathcal{H}_c dt + \Pi_{t,ij} dW_-^i \quad P_{T,j} = \partial_j \Phi(x)|_{x=X_T}. \quad (4.22)$$

The maximum principle requires that

$$P_{t,j} = g_{kj} (v_t^k - iu_t^k) + A_j, \quad (4.23)$$

which implies that $P_{t,j}$ serves as the canonical momentum in the maximum principle. Here, the real part of the momentum is related to the current velocity, given by $\text{Re}\{P_{t,j}\} = g_{kj} v_t^k + A_j$, while the osmotic velocity appears in the imaginary part, $-\text{Im}\{P_{t,j}\} = g_{kj} u_t^k$.

We are interested in finding feedback solutions $v_{q,t}^j = v_q^j(t, X_t)$. Using the complex Itô

²Recall that $h_i^i h_j^j = \sigma^2 g^{ij}$.

formula [Pav95b] for a smooth function f on the manifold, we obtain

$$df = \left[\partial_t + \left(v_{q,t}^j + \frac{i}{2} \sigma^2 g^{kl} \Gamma_{kl}^j \right) \partial_j - i \frac{\sigma^2}{2} g^{jk} \partial_{jk}^2 \right] f dt + \partial_j f h_k^j dW_t^{q,k} \quad (4.24)$$

$$= \left[\partial_t + v_q^j \partial_j - i \frac{\sigma^2}{2} \Delta \right] f dt + \partial_j f dW_t^{q,j}. \quad (4.25)$$

Then considering the feedback momentum

$$P_j(t, x) = g_{kj}(x)(v^k(t, x) - iu^k(t, x)) + A_j(t, x), \quad (4.26)$$

and applying the complex Itô formula (4.25), the feedback matrix reads

$$\Pi_{t,kl} = \frac{1+i}{2} h_l^j \partial_j (P_k). \quad (4.27)$$

Equations (4.22) and (4.23) together with Nelson's FBSDEs (4.19) are the quantum Hamilton equations. In the classical limit, the stochastic terms vanish, and the terms, including the osmotic velocity, i. e. $v_{q,t}^i = v_t^i - iu_t^i \rightarrow v_t^i$. The complex stochastic Hamiltonian \mathcal{H} reduces to the real classical Hamiltonian $\mathcal{H}_{cl} = v^j p_j - \mathcal{L}$ in equation (4.15) with $p_j = g_{ij} v^i + A_j$ and the classical equations of motion are obtained

$$\begin{aligned} dq_j &= \frac{\partial \mathcal{H}_{cl}}{\partial p_j} \\ dp_j &= -\frac{\partial \mathcal{H}_{cl}}{\partial q_j}. \end{aligned} \quad (4.28)$$

Relation to the Schrödinger equation

The equations at hand give rise to the Schrödinger equation

$$i\hbar \partial_t \psi = -\frac{\hbar^2}{2} \Delta_M \psi + V \psi \quad (4.29)$$

on the manifold M with Δ_M as the Laplace-Beltrami operator. Note that Δ_M , as written here, includes the system's structure through the metric g . E.g., for a particle with mass m we define $g_{ij} = m\delta_{ij}$ so that $\Delta_M = \delta^{ij}/m\partial_{ij}$. In general, $-\hbar^2 \Delta_M$ should be replaced by $g^{kl}(-i\hbar \nabla_k - A_k)(-i\hbar \nabla_l - A_l)$ [Dan70]. The vector potential, $A = 0$, is set to zero for brevity.

The osmotic and current velocity associated to ψ are calculated as

$$u^j = \sigma^2 g^{kj} \Re\{\partial_k \psi / \psi\} \quad \text{and} \quad v^j = \sigma^2 g^{kj} \Im\{\partial_k \psi / \psi\}. \quad (4.30)$$

I.e., with $\sigma^2 = \hbar$ for the quantum momentum³

$$P_j = g_{kj}(v^j - iu^j) = (P_j^v - iP_j^u) = -i\hbar \frac{\partial_j \psi}{\psi}. \quad (4.31)$$

Putting this into the rhs of equation (4.29) gives

$$\frac{1}{\psi} \left(-\frac{\hbar^2}{2} \Delta_M \psi + V \psi \right) = \frac{1}{2} g^{kj} P_k P_j - \frac{i\hbar}{2} g^{kl} \Gamma_{kl}^j P_j + \frac{i\hbar}{2} g^{kj} \partial_k P_j + V. \quad (4.32)$$

If we compare this with the stochastic Hamiltonian (4.20) with the feedback processes $P(t, x)$,

³As written here, σ^2 is a constant, while the diffusion coefficient matrix is given by $\sigma^2 g^{-1}$.

$\Pi(t, x)$ from equations (4.26) and (4.27) we arrive at (4.32), i.e.,

$$\mathcal{H}(t, x, v_q(t, x, P), P(t, x), \Pi(t, x)) = \frac{1}{\psi} \left(-\frac{\hbar^2}{2} \Delta_M \psi + V \psi \right). \quad (4.33)$$

Hence, there is a direct relation between the Hamilton operator \hat{H} on the manifold to the stochastic Hamiltonian. Moreover, the terms in $\mathcal{H}(t, x, v_q(t, x, P), P(t, x), \Pi(t, x))$ involving the imaginary unit i correspond to the second-order terms outlined in equation (39) of reference [HZ23]. These terms are introduced to derive a similar version stochastic Hamilton's equations from the so-called stochastic geometric mechanics.

Again, if ψ is in an eigenstate, i.e., $-\frac{\hbar^2}{2} \Delta_M \psi + V \psi = E_Q \psi$, the stochastic Hamiltonian along the optimal feedback controls is constant, $\mathcal{H} = E_Q$, contrary to the stochastic energy

$$E(t, X_t) = \frac{g^{ij}}{2} (P_j^v(t, X_t) + P_j^u(t, X_t))(P_i^v(t, X_t) + P_i^u(t, X_t)) + V(t, X_t), \quad (4.34)$$

where $E[E(t, X_t)] = E_Q$.

The QHE (4.22) are closely related to the Schrödinger equation due to the close relationship between the stochastic Hamiltonian and the Schrödinger equation. Consider the drift term in the momentum equations (4.22),

$$-\partial_i \mathcal{H} = -\partial_i V + \frac{1}{2} \partial_i (g^{kj}) g^{kl} g^{jm} P_l P_m - \frac{i}{2} \hbar \left[\partial_i \left(g^{kl} \Gamma_{kl}^j \right) P_j + (\partial_i g^{kl}) \partial_k P_l \right]. \quad (4.35)$$

The classical equations in curvilinear coordinates contain the first two terms on the right-hand side of the equation, which can be regarded as an effective potential when taken together. Section 5.3 demonstrates this for the spinning particle, while Section 4.4 explores their application in the context of the hydrogen atom, where these terms contribute to the effective potential associated with the angular momentum expectations. Finally, it is worth noting that the terms multiplied by \hbar vanish in the classical limit.

Assuming the existence of scalar potentials S and R such that the feedback processes $P_j^v = \partial_j S$ and $P_j^u = \hbar \partial_j R$ for $P_j = P_j^v - iP_j^u$, the drift term of the complex Itô formula (4.25) applied to $P_j = \partial_j S - i\hbar \partial_j R$ should be equal to equation (4.35). By separating the real and imaginary parts, we obtain a set of coupled partial differential equations for the fields S and R .

To establish the connection between the quantum hydrodynamics equations and the Madelung equations, we apply ∂_j to (4.29), where ψ is replaced by (4.31). This yields the same set of partial differential equations as the approach using the complex Itô formula, as both methods lead to the Madelung equations. A detailed derivation of these partial differential equations on the manifold in local coordinates can be found in section 3 of [Dan70]. However, the connection between these formalisms is only established if the momentum fields are gradients of scalar fields, for example, if $\partial_j P_i^u = \hbar \partial_j \partial_i R = \hbar \partial_i \partial_j R = \partial_i P_j^u$.

The following section will apply the derived quantum Hamilton equations in curvilinear coordinates, specifically spherical coordinates. Finally, we will use them to describe the hydrogen atom by utilizing the rotation symmetry, which allows a solution to the two-body problem similar to the Schrödinger theory. This concludes this relatively dry chapter on stochastic quantum mechanics on manifolds.

4.4 Example: Hydrogen atom

The hydrogen atom was discussed in section 3.3.2 using momentum conservation, which allowed to separate the motion of the center of mass from the relative coordinate R_t . In analogy to classical mechanics, this two-body problem can be further simplified under a coordinate transformation due to the isotropy of the system, which refers to the conservation

of the total angular momentum

$$L_t^{\text{total}} = \sum_i m^i R_t^i \times (v^i(t, R_t^i) + u^i(t, R_t^i))$$

under expectation $E[dL_t^{\text{total}}] = 0$, where R_t^i denotes the position of particle i . This allows us to further reduce the dimension of the two-body problem, where the angular part can be treated separately from the radial part.

We may introduce spherical coordinates $(r, \vartheta, \varphi) \in (0, \infty) \times (-\pi/2, \pi/2) \times [0, 2\pi)$ with corresponding stochastic processes $(X_t^1, X_t^2, X_t^3) = (r_t, \Theta_t, \Phi_t) = (r(R_t), \vartheta(R_t), \varphi(R_t))$ in local coordinates. The induced metric g is diagonal with $g_{rr} = \mu, g_{\vartheta\vartheta} = \mu r^2, g_{\varphi\varphi} = \mu r^2 \sin^2 \vartheta$ such that the matrix

$$H = (h_k^j) = \begin{pmatrix} \tilde{\sigma} & 0 & 0 \\ 0 & \frac{\tilde{\sigma}}{r} & 0 \\ 0 & 0 & \frac{\tilde{\sigma}}{r \sin \vartheta} \end{pmatrix} \quad (4.36)$$

with the diffusion coefficient $\tilde{\sigma} = \sqrt{\hbar/\mu}$. This leads to forward (backward) SDE according to (4.4) as follows,

$$\begin{aligned} dr_t &= \left(v^r \pm u^r \pm \frac{\hbar}{\mu r_t} \right) dt + \tilde{\sigma} dW_{\pm,t}^r \\ d\Theta_t &= \left(v^\vartheta \pm u^\vartheta \pm \frac{\hbar}{2\mu r_t^2} \cot \Theta_t \right) dt + \frac{\tilde{\sigma}}{r_t} dW_{\pm,t}^\vartheta \\ d\Phi_t &= (v^\varphi \pm u^\varphi) dt + \frac{\tilde{\sigma}}{r_t \sin \Theta_t} dW_{\pm,t}^\varphi. \end{aligned} \quad (4.37)$$

Equations (4.37) contain additional drift terms that are a consequence of constructing the Brownian motion in curvilinear coordinates following section 4.1. For example, the term $\hbar/\mu r_t$ induces a probabilistic drift that arises from fluctuations in three dimensions. These fluctuations tend to push the particle away from the center $r = 0$.

Generally, these drift terms emerge due to the non-zero variance of the stochastic process associated with the particle's position in the mean square limit. Consequently, they vanish in the classical limit. As a result of these random fluctuations, the ground state of the hydrogen atom is stable in the stochastic picture.

The stochastic optimal control problem discussed in section 4.3 leads to the definition of a stochastic Hamiltonian

$$\mathcal{H} = \frac{1}{2\mu} \left(P_r^2 + \frac{1}{r_t^2} P_\vartheta^2 + \frac{1}{r_t^2 \sin^2 \Theta_t} P_\varphi^2 + i \frac{\hbar}{r_t^2} \cot \Theta_t P_\vartheta + i \frac{2\hbar}{r_t} P_r \right) + \frac{e_0^2}{r_t} + \frac{1+i}{2} \text{Tr}[\Pi_t H^T], \quad (4.38)$$

where we used shorthand notation $P_j = P_{t,j}$ for the stochastic processes. This Hamiltonian incorporates the classical terms, including the dependency on the metric as well as non-classical terms involving \hbar . The comparison to the Laplace operator in spherical coordinates

$$\Delta = \left[\partial_r^2 + \frac{1}{r^2} \partial_\vartheta^2 + \frac{\cot \vartheta}{r^2} \partial_\vartheta + \frac{1}{r^2 \sin^2 \vartheta} \partial_\varphi^2 + \frac{2}{r} \partial_r \right] \quad (4.39)$$

shows that the two approaches exhibit similarities. In particular, the non-classical terms with \hbar are essential for the correspondence between P_j and $-i\hbar\partial_j$ to hold. This connection is critical for understanding the relationship between stochastic and quantum mechanics, as it emphasizes the importance of fluctuation terms in describing physical systems.

The Hamiltonian given in equation (4.38) is associated with backward stochastic differ-

ential equations (4.22) for the costate process $P_t = (P_r, P_\vartheta, P_\phi)$

$$\begin{aligned} dP_r &= \left(-\frac{e_0^2}{r_t^2} + i\frac{\hbar P_r}{r_t^2} + \frac{1}{\mu r_t^3} \left[P_\vartheta^2 + \frac{P_\varphi^2}{\sin^2 \Theta_t} + i\hbar \cot \Theta_t P_\vartheta \right] + i\frac{\tilde{\sigma}}{r_t^2} \left[\Pi_{\vartheta\vartheta} + \frac{\Pi_{\varphi\varphi}}{\sin \Theta_t} \right] \right) dt \\ &\quad + (\Pi_t dW_t^-)_r \\ dP_\vartheta &= \frac{1}{\mu r_t^2 \sin^2 \Theta_t} \left(\cot \Theta_t P_\varphi^2 + i\frac{\hbar}{2} P_\vartheta + i r_t \tilde{\sigma} \cot \Theta_t \Pi_{\varphi\varphi} \right) dt + (\Pi_t dW_t^-)_\vartheta \\ dP_\varphi &= (\Pi_t dW_t^-)_\varphi, \end{aligned} \quad (4.40)$$

with the matrix-values stochastic process

$$\Pi_t = \begin{pmatrix} \Pi_{rr} & \Pi_{r\vartheta} & \Pi_{r\varphi} \\ \Pi_{\vartheta r} & \Pi_{\vartheta\vartheta} & \Pi_{\vartheta\varphi} \\ \Pi_{\varphi r} & \Pi_{\varphi\vartheta} & \Pi_{\varphi\varphi} \end{pmatrix} \quad \text{and} \quad \Pi_t dW_t^- = \begin{pmatrix} (\Pi_t dW_t^-)_r \\ (\Pi_t dW_t^-)_\vartheta \\ (\Pi_t dW_t^-)_\varphi \end{pmatrix}. \quad (4.41)$$

According to the maximum principle, the canonical momenta are given by $P_j = g_{jk}(v_t^k - iu_t^k)$.

The classical equations do not include drift terms involving i or \hbar . In the stationary state, the current velocity v , which represents the real part of the momentum P_t , is zero in the ground state and only contributes to the z -component of the angular momentum $P_\varphi = \mu g_{\varphi\varphi} v^\varphi = L_z$ for excited states. This property is reflected in the SDE (4.40), where a constant feedback process

$$P_\varphi(t, X_t) = m \in \mathbb{R} \quad (4.42)$$

satisfies the QHE. From Schrödinger's theory, we know that $m \in \mathbb{Z}$. However, at this point, the QHE lack the same additional quantization condition as the Madelung equations mentioned by Wallström [Wal89], so there is no restriction on the angular momentum being quantized under expectation. The quantization in the framework of the QHE is restored by constructing the states with partner Hamiltonians.

For this, we can define the real-valued momentum denoted with a small letter as $p_j = g_{jk}(v_t^k + u_t^k) = P_j^v + P_j^u$ and the angular momentum as $L_t = \mu(r_t \times (v_t + u_t))$. Using partial integration in the calculation of $E[L_t^2]$, we obtain

$$\begin{aligned} E[L_t^2] &= E \left[p_\vartheta^2 + \frac{p_\varphi^2}{\sin^2 \Theta_t} \right] \\ &= E \left[-p_\vartheta^2 - \hbar \cot \Theta_t p_\vartheta + \frac{p_\varphi^2}{\sin^2 \Theta_t} - \hbar \left(\partial_\vartheta p_\vartheta + \frac{\partial_\varphi p_\varphi}{\sin^2 \Theta_t} \right) \right] = E[\tilde{L}_t^2], \end{aligned} \quad (4.43)$$

where we defined a reformulated version of the square of the angular momentum \tilde{L}_t^2 . If we assume that the angular part can be treated separately from the radial part, we can rewrite the SDE (4.40) for the real-valued processes r_t and $p_r = \mu u_r(r_t)$

$$\begin{aligned} dr_t &= \left(u_r(r_t) + \frac{\hbar}{\mu r_t} \right) dt + \sqrt{\frac{\hbar}{\mu}} dW_t^+ \\ du_r(r_t) &= \frac{1}{\mu r_t^2} \left(e_0^2 + \hbar u_r(r_t) + \frac{\tilde{L}_t^2}{\mu r_t} \right) dt + \sqrt{\frac{\hbar}{\mu}} \partial_r u_r(r_t) dW_t^-. \end{aligned} \quad (4.44)$$

The solution to (4.44) for the ground state with zero mean angular momentum leads to $\tilde{L}_t = 0$ and can be solved numerically [BPGP19]. It is isotropic, where the radial projection of the osmotic velocity is constant, namely $\tilde{u}_r = -\frac{\hbar}{a_0 \mu}$ as shown in figure 4.2. It agrees with the solution in section 3.3.2, which corresponds to the s orbital. See figure 3.2.

Excited states

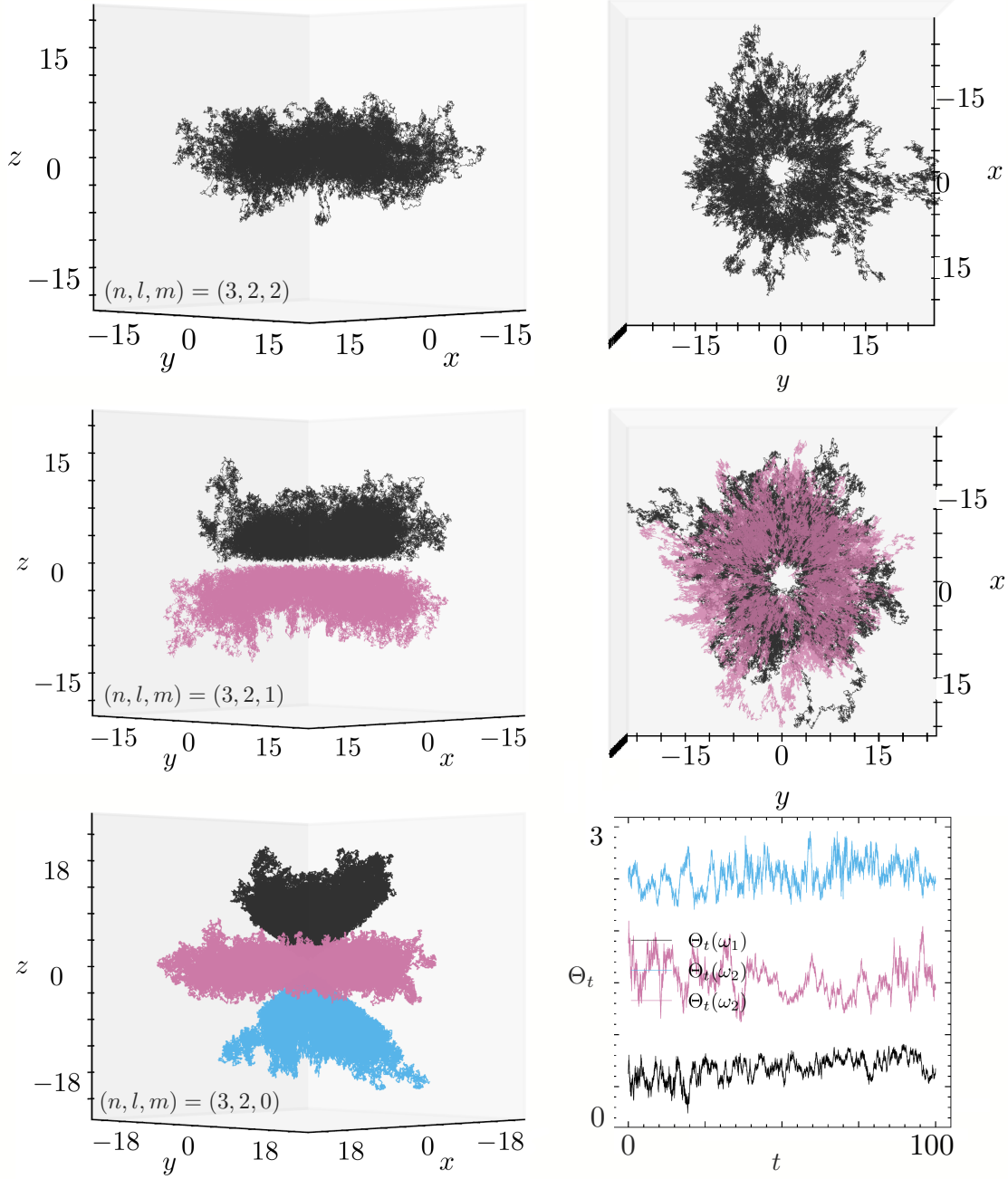


Figure 4.1: The picture depicts sample paths $n = 3, l = 2$ and $m = 2, 1, 0$. These plots correspond to the radial ground states $u_{r,0}^{(2)}$ to the second partner potential V_2 , i.e., $E_{n=3}^Q$. The top row depicts a sample path viewed from two different perspectives for $n = 3, l = 2, m = 2$. The second row depicts two sample paths from different angles for $n = 3, l = 2, m = 1$. Here the $z = 0$ is repulsive, such that the particles can not cross the z plane. The bottom row depicts $n = 3, l = 2, m = 0$ for three sample trajectories, where the stochastic realizations of the azimuthal angle Θ_t for the sample paths on the bottom right illustrate three disjoint regions depending on ϑ . Note that the radial probability densities of all the states shown here are node-free as they describe the ground state to V_2 .

In standard quantum mechanics, the excited states of the radial part can be determined very elegantly with the SUSY approach [VMB90], where the Hamilton operator has to be factorized, leading to partner Hamiltonians sharing the same energy spectrum. Similarly, the excited states for the hydrogen atom in the QHE (4.44) can be determined with the help of partner potentials if the choice of the radial osmotic velocity is appropriate. See e.g.,

section 3.3.1 or ref. [BPGP19] for more details.

Consider an adjusted osmotic velocity

$$\tilde{u}_r := u_r + \frac{\hbar}{\mu r}, \quad (4.45)$$

which is exactly the drift term in (4.44) for dr_t . This is in analogy to the transformation of the radial wave function $\tilde{\psi}_r(r) = r\psi_r(r)$ when solving the Schrödinger equation. It allows us to find a (SUSY-)decomposition of the adjusted Hamilton operator. Note that in this case $\tilde{u}_r = \hbar/\mu \partial_r \ln \psi_r$.

We denote the potential of the problem under consideration as V_0 , namely the Coulomb potential. Then, the first partner potential w.r.t. the definition of \tilde{u}_r is given by

$$V_1 = V_0 - \hbar \partial_r \tilde{u}_{r,0}^{(0)} = V_0 + \frac{\hbar^2}{\mu r^2} \quad (4.46)$$

Here, $u_{0,r}^{(0)}$ is the radial osmotic velocity of the ground state, denoted by superscript (0), with respect to the potential V_0 , denoted by subscript 0. If we use the exact solution $u_{0,r}^{(0)} = -\frac{\hbar}{\mu a_0}$, where a_0 is the Bohr radius, then V_1 becomes the effective potential with angular momentum quantum number $l = 1$. This is seen by separating the radial part from the angular parts in the solution of the Schrödinger equation, which leads to the effective potential

$$V_{\text{eff}}^l(r) = V_0 + \frac{\hbar^2}{2\mu} \frac{l(l+1)}{r^2} \quad (4.47)$$

for the radial part. Therefore, the first partner potential in the stochastic picture V_1 gives the spectrum for $l = 1$. It should be noted that the ground state energy of this potential is equal to the first excited state of V_0 . This is also valid for the second partner potential

$$V_2 = V_1 - \hbar \partial_r \tilde{u}_{r,0}^{(1)} = V_0 + 2 \frac{\hbar^2}{\mu r^2} - \hbar \partial_r \underbrace{\left[-\frac{\hbar}{2\mu a_0} + \frac{\hbar}{\mu r} \right]}_{u_{r,0}^{(1)}} = V_0 + 3 \frac{\hbar^2}{\mu r^2}. \quad (4.48)$$

In general, the ground state velocities for the partner potential $V_l = V_0 + \frac{l(l+1)\hbar^2}{2\mu r^2}$, where $l \in \mathbb{N}_0$, are given by $u_{r,0}^{(l)} = -\hbar/(l+1)\mu a_0 + l\hbar/\mu r$. These ground-state velocities are non-singular ($r > 0$), corresponding to node-free radial wave functions. The energy of these states can be calculated via the expectation value with respect to time t as

$$E[E_{n,l=n-1}] = \lim_{T \rightarrow \infty} \frac{1}{T} \int_0^T \left(\frac{\mu}{2} \left(u_{r,n-1}^{(n-1)}(r_t) \right)^2 + V_{n-1}(r_t) \right) dt = E_n^Q, \quad (4.49)$$

where $E_n^Q = -E_{\text{Ryd}}/n^2$ with the Rydberg energy E_{Ryd} denotes the quantized eigenvalues from non-relativistic quantum mechanics. Hence, we see that the radial osmotic velocity $u_{nl} = u_{r,n-l-1}^{(l)}$ corresponds to the radial eigenstates $\psi_{r,nl}$ with quantum numbers n, l in Hilbert space.

The process for determining the osmotic velocities within the presented formalism is illustrated schematically in figure 4, ref. [BPGP19]. It is worth noting that the states with $l = n - 1$ are the ground states of the partner potentials V_l and thus node-free. The singularities in the osmotic velocities of states like $u_{r,1}^{(0)}$ ($n = 2, l = 0$) or $u_{r,1}^{(1)}$ ($n = 2, l = 1$) depicted in figure 4.2 arise due to the operators that are explicitly written in [BPGP19]. The state corresponding to $n = 2, l = 0$ is also shown in figure 4.3.

The supersymmetric procedure for the QHE leads to a constant expectation value of the

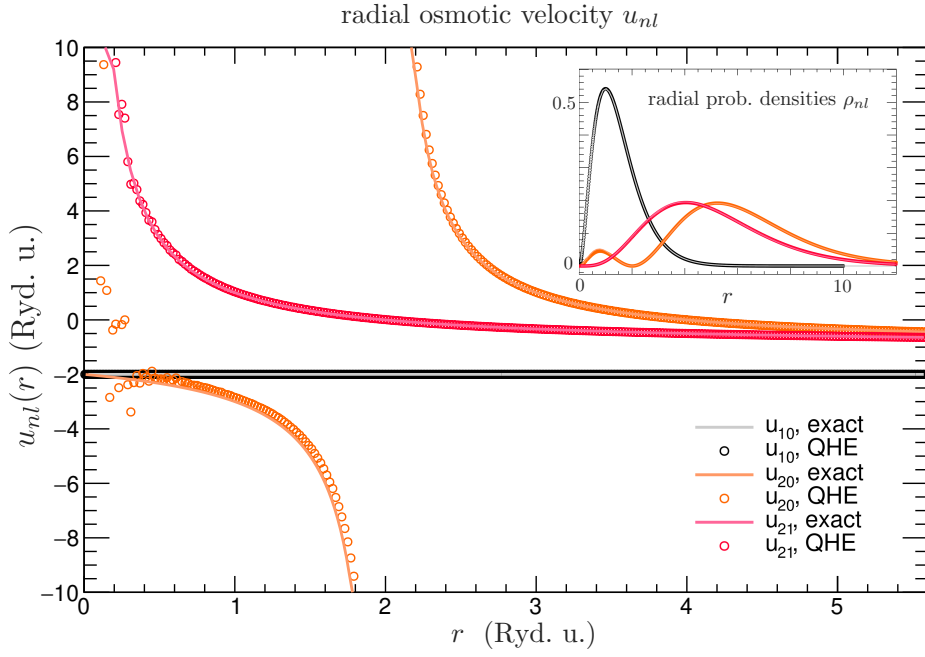


Figure 4.2: The picture depicts the radial osmotic velocities of selected states of the hydrogen atom. The numerical results calculated from the partnerpotentials within the QHE are shown as circles. The analytical solutions derived from the wave functions are depicted as lines. The inset depicts the associated radial probability distributions.

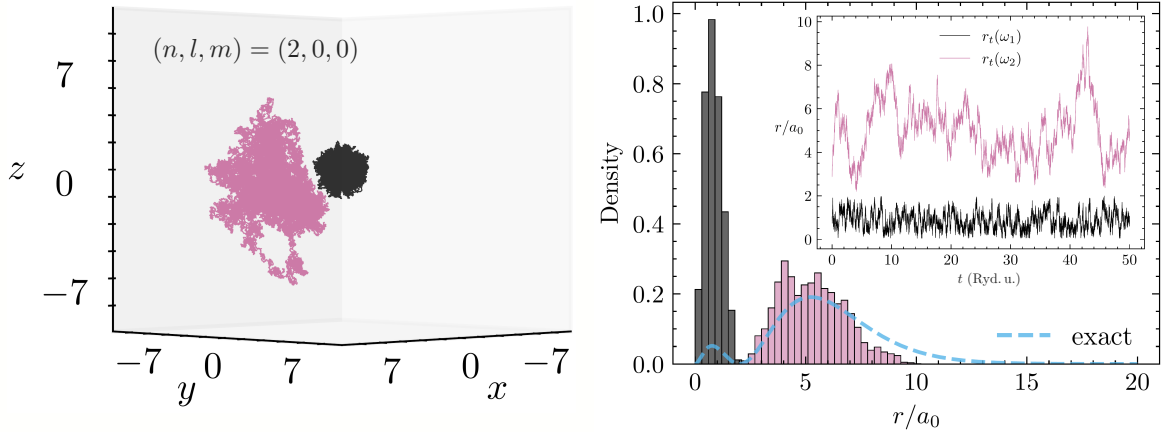


Figure 4.3: The figure depicts a finite time span of two sample trajectories in the first excited state with zero angular momentum, i.e., $n = 2, l = 0, m = 0$. The plot to the right shows the histogram as a function of the distance for the black and pink sample path in comparison with the exact probability density in blue (dashed). The inset shows that $r = 2$ is repulsive. Hence, the black particle starting within $0 < r < 2$ stays close to the origin, which leads to the different visiting histogram in comparison with the probability distribution.

square of the angular momentum in (4.44)

$$E[L_t^2] = \hbar^2 l(l+1) \quad (4.50)$$

so that due to $E[L_t^2] = \tilde{L}_t^2$ we have

$$\tilde{L}_t^2 = -p_\vartheta^2 - \hbar \cot \Theta_t p_\varphi + \frac{p_\varphi^2}{\sin^2 \Theta_t} - \hbar \left(\partial_\vartheta p_\varphi + \frac{\partial_\varphi p_\varphi}{\sin^2 \Theta_t} \right) = \hbar^2 l(l+1). \quad (4.51)$$

Hence, the equation above is a condition on the angular momenta p_φ and p_ϑ . With $p_\varphi = m \in \mathbb{Z}$ fixed, also p_ϑ is determined by the equation above. This allows us to determine the corresponding angular velocities to the hydrogen atom for the quantum numbers n, l and m , which are used to generate the sample paths for a few orbitals shown in figure 4.1.

Consider the second partner potential, for example. The ground state for the radial part $u_{r,n-l-1=0}^{(l=2)}$ to V_2 from equation (4.48) is unique. However, the identification $\tilde{L}_t^2 = \hbar^2 2(2+1)$ allows for multiple solutions concerning the angular momenta p_ϑ and p_φ . Figure 4.1 shows the solutions for three different choices of $L_z = m$, namely $m = 0, 1, 2$, as calculated from the QHE and (4.43).⁴ While the radial probability is node-free, the diffusion may still be singular due to the azimuthal angle ϑ as shown for $(n, l, m) = (3, 2, 1)$ and $(n, l, m) = (3, 2, 0)$. Here the orbitals agree with the hydrogen atom orbitals as determined from the wave function.

The relation between the stochastic quantity \tilde{L}_t^2 and a constant is analogous to the relation between the stochastic Hamiltonian and the energy for eigenstates. For an eigenstate ψ of \hat{L}^2 , i.e. $\hat{L}^2\psi = \hbar l(l+1)\psi$, we have

$$\hat{L}^2\psi = \tilde{L}_t^2\psi. \quad (4.52)$$

This brings us back to the discussion of the effective potential in the stochastic theory, where the Hamiltonian (4.38) can be rewritten as

$$\mathcal{H} = \frac{1}{2\mu} \left(P_r^2 + i \frac{2\hbar}{r_t} P_r \right) + V_{\text{eff}}^l(r_t). \quad (4.53)$$

The effective potential described by equation (4.47) applies to eigenstates where the angular and radial parts are decoupled. It should be noted that in this case, the matrix terms contribute to the effective potential from equation (4.47) if it is identified with

$$V_{\text{eff}}^l = \frac{1}{\mu r_t^2} \left(e_0^2 + \hbar u_r + \frac{\tilde{L}_t^2}{\mu r_t} \right). \quad (4.54)$$

Additionally, the energy E_n^Q along the critical stochastic path can be obtained from the Hamiltonian (4.53) and depends on n , similar to the analysis in the previous section. These energies agree with quantum predictions.

In conclusion, the treatment of the QHE presented in this chapter enables us to describe the stochastic motion in curvilinear coordinates, as illustrated by the hydrogen atom in spherical coordinates. Moreover, it allows solving the hydrogen atom in analogy to the classical Kepler problem. The next chapter will introduce the orientation degree of freedom.

⁴For example, if $L_z = p_\varphi = 2$, then the partial differential equation $\tilde{L}_t^2 = 6\hbar^2$ is fulfilled for $p_\vartheta = 2 \cot \Theta_t$.

Chapter 5

Rotating bodies in quantum Hamilton equations

Spin is one of the fundamental concepts in quantum mechanics, which describes an intrinsic angular momentum of a particle. It is a quantum mechanical property that can take on discrete values, and it plays a crucial role in many quantum phenomena, including the stability of atoms, the behavior of magnetic materials, and the structure of (sub-)atomic particles.

Although the term spin is commonly associated with the rotation of a physical object, in quantum mechanics, it is usually referred to as an intrinsic property of a quantum particle that has no classical counterpart. The prevailing perspective nowadays is due to quantum field theory, see, e.g., [IZ12], which successfully describes relativistic quantum mechanics. From there, one usually constructs representations of the Lorentz group, which are generated by rotation and boost operators fulfilling the usual commutation relations. Then, depending on the representation, one ends up with a scalar or spinor or a vector. From that, the spin is added as an intrinsic label due to the properties of the mathematical group. In the case of electrons, for example, the representation is a bispinor, i.e., a vector in \mathbb{C}^4 from where it is inferred that the particle is a fermion with spin $\frac{\hbar}{2}$. In the limit of small velocities, the non-relativistic descriptions of quantum mechanics are recovered, e.g., the Schrödinger equation or the Pauli equation [Pau25].

In the early days of quantum mechanics, classical models have been proposed that describe the properties of quantum spin based on extended and solid particles. These models, including those developed by Goudsmith and Uhlenbeck [UG25], Reiche [Rei26], Kronig [KR27]¹, can reproduce the well-known properties of spin. However, they were dismissed early on due to their inconsistencies with special relativity. For instance, if elementary particles were extended rather than point-like, the shell of an electron would have to rotate superluminally to match the magnitude of its spin angular momentum. In contrast, the stochastic theory avoids conflicts with special relativity due to non-differentiable trajectories from a technical perspective.² Therefore, one may argue that it is able to provide a physical picture of quantum spin.

The classical generalization of quantum spin in terms of a rotational stochastic process was put forward by Dankel [Dan70]. It builds on Bopp and Haag's [BH50] postulated Hamiltonian for a charged ball with radius R . In the limit $R \rightarrow 0$, the Hamiltonian divides into copies of the regular Pauli-Hamiltonian [Wal90]. Based on that model, Dankel [Dan70, Dan77] showed that each sufficiently smooth wave function, derived from the eigenfunctions of the Schrödinger equation on the manifold, corresponds to an associated Markov process on the manifold $\mathbb{R}^3 \times SO(3)$, which has the same quantum expectation values. In this case, the spin is a continuous random variable, and the values of the spin components, which are measurable as the expectation values of the angular velocities, are quantized.

¹Kronig apparently developed a similar model compared to Uhlenbeck in 1924 which he dismissed at first.

²The (mean) velocity fields, however, would have to surpass the speed of light.

This chapter focuses on the derivation of the quantum Hamilton equations that are associated with a model of a rotating extended particle. To achieve this, a Lagrangian is proposed in analogy to classical theory of a rotating charge, and the stochastic variational principle in section 4.3 is applied to the group of rotation $SO(3)$. This allows to study the relation between stochastic spin representation and the non-relativistic limit of the representations of quantum spin.

The chapter is organized as follows. We first introduce the spin models proposed in stochastic mechanics, especially the one put forward by Dankel. Then, we revisit a classical Lagrangian and derive the equations of motion. Next, we transfer the classical Lagrangian to the stochastic picture and derive the QHE for a freely spinning particle. Finally, we discuss the spin states that follow from the calculation of the QHE by analyzing its expectation values.

5.1 The model of a rotating particle in stochastic mechanics

5.1.1 Spin in quantum mechanics

The spin angular momentum in quantum mechanics is typically associated with a vector operator \hat{s}_i , defined similarly to the orbital angular momentum through commutation relations given by

$$[\hat{s}_i, \hat{s}_j] = i\hbar\epsilon_{ijk}\hat{s}_k \quad \text{and} \quad [\hat{s}^2, \hat{s}_i] = 0. \quad (5.1)$$

The eigenstates of the two operators, denoted by $|jm\rangle$ in Dirac notation, satisfy the following conditions

$$\begin{aligned} \hat{s}^2|jm\rangle &= \hbar^2 j(j+1)|jm\rangle \\ \hat{s}_z|jm\rangle &= \hbar m|jm\rangle \\ (\hat{s}_x \pm i\hat{s}_y)|jm\rangle &= \hbar\sqrt{j(j+1) - m(m \pm 1)}|j(m \pm 1)\rangle, \end{aligned} \quad (5.2)$$

where j is the spin quantum number and m the spin projection onto the z axis. Consequently, the spin's expectation values can be seen as a vector quantity with a fixed magnitude and quantized direction. Unlike the orbital angular momentum, however, half-integer values are allowed for the spin.

The spin itself is not accessible directly, but its coupling to position in space, for example. This is due to the magnetic moment associated with the particle, which follows in the classical model of a rotating charged particle. The magnetic moment, however, differs by a factor $g \neq 1$ from the classical model. For a particle with uniform and equal charge and mass distribution, the classical gyromagnetic factor is given by $\gamma = \frac{q}{2m}g$ with $g = 1$. From experiments, it is well-known that the g factor generally has different values. Hence, from a classical point of view, a non-trivial g -factor arises if the charge and mass distributions are not the same for a particle with charge q and mass m .³

For instance, consider the electron, where $g = 2$ in the non-relativistic limit. This value follows from the relativistic description of the electron in quantum mechanics, namely the Dirac equation [Dir26, LL67]. This is associated with a Clifford algebra for the linear operators that have to be represented by 4×4 dimensional complex-valued matrices, which act on a 4-component wave function $\psi = (\phi^T, \chi^T)^T$. When considering particles in an external magnetic field and introducing minimal coupling, one can eliminate one of the bispinors, namely χ , and obtain the Pauli equation for spinor ϕ in the non-relativistic limit

$$\left[i\hbar\partial_t - e\Phi - \frac{1}{2m}(\hat{p} + eA)^2 - \frac{\hbar e}{2m}\hat{\sigma} \cdot B \right] \phi = 0.$$

³More generally, $g \neq 1$ if the back interaction of the moving charges with their Maxwell fields is taken into account. See [Spo04] for more details.

Here, $\hat{\sigma} = (\hat{\sigma}_x, \hat{\sigma}_y, \hat{\sigma}_z)$ represents the vector of the Pauli matrices, $q = -e$ is the electron's charge, A is the vector potential, B is the magnetic field and Φ is the electric potential. Hence, the Pauli equation introduces a term that couples the spin to the magnetic field in addition to the Schrödinger equation. The magnetic moment of a particle can be defined as $\hat{\mu} = \frac{e\hbar}{2m} \hat{s} = \mu_B \hat{s}$, where $\hat{s} = \frac{\hat{\sigma}}{2}$ is the actual spin-1/2 operator, and μ_B is the Bohr magneton. This leads to a factor of 2 in the electron's gyromagnetic ratio. The spinor $\phi = (\phi_1, \phi_2)$ can usually be considered as a superposition of $\phi_1 = |j = 1/2, m = 1/2\rangle$ and $\phi_2 = |j = 1/2, m = -1/2\rangle$. This is generalized to higher spins accordingly.

The basic properties of the spin described here can be described by a classical model of spin in stochastic mechanics for non-relativistic systems. This is shown in the following.

5.1.2 Spin in stochastic mechanics

Generalizing the formalism and interpretation of classical mechanics, stochastic mechanics describes a quantum system in terms of a Markovian stochastic process in the configuration space. Thus, in analogy, the classical generalization in the case of quantum spin would then require a rotational stochastic process based on the assumption of the classical counterpart.

In our model, we assume that diffusion takes place on the manifold $M = \mathbb{R}^3 \times SO(3)$ (instead of $\tilde{M} = \mathbb{R}^3 \times SU(2)$ in quantum mechanics), where \mathbb{R}^3 covers the translational and $SO(3)$ the orientational degrees of freedom. The velocity for the translation in \mathbb{R}^3 describes the motion of the particle's center of mass (COM). The angular velocity describes the change of orientation with respect to the COM. It is an element of the Lie algebra $\mathfrak{so}(3)$, which is the tangent space of the Lie group $SO(3)$.

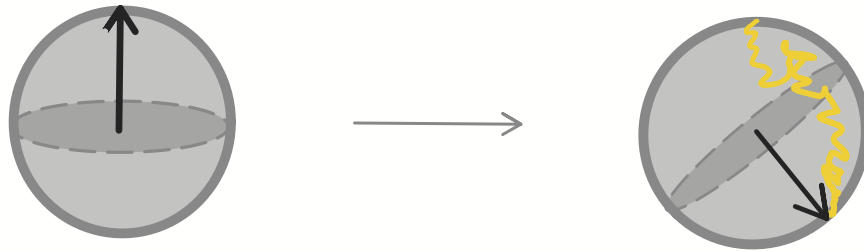


Figure 5.1: The diagram illustrates extension of the point particle concept by giving it an orientation. The particle's orientation undergoes random fluctuations over time in response to its interaction with the surrounding governed by a SDE.

The Bopp-Haag-Dankel model [BH50, Dan70] gives a more intuitive explanation of ascribing a moment of inertia $I_m > 0$ to the considered particle than to a point particle in Nelson's suggestions later [Nel85]. Either way, both consider the limit of a vanishing moment of inertia $I_m \rightarrow 0$, which in Dankel's case is due to the radius going to zero. The value of I_m does not influence the spin expectation values.

Furthermore, Dankel showed that to each sufficiently smooth wave function on the manifold $\mathbb{R}^3 \times SU(2)$, there is an associated Markov process on the manifold $\mathbb{R}^3 \times SO(3)$ leading to the same quantum averages. The random variable for the spin is continuous, as opposed to the discrete values of spin components that are measurable, i.e., the expectation values of the angular velocities are quantized. Note that the wave function is defined on $SU(2)$, whereas the diffusion is defined on $SO(3)$.⁴ The spin for fermions in quantum mechanics starting from the Dirac equation, e.g., is associated with $SU(2)$ and not $SO(3)$. The unitary group $SU(2)$, a simply connected space, is the double cover of the rotation group $SO(3)$, which is not simply connected.⁵ The use of $SU(2)$ is important in the case of 2π rotations. Consider,

⁴It should be noted that the stochastic diffusions can be defined on $SU(2)$ as shown by Faris [Far82].

⁵For more details on $SO(3)$ and its connection to $SU(2)$, see appendix D.1.

e.g., the wave function $\psi(x, \Theta)$, where Θ denotes the orientation dependency. A 2π rotation in $SU(2)$ is associated with $-\Theta$, while on $SO(3)$ we end up with Θ again. The wave function is then split in two classes, namely $\psi(x, \Theta) = \psi(x, -\Theta)$ for bosons and $\psi(x, \Theta) = -\psi(x, -\Theta)$ for fermions [Nel85]. This is different in stochastic mechanics, where the velocity fields are defined on $SO(3)$ for both cases.

Approaches of rotating charge distributions [dIPA71, CdIPA71] similar to Dankel's model can be found in the literature related to stochastic electrodynamics, see, e.g., the book of Peña and Cetto [dIPCVH15] for an overview, where spin is a result of the interaction with the *zero-point field* [DAJL82]. There is also work based on a discrete configuration space for spin- $\frac{1}{2}$ particles [GM84, DAJL82], where spin is treated as a discrete random variable, e.g., considering a Markov process $\xi(t) = (X_t, S_t) \in \mathbb{R}^3 \times \{-1, 1\}$. In these, there is no construction of a model proposed. They rather start from the Pauli equation, knowing that the random variables are discrete. This thesis will rely on the model proposed by Bopp and Dankel.

5.1.3 Construction of the stochastic process

The rotational diffusion introduced by Dankel [Dan70] is discussed in analogy to the translational Brownian motion, where the system is subject to a background field that changes its position and orientation, thus its angular momentum. Mathematically, this can be tracked via an element R_t representing the orientation at time t in the group of rotations $SO(3)$. It is important to note that the rotational process R_t does not describe a rotation at time t , but rather the change in the body's orientation that occurs between time 0 and t . The change of orientation then describes the particle's spin and is described by the SDE

$$dR_t = R_t[\omega]_{\times} dt + R_t \sigma_I \tilde{h}_i \circ dW_t^i, \quad (5.3)$$

where $[\omega]_{\times}$ denotes an element of the Lie algebra $\mathfrak{so}(3)$ and ω is the corresponding vector representation in \mathbb{R}^3 ; see appendix D.1. Furthermore, \tilde{h}_i is a suitable function depending on the considered metric in local coordinates, W_t is a 3-dimensional Wiener process, and σ_I is the coupling constant to the background field.

In analogy to Nelson's construction in flat space, the drift field in the form of the vector representation $\omega = \omega_v + \omega_u$ is the sum of current and osmotic angular velocity, respectively. They are the counterparts of the two velocity fields concerning translation. Similarly, the diffusion constant σ_I^2 has to be the quotient of \hbar and something with the unit of moment of inertia to give it a physical meaning. The simplest choice would be to define $\sigma_I^2 = \frac{\hbar}{I_m}$ where $I_m > 0$ is the moment of inertia of the particle, and to assume that the particle's I_m is the same for all principal axes. In the general case $\sigma_I = \hbar I_m^{-1}$ would be a matrix. Hence, in this model, the inertia associated with the mass distribution I_m steps in the role of the mass and determines the strength of the random kicks to the particle's orientation. In summary, we have the correspondences

$$\begin{aligned} X_t, m &\rightarrow R_t, I_m \\ v, u &\rightarrow \omega_v, \omega_u \\ \sigma^2 = \frac{\hbar}{m} &\rightarrow \sigma_I^2 = \frac{\hbar}{I_m}. \end{aligned} \quad (5.4)$$

As illustrated in figure 5.1, instead of using $R_t \in SO(3)$, it is also possible to assign an orientation to the particle in the form of a vector $N_t \in \mathbb{R}^3$, allowing the above SDE to be rewritten as

$$dN_t = N_t \times [(\omega_v + \omega_u)dt + \sigma_I dW_t], \quad (5.5)$$

where the cross-product ensures that only the direction of the orientation is changed. In this case, we can visualize the change of orientation by tracing the tip of the orientation vector on the sphere in \mathbb{R}^3 .

Since the considered configuration space $SO(3)$ is not flat, the stochastic analysis follows the formalism used in section 4.3. Due to the dimension of $SO(3)$, the charts are mostly based on three parameters.⁶ Here we use Euler angles denoted by $\theta = (\vartheta, \varphi, \chi) \in [0, \pi] \times [-\pi, \pi]^2$ as local coordinates in flat euclidean space.

Describing the rotation with Euler angles

Think of a laboratory frame with axes x_1, x_2, x_3 fixed and the body fixed frame $\tilde{x}_1, \tilde{x}_2, \tilde{x}_3$ into which the rotation would take the reference frame. The three angles describe three consecutive rotations in the 3 1 3 or $z x z$ -convention (see figure 5.2):

- rotation around x_3 -axis by angle φ ($x_1 \rightarrow x'_1, x_2 \rightarrow x'_2, x_3 \rightarrow x_3$)
- rotation around x'_1 -axis by angle ϑ ($x'_1 \rightarrow x'_1, x'_2 \rightarrow x''_2, x_3 \rightarrow \tilde{x}_3$)
- rotation around x'_3 -axis by angle χ ($x'_1 \rightarrow \tilde{x}_1, x'_2 \rightarrow \tilde{x}_2, \tilde{x}_3 \rightarrow \tilde{x}_3$)

so that $\theta = (\vartheta, \varphi, \chi)$ denotes the orientation of the objects in the laboratory frame. This rotation is intrinsic, which means that the rotations are carried out about the axes of the rotating coordinate system.

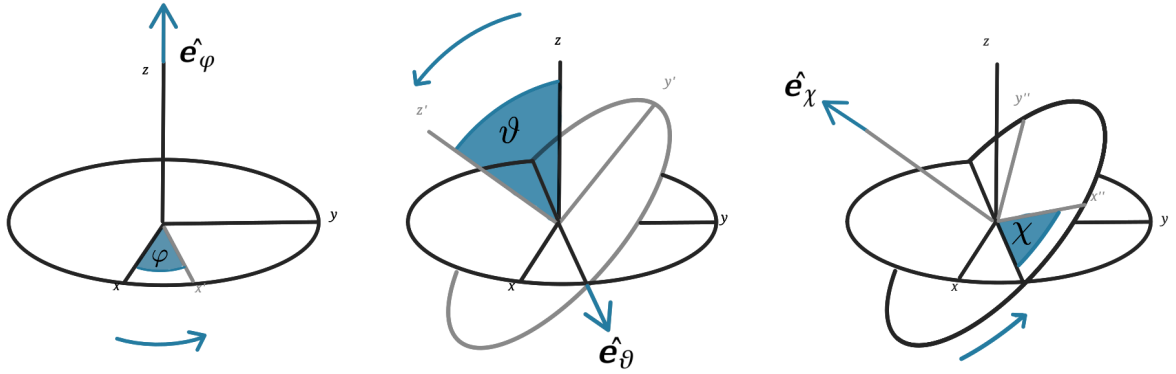


Figure 5.2: The three consecutive rotations in the $z x z$ -convention of the Euler angles are shown from left to right. The first rotation is about the z axis by the precession angle φ . The second rotation is carried out about the x' axis by the nutation angle ϑ . The intrinsic rotation around the z' axis is quantified by χ .

The metric on $SO(3)$ for the considered Euler angles is given by

$$(g_{ij}) = \begin{pmatrix} 1 & 0 & 0 \\ 0 & 1 & \cos \vartheta \\ 0 & \cos \vartheta & 1 \end{pmatrix} \quad \text{with its inverse} \quad (g^{ij}) = \begin{pmatrix} 1 & 0 & 0 \\ 0 & \frac{1}{\sin^2 \vartheta} & -\frac{\cos \vartheta}{\sin^2 \vartheta} \\ 0 & -\frac{\cos \vartheta}{\sin^2 \vartheta} & \frac{1}{\sin^2 \vartheta} \end{pmatrix}. \quad (5.6)$$

Given a vector $(v^\vartheta, v^\varphi, v^\chi)^T$ in the reference frame, the corresponding vector in cartesian coordinates reads

$$(v^1, v^2, v^3)^T = J_L(v^\vartheta, v^\varphi, v^\chi)^T = (e_\vartheta \ e_\varphi \ e_\chi) (v^\vartheta, v^\varphi, v^\chi)^T \quad (5.7)$$

where J_L is the left Jacobian given in (D.3) with the basis vectors $e_\vartheta = (\cos \varphi, \sin \varphi, 0)^T$, $e_\varphi = (0, 0, 1)^T$ and $e_\chi = (\sin \varphi \sin \vartheta, -\cos \varphi \sin \vartheta, \cos \vartheta)^T$ pointing along each axes of rotation of the corresponding angle. Analogously for the body fixed frame denoted by prime, there is

$$(v'^1, v'^2, v'^3)^T = J_R(v'^\vartheta, v'^\varphi, v'^\chi)^T = (e'_\vartheta \ e'_\varphi \ e'_\chi) (v'^\vartheta, v'^\varphi, v'^\chi)^T \quad (5.8)$$

⁶In some cases, it is better to consider four parameters with an additional constraint, e.g., quaternions which represent $SU(2)$. This can be helpful in the numerical treatment of rotations.

where J_R is the right Jacobian given in (D.4) with $e'_\vartheta = (\cos \chi, -\sin \chi, 0)^T$, $e'_\chi = (0, 0, 1)^T$ and $e'_\varphi = (\sin \vartheta \sin \chi, \sin \vartheta \cos \chi, \cos \vartheta)^T$.

This allows us to write the SDE for the stochastic processes $\Theta_t = (\Theta_t, \Phi_t, \mathcal{X}_t)$ in local coordinates given in equation (4.4) and (4.9) for the corresponding orientation angles $\theta = (\vartheta, \varphi, \chi)$ as follows

$$\begin{aligned} d\Theta_t &= \left[\omega_v^\vartheta \pm \omega_u^\vartheta \mp \frac{\sigma_I^2}{2} \cot \Theta_t \right] dt + h_j^\vartheta dW_{\pm,t}^j \\ d\Phi_t &= [\omega_v^\varphi \pm \omega_u^\varphi] dt + h_j^\varphi dW_{\pm,t}^j \\ d\mathcal{X}_t &= [\omega_v^\chi \pm \omega_u^\chi] dt + h_j^\chi dW_{\pm,t}^j, \end{aligned} \quad (5.9)$$

where $W_{\pm,t}^j$ are the components of a three-dimensional forward/backward Wiener process, and the matrix elements h_j^i are associated with the J_L^{-1} given in (D.5)

$$(h_j^i) = (h^\vartheta \ h^\varphi \ h^\chi) = \sigma_I \begin{pmatrix} \cos \varphi & -\cot \vartheta \sin \varphi & \frac{\sin \varphi}{\sin \vartheta} \\ \sin \varphi & \cot \vartheta \cos \varphi & -\frac{\cos \varphi}{\sin \vartheta} \\ 0 & 1 & 0 \end{pmatrix} \quad (5.10)$$

so that $h^i(\vartheta, \varphi) \cdot h^j(\vartheta, \varphi) = \sigma_I^2 g^{ij}(\vartheta)$. The components $\omega^j = \omega \cdot e^j$ denote the angular velocities projected onto the basis vectors of the three consecutive rotations. These equations demonstrate that as the moment of inertia decreases, and $I_m \rightarrow 0$, the Brownian motion of the orientation becomes increasingly jiggly, with $\sigma_I \rightarrow \infty$.

The FBSDEs for the local coordinates (5.9) represent the conservative diffusion on the group of rotations. They will be used as a constraint for the stochastic optimal control problem, allowing the derivation of SDEs for the canonical angular momenta. In line with Nelson's postulate for a stochastic Newton law, on the other hand, the angular velocity fields $\omega_v(t, \theta)$ and $\omega_u(t, \theta)$ obey coupled partial differential equations, which are related to the Madelung equations on $SO(3)$ [Dan70].

Moreover, in the deterministic term of $d\Theta_t$ in equations (5.9), there is also a divergent term that tends to keep ϑ away from the second rotation axis x_1' . This is due to the singularity of the coordinate description in Euler angles. If the ϑ -rotation has the value 0 or π , the φ and χ rotations rotate around the same axis, and thus one loses a degree of freedom, which is also known as the gimbal lock. Hence, it is necessary to point out that, e.g., similar to spherical coordinates where the radius $r > 0$, if $\Theta_{t=0} = 0$ or $\Theta_{t=0} = \pi$ a different set of coordinates has to be used.

The following section considers the classical limit for rigid bodies with non-vanishing inertia ($\sigma_I^2, \omega_u \rightarrow 0$) and derives the differential equations for the canonical angular momenta corresponding to the Euler angles given here. Together with the differential equations given in (5.9) in the classical limit, they describe a classically rotating particle.

5.2 Spinning bodies in classical mechanics

In this thesis, it is assumed that the mass ρ_m and charge distribution ρ_c are strongly localized compared to the typical distance traveled [BH50, Spo04] and that the rotor is symmetric, such that the moments of inertia along the principal axes of the body are equal. This results in the inertia for the mass being $I_{\text{mass}} = I_m \mathbb{I}$ and the inertia for the charge distribution being $I_{\text{charge}} = I_c \mathbb{I}$, with the identity matrix \mathbb{I} .⁷

In classical mechanics, the magnetic moment M' associated with the spinning ball of charge and corresponding inertia I_c is given by $M' = I_c \omega'$. In contrast, the mass distribution with inertia I_m is related to an angular momentum $\Sigma' = I_m \omega'$, where ω' is the angular veloc-

⁷In a more general, even relativistic, scenario, a moment of inertia can be defined for the mass distribution ρ_m and the charge distribution ρ_c , including non-symmetrical distribution. In this case, we have two different

ity in the body's reference frame. The assumption in this model is that of a spinning particle, such that the magnetic moment in the reference frame is related to its angular momentum and angular velocity ω by $M = \gamma \Sigma$ in the reference frame. The gyromagnetic factor $\gamma = \frac{I_c}{I_m}$ depends on the ratio of I_c and I_m .

The system can be described via a Lagrangian, where the kinetic term of the rotation and the interaction with an external magnetic field B are given by $T_s = \frac{1}{2} I_m \omega^2$ and $V_s = -M \cdot B = -I_c \omega \cdot B$, respectively. The rotational kinetic energy reads

$$T^{\text{spin}} = \frac{1}{2} g_{ij}^I \omega^i \omega^j \quad (5.13)$$

with the metric $g_{ij}^I = I_m g_{ij}$, $g_I^{ij} = g^{ij}/I_m$ as defined in equations (5.6). If we allow an external field to act on the system, we get the Lagrangian $\mathcal{L} : M \times T_x M \times \mathbb{R}$

$$\mathcal{L}_s = T_s - V_m = \frac{1}{2} g_{ij}^I \omega^i \omega^j + I_c \omega^i B_i \quad (5.14)$$

where the magnetic field is given by $B_i = \varepsilon_i^{kl} \partial_k A_l = (\nabla \times A)_i$ and A is the vector potential. The canonical angular momentum is then defined as

$$\Omega_j = \frac{\partial \mathcal{L}}{\partial \omega^j} = g_{ij}^I \omega^i + I_c B_j, \quad (5.15)$$

with the angular velocities in terms of the momenta above

$$\omega^j = g_I^{ij} (\Omega_i - I_c B_i). \quad (5.16)$$

Then the classical Hamiltonian is obtained as

$$\mathcal{H}_s = \omega^i \Omega_i - \mathcal{L} \quad (5.17)$$

$$= \frac{1}{2 I_m} g^{ij} \Omega_i \Omega_j - \gamma g^{ij} \Omega_i B_j + \frac{I_m \gamma^2}{2} g^{ij} B_i B_j. \quad (5.18)$$

From that, it is straightforward to derive Hamilton's equation of motion in the classical case. The equations of motion (cf. (5.9)) concerning the change of orientation read

$$\begin{aligned} d\vartheta &= \left[\frac{\Omega_\vartheta}{I_m} - \gamma B_\vartheta \right] dt \\ d\varphi &= \left[\frac{\Omega_\varphi - \cos \vartheta \Omega_\chi}{I_m \sin^2 \vartheta} - \gamma g^{\varphi j} B_j \right] dt \\ d\chi &= \left[\frac{\Omega_\chi - \cos \vartheta \Omega_\varphi}{I_m \sin^2 \vartheta} - \gamma g^{\chi j} B_j \right] dt, \end{aligned} \quad (5.19)$$

moments of inertia, given by

$$I_m = \int_{\mathbb{R}^3} \rho_m(r) (\mathbb{I}r - r r^T) dr \quad (5.11)$$

$$I_c = \int_{\mathbb{R}^3} \rho_c(r) (\mathbb{I}r - r r^T) dr, \quad (5.12)$$

However, to account for such a scenario, one needs to include the particle's interaction with the field generated by its own motion, as discussed in [Spo04, IKS15].

while the change of canonical angular momentum is governed by

$$\begin{aligned}
d\Omega_\vartheta &= \left[\frac{1}{I_m \sin^3 \vartheta} (\cos \vartheta (\Omega_\chi^2 + \Omega_\varphi^2) - (1 + \cos^2 \vartheta) \Omega_\chi \Omega_\varphi) \right. \\
&\quad \left. + \gamma \csc^2 \vartheta (\Omega_\varphi - \cos \vartheta \Omega_\chi) (B_x \cos \varphi - B_y \sin \varphi) \right] dt \\
d\Omega_\varphi &= \gamma [\Omega_\vartheta (\sin \varphi B_x - \cos \varphi B_y) + \csc \vartheta \Omega_\chi (-\sin \varphi B_y - \cos \varphi B_x) \\
&\quad + \cot \vartheta \Omega_\varphi (\sin \varphi B_y - \cos \varphi B_x)] dt \\
d\Omega_\chi &= 0.
\end{aligned} \tag{5.20}$$

Solving the equations of motion for a classically spinning particle is a complex task that

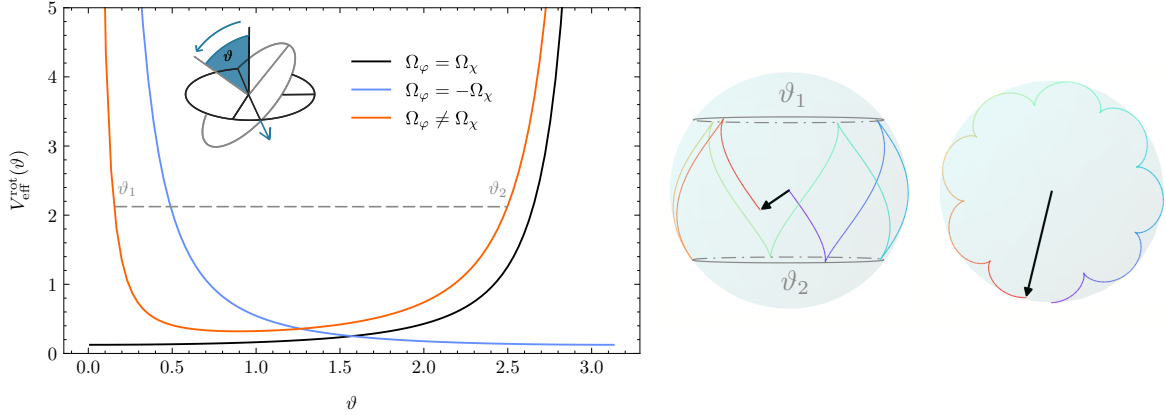


Figure 5.3: The left plot shows the effective potential for different values of the angular velocities Ω_φ and Ω_χ , plotted against the angle ϑ . The nutation angle is also shown in the inset. To the right of the figure, two spheres depict an example trajectory of a rotation when $\Omega_\varphi \neq \Omega_\chi$, represented by the tip of a body-fixed unit vector from two different perspectives. The particle's orientation has two classical turning points, denoted as ϑ_1 and ϑ_2 .

heavily depends on the chosen parameters. Despite this, some valuable observations can be made. For example, the Lagrangian in Euler angles gives rise to an effective rotation potential,

$$V_{\text{eff}}^{\text{rot}}(\vartheta, \Omega_\varphi, \Omega_\chi) = \frac{1}{2I_m \sin^2 \vartheta} (\Omega_\varphi^2 + \Omega_\chi^2 - 2 \cos \vartheta \Omega_\chi \Omega_\varphi). \tag{5.21}$$

similar to the potential barrier encountered in the central potential problem. This potential, denoted by $V_{\text{eff}}^{\text{rot}}(\vartheta, \Omega_\varphi, \Omega_\chi)$ in equation (5.21), illustrates the behavior of the orientation angles ϑ, φ, χ and their role in describing rotations in a stochastic context. From equations (5.19) and (5.20), it follows that the canonical momentum for χ is a constant of motion independent of the magnetic field, as it describes the intrinsic rotation around the body-fixed \tilde{z} axis. Moreover, when the magnetic field has only a z component, the canonical momentum for φ is also a constant of motion. Although the rotation itself can be complex, the momentum relations in equation (5.20) simplify for $B = B_z e_z$ as follows

$$d\Omega_\vartheta = \partial_\vartheta V_{\text{eff}}^{\text{rot}}(\vartheta, \Omega_\varphi, \Omega_\chi) dt \tag{5.22}$$

$$d\Omega_\varphi = 0, \quad d\Omega_\chi = 0. \tag{5.23}$$

Since $\Omega_\varphi, \Omega_\chi$ are constants, the change of ϑ is described by the shape of the effective potential, which depends on the initially chosen values of Ω_φ and Ω_χ . Some $V_{\text{eff}}^{\text{rot}}$ are depicted in figure 5.3 for different choices of canonical angular momenta $\Omega_\varphi, \Omega_\chi$.

For $\Omega_\varphi \neq \Omega_\chi$ the angle ϑ follows an oscillatory movement as shown in the inset of figure 5.3. This behavior is a consequence of the shape of the effective potential illustrated in orange. For the other two combinations, the potentials lead to a parallel or antiparallel

alignment of the particle's orientation w.r.t. to the chosen z -axis⁸ since the effective potential has minima at nutation angles $\vartheta = 0$ and $\vartheta = \pi$ in some cases. The effective potential will play a similar role in the subsequent discussion of the QHE for a freely spinning top, where the values of Ω_φ and Ω_χ are critical to the determination of the spin projections. Finally, analytic solutions and a discussion for a classically spinning object can be found in more depth in [BBM92].

Returning to Cartesian coordinates, we can express the angular momentum $\Sigma = I_m\omega$ using (5.16) as follows

$$\begin{aligned}\Sigma^x + I_c B_x &= \cos \varphi \Omega_\vartheta + \frac{\sin \varphi}{\sin \vartheta} \Omega_\chi - \frac{\sin \varphi \cos \vartheta}{\sin \vartheta} \Omega_\varphi \\ \Sigma^y + I_c B_y &= \sin \varphi \Omega_\vartheta - \frac{\cos \varphi}{\sin \vartheta} \Omega_\chi + \frac{\cos \varphi \cos \vartheta}{\sin \vartheta} \Omega_\varphi \\ \Sigma^z + I_c B_z &= \Omega_\varphi.\end{aligned}\tag{5.24}$$

The equations presented above allow us to define the terms on the right-hand side as the canonical angular momenta $s = \Sigma + I_c B$, similar to the classical canonical momentum. In this case, the j th component of the spin momentum in Cartesian coordinates is given by $s^j = (J_L)_i^j g_I^{ik} \Omega_k$. For example, $d\Omega_\varphi = \gamma(s \times B)_z dt = ds^z$. It is important to note that the spin s defined here is not only the kinetic angular momentum Σ but also the external field B multiplied by coupling constants, i.e., the canonical spin angular momentum. By converting the momentum equations (5.20) to Cartesian coordinates, we obtain the classical precession equation for a spinning particle,

$$ds = \gamma [s \times B] dt\tag{5.25}$$

or equivalently

$$I_m d\omega = I_c [\omega \times B - \dot{B}] dt.\tag{5.26}$$

The Hamiltonian expressed in terms of the canonical angular momentum is given by

$$\mathcal{H}_s^{cl} = \frac{s^2}{2I_m} - \gamma s \cdot B + \frac{I_m \gamma^2}{2} B^2.\tag{5.27}$$

When considering a constant magnetic field along the z -axis, the z -component of s remains constant, leading to the precession of the spin s around the magnetic field. It is also possible to demonstrate, using Poisson brackets, that s^2 is a constant of motion, that s precesses with $\dot{s} = s \times B$, and that $\{s_i, s_j\} = \varepsilon_{ijk} s_k$ [BBM92].

5.3 Quantum Hamilton equations of spinning particles

Let us examine the stochastic processes $\Theta_t = (\Theta_t, \Phi_t, \mathcal{X}_t)$, which represent the continuously changing orientation of the particle. In the case of pure rotation, Nelson's forward-backward SDEs can be expressed using the selected Euler angles (5.9). The combination into a single complex SDE as shown in equation (4.19) results in the following set of equations

$$\begin{aligned}d\Theta_t &= \left[\omega_q^\vartheta + i \frac{\sigma_I^2}{2} \cot \Theta_t \right] dt + h_j^\vartheta dW_{q,t}^j \\ d\Phi_t &= \omega_q^\varphi dt + h_j^\varphi dW_{q,t}^j \\ d\mathcal{X}_t &= \omega_q^\chi dt + h_j^\chi dW_{q,t}^j\end{aligned}\tag{5.28}$$

⁸Note that the orientation angles, including the nutation ϑ , describe the orientation of the particle and not necessarily its spin, which is related to the change of the orientation.

Here, $W_{q,t}^j$ denotes independent quantum Wiener processes for each j , and, again, h_l^i represents the left Jacobian J_L given in the appendix D.2 with $h_l^i h_l^j = \sigma_I g^{ij}$. The components $\omega_q^j = \omega_v^j - i\omega_u^j$ denote the quantum angular velocities.

For the cost function given in equation (4.18), we take the classical Lagrangian \mathcal{L} from equation (5.14) and introduce the quantum angular velocity $\omega_{q,t} = \omega_{v,t} - i\omega_{u,t}$ as stochastic control, instead of the classical velocity ω . The aim is to find solutions in the form of feedback controls, i.e., $\omega_{q,t} = \omega_q(t, \theta)$.

The corresponding stochastic Hamiltonian from equation (4.20) in Euler angles reads

$$\mathcal{H}_s = -\frac{g_{kj}^I}{2} \omega_{q,t}^k \omega_{q,t}^j - I_c B_j \omega_{q,t}^j + \Omega_j v_{q,t}^j + i \frac{\sigma_I^2}{2} \cot \Theta_t \Omega_j - \frac{(1+i)}{2} \text{Tr}\{\Pi_t H^T\}, \quad (5.29)$$

where we introduce the costate processes Ω_t and Π_t ⁹ and use shorthand $\Omega_j = \Omega_{j,t} = g_{ij}^I \omega_{q,t}^j + I_c B_j$. The latter equality follows from the extremization of the Hamiltonian w.r.t. $\omega_{q,t}$.

The QHE (4.22) for the canonical angular momenta depending on Euler angles can be written in a compact form as follows

$$\begin{aligned} d\Omega_\vartheta &= \left[\partial_\vartheta V_{\text{eff}}^{\text{rot}}(\Theta_t, \Omega_\varphi, \Omega_\chi) + \frac{\gamma}{\sin^2 \Theta_t} (\Omega_\varphi - \cos \Theta_t \Omega_\chi) (B_x \cos \Phi_t - B_y \sin \Phi_t) \right. \\ &\quad \left. + i \frac{\hbar \Omega_\vartheta}{2 I_m \sin^2 \Theta_t} + \frac{1+i}{2 \sin^2 \Theta_t} \sigma_I f_\vartheta(\Theta_t, \Phi_t, \Pi_t) \right] dt + \Pi_{\vartheta j} dW_{-,t}^j \\ d\Omega_\varphi &= \left[\gamma [s \times B]_z + \frac{1+i}{2 \sin \Theta_t} \sigma_I f_\varphi(\Theta_t, \Phi_t, \Pi_t) \right] dt + \Pi_{\varphi j} dW_{-,t}^j \\ d\Omega_\chi &= \Pi_{\chi j} dW_{-,t}^j \end{aligned} \quad (5.30)$$

with the rotational effective potential (5.21) from the classical analysis. In addition we introduce the functions f_ϑ, f_φ as follows

$$\begin{aligned} f_\vartheta(\vartheta, \varphi, \Pi_t) &= \sin \varphi (\Pi_{\vartheta\varphi} - \Pi_{\vartheta\chi} \cos \vartheta) + \cos \varphi (\Pi_{\varphi\chi} \cos \vartheta - \Pi_{\varphi\varphi} \csc \vartheta) \\ f_\varphi(\vartheta, \varphi, \Pi_t) &= \cos \varphi (\Pi_{\vartheta\chi} - \Pi_{\vartheta\varphi} \cos \vartheta + \Pi_{\varphi\vartheta} \csc \vartheta) \\ &\quad - \sin \varphi (\Pi_{\vartheta\vartheta} \csc \vartheta + \Pi_{\varphi\varphi} \cos \vartheta - \Pi_{\varphi\chi}). \end{aligned} \quad (5.31)$$

The momentum equations (5.30) may be written in terms of the Cartesian spin vector s_t as

$$ds_t = \gamma [s_t \times B] dt + \sigma_I^2 T(\Theta_t, \Phi_t, \tilde{\Pi}_t) dt + s_t \times (\tilde{\Pi}_t dW_{-,t}), \quad (5.32)$$

where $\tilde{\Pi}_t = J_L^{-1} \Pi_t$. T is an additional quantum torque depending on ϑ, φ and $\tilde{\Pi}_t$ following f_ϑ, f_φ in equation (5.30) and has only x and y components. Hence, the classical equations are recovered for $\sigma_I^2 \rightarrow 0$, where $\Pi_t, \tilde{\Pi}_t$ vanish, and the spin $s_t = s(t)$ is a real quantity. Note that in the present case, ‘‘classical limit’’ refers to $\hbar/I_m \rightarrow 0$ with $\Omega_j = \Omega_j^v - i\Omega_j^u \rightarrow \Omega_j^v$, since the diffusive behavior disappears, i.e., $\Omega_j^u \rightarrow 0$.

The final step in the derivation of the quantum Hamilton equations is related to the constraint that the controls for the momenta should be feedback controls, i.e., $\Omega_t = \Omega(t, \theta)$. Assuming that the momenta depend on time t and on the orientation variables θ , there is due to the complex Itô formula (4.25)

$$\Pi_{jl} = \frac{1+i}{2} h_l^k \partial_k \Omega_j = \frac{1+i}{2} (J_{\vartheta, \varphi, \chi} \Omega H)_{jl} \quad (5.33)$$

with $J_{\vartheta, \varphi, \chi} \Omega$ as Jacobi matrix for the rotational momentum Ω_j . Note that the feedback momentum here is still complex, i.e., $\Omega_j(t, \theta) = g_{jk}^I (\omega_v^k(t, \theta) - i\omega_u^k(t, \theta)) + B_j(t, \theta)$. Then f_ϑ and

⁹ $\Omega_t = P_t$ in this case.

f_φ in equations (5.30) may be rewritten with the partial derivatives

$$f_\vartheta(\vartheta, \varphi) = \frac{(1+i)\sigma_I}{4\sin\vartheta} (\partial_\varphi\Omega_\chi + 2\partial_\chi\Omega_\varphi - 2(\partial_\varphi\Omega_\varphi + \partial_\chi\Omega_\chi) \cos\vartheta + \partial_\varphi\Omega_\chi \cos(2\vartheta)) \quad (5.34)$$

$$f_\varphi(\vartheta, \varphi) = \frac{(1+i)\sigma_I}{2} (\partial_\vartheta\Omega_\chi - \partial_\chi\Omega_\vartheta + \cos\vartheta(\partial_\varphi\Omega_\vartheta - \partial_\vartheta\Omega_\varphi)) \quad (5.35)$$

In the next subsection, we consider freely spinning particles, which allows us to simplify, e.g., $f_\vartheta = f_\varphi = 0$, and solve the QHE (5.28) and (5.30) for a freely spinning particle. Before that, we will consider the associated spin operators.

Correspondence to spin operators

The stochastic Hamiltonian (5.29) in terms of the feedback momenta reads

$$\begin{aligned} \mathcal{H}_s &= \frac{\Omega^2}{2I_m} - \gamma\Omega \cdot B + \frac{I_m\gamma^2 B^2}{2} + i\frac{\sigma_I^2}{2} \cot\vartheta\Omega_\vartheta + i\sigma_I^2 g^{kl} \partial_k\Omega_l \\ &= \frac{1}{2I_m} g^{ij}\Omega_i\Omega_j + i\frac{\sigma_I^2}{2} \cot\vartheta\Omega_\vartheta - \gamma g^{ij}\Omega_i B_j + \frac{I_m\gamma^2}{2} g^{ij} B_i B_j + i\sigma_I^2 g^{kl} \partial_k\Omega_l. \end{aligned} \quad (5.36)$$

Similar to the Schrödinger quantization of a classical Hamiltonian, it is possible to quantize the classical part of Hamiltonian (5.36), i.e., with $\sigma_I \rightarrow 0$ and by replacing $\Omega_j \rightarrow -i\hbar\partial_j$ in (5.24) there is

$$\hat{s}^2 = -\hbar^2 (g^{ij}\partial_{ij}^2 + \cot\vartheta\partial_\vartheta) \equiv -\hbar^2 \Delta. \quad (5.37)$$

We see a direct correspondence if we set $B = 0$ in the stochastic Hamiltonian (5.36). The considered Laplace Beltrami operator Δ has eigenfunctions for eigenvalues $j(j+1)$, where $j \in \{\frac{n}{2} | n \in \mathbb{N}_0\}$. Bopp & Haag [BH50] and also Rosen [Ros51] showed that, in general two-valued, representations $D_{\mu\nu}^s(\vartheta, \varphi, \chi)$ form a complete orthonormal basis, $|\mu|, |\nu| \leq js$. Two valued here refers to one of the two angles φ or χ taking values in $[-2\pi, 2\pi)$ instead of $[-\pi, \pi)$. By restricting the eigenfunctions to the subgroup of single-valued function, i.e. $\varphi, \chi \in [-\pi, \pi)$, these describe only integer j . This means if j is half an odd-integer, then the eigenfunctions are double-valued. Similar explanations were found in earlier works by Phillips [PT27] for integer spins on $SO(3)$ and Casimir [Cas32] including half-integer spins on $SU(2)$.

For example, the eigenfunctions for Δ on $SO(3)$ can be expressed as

$$D_{\mu\nu}^{\frac{1}{2}}(\vartheta, \varphi, \chi) = \exp(i(\mu\varphi + \nu\chi)) i^{\frac{1}{2}+\mu} \cos\frac{\vartheta}{2}. \quad (5.38)$$

for $B = 0$, $j = \frac{1}{2}$, and $\mu = \nu = \pm j$. These eigenfunctions can be utilized to return to the stochastic formalism, where the osmotic velocities are determined using the wave function's standard form through the potentials $R(\vartheta)$ and $S(\varphi, \chi)$ in the exponent. Specifically, we define

$$\omega_u^i = g_I^{ij} 2\hbar\partial_j R \quad (5.39)$$

$$\omega_v^i = g_I^{ij} 2\hbar\partial_j S. \quad (5.40)$$

Finally, for $\mu = \nu = \pm 1/2$, we obtain

$$\omega_u = -\frac{\hbar}{2I} \tan\frac{\vartheta}{2} e_\vartheta \quad \text{E}[I\omega_u] = 0 \quad (5.41)$$

$$\omega_v = \pm \frac{\hbar}{2I} \frac{1}{1 + \cos\vartheta} (e_\varphi + e_\chi) \quad \text{E}[I\omega_v] = \pm \frac{\hbar}{2} e_\varphi \quad (5.42)$$

and

$$\mathbb{E}[I^2(\omega_u + \omega_v)^2] = \frac{3\hbar^2}{4}. \quad (5.43)$$

Here, e_φ denotes the rotation around the z axis in the reference frame, and the average $\mathbb{E}[\cdot]$ is taken as an ensemble average. In these particular cases, the ensemble average of the spin is directed along the φ rotation axis. Therefore, *spin up* corresponds to $\mathbb{E}[I\omega_v] = \frac{\hbar}{2}e_\varphi$, and *spin down* corresponds to $\mathbb{E}[I\omega_v] = -\frac{\hbar}{2}e_\varphi$. It is worth noting that the inertia I_m does not factor into the expectation values. Moreover, higher values of the spin quantum number s are also compatible with the anticipated values from quantum mechanics [Dan77]. These states can be recovered in the numerical solutions to the QHE for a freely spinning particle, see section 5.3.

Connection to Wigner functions

Consider the common set of eigenvectors or pure spin states $|jm\rangle$ given in (5.1) and (5.2). These eigenvectors can be rotated with a matrix \mathcal{R} described with the zxz Euler angles $(\vartheta, \varphi, \chi)$ in order to get the so-called Wigner-D-functions [Wig31]

$$D_{m'm}^j(\vartheta, \varphi, \chi) = \langle jm' | \mathcal{R}(\vartheta, \varphi, \chi) | jm \rangle \quad (5.44)$$

in the zxz convention. The matrix D^j itself is unitary, and it is an irreducible representation of $SU(2)$, with $j \in \{n/2 | n \in \mathbb{N}\}$, and of $SO(3)$, with $j \in \mathbb{N}$.

The elements $D_{m'm}^s$ are functions of the Euler angles $\theta = (\vartheta, \varphi, \chi)$ and form a complete set $\int d\theta D_{l'm'}^j D_{lm}^j = \delta_{l'l} \delta_{m'm} \delta_{j'j}$. Hence, for each wave function $|\psi\rangle$ in the Hilbert space $M = \mathbb{R}^3 \times SO(3)$ we can expand

$$|\psi\rangle = \sum_{j,m} c_j^m D_{ml}^j, \quad (5.45)$$

which is referred to as Peter-Weyl Decomposition [PW27]. Here l is fixed, c_j^m may depend on time and position and $D_{ml}^j = \langle \theta | jm \rangle$. Then the Wigner-D functions associate the momentum representation $|jm\rangle$ to the orientation representation $|\theta\rangle$ [Hol95]. For j (and l) fixed, for example, we end up with the $2j + 1$ functions D_{ml}^j associated to the spinor representation for a non-relativistic spin- j particle.

Take the canonical angular momentum from (5.24), namely $s = \Sigma + I_c B$. Now replace Ω_j by $i\hbar\partial_j$. This operator, \hat{J} , acting on the Euler angles ϑ, φ, χ has the eigenvalues

$$\hat{J}_z D_{m'm}^{j*}(\vartheta, \varphi, \chi) = \hbar m' D_{m'm}^{j*}(\vartheta, \varphi, \chi) \quad (5.46)$$

$$\hat{J}^2 D_{m'm}^{j*}(\vartheta, \varphi, \chi) = \hbar^2 j(j+1) D_{m'm}^{j*}(\vartheta, \varphi, \chi), \quad (5.47)$$

where $D_{m'm}^{j*}$ is the complex conjugate of $D_{m'm}^j$ and

$$\begin{aligned} \hat{J}_x &= -i\hbar \left(\cos \varphi \partial_\vartheta + \frac{\sin \varphi}{\sin \vartheta} \partial_\chi - \frac{\sin \varphi \cos \vartheta}{\sin \vartheta} \partial_\varphi \right) \\ \hat{J}_y &= -i\hbar \left(\sin \varphi \partial_\vartheta - \frac{\cos \varphi}{\sin \vartheta} \partial_\chi + \frac{\cos \varphi \cos \vartheta}{\sin \vartheta} \partial_\varphi \right) \\ \hat{J}_z &= -i\hbar \partial_\varphi \\ \hat{J}^2 &= -\hbar^2 (g^{ij} \partial_{ij} + \cot \vartheta \partial_\vartheta). \end{aligned} \quad (5.48)$$

The operator \hat{J} is the same as the one proposed by Bopp and Haag [BH50] and fulfills the usual commutation relations (5.1) for angular momentum operators. Moreover, the Wigner-D representations $D_{m'm}^{j*}$ are the same eigenfunctions as given in (5.38) and will be used as

a reference in the numerical calculation of the QHE for the freely spinning particle.

5.4 Freely spinning particle

This section focuses on the numerical solution to the QHE (5.28) and (5.30) for a freely rotating particle. Specifically, we aim to find stationary processes $(\Theta_t, \Omega(t, \Theta_t))$ that satisfy equations (5.28), (5.30) and minimize the energy of the system.

Without any assumption about the external field, we have $E[d\Omega_\chi] = 0$, meaning that the particle's eigenrotation is constant on average. By assuming optimal feedback controls, namely $\Omega_\chi = \Omega_\chi(t, \theta)$, a trivial solution to the backward equation is a constant $\hbar\nu \in \mathbb{C}$.

In a second step, we can choose $B = B e_z$ such that $(s \times B)_z = 0$. Furthermore, we assume that the feedback solutions for the canonical angular momenta are decoupled, i.e., $\Omega_\vartheta(\vartheta), \Omega_\varphi(\varphi)$, so that $f_\varphi = f_\vartheta = 0$; see equation (5.31). Then, the drift term for $d\Omega_\varphi$ is zero. Hence, a similar argument holds for constant $\Omega_\varphi = \Omega_\varphi(t, \theta)$. This is due to the specific choice of symmetry in the zxz Euler angle parametrization and the fact that the magnetic field is inherited in the canonical angular momentum $\Omega_\varphi = g_{\varphi j}^I \omega_q^\varphi + I_c B_z$. Note that in cases of constant $\Omega_\varphi, \Omega_\chi$, the contravariant angular velocity components $\omega_q^\varphi = \frac{1}{I_m \sin^2 \vartheta} (\Omega_\varphi - \cos \vartheta \Omega_\chi) - \gamma B_z$ and $\omega_q^\chi = \frac{1}{I_m \sin^2 \vartheta} (\Omega_\chi - \cos \vartheta \Omega_\varphi)$ depend on ϑ , for example. Hence, the drift terms in equations (5.28) for $d\varphi$ and $d\chi$ are not constant for constant canonical angular momenta $\Omega_\varphi, \Omega_\chi$.

The properties of the real-valued current and osmotic angular velocities, i.e., the corresponding angular momenta Ω_i^v and Ω_i^u imply that $\Omega_\varphi^u = \Omega_\chi^u = 0$. This is because $\omega_u^i \sim \nabla^i \log \rho$, and thus the expectation value of the osmotic velocity $E[I_m \omega^u] = E[I(\omega_\vartheta^u e_\vartheta + \omega_\varphi^u e_\varphi + \omega_\chi^u e_\chi)] = 0$ must vanish. We can conclude that the angular momenta $\Omega_\chi = \hbar\nu$ and $\Omega_\varphi = \hbar\mu$ with real-valued constants $\mu, \nu \in \mathbb{R}$ are solutions of the QHE for the momenta (5.30) as feedback controls. The constant μ corresponds to the precession around the z -axis in the lab frame, while ν corresponds to the eigenrotation in the body frame, according to the definitions of the Euler angles.

In the final step, we can separate the real and imaginary parts of equations (5.30) and express the SDE for the canonical angular momentum in real space as $\Omega_j^v + \Omega_j^u$. This gives

$$\begin{aligned} d\Theta_t &= \frac{1}{I} [\Omega_\vartheta^v \pm \Omega_\vartheta^u \mp \frac{\hbar}{2} \cot \Theta_t] dt + h_j^\vartheta \cdot dW_{\pm, t}^j \\ d(\Omega_\vartheta^v + \Omega_\vartheta^u) &= \left[\partial_\vartheta V_{\text{eff}}^{\text{rot}}(\Theta_t, \mu, \nu) + \frac{\sigma_I^2}{2 \sin^2 \Theta_t} (\Omega_\vartheta^u - \Omega_\vartheta^v) \right] dt + h_j^k \partial_k (\Omega_\vartheta^u + \Omega_\vartheta^v) dW_{-, t}^j \quad (5.49) \\ \Omega_\varphi^v &= \hbar\mu \\ \Omega_\chi^v &= \hbar\nu. \end{aligned}$$

If both μ and ν are zero, the trivial feedback solution for the ϑ component is $\Omega_\vartheta^v(\vartheta) = \Omega_\vartheta^u(\vartheta) = 0$. Otherwise, a numerical solution can be obtained for the QHE.

The assumptions presented for a spinning particle under a constant magnetic field along z in this section enable a solution to the QHE in the stationary case where the probability distribution is time-independent. Furthermore, in the stationary case, we can make the assumption that $\Omega_\vartheta^v = 0$, which simplifies equations (5.9) and (5.30) to effectively describe a one-dimensional problem, as follows

$$\begin{aligned} d\Theta_t &= \frac{1}{I_m} [\pm \Omega_\vartheta^u \mp h/2 \cot \vartheta] dt + h_j^\vartheta dW_{t \pm}^j \\ d\Omega_\vartheta^u &= \left[\partial_\vartheta V_{\text{eff}}^{\text{rot}}(\Theta_t, \mu, \nu) + \frac{\hbar}{2 I_m \sin^2 \Theta_t} \Omega_\vartheta^u \right] dt + h_j^k \partial_k \Omega_\vartheta^u dW_{-}^j \quad (5.50) \\ \Omega_\varphi^v &= \hbar\mu, \quad \Omega_\chi^v = \hbar\nu. \end{aligned}$$

This coupled system of FBSDEs can be solved numerically in line with the algorithm given

in the appendix B. The detailed numerical description is given in the following subsection.

5.4.1 Numerical solution

Our objective is to determine a feedback control function $\Omega_\vartheta(\vartheta)$ for given $\Omega_\varphi = \hbar\mu$, $\Omega_\chi = \hbar\nu$. To obtain the stationary solution of the coupled stochastic differential equations (5.50), we can use either the forward or backward SDE for the angle Θ_t . In this numerical solution, we use the forward equation for $d\Theta_t$ coupled to the backward SDE for the canonical angular momentum.

We introduce dimensionless variables with a time scale c_t , such that $t = c_t\tilde{t}$, $\omega^j = \tilde{\omega}^j/c_t$, and $dW = \sqrt{c_t}d\tilde{W}$. Since the unit of Ω_j is the same as $[I_m\omega_j] = Js$, we define the canonical angular momentum as multiples of the reduced Planck constant, $\Omega_j = \hbar\tilde{\Omega}_j$. This gives us the following equations

$$\begin{aligned} d\Theta_t &= [\tilde{\Omega}_\vartheta^u - 1/2 \cot \Theta_t] \frac{\hbar c_t}{I_m} d\tilde{t} + \sqrt{\frac{\hbar c_t}{I_m}} \tilde{h}_j^\vartheta d\tilde{W}_{t,+}^j, \\ d\tilde{\Omega}_\vartheta^u &= \left[\partial_\vartheta V_{\text{eff}}^{\text{rot}}(\Theta_t, \mu, \nu) + \frac{\tilde{\Omega}_\vartheta^u}{2 \sin^2 \vartheta} \right] \frac{\hbar c_t}{I_m} d\tilde{t} + \sqrt{\frac{\hbar c_t}{I_m}} \tilde{h}_j^k \partial_k \tilde{\Omega}_\vartheta^u d\tilde{W}_-^j. \end{aligned} \quad (5.51)$$

Thus, the natural choice for the time scale is $c_t = I_m/\hbar$. This eliminates other fundamental constants from the equations of motion for a freely spinning particle. Furthermore, when $I_m \rightarrow 0$, the time scale also goes to zero.

The Euler-Maruyama discretization of equation (5.51) for timestep $n \in \{0, \dots, N\}$ is given by

$$\begin{aligned} \Theta_{n+1} &= \Theta_n + [\tilde{\Omega}_{\vartheta,n}^u - 1/2 \cot \Theta_n] \Delta\tilde{t} + \tilde{h}_j^\vartheta \Delta\tilde{W}_{+,n}^j \\ \tilde{\Omega}_{\vartheta,n}^u &= \frac{\sin^2 \Theta_n}{\sin^2 \Theta_n + 2\Delta\tilde{t}} \left[\tilde{\Omega}_{\vartheta,n+1}^u + \partial_\vartheta V_{\text{eff}}^{\text{rot}}(\Theta_n, \mu, \nu) \Delta\tilde{t} + \tilde{h}_j^\vartheta \partial_k \tilde{\Omega}_{\vartheta,n}^u \Delta\tilde{W}_{-,n}^j \right]. \end{aligned} \quad (5.52)$$

Here, an implicit scheme for the backward equation was used. Equations (5.52) can be simplified by taking into account that the feedback process $\tilde{\Omega}_\vartheta^u(\vartheta)$ depends only on ϑ , but not on ϕ and χ . This leads to:

$$\begin{aligned} \Theta_{n+1} &= \Theta_n + [\tilde{\Omega}_{\vartheta,n}^u - 1/2 \cot \Theta_n] \Delta\tilde{t} + \Delta\tilde{W}_{+,n} \\ \tilde{\Omega}_{\vartheta,n}^u &= \frac{\sin^2 \Theta_n}{\sin^2 \Theta_n + 2\Delta\tilde{t}} \left[\tilde{\Omega}_{\vartheta,n+1}^u + \partial_\vartheta V_{\text{eff}}^{\text{rot}}(\Theta_n, \mu, \nu) \Delta\tilde{t} + \partial_\vartheta \tilde{\Omega}_{\vartheta,n}^u \Delta\tilde{W}_{-,n} \right]. \end{aligned} \quad (5.53)$$

For the numerical treatment, one can use either equation in (5.53) as is or rewrite it by taking conditional expectation with respect to the filtration \mathcal{P}_n generated by the forward process Θ_n up to time-step n

$$\tilde{\Omega}_{\vartheta,n}^u = \frac{\sin^2 \Theta_n}{\sin^2 \Theta_n + 2\Delta\tilde{t}} \left(\partial_\vartheta V_{\text{eff}}^{\text{rot}}(\Theta_n, \mu, \nu) + \left[\tilde{\Omega}_{\vartheta,n+1}^u \middle| \mathcal{P}_n \right] \Delta\tilde{t} \right). \quad (5.54)$$

The initial value of Θ_t , denoted by Θ_0 , is chosen randomly from a uniform distribution over the interval $(0, \pi)$. The final value of the feedback process $\tilde{\Omega}_\vartheta^u$ at time T , denoted by $\tilde{\Omega}_{\vartheta,T}^u$, is calculated iteratively using the angle ϑ as input to the osmotic angular velocity function $\tilde{\Omega}_\vartheta^u(\vartheta)$.

To numerically compute the solution, a Euler-Maruyama discretization of (5.51) with a time-step $\Delta\tilde{t} = 0.01$ and $N = 100$ time-steps is used. We generate 10^5 sample paths per iteration using the conditional expectation. Results are shown in figures 5.4 and 5.7.

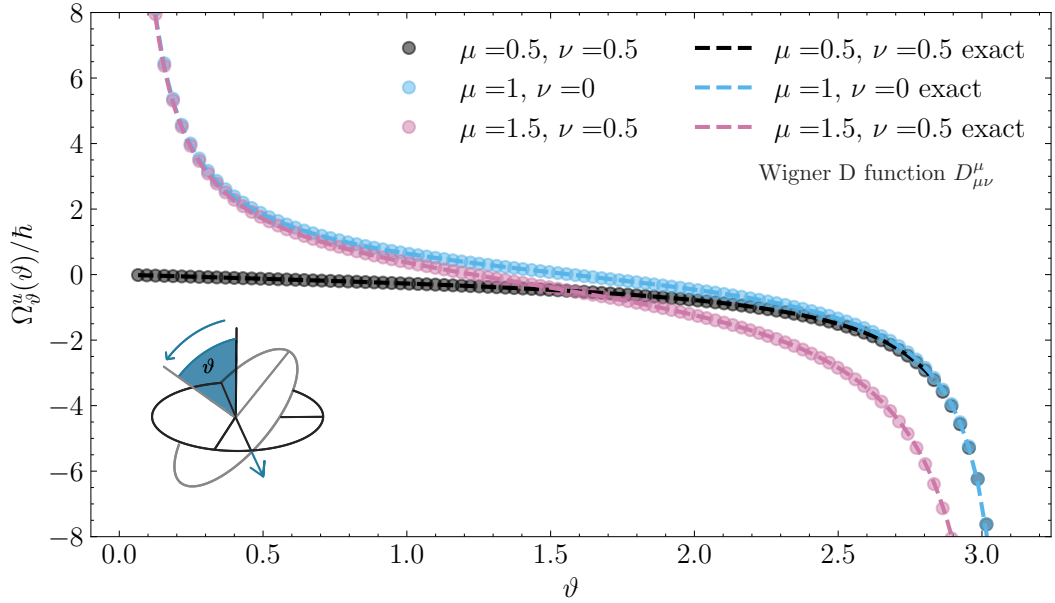


Figure 5.4: The plot compares the numerically calculated velocity fields (circles) and the corresponding “exact” fields obtained from the eigenfunctions (dashed lines) for the rigid spin operator [BH50] for three different combinations of μ and ν , as given in equation (5.38).

5.4.2 Results

The figure 5.4 displays numerical results for the optimal feedback control of the osmotic canonical angular momentum Ω_{ϑ}^u . It shows three different choices of constants μ and ν as points, while the dashed lines represent the exact velocities calculated from the Wigner functions $D_{\mu\nu}^{\mu}$ for the rigid spin operator. These Wigner functions are derived in ref. [BH50] and explained in section 5.3. The calculated velocities are in perfect agreement with those obtained from the Wigner functions.

For example, consider the two cases $\mu = \nu = \frac{1}{2}$ (black) and $\mu = 1, \nu = 0$ (red). In the latter case, Ω_{ϑ}^u keeps the nutation angle of the particle’s orientation between 0 and π . The black curve, on the other hand, shows that the osmotic velocity tries to keep the orientation parallel to the z axis, i.e., $\vartheta = 0$.

The Wigner-D representations $D_{\mu\nu}^j$ generally have nodes where $\mu, \nu \leq j$, and j is the spin quantum number. However, for $|\mu| = j$ or $|\nu| = j$, the Wigner functions are node-free except for the boundaries $\vartheta = 0, \pi$. This property allows the determination of the critical processes in the numerical treatment of the QHE. It corresponds to the system’s lowest energy given the initial (or final) conditions, i.e., $\Omega_{\varphi} = \hbar\mu$ and $\Omega_{\chi} = \hbar\nu$. This suggests that the QHE given in (5.51) give rise to spin states where the spin quantum number and the spin projection number are the same, i.e., $\mu = j = m$. The ground state should describe the non-singular diffusion that corresponds to the Wigner functions.

Spin- $\frac{1}{2}$ process

Consider the numerical solution to $\mu = -\nu = \frac{1}{2}$ in (5.50). After sufficient iteration runs in the numerical algorithm, one can visualize a sample trajectory Θ_t of the orientation and the canonical angular momentum s_t . The change of orientation for a particle in terms of the Euler angles is visualized in the left of figure 5.5. It shows the trace of the tip of the unit vector (black arrow) along the x -axis in the body frame over time. The rotation of the vector (and the particle) is characterized by the Euler angles $(\vartheta, \varphi, \chi)$, namely their stochastic processes $(\Theta_t, \Phi_t, \mathcal{X}_t)$ for a realization, as shown to the right of figure 5.5. The Euler angles were calculated by numerically integrating the forward SDEs (5.9).

The φ -component is stochastically periodic due to an additional constant drift that de-

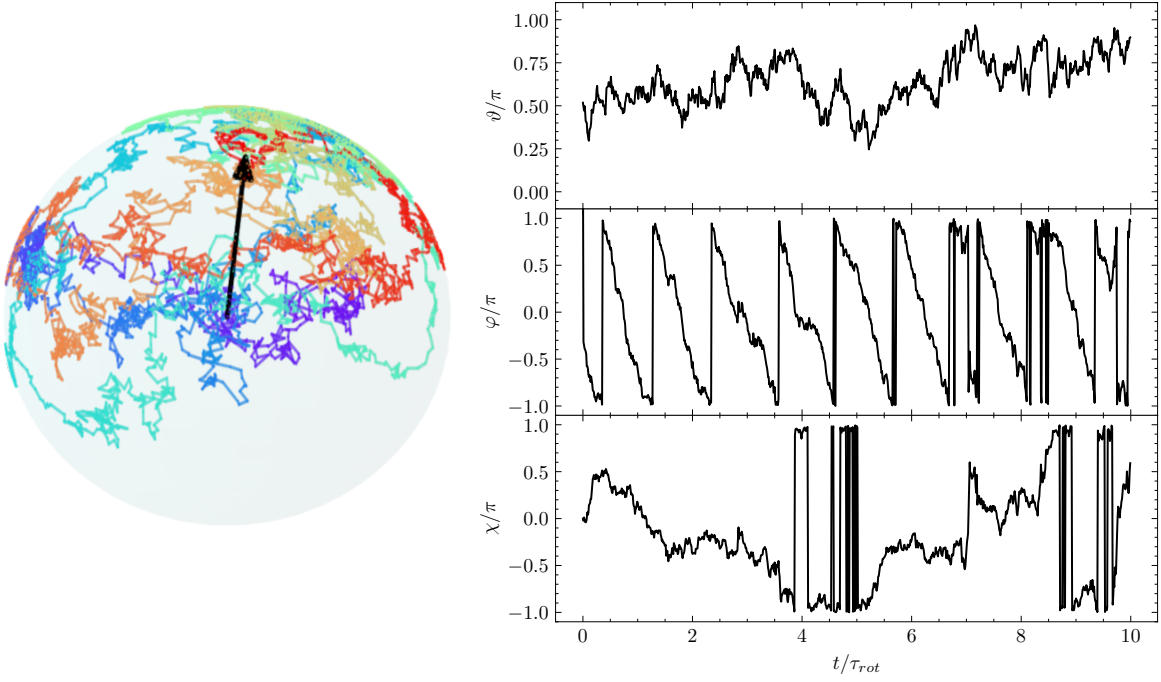


Figure 5.5: The plots presented here are based on a realization of the stochastic process Θ_t in an external field of $B = B e_z$ together with the backward integration for the canonical angular momenta, obtained from the numerical solution of the QHE (5.50) with $\mu = -\nu = -1/2$. The plot on the left shows the change in orientation as a unit vector (black arrow) fixed in the body frame, with the trace visualizing the path of the vector. The three stacked graphs on the right display the corresponding Euler angles $\vartheta, \varphi, \chi \in [0, \pi] \times [-\pi, \pi]^2$ as a function of time, calculated from equation (5.50).

depends on the magnitude of the external magnetic field, since $\omega_v^\varphi = g_I^{\varphi j} \frac{\hbar}{I_m} \Omega_j^v - \gamma B$. The characterization of this state can be done easily by calculating the spin

$$s_t = s_t^v + s_t^u = I_m(\omega_t^v + \omega_t^u) = g_I^{kl}(\Omega_k^u + \Omega_k^v)e_l \quad (5.55)$$

as the sum of current and osmotic angular velocity. The time-dependent components of the stochastic process s_t are illustrated in figure 5.6. It is evident that the x (black) and y (blue) components of the spin in stochastic mechanics are clearly stochastic, whereas the z (magenta) component is constant at $-\frac{\hbar}{2}$.¹⁰ By using the angular velocities $\Omega_\vartheta^u = -\frac{\hbar}{2} \cot \frac{\vartheta}{2}$ (also shown in figure 5.4) and $\Omega_\varphi^v = -\Omega_\chi^v = -\frac{\hbar}{2}$, we can calculate the spin fields as feedback control as follows

$$s(\vartheta, \varphi) = s_v(\vartheta, \varphi) + s_u(\vartheta, \varphi) = \frac{\hbar}{2} \begin{pmatrix} -\cot \frac{\vartheta}{2} (\cos \varphi + \sin \varphi) \\ \cot \frac{\vartheta}{2} (\sin \varphi - \cos \varphi) \\ -1 \end{pmatrix}, \quad (5.56)$$

which represents a spin-down state.

To further confirm this, compare the expectation values of the stochastic process with the usual eigenvalues of a pure spin state $|jm\rangle$ in Dirac notation with the spin quantum number j and the spin projection number m . In this context, $\langle \hat{s}_z \rangle_{jm} = \hbar m$ and $\langle \hat{s}^2 \rangle_{jm} = \hbar^2 j(j+1)$, where $\langle \cdot \rangle_{jm}$ denotes the quantum expectation with respect to the state $|jm\rangle$. The stochastic analogue of these values are the ensemble averages given by

$$\begin{aligned} \mathbb{E}[s] &= \mathbb{E}[s_v + s_u], \\ \mathbb{E}[s^2] &= \mathbb{E}[(s_v + s_u)^2]. \end{aligned} \quad (5.57)$$

¹⁰The spin components of s_t in the figure are plotted from the numerical evaluation of the BSDE for Ω_t and not from the feedback fields $s(t, \Theta_t)$.

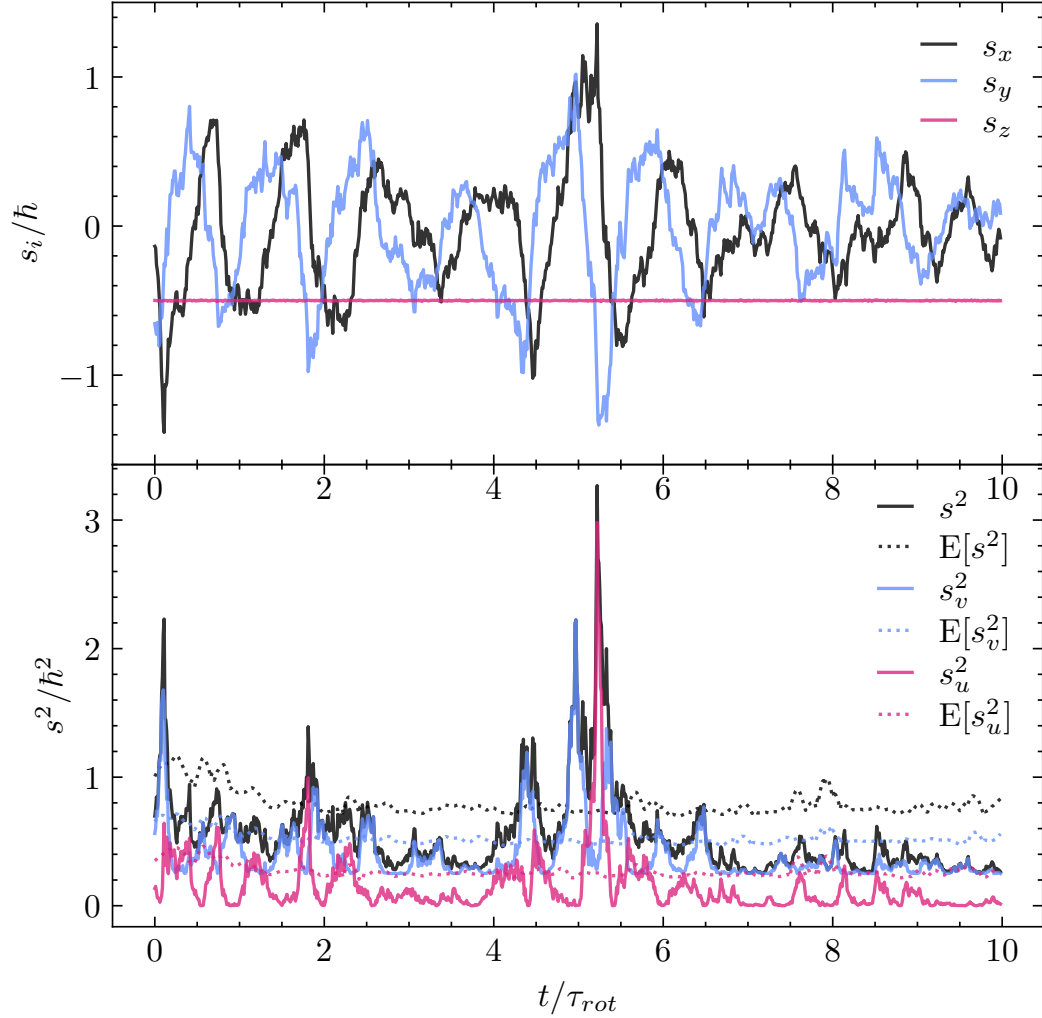


Figure 5.6: The top plot shows the components of the spin s_t as a function of time for the same sample path as shown in figure 5.5. It is apparent that the z component of the spin is constant. (The barely visible small scale fluctuations of the s_z component are due to the numerical accuracy in the calculation.) The lower plot shows the squares of the current and osmotic spins s_v^2 (blue) and s_u^2 (magenta), as well as the total spin $s^2 = (s_v + s_u)^2$ (black). The dotted lines show the ensemble average of 1000 sample paths, indicating constant expectation values of the spins.

For the example shown in figure 5.6, this leads to $E[s_u] = 0$ and $E[s_v] = -\frac{\hbar}{2}e_z$, indicating that there is no osmotic contribution to $E[s]$. However, this is not the case for the magnitude of the spin shown in the lower plot in figure 5.6. Unlike $s_z(\vartheta, \varphi)$, the stochastic process $s^2(\vartheta, \varphi)$ is not constant. It is a combination of the current angular velocity proportion $E[s_v^2] = \frac{\hbar^2}{2}$ (dotted blue) and the non-vanishing contribution of the osmotic angular velocity $E[s_u^2] = \frac{\hbar^2}{4}$ (dotted magenta). Therefore, the expected magnitude is $E[s^2] = \frac{3}{4}\hbar^2$, which leads to an energy

$$\mathcal{H}_s = E[E_s] = E \left[\frac{s^2}{2I_m} - \gamma s \cdot B + \frac{I_m \gamma^2 B^2}{2} \right] = \frac{3\hbar^2}{8I_m} + \gamma \frac{\hbar}{2} B_z + \frac{I_m \gamma^2 B^2}{2}, \quad (5.58)$$

where the stochastic Hamiltonian for the spin \mathcal{H}_s is defined in equation (5.36). We see, that I_m does not enter the spin expectations $E[s]$ and $E[s^2]$, but it does so for the energy, where the limit $I_m \rightarrow 0$ leads to a singular term of the particle's energy due to the spin.

Spin expectations in the general case

The presented results of equations (5.50) demonstrate that the stochastic expectation values of the spin are determined by the parameter μ . In particular,

$$\begin{aligned} E[s] &= E[I_m(\omega_v + \omega_u)] = E[g^{kl}(\Omega_k^u + \Omega_k^v)e_l] = \hbar\mu e_\varphi \\ E[s^2] &= E[I_m^2(\omega_u^2 + \omega_v^2)] = E[(g^{kl}(\Omega_k^u + \Omega_k^v)e_l)^2] = \hbar^2|\mu|(|\mu| + 1), \end{aligned} \quad (5.59)$$

where s denotes the spin vector, and e_φ is the unit vector in the azimuthal direction. Note that the parameter ν determines the spin projection in the body frame, while μ is related to the reference frame.

The above results imply that the numerical solutions of the spin QHE (5.50), illustrated in figure 5.4, are solely determined by the constant μ . These solutions correspond to spin states with $j = |m|$. For instance, for a spin- $1/2$ particle in a magnetic field oriented along the z -axis, the spin down eigenstate corresponds to $\mu = -\frac{1}{2}$, i.e. $E[s] = -\frac{\hbar}{2}e_z$, whereas $\mu = \frac{1}{2}$ corresponds to the spin up state.

At this point there are two open questions emerging from the discussed solutions. The first is related to the quantization of the values for μ (and ν). Secondly, states with $j > |m|$ cannot be evaluated directly from the QHE. Certain spin states, such as $j = 2$ and $m = 0$, cannot be determined without additional restrictions or rules. This is because the QHE only provide a means to solve an optimization problem that leads to the node-free *ground state* of the problem [BPGP19]. These questions are adressed in the following in more detail.

The quantization condition

In this model there is no argument to restrict μ (and ν) to quantized values. E.g., any real $\mu \in \mathbb{R}$ leads to a solution of the QHE (5.30). However, the QHE describe a process for which also a description in terms of the Schrödinger equation exist, i.e., the Hamilton-Jacobi formulation of this process. While all of the spin diffusions are defined on $SO(3)$, the corresponding wave functions $\psi(\vartheta, \varphi, \chi)$ are properly defined for integer and half-integer μ, ν only, where the integral values lead to wave functions defined on $SO(3)$. The half-integer values lead to wave functions on the covering space $SU(2)$ [Nel66].

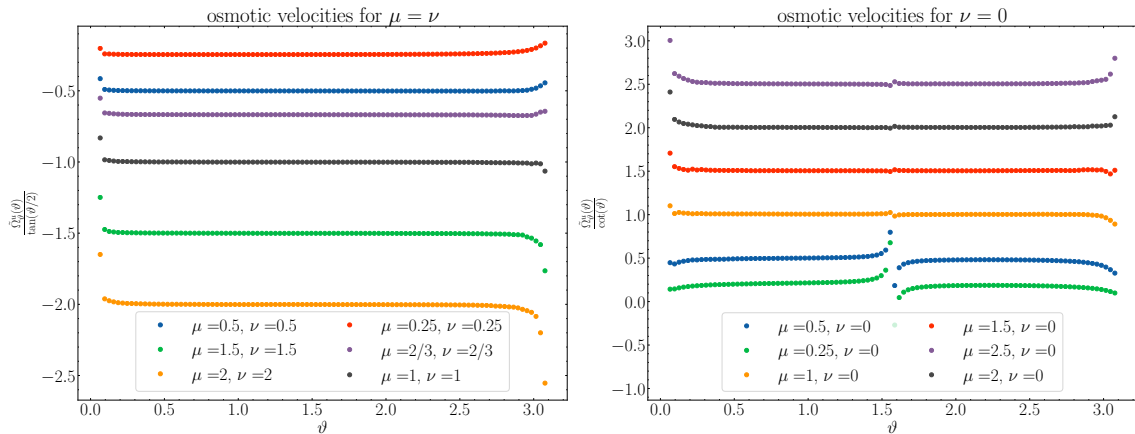


Figure 5.7: The numerical results for $\Omega_y^u / \tan(\vartheta/2)$ as a function of the rotation angle ϑ , for various values of $\mu = \nu$, are displayed in the figure on the left. These results suggest that Ω_y^u can be represented as $-\mu \tan(\vartheta/2)$. On the right side of the figure, the results for $\Omega_y^u / \cot \vartheta$ are shown for different values of μ with ν set to 0. These results indicate that Ω_y^u can be expressed as $\mu \cot \vartheta$ (noting that $\cot \vartheta$ equals 0 at $\vartheta = \pi/2$).

In more detail, from the functions $D_{\mu\nu}^j(\vartheta, \varphi, \chi) = N \exp i(\mu\varphi + \nu\chi)d_{\mu\nu}^j(\vartheta)$, we can see that for $(\varphi, \chi) \in [-\pi, \pi]^2$ and $\mu, \nu \in \mathbb{Z}$, the wave function is single-valued. However, if we consider the double cover of $SO(3)$, which can be described by the Euler angles ϑ, φ, χ if

$(\varphi, \chi) \in [-2\pi, 2\pi]$, then $\exp i(\mu + \nu)$ allows half-integer values for μ and ν [BH50]. If we rotate around the z -axis by 2π , i.e., $\varphi \rightarrow \varphi + 2\pi$, the wave function picks up a minus sign. On the other hand, for $(\varphi, \chi) \in [-\pi, \pi]^2$, the wave function remains unchanged under 2π rotation. By using the single- and double-valued eigenfunctions to the Laplace-Beltrami operator on $SO(3)$, we end up with the usual boson and fermion symmetries for the wave function related to the simply connected double cover of $SO(3)$.

From the QHE alone the velocity fields for the considered eigenstates show no sign of single or double valuedness. The diffusions are defined on $SO(3)$ since there is no need to extend $(\varphi, \chi) \in [-\pi, \pi]^2$ to $(\varphi, \chi) \in [-2\pi, 2\pi]^2$ at this point. The numerical solution to the QHE allows any real constant for μ and ν . This is illustrated in figure 5.7 where we have solutions to pairs of μ, ν which are not described by single- or even double-valued eigenfunctions, e.g., $\mu = \nu = 2/3$. Taking into account the wave functions corresponding to the stochastic velocity fields, however, leads to the usual quantization of μ, ν to half-integers for single- and double-valued wave functions [BH50].

This is in line with the argument by Takabayashi and Wallström as discussed in section 2.5, where an additional quantization condition has to be added ad-hoc for a closed-loop integral of the current (angular) velocity. An alternative for the quantization is offered by the use of partnerpotentials considering the spin in stochastic mechanics. This is discussed in the following.

5.4.3 Quantization of the spin states

It has been shown that the eigenfunctions of the Laplace-Beltrami operator on the rotation group $SO(3)$ and $SU(2)$ share the same eigenvalues as the spin operator [BH50]. Furthermore, stochastic processes based on these eigenfunctions yield the same expected values for the spin [Dan70]. Previous sections have also demonstrated that the stochastic Hamiltonian equations, derived from the Madelung equations, are related to the Schrödinger equation.

Nevertheless, the solutions to the QHE and the Schrödinger equation generally differ. As previously mentioned, the Madelung equations produce a broader set of solutions that can be constrained to those of the Schrödinger equation by imposing an additional ad-hoc “quantization rule” associated with the phase factor of the wave function [Wal94]. Therefore, it is unsurprising that the QHE also yield a more general set of solutions than those of the Schrödinger equation.

To introduce quantization in the spin QHE, we can use supersymmetric Hamiltonian theory, which can be incorporated into the framework of stochastic mechanics [Gri91, KPGP18, BPGP19]. This allows us to generate higher spin states.

Integer spin

For instance, consider the trivial ground state of the freely spinning top, $\Omega_{\vartheta,0}^u = 0$, which serves as our reference value and corresponds to a spin-0 state with quantum numbers $j = 0, m_j = 0$. Recall that

$$d\Theta_t = [\Omega_{\vartheta}^u - \hbar/2 \cot \Theta_t] dt / I_m + \hbar_k^{\vartheta} \cdot dW_{+,t}^k. \quad (5.60)$$

To determine the supersymmetric partner, we can follow a similar approach to that used for the hydrogen atom in section 4.4 or ref. [BPGP19] and define

$$\tilde{\Omega}_{\vartheta}^u = \Omega_{\vartheta}^u - \frac{\hbar}{2} \cot \vartheta, \quad (5.61)$$

which is related to how we factorize the Hamilton operator.

To calculate the first partner potential, we start with $V_0 = 0$, the ground state potential,

and obtain

$$V_1 = V_0 - \frac{\hbar}{I_m} \partial_\vartheta \tilde{\Omega}_{\vartheta,0}^u = \frac{\hbar^2}{2I_m \sin^2 \vartheta}. \quad (5.62)$$

Comparing V_1 with the effective potential

$$V_{\text{eff}}(\vartheta) = \frac{1}{2I_m \sin^2 \vartheta} (\Omega_\varphi^{v2} + \Omega_\chi^{v2} - 2 \cos \vartheta \Omega_\chi^{v2} \Omega_\varphi^{v2}), \quad (5.63)$$

we find that

$$V_1 = V_{\text{eff}} \quad (5.64)$$

for either

$$\Omega_{\varphi,1}^v = \pm \hbar, \Omega_{\chi,1}^v = 0 \quad \text{or} \quad \Omega_{\varphi,1}^v = 0, \Omega_{\chi,1}^v = \pm \hbar. \quad (5.65)$$

This suggests that the new partner potential V_1 obtained from the ground state $\Omega_{\vartheta,0}^u = 0$ leads to the effective potential of a spin state with corresponding quantum numbers $j = 1, m_j = 1$.

Further progress can be made by solving the QHE using the potential V_1 or the Laplace-Beltrami operator's corresponding eigenfunction. Both methods yield $\Omega_{\vartheta,1}^u = \hbar \cot \vartheta$ for the first excited state. This, in turn, enables the calculation of the next partner potential

$$V_2 = V_1 - \frac{\hbar}{I_m^2} \partial_\vartheta \tilde{\Omega}_{\vartheta,1}^u = \frac{4\hbar^2}{2I_m \sin^2 \vartheta} \quad (5.66)$$

Comparison with the effective potential yields

$$V_{\text{eff}} = V_2 \quad \text{if} \quad \Omega_{\varphi,2}^v = \pm 2\hbar, \Omega_{\chi,2}^v = 0 \quad \text{or} \quad \Omega_{\varphi,2}^v = 0, \Omega_{\chi,2}^v = \pm 2\hbar$$

with $\Omega_{\vartheta,1}^u = 2\hbar \cot \vartheta$. Generally speaking, choosing $\tilde{\Omega}_\vartheta^u = \Omega_\vartheta^u - \hbar/2 \cot \vartheta$ gives the eigenstates for integer spin eigenvalues $n \in \mathbb{Z}$

$$\Omega_{\varphi,n}^v = n\hbar, \Omega_{\chi,n}^v = 0 \quad \text{or} \quad \Omega_{\varphi,n}^v = 0, \Omega_{\chi,n}^v = n\hbar \quad (5.67)$$

with $\Omega_{\vartheta,n}^u = n\hbar \cot \vartheta$. Similar to the hydrogen atom in section 4.4, the ground state solutions to the partner potentials lead to different quantized spin eigenstates. The choice of $\tilde{\Omega}_\vartheta^u$ here gave a way to determine the integer spin eigenstates.

Half-integer spin

It is also possible to generate the half-integer spin values starting from the trivial zero ground state by using a different decomposition, namely $\tilde{\Omega}_\vartheta^u = \Omega_\vartheta^u - \frac{\hbar}{4} \tan \frac{\vartheta}{2}$. Then, the first partner potential is given by

$$V_1 = V_0 - \frac{\hbar}{I_m} \partial_\vartheta \tilde{\Omega}_{\vartheta,0}^u = \frac{\hbar^2}{8I_m \cos^2 \frac{\vartheta}{2}} \quad (5.68)$$

Comparing this to the effective potential gives

$$V_{\text{eff}} = V_1 \quad \text{for} \quad \Omega_{\varphi,1}^v = \Omega_{\chi,1}^v = \pm \frac{\hbar}{2}. \quad (5.69)$$

This can be generalized for the eigenstates $n \in \frac{1}{2}\mathbb{Z}$ in analogy to the integer case. By choosing $\tilde{\Omega}_{\vartheta}^u = \Omega_{\vartheta}^u - \frac{\hbar}{4} \tan \frac{\vartheta}{2}$, the n th supersymmetric partner has the following eigenvalues

$$\Omega_{\varphi,n}^v = \pm n\hbar, \quad \Omega_{\chi,n}^v = \pm n\hbar \quad (5.70)$$

with $\Omega_{\vartheta,n}^u = -n\hbar \tan \frac{\vartheta}{2}$.

Jumping between different spin projection values m_j with constant value j

The two subsections established a way to determine states from the QHE for a freely spinning particle leading to quantized values of μ and ν . These states correspond to node-free Wigner-D functions $D_{m_j m'_j}^j = D_{\mu\nu}^j$. Using the operator \hat{J} defined in equations (5.48), one can transition between certain states with different values of m_j by applying the ladder operators

$$\hat{J}_{\pm} = (\hat{J}_x \pm i\hat{J}_y) D_{m_j m'_j}^j = \hbar \sqrt{j(j+1) - m_j(m_j \pm 1)} D_{(m_j \pm 1) m'_j}^j \quad (5.71)$$

In analogy to the canonical angular momentum in equation (5.24), it is possible to define the stochastic equivalent of \hat{J}_{\pm} as

$$s_{\pm}(\vartheta, \varphi, \Omega_{\varphi}^v, \Omega_{\chi}^v) = s_x \pm i s_y = e^{\pm i\varphi} \left(\Omega_{\vartheta}^u \pm \frac{1}{\sin \vartheta} (\Omega_{\chi}^v - \cos \vartheta \Omega_{\varphi}^v) \right). \quad (5.72)$$

Using equation (5.71), it can be inferred that the values of $\Omega_{\vartheta,j,m_j \pm 1}^u$ can be calculated from $\Omega_{\vartheta,s,m}^u$ using

$$\Omega_{\vartheta,j,m_j \pm 1}^u = \hbar \frac{\partial_{\vartheta} s_{\pm}}{s_{\pm}} + \Omega_{\vartheta,j,m_j}^u, \quad (5.73)$$

provided that $s_{\pm} \neq 0$. However, if $s_{\pm} = 0$, then $|m_j \pm 1| > j$.

In summary, the aforementioned states that follow from the QHE for a freely spinning particle lead to quantum numbers $j = |m|$ or, in other terms, to $E[s^2] = \hbar^2 |m_j| (|m_j| + 1)$ and $E[s] = \hbar m_j e_{\varphi}$. Take for example $j = m_j = 1$ which state is determined with the QHE (5.50) by choosing $\mu = \nu = \hbar$ leading to $\Omega_{\vartheta,(j=)1,(m_j=)1}^u = -\hbar \tan(\vartheta/2)$. With (5.73) for going 'down' this yields

$$\Omega_{\vartheta,1,0}^u = \hbar \frac{\partial_{\vartheta} (-\hbar \tan(\vartheta/2) + 1/\sin \vartheta (1 - \cos \vartheta))}{-\hbar \tan(\vartheta/2) + 1/\sin \vartheta (1 - \cos \vartheta)} - \hbar \tan(\vartheta/2) = \cot \vartheta, \quad (5.74)$$

which is by the way equivalent to the result when $\mu = 1$ and $\nu = 0$ in (5.50). From the latter result, it is also possible to determine

$$\Omega_{\vartheta,1,-1}^u = \cot \frac{\vartheta}{2} \quad (5.75)$$

In the end, it is possible to determine the same set of states that follow from the Laplace-Beltrami operator with the help of the quantum Hamilton equations only. Putting all together, the (complex) spin field in the reference frame reads

$$s = \frac{\hbar}{2} \begin{pmatrix} -(j + m_j) \tan \frac{\vartheta}{2} e^{-i\varphi} + (j - m_j) \cot \frac{\vartheta}{2} e^{i\varphi} \\ i \left((j + m_j) \tan \frac{\vartheta}{2} e^{-i\varphi} - (j - m_j) \cot \frac{\vartheta}{2} e^{i\varphi} \right) \\ 2m_j \end{pmatrix} \quad (5.76)$$

where j is the spin quantum number and $m_j = -j, j + 1, \dots, j$ is the z projection of the spin field.

Figure 5.8 shows a stochastic realization of a spin-1 particle with $m_j = 0$. Here the z

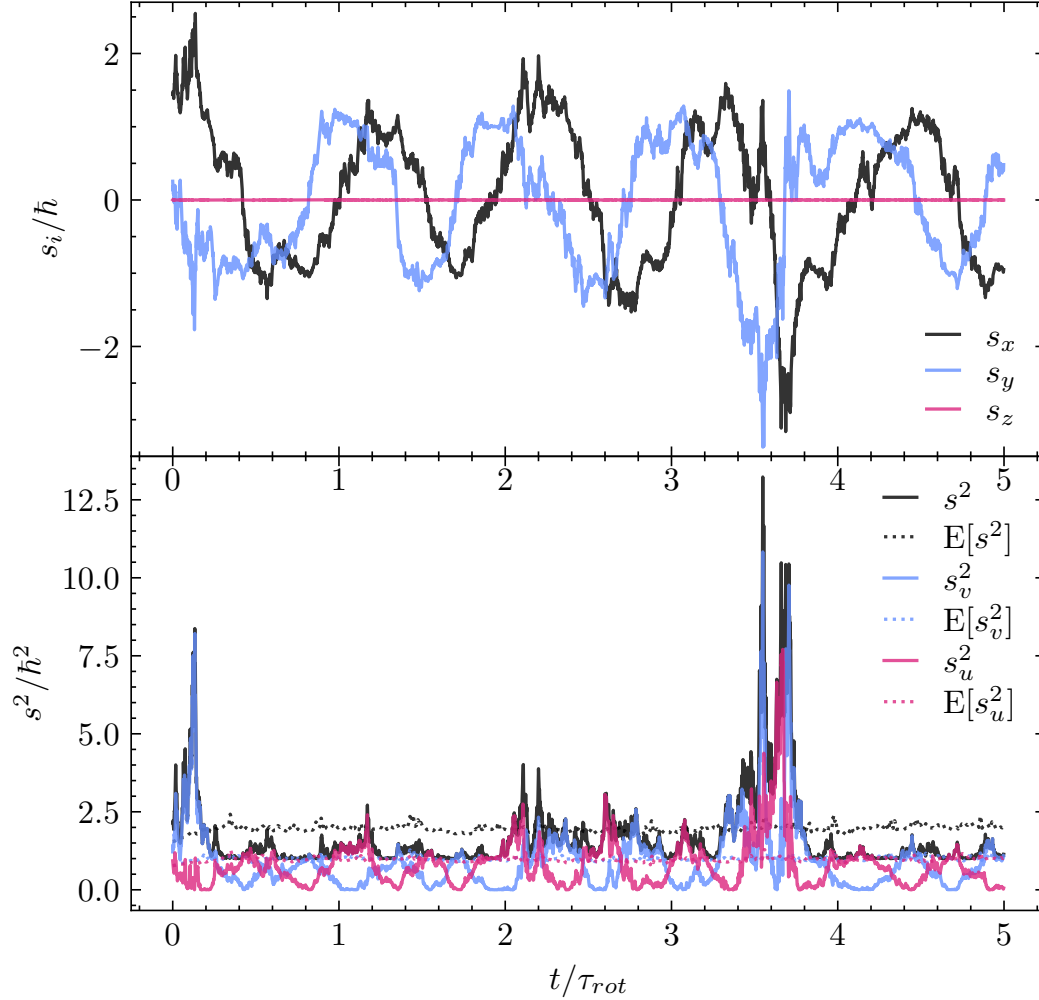


Figure 5.8: The plot shows the stochastic spin corresponding to a $j = 1, m_j = 0$ state similar to figure 5.6. The z component of the spin (magenta) is zero. The lower plot shows the squares of the current and osmotic spin, s_v^2 (blue) and s_u^2 (magenta), as well as the total spin $s^2 = (s_v + s_u)^2$ (black). The dotted lines show the ensemble average of 1000 sample paths, indicating constant expectation values of the spin with $E[s_v^2] \approx \hbar^2$, $E[s_u^2] \approx \hbar^2$ and $E[s^2] \approx 2\hbar^2$.

component of the stochastic spin is 0 so that $E[s_t] = 0$. The ensemble average of the square of the stochastic spin yields $E[s_t^2] = 2\hbar^2$ with $E[s_{u,t}^2] = E[s_{v,t}^2] = \hbar^2$.

5.4.4 Relation to the Pauli equation

Before discussing the coupling of spin to position in space, we relate the spin states derived in this section to the standard treatment in quantum mechanics, where spin is commonly described using spinors. The spinors are column vectors of complex functions $\psi_i(t, x)$, where the number of components depends on the particle's spin or the specific model being used. For example, a spin- $\frac{1}{2}$ particle is typically described by a two-component spinor, which can be used to derive the Pauli equation in the non-relativistic limit. In contrast, the Lorentz-invariant 4-spinor by Dirac is used to describe relativistic particles.

The depiction in the form of a spinor is comparable with a superposition of different quantum states $\Psi = \sum_i \psi_i |i\rangle$ with basis $|i\rangle = (0, \dots, 0, 1, 0, \dots)^T$. There is no information on the spin in $\psi_i(t, x)$ only, hence by writing

$$\Psi(t, x) = \sum_i \psi_i(t, x) |i\rangle \quad (5.77)$$

there is a factorization of the spatial and spin-dependent part for each spinor component. However, the information about the particle's spin is not contained in the individual components of the spinor but rather in the matrix operators in the Hamiltonian that couple the spin to the translational motion.

In this discussion, the non-relativistic stochastic formalism is related to the eigenvectors $|i\rangle$, represented by the corresponding eigenfunctions calculated from the freely spinning model in the QHE. For instance, when $\Omega_\varphi = \Omega_\chi = \hbar/2, \Omega_\vartheta = -i\hbar/2, \tan \vartheta/2$, an associated eigenfunction $e_1(\vartheta, \varphi, \chi) = N e^{i(\varphi+\chi)/2} \cos \vartheta/2$ exists such that $\Omega_k = -i\hbar \partial_k e_1$, where N is a normalization factor. Depending on the Euler angles, the eigenfunctions $e_i(\vartheta, \varphi, \chi)$ and $|i\rangle$ have the same eigenvalues:

$$\hat{s}_z |i\rangle = \hbar m_i |i\rangle \quad (5.78)$$

$$\hat{s}_z e_i(\vartheta, \varphi, \chi) = \hbar m_i e_i(\vartheta, \varphi, \chi). \quad (5.79)$$

With $\hat{s}^2 |i\rangle = \hbar^2 j(j+1) |i\rangle$, the basis vector $|i\rangle$ and the eigenfunctions $e_i(\vartheta, \varphi, \chi)$ are identified with the momentum representation $|jm_i\rangle$. For instance, a new basis for spin- $\frac{1}{2}$ particles in the Pauli-equation, represented by a two-component spinor

$$\Psi = (\psi_1 \ \psi_2) \quad (5.80)$$

can be represented as

$$\tilde{\Psi} = \psi_1 e_1(\vartheta, \varphi, \chi) + \psi_2 e_2(\vartheta, \varphi, \chi). \quad (5.81)$$

Note that the eigenfunctions are the elements of the Wigner-D matrix $e_i = D_{il}^j$ for $j = l = \frac{1}{2}$ (cf. equation (5.45)).

According to the definition used here, two different spin (expectation) values can be calculated. The first one is the orientational average $\bar{s}(t, x)$ associated with the spin field $s(t, x, \theta) = I_m \omega(t, x, \theta) + \gamma I_m B(t, x)$, as introduced in [Hol95],

$$\bar{s} = \frac{1}{\bar{\rho}} \int d\theta s \rho = \frac{1}{\bar{\rho}} \int d\theta \tilde{\Psi}^* \hat{s} \tilde{\Psi} = \frac{1}{\Psi^\dagger \Psi} \Psi^\dagger \hat{s} \Psi \quad (5.82)$$

Here, $d\theta = \sin \vartheta d\varphi d\vartheta d\chi$ and $\bar{\rho} = \int d\theta \rho = \int d\theta \tilde{\Psi}^* \tilde{\Psi}$.¹¹ The correspondence to the spin matrices follows from the orthogonality of e_i , given by

$$\int d\theta e_i^*(\vartheta, \varphi, \chi) e_j(\vartheta, \varphi, \chi) = \delta_{ij}. \quad (5.83)$$

The second expectation value, denoted by $\langle \hat{s} \rangle$, refers to the integration over the whole space at a time t and is given by

$$\langle \hat{s}(t) \rangle = \int dx \Psi^\dagger \hat{s} \Psi = \int dx d\theta \tilde{\Psi}^* \hat{s} \tilde{\Psi}. \quad (5.84)$$

The stochastic picture here suggests a more detailed understanding of the actual (random) behavior of the orientation, where the (measurable) spin represented by spinors can be viewed as the orientational average. The spin operator acting on the spinors is then the marginal spin at a position x in space as a result of the ensemble average over all possible orientations with respect to $\rho(t, x, \theta)$.

This approach is justified by considering the translational and rotational diffusion time scales. In particular, the orientation changes rapidly compared to the changes in position. This is why stochastic models of eigenrotation usually consider a limit where the orientation is averaged out [BH50, Dan70, Nel85, Wal90]. These orientational averages will be

¹¹For a given field $f(t, x, \theta)$, we have $\bar{f} = \frac{1}{\bar{\rho}} \int d\theta f \rho$ accordingly.

used in the stochastic analysis of the Stern-Gerlach experiment and the EPRB paradox in the upcoming chapter

Chapter 6

Spinning particles moving in space

In most experiments, it is impossible to determine a particle's orientational degree of freedom directly. However, this information can be inferred through methods such as a Stern-Gerlach experiment, in which the particle's spin is indirectly measured by its coupling to translation in space. This also applies to measurements of the spin of entangled objects.

A stochastic process is required to describe these experiments, which combines space and rotation diffusion. For a single particle, the stochastic process $Y_t \in M = \mathbb{R}^3 \times SO(3)$ is augmented, $Y_t = (X_t(Y_t), R_t(Y_t))$, where X_t represents the position in space and R_t represents a rotation of the body as introduced in section 5.1.3. Nelson's construction of the



Figure 6.1: The figure illustrates the combination of a stochastic process regarding position and orientation. A quantum object with mass m and inertia I_m is subjected to random perturbations with diffusion constants $\sigma^2 = \hbar/m$ and $\sigma^2 = \hbar/I_m$ as shown to the left. The stochastic motion is governed by an adjusted version of Newton's law, as shown on the right.

conservative diffusion system consists of forward-backward SDEs for dX_t and dR_t , which are provided in the previous sections

$$dX_t = [v(t, Y_t) \pm u(t, Y_t)] dt + \sigma_m dW_{\pm, t} \quad (6.1)$$

$$dR_t = R_t[\omega_v(t, Y_t) \pm \omega_u(t, Y_t)]_{\times} dt + R_t \sigma_I h_i \circ dW_{\pm, t}^i. \quad (6.2)$$

The stochastic process is described by the velocity fields v, ω_v and u, ω_u . These are the current and osmotic (angular) velocities, respectively. They obey a set of partial differential equations following the stochastic definition of the Newton law for a classical force F [Dan70]. The diffusion constant is split into σ_m and σ_I , corresponding to diffusion in \mathbb{R}^3 and rotation in $SO(3)$. The definition of σ_I , as given in section 5.1.3, is analogous to $\sigma_m^2 = \frac{\hbar}{m}$, which considers the diffusion of a particle with mass m . The difference between the two constructions is related to the definition of the diffusion constant, where σ_I leads to an increasingly fast wiggling spin diffusion as the moment of inertia I_m approaches 0.

The coupling of the two processes in the framework of the QHE is a combination of the flat case in section 3.2.2 and the analysis for the rotating body in section 5. It is assumed that there is a time-reversible stochastic process that covers the spatial space and the space of ro-

tations. This process couples the orientation to the position, even in cases where the classical coupling terms are absent. This enables the discussion of the quantized spin properties of a particle after interacting with a magnetic field, as in the Stern-Gerlach experiment. In this experiment, a non-classical torque term is related to the osmotic contribution of the velocity fields, which aligns the spins in the field-free region. This behavior is more apparent in the case of entangled particles, where the particle pairs cannot be described as single particles anymore. As a consequence of the non-separability of the probability distribution, this leads to non-local velocity fields.

In the context of $M = \mathbb{R}^3 \times SO(3)$, two distinct timescales are evident for the diffusions. The timescale for translation depends on the particle's mass and the typical distance it travels, denoted by l . Specifically, $\tau_{\text{trans}} = \frac{m}{\hbar} l^2$. Meanwhile, rotational diffusion scales with the moment of inertia I_m , such that $\tau_{\text{rot}} = \frac{I_m}{\hbar}$. For a classical, spherically symmetric distribution, $I_m \approx mR^2$, where R represents the classical radius of the particle. Typically, R or its upper bound is several orders of magnitude smaller than the translational length scale, i.e., $R \ll l$. Consequently, the jittery rotational diffusion can be approximated by taking the limit as $I_m \rightarrow 0$ [Wal90, Nel85], whereby one deals with averaged values.

The implications of this limit are illustrated in the simulation of one spin measurement, namely the Stern-Gerlach (SG) experiment, and in the discussion of simultaneous measurements on spin pairs, which addresses the Einstein-Podolsky-Rosen-Bohm (EPRB) thought experiment. These examples show that considering averaged quantities of the spin to account for the measurement results suffice.

The structure of this chapter is as follows: First, we derive the classical Hamilton equations for a rigid rotor moving in space. Then, we generalize to the quantum Hamilton equations. Subsequently, we apply the QHE, where the spin is coupled to the position, which includes the system of a charged particle in a constant magnetic field and the idealized Stern-Gerlach experiment. Finally, we analyze the EPRB thought experiment in the framework of quantum mechanics.

6.1 Hamilton equations of motion

The discussion of the classical problem follows section 5.2. In addition to the spinning particle with magnetic moment M , the Lagrangian includes the spatial motion in the kinetic energy as follows

$$T = T^{\text{trans}} + T^{\text{spin}} = \frac{1}{2} m_{ij} v^i v^j + \frac{1}{2} g_{ij}^I \omega^i \omega^j \quad (6.3)$$

where the mass metric is given by $(m_{ij}) = m\mathbb{I}$, and the system's Lagrangian is enhanced as $\mathcal{L} : M \times T_x M \times \mathbb{R}$

$$\mathcal{L} = T - V = \frac{1}{2} m_{ij} v^i v^j + qv^i A_i + \frac{1}{2} g_{ij}^I \omega^i \omega^j + \gamma I_m \omega^i B_i - V \quad (6.4)$$

where A_i are the covariant components of the vector potential, the magnetic field is given by $B_i = \varepsilon_i^{kl} \partial_k A_l = \nabla \times A$, and V is the potential. The canonical momenta are defined as follows

$$\begin{aligned} p_j &= \frac{\partial \mathcal{L}}{\partial v^j} = m_{ij} v^i + qA_j \\ \Omega_j &= \frac{\partial \mathcal{L}}{\partial \omega^j} = g_{ij}^I \omega^i + I_c B_j, \end{aligned}$$

and the velocities in terms of the momenta above read

$$\begin{aligned} v^j &= m^{ij}(p_i - qA_i) \\ \omega^j &= g_I^{ij}(\Omega_i - I_c B_i). \end{aligned} \quad (6.5)$$

Then, the classical Hamiltonian is obtained as

$$\begin{aligned} \mathcal{H} &= v^i p_i + \omega^i \Omega_i - \mathcal{L} \\ &= \frac{1}{2} m^{ij} p_i p_j - q m^{ij} p_i A_j + \frac{q^2}{2} m^{ij} A_i A_j \\ &\quad + \frac{1}{2I_m} g^{ij} \Omega_i \Omega_j - \gamma g^{ij} \Omega_i B_j + \frac{\gamma^2}{2} g_I^{ij} B_i B_j \\ &= \frac{(p - qA)^2}{2m} + \frac{s^2}{2I_m} - \gamma s \cdot B + \frac{\gamma^2 I_m}{2} B^2. \end{aligned} \quad (6.6)$$

The equations of motion for the rotational part remain unchanged compared to the spin-only case, so the classical momentum equations read

$$\begin{aligned} dp &= [q(E + v \times B) + I_c \nabla(\omega \cdot B)] dt \\ ds &= \gamma s \times B dt - I_c dB. \end{aligned} \quad (6.7)$$

It is assumed that the external field depends only on the spatial variables and not on the body's orientation for simplicity. Then, the coupling term between translational and rotational motion is given by $I_c \nabla(\omega \cdot B)$ where ∇ acts on B . This requires an inhomogeneity in the external magnetic field as in Stern-Gerlach-like experiments. When a constant magnetic field is applied along the z axis, the s_z component remains constant, which results in a precession of the spin s around the magnetic field.

The following section derives the generalized Hamilton equations in the stochastic setting based on the classical given in this section. After that, a constant and an inhomogeneous magnetic field are discussed based on these QHE.

6.2 Quantum Hamilton equations

We generalize the deterministic optimal control problem from the previous section by replacing the classical velocities v, ω with the quantum velocities $v^q = v - iu, \omega^q = \omega_v - i\omega_u$ in the classical Lagrangian (6.4). The velocity fields serve again as stochastic optimal controls $v^q = v_t^q, \omega^q = \omega_t^q$. For an analogy to the derivation of the QHE on a manifold in section 4.3, we redefine the quantum velocity $\tilde{v}_t^q = (v_t^q, \omega_t^q)$ and the vector field correspondingly $\tilde{A} = (qA, I_c B)$. The metric \tilde{g}_{ij} is then composed of a metric concerning the mass, i.e., $g_{ij}^m = m\mathbb{I}$, and concerning the inertia $g_{ij}^I = I_m g_{ij}$ defined in section 5.6 for the xxz Euler angles, as follows

$$\tilde{g}_{ij} = \begin{pmatrix} m\mathbb{I}_{3 \times 3} & 0 \\ 0 & g_{kl}^I \end{pmatrix}. \quad (6.8)$$

The usual procedure allows setting up the cost function (4.18) and the stochastic Hamiltonian (4.20)

$$\mathcal{H}_c = -\frac{\tilde{g}^{kj}}{2} \tilde{v}_{q,t}^k \tilde{v}_{q,t}^j - \tilde{A}_j \tilde{v}_{q,t}^j + V + \tilde{P}_{t,j} (\tilde{v}_{q,t}^j - i\tilde{g}^{kl} \tilde{\Gamma}_{kl}^j / 2) - \frac{1+i}{2} \text{Tr}\{\tilde{\Pi} \tilde{H}^T\} \quad (6.9)$$

with matrix $\tilde{H} = (\sigma h_j^i)$ for the generalized coordinates are $\tilde{x} = (x, \theta) = (x, y, z, \vartheta, \varphi, \chi)$. The corresponding momentum equations given in equations (4.22) for the costate variables

$\tilde{P}_t = (P_t, \Omega_t)$ with $\tilde{\Pi}_t = \begin{pmatrix} \sqrt{\hbar/m}\Pi_t^{xx} & \sqrt{\hbar/I_m}\Pi_t^{x\theta} \\ \sqrt{\hbar/m}\Pi_t^{\theta x} & \sqrt{\hbar/I_m}\Pi_t^{\theta\theta} \end{pmatrix} \in \mathbb{C}^{6 \times 6}$ for each of the components read

$$\begin{aligned}
dP_j &= [F_j^{\text{Lor}} - I_c \nabla_j (\omega_t^q \cdot B)] dt + dA_j \\
&\quad + \sqrt{\frac{\hbar}{m}} \Pi_{ij}^{xx} dW_-^i + \sqrt{\frac{\hbar}{I_m}} \Pi_{kj}^{x\theta} dW_-^k \\
d\Omega_\vartheta &= [\partial_\vartheta V_{\text{eff}}^{\text{rot}}(\Theta_t, \Omega_\varphi, \Omega_\chi) + \frac{\gamma}{\sin^2 \Theta_t} (\Omega_\varphi - \cos \Theta_t \Omega_\chi) (B_x \cos \Phi_t - B_y \sin \Phi_t) \\
&\quad + i \frac{\hbar \Omega_\vartheta}{2 I_m \sin^2 \Theta_t} + \frac{1+i}{2 \sin^2 \Theta_t} \sigma_I f_\vartheta(\Theta_t, \Phi_t, \tilde{\Pi}_t)] dt \\
&\quad + \sqrt{\frac{\hbar}{m}} \Pi_{\vartheta j}^{\theta x} dW_-^j + \sqrt{\frac{\hbar}{I_m}} \Pi_{\vartheta k}^{\theta\theta} dW_-^k \\
d\Omega_\varphi &= \left[\gamma [s \times B]_z + \frac{1+i}{2 \sin \Theta_t} \sigma_I f_\varphi(\Theta_t, \Phi_t, \tilde{\Pi}_t) \right] dt \\
&\quad + \sqrt{\frac{\hbar}{m}} \Pi_{\varphi j}^{\theta x} dW_-^j + \sqrt{\frac{\hbar}{I_m}} \Pi_{\varphi k}^{\theta\theta} dW_-^k \\
d\Omega_\chi &= \sqrt{\frac{\hbar}{m}} \Pi_{\chi j}^{\theta x} dW_-^j + \sqrt{\frac{\hbar}{I_m}} \Pi_{\chi k}^{\theta\theta} dW_-^k,
\end{aligned} \tag{6.10}$$

with the maximum principle leading to $P_t = m v_t^q + qA$ and $\Omega_{t,k} = g_{kl}^I \omega_{q,t}^l + I_c B_k$. The indices $i, j \in \{x, y, z\}$ and $k, l \in \{\vartheta, \varphi, \chi\}$, and F_j is the Lorentz force $F_j = -\partial_j V - \partial_t A_j - \varepsilon_{jin} g^{in} (p_i - A_i) B_n$. Here, it is assumed that the potential V does not depend on the orientation and B may depend on spatial coordinates, but for simplicity, not on time.

Note that the drift terms of the SDE for the components of Ω_t are the same as in the case of a freely rotating particle (5.30). This suggests that it is possible to search for solutions to the QHE where we assume that the particles are in a spin eigenstate decoupled from translation as described in section 5.4 if $B = B_z e_z$. This is the basis in the spinor representation, where each entry $\psi_i(t, x)$ of the spinor $\Psi(t, x) = (\psi_1(t, x), \psi_2(t, x), \dots)$ can be associated with a product wave function $\psi_i(t, x) e_i(\theta)$. The function $e_i(\theta)$ denotes eigenfunction of the spin eigenstate with spin quantum numbers j and m_i , i.e., $\hat{s}^2 e_i = \hbar^2 j(j+1) e_i$, $\hat{s}_z e_i = \hbar m_i e_i$; cf. section 5.4.4. Hence, the spinor representation can be viewed as a linear combination of freely spinning particle eigenstates which is a special case of the QHE (6.10).

We can point out two differences to the treatment given in the previous section for a freely spinning particle 5.3:

- 1) The gradient $-I_c \nabla_j (\omega_t^q \cdot B) = g^{kl} (I_c B_k - \Omega_k) I_c \partial_j B_l$ describes the classical coupling term.
- 2) There are “mixed” noise terms like $\sqrt{\frac{\hbar}{m}} \Pi_{\vartheta j}^{\theta x} dW_-^j + \sqrt{\frac{\hbar}{I_m}} \Pi_{\vartheta k}^{\theta\theta} dW_-^k$ which describe a possible coupling of the feedback fields $v^q(t, x, \theta)$ to the orientation and $\omega^q(t, x, \theta)$ to the position without any external field.

The first point reflects the classically expected deflection of a magnetic moment in a field gradient B , which is the basic need for the description of the Stern-Gerlach experiment. This term alone, however, cannot account for the beam splitting into “quantized” channels, as will be discussed in section 6.4.

The second point refers to the occurrence of the rotational diffusion coefficient $\sigma_I = \sqrt{\hbar/I_m}$ in the SDEs for the translational momentum and the coefficient $\sigma_m = \sqrt{\hbar/m}$ in the SDEs for the angular momentum. If we consider the momenta as feedback controls $P(t, x, \theta)$ and $\Omega(t, x, \theta)$ depending on the time t and on the spatial and orientational variables, there is

$$\Pi_{ji}^{xx} = \partial_i P_j \tag{6.11}$$

$$\Pi_{jk}^{x\theta} = \frac{1}{\sigma_I} h_k^l \partial_l P_j \tag{6.12}$$

for the momentum P_j and

$$\Pi_{kl}^{\theta\theta} = \frac{1}{\sigma_I} h_l^n \partial_n \Omega_k \quad (6.13)$$

$$\Pi_{kj}^{\theta x} = \partial_j \Omega_k. \quad (6.14)$$

for the rotational momentum Ω_l where $i, j \in \{x, y, z\}$ and $k, l, n \in \{\vartheta, \varphi, \chi\}$. Hence, $\Pi^{x\theta} = \nabla_\theta P$ and $\Pi^{\theta x} = \nabla \Omega$ do not vanish if the feedback momentum $P(t, x, \theta)$ depends on the orientation and $\Omega(t, x, \theta)$ depends on the position in space. Such coupling terms are required to describe non-classical interactions in the Stern-Gerlach experiment or the entanglement of spins, for example.

Semiclassical limit

The limit $\hbar \rightarrow 0$ in (6.10) leads to the classical equations of motion (6.7) of a rigid charge. Similar to the discussion in section 3.2.2, we may also consider the semiclassical limit in the sense of the total time derivative $\frac{d_{cl}}{dt} = \partial_t + v \cdot \nabla + \omega_v \cdot \nabla_\theta$, where ∇_θ describes the nabla operator acting on the angle variables. The real part of the QHE (6.10) in combination with the complex Itô formula (4.25) leads to an equation for the current velocity v of the center of mass

$$m \frac{d_{cl} v}{dt} = F^{\text{Lor}} - I_c \nabla(\omega \cdot B) \quad (6.15)$$

$$+ (u \cdot \nabla + \frac{\hbar}{2m} \Delta) u \quad (6.16)$$

$$+ (\omega_u \cdot \nabla_\theta + \frac{\hbar}{2I_m} \Delta_\theta) u. \quad (6.17)$$

The terms in the second and third row are related to ∇ acting on the osmotic kinetic energies $E[-\frac{m}{2}u^2]$ and $E[-\frac{I_m}{2}\omega_u^2]$ in the stochastic Lagrangian. Hence, the angular velocity contributes similarly to the semiclassical effective potential

$$\begin{aligned} V_{\text{eff}} &= V - \frac{m}{2}u^2 - \frac{\hbar}{2}\nabla \cdot u - \frac{I_m}{2}\omega_u^2 - \frac{\hbar}{2}\nabla_\theta \cdot \omega_u \\ &= V + V_Q + V_{Q_s}, \end{aligned} \quad (6.18)$$

where $V_Q = -\frac{m}{2}u^2 - \frac{\hbar}{2}\nabla \cdot u$ and $V_{Q_s} = -\frac{I_m}{2}\omega_u^2 - \frac{\hbar}{2}\nabla_\theta \cdot \omega_u$. In a similar fashion, we can derive the total time derivative for the current angular velocity ω_v

$$\frac{d_{cl}\omega_v}{dt} = \gamma\omega_v \times B - \gamma\dot{B} - \frac{1}{I_m}\nabla_\theta(V_Q + V_{Q_s}). \quad (6.19)$$

See also appendix E for more details.

These semiclassical equations reveal a strong coupling between the motion of the center of mass, including the particle's orientation. The coupling can occur without external fields due to osmotic velocity fields. If the (angular) osmotic velocity does not depend on the orientation (position) variables, the two diffusions are decoupled in the field-free regions. This decoupling is described by a separable distribution $\rho(t, x, \theta) = \rho_x(t, x)\rho_\theta(t, \theta)$. Again, the osmotic velocity implicitly accounts for the quantum behavior in the QHE. Consequently, any non-trivial initial distribution results in quantum effects driven by the osmotic velocity since it is the gradient of the probability.

Solving the quantum Hamilton equations derived in this section is generally challenging. Nonetheless, we can solve the QHE under certain assumptions, as demonstrated in the following examples. First, we examine a constant magnetic field in the symmetric gauge to recreate the Landau levels. Subsequently, we will discuss the spin measurement. Finally, the chapter concludes with a discussion on the measurement of (entangled) particle pairs.

6.3 Anomalous Zeeman effect

Consider the simplest case of (anomalous) Zeeman splitting first. The energy of a particle is contributed by both translational and rotational motion, given by the equation

$$E = E_{\text{trans}} + E_{\text{rot}} = E \left[\frac{m}{2}(v^2 + u^2) + qv \cdot A \right] + E \left[\frac{1}{2I_m}s^2 - \gamma_s \cdot B \right] \quad (6.20)$$

This energy expression highlights the Zeeman splitting of energies caused by the interaction between an external field and the particle's dynamical magnetic moment. In the case of a constant magnetic field, using the symmetric gauge where $\nabla \cdot A = 0$ and $\nabla \times A = B e_z$, the classical coupling term in the QHE (6.10) vanishes. Thus, the translation is decoupled from the spin. The stochastic Hamiltonian given in (4.20) can be expressed in terms of canonical momenta $(P_{\rho,t}, P_{\phi,t}) = (mv_t^\rho, m\rho^2(\omega_B + v_t^\phi))$ in polar coordinates (ρ, ϕ) , where $\omega_B = \frac{eB}{2m}$ and the z component of the angular momentum $L_z = P_{\phi,t}$. The QHE for the translational motion read

$$d\rho_t = \left[\frac{P_{\rho,t}}{m} + \frac{\hbar}{2m\rho_t^2} \right] dt + \sqrt{\frac{\hbar}{m}} dW_{+,t}^\rho \quad (6.21)$$

$$d\phi_t = \left[\frac{L_z}{m\rho_t^2} - \omega_B \right] dt + \frac{1}{\rho_t} \sqrt{\frac{\hbar}{m}} dW_{+,t}^\phi \quad (6.22)$$

$$dP_{\rho,t} = \left[-m\omega_B^2\rho_t + \frac{L_z^2}{m\rho_t^2} - i\frac{\hbar P_{\rho,t}}{2m\rho_t^2} + \frac{\sigma_m}{\rho_t^2} \Pi_{\phi\phi} \right] dt + \Pi_{\rho j} dW_{-,t}^j \quad (6.23)$$

$$dP_{\phi,t} = \Pi_{\phi j} dW_{-,t}^j. \quad (6.24)$$

We can immediately deduce that a constant feedback momentum $P_{\phi,t} = L_z = \text{const}$ is a solution to (6.24). This effectively describes a symmetric harmonic oscillator in the $x - y$ plane due to the presence of $-m\omega_B^2\rho$ in (6.23) which results from the field term A^2 . As a result, Landau levels emerge, where the angular momentum L_z and its expectation value $E[L_z]$ remain constant.

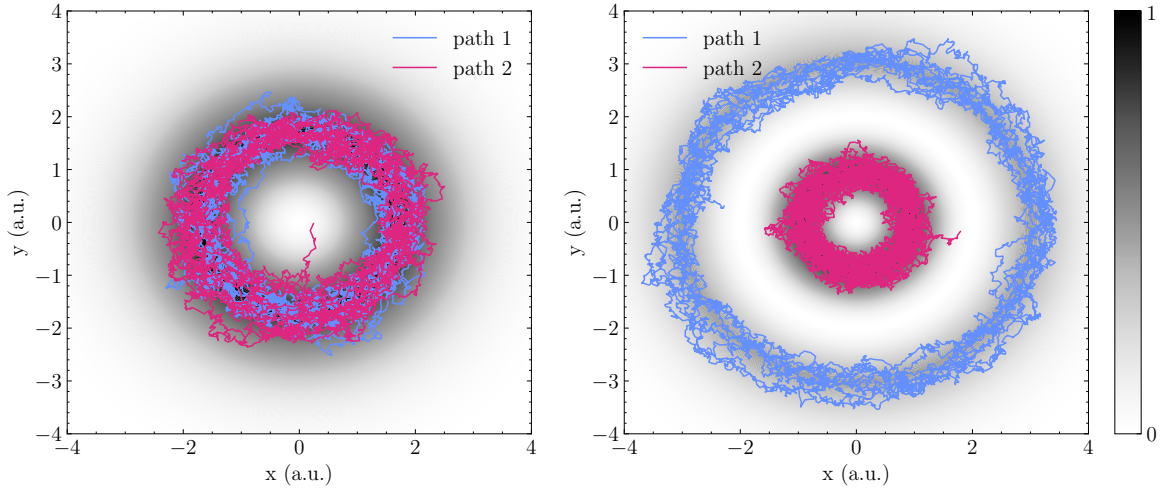


Figure 6.2: The graphs display the $z = 0$ plane for two sample trajectories, represented by blue and red lines. These paths are superimposed on a contour map illustrating the corresponding probability distribution for a perpendicular uniform magnetic field in the symmetric gauge. In the left plot, the state exhibits an energy expectation value of $E[E] = \hbar\omega_B + E[\frac{p_z^2}{2m}] + E_{\text{rot}}$, along with an angular momentum of $E[L_z] = -\hbar$. On the other hand, the right graph represents an energy state with $E[E] = 2\hbar\omega_B + E[\frac{p_z^2}{2m}] + E_{\text{rot}}$ and $E[L_z] = -\hbar$. Here, $\omega_B = \frac{eB}{2m}$.

Figure 6.2 illustrates the lowest two non-trivial states in the $x - y$ plane for an electron with charge $q = -e$ in atomic units, where $\hbar = m = e = 1$. The sample paths were ob-

tained by numerically solving the stochastic differential equations (6.21)-(6.24) for the polar coordinates (ρ, ϕ) .

By neglecting the coupling to any orbital angular momentum, the system under consideration is analogous to the free case discussed earlier. Therefore, the solutions for the QHE described by equation (5.50) regarding the spin are applicable. Consequently, for a spin-1/2 particle with potential spin projections $E[s_z] = \pm\hbar/2$, the interaction term $\gamma s \cdot B$ in equation (6.20) introduces an additional energy splitting of $\Delta E_{\text{Zeeman}} = \pm\hbar\omega_B$, where the gyromagnetic factor of the electron is given by $\gamma = \frac{I_m}{I_c} = \frac{e}{m}$.

It should be noted that the graphs presented in figure 5.5 also pertain to this problem. However, the timescales in those figures differ due to the chosen timescale for rotation, $\tau_{\text{rot}} = \frac{I_m}{\hbar} \approx \frac{mr_e^2}{\hbar} \approx 10^{-34} \text{ s}$, where r_e denotes an upper bound on the electron's radius of 1 am. This timescale is considerably smaller than the timescale in atomic units, $\tau_{\text{trans}} \approx 10^{-17} \text{ s}$, employed here. The coupling between position and orientation becomes evident in the presence of an inhomogeneous external field, as exemplified by the Stern-Gerlach experiment, which will be further discussed in the subsequent section.

6.4 Stern-Gerlach experiment

A particle's orientation and spin can only be measured indirectly, e.g., via position measurements, when the magnetic moment interacts with the measurement fields in such a way that the position is changed depending on the orientation of the magnetic moment. It is, therefore, necessary to study the coupling of the particle's position to its magnetic moment to gain information about the spin. In the stochastic model, the stochastic change of the orientation is the underlying variable that gives rise to the magnetic moment. Unlike the standard treatment in quantum mechanics, the stochastic model allows for the description of the motion of individual particles and their spins during the measurement. This is studied with the help of the QHE (6.10) derived earlier.

6.4.1 Experimental setup

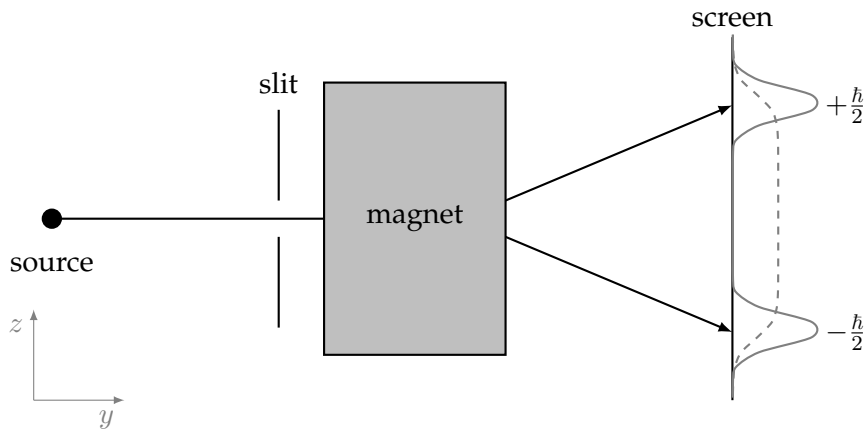


Figure 6.3: The two-dimensional sketch illustrates an idealized Stern-Gerlach experiment for a beam of spin- $\frac{1}{2}$ particles. Quantum mechanics predicts a bimodal distribution of particles at the screen (solid grey) for randomly oriented spins, which contrasts the classically expected statistics (dashed grey).

The first experimental confirmation of a quantized magnetic moment of silver atoms carried out by Stern and Gerlach in 1922 [GS22b] will serve as a reference to study the coupling in the context of the QHE. An idealized version of the Stern-Gerlach (SG) experiment is shown in figure 6.3. The parameters are close to the experiment by Stern and Gerlach [GS22b, GS22a] as given in Table 6.1. The emission of silver atoms from an oven creates a beam of particles with random spin expectation values. They enter a magnet through a Gaussian slit with width σ_0 at, say, time $t = 0$. The momentum in y direction $E[p_y]$ is assumed to follow from the thermal velocity distribution conform to the oven's temperature. The atom's transversal momentum in z direction is $E[p_z] = 0$. The inhomogeneous magnetic field $B = bx e_x + (B_0 + bz) e_z$ acts along the y axis from 0 to d_1 . A detector screen is put at a distance d_2 from the end of the magnet.

The strength of the magnetic field is mostly determined through B_0 . It is strong enough to lead to a rapid precession of the spin around the magnetic field with frequency $\omega_B = \frac{qB_0}{2m}$ compared to the translation in space. The gradient term $bz \ll B_0$ of the magnetic field accounts for the momentum gain in z direction depending on the particle's spin and thus the separation of the spins at a detector after the magnet. The third dimension perpendicular to the translation in y , and the magnetic field are neglected. Since $bx \ll B_0$ and thus $B_x \ll B_z$ one may set

$$B \approx (B_0 + bz) e_z. \quad (6.25)$$

E.g., in terms of the spinor describing the SG experiment in the magnet B_x leads to a rapidly oscillating phase in each spinor component. Note that B in (6.25) violates the Maxwell equation $\nabla \cdot B \neq 0$ and that the magnetic field is assumed to vanish outside the magnet. These simplifications are accepted in the following since they are not significant to the discussion of the beam splitting from the perspective of the QHE.

Classical description

From a classical point of view, the direction of the magnetic moment w.r.t. the inhomogeneity of the magnetic field determines the deflection of the particle. The net magnetic moment of the silver atom is due to the 5s electron, where the orbital angular momentum is 0. Hence, from classical mechanics we expect a broad distribution at the screen for random spin orientations due to the high temperature. The interesting point about the experiment is that the deflection seems to show only magnetic moments with distinct quantized projections along the measured axis prior to the measurement, e.g., parallel and antiparallel to the field for a spin $1/2$ particle. A change of the measurement axis leads to the same splitting while the preparation of the atoms is unchanged. The deflection into separate beams is also unaffected by the starting configuration of spins, e.g., if the magnetic moments are preselected by another SG experiment.

The transverse momentum p_z in the classical picture is changed due to the acceleration $M_z \partial_z B_z$, where M is the particle's magnetic moment. On the other hand, the motion for the spin leads to a precession of the magnetic moment around B_z in the field. I.e., the projection of the magnetic moment M_z (or s_z) is constant, leading to a splitting of the classical beam according to the maximal transverse momenta in each direction

$$p_{\max} = |M_z| \int_0^{T_m} \partial_z B_z dt. \quad (6.26)$$

The integral (6.26) covers the time spent in the magnetic field T_m . Since $M_z(0) = M_z(t) = \text{const}$ the spin projection s_z at $t = 0$ determines the deflection of the particles. I.e., a beam of silver atoms with randomly distributed spins at the entrance of the magnetic field would lead to a broadening of the incident beam according to the transverse momentum distribution $p_z^{\text{classical}} \in [-p_{\max}, p_{\max}]$.

Standard description in non-relativistic quantum mechanics

The prevailing view among physicists in non-relativistic quantum mechanics is that when an atom with net spin enters an inhomogeneous magnet, its state is in a superposition of spin-up and spin-down states. The probability of the atom being deflected either parallel or anti-parallel to the magnetic field gradient is defined by the squared magnitude of the associated coefficients. The detection of the atom in one of the channels is accompanied by the wave function collapse onto the corresponding component of the linear combination.

In textbooks this experiment is usually described by the Pauli-spinor $\psi = \begin{pmatrix} \psi_+ \\ \psi_- \end{pmatrix}_z$. The $(\cdot)_z$ indicates that the basis of ψ corresponds to the measurement axis chosen as z . The spinor components in this experiment are associated with the strength of the up and down spin states w.r.t. to the measurement axis so that the squared modulus of each component may be read as probabilities. The Pauli-Hamiltonian in the magnet reads

$$\hat{H} = \frac{\hat{p}^2}{2m} - \gamma \hat{s}_z (B_0 + bz). \quad (6.27)$$

The inclusion of the B_x component to satisfy the Maxwell equations would give rise to rapid oscillations which can be put into the phase factor [Pla92]. In terms of Pauli matrices, the operator \hat{s}_z is diagonal and hence the components ψ_{\pm} of the spinor decouple in (6.27). The

magnetic energy reads $\mp|M_z|(B_0 + bz)$ where $M_z = \langle \gamma \hat{s}_z \rangle$ and $\langle \cdot \rangle$ denotes expectation w.r.t. ψ . Thus, ψ_+ is subject to a force $M_z b$ while ψ_- is subjected to a force $-M_z b$ so that the beams will split according to the probabilities associated with the spinor components.

The mean trajectories for the particles may be calculated within the Heisenberg picture. Since \hat{H} in (6.27) commutes with \hat{s}_z , the expectation $\langle \hat{s}_z \rangle$ is a constant of motion

$$\frac{d}{dt} \langle \hat{s}_z \rangle = 0. \quad (6.28)$$

The commutator $[\hat{H}, \hat{p}_z] = \gamma b \hat{s}_z$ leads to the constant mean force

$$\frac{d}{dt} \langle \hat{p}_z \rangle = -\gamma b \langle \hat{s}_z \rangle \quad (6.29)$$

in the magnetic field. Here the time evolution of a time-dependent operator \hat{O} is given by Heisenberg's equation of motion $\frac{\hbar}{i} \frac{d}{dt} \hat{O} = [\hat{O}, \hat{H}]$. The transverse displacement $\hat{z}(t)$ and momentum $\hat{p}(t)$ follow [SSE88]

$$\hat{z}(t) = \hat{z}(0) + \hat{p}_z(0) \frac{t}{m} + \frac{2\hat{s}_z(0)}{\hbar} \left[\frac{t}{m} \Delta_{p_z}(t) + \Delta_z(t) \right] \quad (6.30)$$

$$\hat{p}_z(t) = \hat{p}_z(0) + \frac{2\hat{s}_z(0)}{\hbar} \Delta_{p_z}(t) \quad (6.31)$$

where $\Delta_z(t) = -\frac{1}{m} \int_0^t M_z b t' dt'$ and $\Delta_{p_z}(t) = \int_0^t M_z b dt'$ for $0 \leq t \leq T_m$ in the magnetic field. After the magnetic field, i.e., $t > T_m$, the transversal displacement and momentum read $\Delta_z = \Delta_z(T_m)$ and $\Delta_{p_z} = \Delta_{p_z}(T_m)$, respectively. It follows from (6.30)-(6.31) that the (mean) trajectories will depend on the initial spin which is determined by the weighting of the spinor components. These equations are compared with the trajectories calculated from the QHE in the following sections.

While the z component of the spin is conserved in expectation, the x, y components oscillate in the magnetic field. For example,

$$\begin{aligned} \hat{s}_+(t) &= \hat{s}_x(t) + i\hat{s}_y(t) \\ &= \exp \left\{ -i \left(\int_0^t M_z B_z(t') dt' + 2\hat{z}(0) \Delta_{p_z}(t) / \hbar - 2\hat{p}_z(0) \Delta_z(t) / \hbar \right) \right\} \hat{s}_+(0), \end{aligned} \quad (6.32)$$

where the term including $B_z = B_0 + bz \approx B_0$ is the leading contribution to the phase factor. The resulting rapid oscillations do not contribute to the deflection of the particles and are therefore not investigated in detail.

The spin measurement in the pilot wave theory, see section 2.4.2, allows a deterministic description of the configuration variables. The spin projection, for example, is not fixed and changes throughout the experiment. The crucial hidden variable in this formalism that fixes the outcome on the screen is the initial position of the particles prior to entering the magnet [Hol95, DHKV88]. The following subsection focuses on the hidden variables of the stochastic model: stochastic processes associated with position and orientation. They allow the determination of probabilities depending on the initial configuration only. I.e., the outcomes depend on both initial position and spin.

6.4.2 Stochastic description

The stochastic model follows the QHE derived in section 6.2 where equations (6.10) concerning the spin are simplified when the magnetic field has a z component only. Note that z component refers to the chosen symmetry axis of the experiment. The coupling in the drift terms of the orientational part to the spatial part is then only due to the inhomogeneity of

the magnetic field

$$F_{\text{mag}} = -\gamma \nabla (I_m \omega \cdot B). \quad (6.33)$$

With $B = B_z(z)e_z$ from (6.25), the QHE given in (6.10) for the momentum equations read

$$m dv_q^k = \gamma I_m \partial_k (\omega_q \cdot B) dt + \tilde{\Pi}_{kj} dW_-^k \quad (6.34)$$

$$d\Omega_\vartheta = \left[\partial_\vartheta V_{\text{eff}}^{\text{rot}} + i \frac{\hbar \Omega_\vartheta}{2 I_m \sin^2 \Theta_t} + \frac{1+i}{2 \sin^2 \Theta_t} \sigma_I f_\vartheta \right] dt + \tilde{\Pi}_{\vartheta j} dW_-^j$$

$$d\Omega_\varphi = \frac{1+i}{2 \sin^2 \Theta_t} \sigma_I f_\varphi dt + \tilde{\Pi}_{\varphi j} dW_-^j \quad (6.35)$$

$$d\Omega_\chi = \tilde{\Pi}_{\chi j} dW_-^j.$$

Hence, the BSDEs concerning the angular momenta in this case yield the drift terms of a freely spinning particle. The coupling of the particle's position to its orientation in the QHE is due to the matrix $\tilde{\Pi}$ since, for example, the feedback momenta $p = p(t, x, \theta)$ can generally depend on all variables. This implies a dependence of $\tilde{\Pi}_{jk}(t, x, \theta) \propto \partial_j p_k(t, x, \theta)$ on all configuration coordinates. For instance, such a coupling follows in the stochastic picture if the expectation values of the spins are not aligned with the measurement setup, as will be shown later.

Solutions to constant s_z expectation

In order to solve the problem at hand, a simplified version of constant spin projection is considered in a first step. We assume that the orientation variables decouple from the motion in space. The discussion of the solutions to the angular momentum equations (6.35) then follows the section regarding the freely spinning particle 5.3. For spin $\frac{1}{2}$ particles the stochastic processes fulfill $E[s^2] = \frac{3\hbar^2}{4}$ and $E[s] = \pm \frac{\hbar}{2} e_z$ for the two eigenstates. The feedback controls for the angular momenta read $\Omega_\varphi = \Omega_\chi = \frac{\hbar}{2}$ and $\Omega_\vartheta = -i \frac{\hbar}{2} \tan \frac{\vartheta}{2}$ for the spin up particle, and $\Omega_\varphi = -\Omega_\chi = -\frac{\hbar}{2}$, $\Omega_\vartheta = -i \frac{\hbar}{2} \cot \frac{\vartheta}{2}$ for the spin down state, respectively. In terms of the spin vector in the reference frame, e.g., the spin up vector from (5.76), there is

$$s = \frac{\hbar}{2} (\tan \vartheta/2 e^{-i\varphi}, -i \tan \vartheta/2 e^{-i\varphi}, 1)^T. \quad (6.36)$$

It follows that the feedback field of the spin along the measurement axis z is constant. Hence, the solutions to (6.34) may be found approximately since the only coupling term in (6.34) is due to the z component of the magnetic field and the angular velocity. With that, the force acting on the particle in the magnetic field is constant, simplifying the search for a solution of the quantum velocity with the help of the QHE.

Quantity	Value
standard atomic weight silver m	1.79×10^{-25} kg
temperature oven	≈ 1500 K
strength magnetic field B_0	5 T
gradient b	$\approx -1.5 \times 10^3 \frac{\text{T}}{\text{m}}$
standard deviation of Gaussian beam σ_0	4×10^{-5} m
length magnet d_1	0.03 m
RMS of velocity v_y	$680 \frac{\text{m}}{\text{s}}$
time spent in magnet T_m	5.15×10^{-5} s
distance magnet to screen d_2	0.06 m

Table 6.1: The table lists the experimental data used as a basis for the numerical simulation. The values are partly taken from the experiment by Stern and Gerlach [GS22b, GS22a].

The further discussion of the Stern-Gerlach experiment by means of the QHE is based on some simplifications. According to the table 6.1, the beam of silver atoms moves at $t = 0$ in the y direction through a slit of Gaussian width σ_0 . This fixes the width of the initial distribution in y, z so that the osmotic velocity is $u(t = 0, x) = \frac{1}{\tau_0}(0, -y, -z)$, where $\tau_0 = \frac{m\sigma_0^2}{\hbar}$. The momentum in the y direction is assumed to stem from the Maxwell-Boltzmann distribution, where the root mean square $v_y = \sqrt{\frac{4k_B T}{m}}$ serves as the semiclassical propagation velocity, i.e., it is the current velocity in the y direction. The other components of v are initially set to 0. The current velocity v_y is assumed to remain constant throughout the experiment. This neglects any spreading effects due to the distribution of the beam in the propagation direction. The length d_1 of the magnet leads semiclassically to an interaction time $T_m = \frac{d_1}{v_y}$ of the beam with the inhomogeneity. After that the field is assumed to vanish, i.e., the motion is field free.

With a constant force acting on the atom, the velocity in the magnet is easy to determine. In the inhomogeneous field the particle with constant $s_z = \pm \frac{\hbar}{2}$ gains a transverse momentum which leads to a time-dependent z -component of the quantum velocity

$$v_z^{q,m}(t, z) = v_{\text{cl}}(t) - \frac{i}{\tau_0 \sigma_t} (-z + z_{\text{cl}}(t)) \quad (6.37)$$

with the definition of a classical velocity

$$v_{\text{cl}}(t) = \frac{\gamma s_z b}{m} t \quad (6.38)$$

and a classical displacement

$$z_{\text{cl}}(t) = \frac{\gamma s_z b}{2m} t^2. \quad (6.39)$$

The quantum velocity given in (6.37) is a solution to the QHE for a constant spin projection s_z . Spreading effects of the distribution depend on the timescale of the experiment, where $\tau_0 = \frac{m\sigma_0^2}{\hbar}$ depends on σ_0 and m and $\sigma_t = 1 + i \frac{t}{\tau_0}$.

At the exit of the magnet at time $t = T_m$ the current velocity has an additional contribution in the z direction $v_m = v_{\text{cl}}(T_m) = \frac{\gamma s_z b}{m} T_m$ and the probability distribution is displaced by $z_m = z_{\text{cl}}(T_m) = \frac{\gamma s_z b}{2m} T_m^2$. This leads to a quantum velocity after the magnet

$$v_z^{q,a}(t', z) = v_m - \frac{i}{\tau_0 \sigma_{t'}} (-z + z_m + v_m t') \quad (6.40)$$

where $t' = t - T_m$. The spreading of the distribution is related to $\frac{t}{\tau_0}$ and higher orders may be neglected if $\sigma_t \sigma_0 \ll |v_m| t$. This implies that the interaction time with the magnetic field's inhomogeneity should fulfill $bT \gg \frac{1}{\gamma \sigma_0}$ such that the change in transversal momentum is large compared to the spreading of the distribution. In this case, one may neglect any higher orders terms in

$$\frac{1}{\sigma_t} = 1 - i \frac{t}{\tau_0} + \mathcal{O} \left(\left(\frac{t}{\tau_0} \right)^2 \right). \quad (6.41)$$

The feedback solutions given in (6.37) and (6.40) may be verified by applying the complex Itô formula (4.25) to the quantum velocities $v_z^{q,a}$ and comparing the drift terms in the momentum equations of the QHE. On average the particles pick up a transversal momentum in the magnet according to their initial spin projection s_z which can be read from the real part in equations 6.37 and (6.40). This is the current velocity. The osmotic velocity encoded in the imaginary part of these equations, ensures that the particle stays close to the classically expected path. Hence, in the special cases of constant spin projections, i.e., the spin states

are aligned with the direction of the field gradients, the stochastic mechanics' description is similar to that expected from classical mechanics. The same interpretation is used in the superposition of the spin eigenstates with Pauli spinors where from a semiclassical point of view each component is deflected as if the spins are either aligned up or down w.r.t. the magnetic field. The conceptual differences to the classical picture and the ordinary treatment in quantum mechanics appear when the spins are randomly oriented before the interaction with the magnetic field.

Randomly oriented initial spins

When the spin- $\frac{1}{2}$ particles have z projections $|E[s_z]| < \frac{\hbar}{2}$, the differences between the two approaches become more pronounced. I.e., the spin expectations are tilted w.r.t. the measurement axis,

$$\begin{aligned} E[s] &= \pm \frac{\hbar}{2} e(\delta_0, \phi_0) \\ E[s^2] &= \frac{3\hbar^2}{4} \end{aligned} \quad (6.42)$$

where the new spin projection axis is along the unit vector

$$e(\delta_0, \phi_0) = (\cos \phi_0 \sin \delta_0, \sin \phi_0 \sin \delta_0, \cos \delta_0). \quad (6.43)$$

Classically, the magnetic moment precesses around the measurement axis in the magnetic field. The z projection, however, is unchanged. Hence, the stochastic description must account for the additional transverse momentum or change of the spin projection onto the measurement axis.

The spin expectations (6.42) imply

$$E[s] = \int s \rho d\theta \neq \int s \rho_{\pm} d\theta \quad (6.44)$$

where ρ is the probability distribution to the rotated spin state and ρ_{\pm} are the probability distributions of the spin-up s_+ and spin-down s_- states with expectations $E[s_{\pm}] = \int s_{\pm} \rho^{\pm} d\theta = \pm \frac{\hbar}{2} e_z$. So the rotation of the angular velocity expectation is accompanied by a change in the probability distributions from ρ_{\pm} to ρ . In the following, the stochastic process of the spin-up state is considered, which is rotated so that $E[s] = \frac{\hbar}{2} e(\delta_0, \phi_0)$. This follows by analogy with the combination of two known solutions of the QHE as described in the appendix F with constants $c_1 = \cos(\delta_0/2) e^{-i\phi_0/2}$ and $c_2 = \sin(\delta_0/2) e^{i\phi_0/2}$. In terms of matrix multiplication, the j th component of the rotated canonical angular momentum reads

$$\Omega_j = \frac{1}{\rho} \begin{pmatrix} \cos^2 \frac{\delta_0}{2} \rho_+ & \frac{1}{2} \sin \delta_0 \sqrt{\rho_+ \rho_-} e^{-\frac{i}{\hbar}(S_- - S_+) - i\phi_0} \\ \frac{1}{2} \sin \delta_0 \sqrt{\rho_+ \rho_-} e^{\frac{i}{\hbar}(S_- - S_+) + i\phi_0} & \sin^2 \frac{\delta_0}{2} \rho_- \end{pmatrix} \begin{pmatrix} \Omega_{+,j} \\ \Omega_{-,j} \end{pmatrix}, \quad (6.45)$$

where the two spin angular momenta $\Omega_{+,j}$ and $\Omega_{-,j}$ correspond to spin up and down states for a spin- $\frac{1}{2}$ particle from section 5.4. Correspondingly, the orientational probability distribution

$$\rho = \cos^2 \frac{\delta_0}{2} \rho_+ + \sin^2 \frac{\delta_0}{2} \rho_- + \sin \delta_0 \sqrt{\rho_+ \rho_-} \cos((S_- - S_+)/\hbar + \phi_0) \quad (6.46)$$

is the new probability distribution, and the functions S_{\pm} must satisfy $\Omega_{\pm,j} = -i\hbar \partial_j S_{\pm}$.¹

Carrying out the calculation given in (6.45), the rotated canonical angular momenta as

¹The combination in equation (6.45) ensures that the QHE for the rotational part - and the associated partial differential equations - are satisfied. This matrix multiplication is the stochastic counterpart to the linear superposition of two solutions to the Schrödinger equation, where it is apparent that in the stochastic theory, the combination is not a simple superposition but a non-linear combination due to the non-linearity of the QHE.

feedback controls of the Euler angles read

$$\begin{aligned}\Omega_\vartheta &= \frac{\hbar}{2\rho} (i \cos \delta_0 \sin \vartheta + \sin \delta_0 (\cos(\phi_0 + \varphi) - i \cos \vartheta \sin(\phi_0 + \varphi))) \\ \Omega_\varphi &= \frac{\hbar}{2\rho} (\cos \delta_0 + \cos \vartheta - i \cos(\phi_0 + \varphi) \sin \delta_0 \sin \vartheta) \\ \Omega_\chi &= \frac{\hbar}{2}\end{aligned}\tag{6.47}$$

with $\rho = (1 + \cos \delta_0 \cos \vartheta + \sin \delta_0 \sin \vartheta \sin(\phi_0 + \varphi))$. The intrinsic rotation Ω_χ in (6.47) is unaffected, whereas the z projection is no longer constant. The corresponding spin vector in the reference frame is thus given by

$$s = \frac{\hbar}{2\rho} \begin{pmatrix} (\cos \phi_0 - i \cos \vartheta \sin \phi_0) \sin \delta_0 + \sin \vartheta (i \cos \delta_0 \cos \varphi + \sin \varphi) \\ -i \cos \phi_0 \cos \vartheta \sin \delta_0 - \sin \phi_0 \sin \delta_0 - \sin \vartheta (\cos \varphi - i \cos \delta_0 \sin \varphi) \\ (\cos \delta_0 + \cos \vartheta - i \cos(\phi_0 + \varphi) \sin \delta_0 \sin \vartheta) \end{pmatrix}.\tag{6.48}$$

The expectation values associated with the spin angular momentum s obey equations (6.42). The latter equations also show that the motion of orientation and position is coupled in the QHE for the momenta (6.34)-(6.35). E.g., the z -component of the spin $s_z(\theta, \delta_0, \phi_0)$ depends in general on the Euler angles $\theta = (\vartheta, \varphi, \chi)$, while the expectation along the z axis is $E[s_z] = \frac{\hbar}{2} \cos \delta_0$. Thus, s_z is not a constant field, so the description of the SG experiment has to include the coupling of the random orientational variables to the translational motion due to classical force term $-\gamma s_z(t, x, \theta, \delta_0, \phi_0)b$. Unfortunately, it is not trivial to derive solutions to the QHE in an analytic form for position and orientation in space. It is, however, possible to describe the present experiment using the solutions for the cases with $E[s_z] = \pm \frac{\hbar}{2}$ discussed earlier in this section.

The solutions for constant spin projections lead to velocity fields in the magnet and after the magnet (6.37)-(6.40). Depending on the spin projections for a spin- $\frac{1}{2}$ particle, there are two known solutions to the QHE: one for spin up and the other for the down state. According to the appendix F, these solutions may be combined to describe solutions in the stochastic picture for random orientations of spin expectations according to (6.47) or (6.48). This combination of the corresponding spin- $\frac{1}{2}$ particles gives a velocity in the magnetic field of

$$v_z^{q,m}(t, z, \Omega_\varphi^{q,m}(t)) = \frac{2}{\hbar} v_{\text{cl}}(t) \Omega_\varphi^{q,m}(t) - \frac{i}{\tau_0 \sigma_t} \left(-z + \frac{2}{\hbar} z_{\text{cl}}(t) \Omega_\varphi^{q,m}(t) \right).\tag{6.49}$$

Here the feedback angular momentum $\Omega_\varphi^{q,m}(t) = \Omega_\varphi^{q,m}(t, z, \theta)$ is written in short-hand notation. The expressions for the angular momenta $\Omega_j^{q,m}(t) = \Omega_j^{q,m}(t, z, \theta)$ in the magnet read

$$\begin{aligned}\Omega_\vartheta^{q,m}(t) &= \frac{\hbar e^{-C_1}}{4|\sigma_t|^2 \rho_m} (i \cos \delta_0 \cosh C_2 \sin \vartheta - i \sin \delta_0 (\cos C_3 + i \cos \vartheta \sin C_3) \\ &\quad - \sin \vartheta \sinh C_2) \\ \Omega_\varphi^{q,m}(t) &= \frac{\hbar}{2} \left(-1 + \frac{1}{1 - i e^{C_2 + i C_3} \tan(\vartheta/2) \tan(\delta_0/2)} \right) \\ \Omega_\chi^{q,m}(t) &= \frac{\hbar}{2}\end{aligned}\tag{6.50}$$

where the probability distribution

$$\rho_m(t, z, \theta) = \frac{1}{|\sigma_t|^2} e^{-C_1} \left(2e^{-C_2} \cos^2(\vartheta/2) \cos^2(\delta_0/2) + 2e^{C_2} \sin^2(\vartheta/2) \sin^2(\delta_0/2) + \sin \vartheta \sin \delta_0 \sin C_3 \right) \quad (6.51)$$

and $C_1 = C_1(t, z) = \frac{z^2 + z_{cl}^2(t)}{\sigma_t \sigma_0^2}$, $C_2 = C_2(t, z) = \frac{2z z_{cl}(t)}{\sigma_t \sigma_0^2}$ and $C_3 = C_3(t, z, \varphi) = \phi_0 + \varphi + \frac{2}{\hbar} m v_{cl}(t) z + \omega_B t$. Here $\omega_B = \frac{\gamma}{2} B_0$ describes the oscillation in the magnetic field due to the strength of the homogeneous field B_0 where $\frac{2}{\hbar} m v_{cl}(t) z \ll \omega_B t$ since $bz \ll B_0$.

After the magnet, the translational and positional velocities are still coupled and evolve with the transversal quantum velocity

$$v_z^{q,a}(t, z, \Omega_\varphi^{q,a}(t)) = \frac{2}{\hbar} v_m \Omega_\varphi^{q,a}(t) - \frac{i}{\tau_0 \sigma_t} \left(-z + \frac{2}{\hbar} (z_m + v_m t) \Omega_\varphi^{q,a}(t) \right) \quad (6.52)$$

where the time-dependent classical quantities $z_{cl}(t)$, $v_{cl}(t)$ are replaced by the classically expected displacement with constant transversal velocity $z_m + v_m t$ and v_m , respectively. The angular momenta in the field-free region are similar to those in the magnet

$$\begin{aligned} \Omega_\vartheta^{q,a} &= \frac{\hbar e^{-C_4}}{4|\sigma_{t'}|^2 \rho_a} \left(i \cos \delta_0 \cosh C_2 \sin \vartheta - \sin \delta_0 (\cos C_6 + i \cos \vartheta \sin C_6) \right. \\ &\quad \left. - i \sin \vartheta \sinh C_5 \right) \\ \Omega_\varphi^{q,a} &= \frac{\hbar}{2} \left(-1 + \frac{1}{1 + i e^{C_5 - i C_6} \tan(\vartheta/2) \tan(\delta_0/2)} \right) \\ \Omega_\chi^{q,a} &= \frac{\hbar}{2} \end{aligned}$$

where the probability distribution

$$\rho_a(t', z, \theta) = \frac{1}{2|\sigma_{t'}|^2} e^{-C_4} \left(2e^{-C_5} \cos^2(\vartheta/2) \cos^2(\delta_0/2) + 2e^{C_5} \sin^2(\vartheta/2) \sin^2(\delta_0/2) + \sin \vartheta \sin \delta_0 \sin C_6 \right) \quad (6.53)$$

with $C_4(t', z) = \frac{z^2 + (z_m + v_m t')^2}{\sigma_{t'} \sigma_0^2}$, $C_5(t', z) = \frac{2z(z_m + v_m t')}{\sigma_{t'} \sigma_0^2}$ and $C_6(z, \varphi) = \phi_0 + \varphi + \frac{2}{\hbar} m v_m z + \phi_B$. The comparison of the quantum velocity fields from the QHE (6.49)-(6.52) with the equations in the Heisenberg picture (6.30)-(6.31) show similar terms. E.g., in the magnet the transversal velocity $\frac{2\hat{s}_z(0)}{\hbar} \Delta p_z(t)$ reappears in the stochastic velocity field as $\frac{2}{\hbar} v_{cl}(t) \Omega_\varphi^{q,m}(t)$ where the complex angular momentum $\Omega_\varphi^{q,m}(t)$ takes the role of the operator $\hat{s}_z(0)$. The terms multiplied with i in (6.49) are related to the shape of the probability distribution, i.e., the localization of the ensemble.

Consider now a scenario where the initial spin component Ω_φ^q is a continuous random variable with vanishing expectation value. The spin- $\frac{1}{2}$ particle should have an equal probability of moving up or down after the interaction with the apparatus. The initial random value of that spin component at $t = 0$ influences the direction the particle is moving as given in equation (6.37). Thus, the probability of ending up in one of the two channels, depends on the direction of the spin. This will be shown in the following subsection w.r.t. the spin average in more detail.

The field equations for the angular momenta (6.50)-(6.53) have no counterpart in the spinor description of quantum mechanics since $\Omega_j^q(t, z, \theta)$ depend on the orientation variables. Hence, the stochastic description offers additional information on the change in the particle's orientation. However, the detailed information on θ and the associated stochastic

spin s is not necessary to describe phenomena in the stochastic picture, which is due to the different timescales of the stochastic processes in position and orientation which is discussed in the explicit numerical solution of the stochastic processes.

In the following subsection, these solutions of the momentum equations allow the solution of Nelson's forward SDE for the configuration variables.

Numerical solution

The evolution of the particles will be given by Nelson's FBSDEs with the derived feedback velocities in the previous subsection. For example, the forward SDE, see equations (2.40) and (5.9), in the magnetic field for the stochastic processes $X_t = (X_t^1, X_t^2)$ and $Y_t = (\Theta_t, \Phi_t, \mathcal{X}_t)$ concerning the position $x = (y, z)$ and orientation $\theta = (\vartheta, \varphi, \chi)$ follow from the velocity fields (6.49)-(6.50),

$$\begin{aligned}
dX_t^1 &= \left[v_0 + \frac{v_0 t - X_t^1}{\tau_0} \right] dt + \sqrt{\frac{\hbar}{m}} dW_+^1 \\
dX_t^2 &= \left[\frac{2}{\hbar} (v_{cl}(t) + z_{cl}(t)/\tau_0) \Omega_\varphi^{v+u} - \frac{X_t^2}{\tau_0} \right] dt + \sqrt{\frac{\hbar}{m}} dW_+^2 \\
d\Theta_t &= \frac{\Omega_\vartheta^{v+u}}{I_m} dt + \sqrt{\frac{\hbar}{I_m}} h_k^\vartheta dW_+^{\theta,k} \\
d\Phi_t &= \left[\frac{\Omega_\varphi^{v+u} - \cos \Theta_t \Omega_\chi^{v+u}}{I_m \sin^2 \Theta_t} - \gamma B_z \right] dt + \sqrt{\frac{\hbar}{I_m}} h_k^\varphi dW_+^{\theta,k} \\
d\mathcal{X}_t &= \frac{\Omega_\chi^{v+u} - \cos \Theta_t \Omega_\varphi^{v+u}}{I_m \sin^2 \Theta_t} dt + \sqrt{\frac{\hbar}{I_m}} h_k^\chi dW_+^{\theta,k}.
\end{aligned} \tag{6.54}$$

The real angular momenta $\Omega_j^{v+u} = \Omega_j^v + \Omega_j^u = \Re(\Omega_j) - \Im(\Omega_j)$ are used in the calculation and the drift terms $\mathcal{O}\left(\left(\frac{1}{\tau_0}\right)^2\right)$ in (6.54) have been neglected. It is important to mention that the y component does not exhibit any spreading effects over the course of the experiment.

The numerical solution requires choosing a characteristic time t_c and length l_c . As mentioned before, the mass inertia $I_m \approx mR^2$, depending on the radius of the modeled extended mass distribution, fixes the time scale $t_c^{\text{rot}} = \frac{I_m}{\hbar}$ of the rotational diffusion. Compared to the time scale $t_c = \frac{m}{\hbar} d_1^2$ suggested by the length of the magnet

$$t_c^{\text{rot}} \approx \frac{m}{\hbar} R^2 \ll \frac{m}{\hbar} d_1^2 = t_c, \tag{6.55}$$

it follows that the change of the orientation is rapid compared to the motion in space. Therefore, during a time step $\Delta t \gg t_c^{\text{rot}}$ (but $\Delta t \ll t_c$) in the simulation of the atoms in the SG experiment, all reachable orientation angles are visited according to their current probability distribution.² E.g., for the spin field $s(t, X_t, Y_t)$ the average

$$\langle s(t, X_t, Y_t) \rangle_{\Delta t} = \frac{1}{\Delta t} \int_t^{t+\Delta t} s(t, X_t, Y_t) dt \tag{6.56}$$

corresponds approximately to the expectation of the spin at (t, x) , if $X_t \approx X_{t+\Delta} = x$ is assumed to be constant during the timespan Δt . This, in turn, allows for a simplification of the diffusion from $\mathbb{R}^3 \times SO(3)$ to \mathbb{R}^3 by taking the orientational averages of the considered quantities. For example,

$$\bar{f}(t, x) = \frac{1}{\bar{\rho}(t, x)} \int f(t, x, \theta) \rho(t, x, \theta) d\theta \tag{6.57}$$

²If the orientational distribution has no zeros the accessible regions of the orientation angles are not separated.

where $\bar{\rho}(t, x) = \int \rho(t, x, \theta) d\theta$ and the integral is meant to cover the whole configuration space concerning the orientation. The averaging simplifies the numerical solution of the SDE (6.54) at the cost of lost details in spin dynamics. From here, averages concerning the orientation variables are used. Hence,

$$\begin{aligned} d\bar{X}_t^1 &= \left[v_0 + \frac{v_0 t - \bar{X}_t^1}{\tau_0} \right] dt + \sqrt{\frac{\hbar}{m}} dW_+^1 \\ d\bar{X}_t^2 &= \left[\frac{2}{\hbar} \left(v_{\text{cl}}(t) + \frac{z_{\text{cl}}(t)}{\tau_0} \right) \bar{\Omega}_\varphi^{v+u} - \frac{\bar{X}_t^2}{\tau_0} \right] dt + \sqrt{\frac{\hbar}{m}} dW_+^2. \end{aligned} \quad (6.58)$$

The orientational average of the spin angular momentum in z direction $\bar{s}_z^{m,v+u}(t, z) = \bar{\Omega}_\varphi^{m,v+u}(t, z)$ in the magnet (similarly for the field-free region) reads

$$\begin{aligned} \bar{\Omega}_\varphi^{m,v+u}(t, z) &= \frac{1}{\bar{\rho}(t, z)} \int \Omega_\varphi^{m,v+u}(t, z, \theta) \rho(t, z, \theta) d\theta \\ &= -\frac{\hbar}{2} \left(1 - \frac{2(1 + \cos \delta_0)}{1 + \exp(4z_{\text{cl}}(t)z/\sigma_t \sigma_0^2) (1 - \cos \delta_0) + \cos \delta_0} \right). \end{aligned} \quad (6.59)$$

The spin average thus depends on the initial spin expectation value through δ_0 . The two cases of spin up ($\delta_0 = 0$) and down ($\delta_0 = \pi$) again lead to $\bar{\Omega}_\varphi^{m,v+u}(t, z) = \pm \hbar/2$.

Last but not least, with the considerations of orientational averages it is apparent that the stochastic theory including $SO(3)$ hints at a more detailed description of spin dynamics where the orientation is a continuous random variable. As opposed to the translational motion the spin space is considered to be discrete in the standard treatment of spin. The theory of the spin as an intrinsic property of the particle is confirmed by many experiments. Putting the orientation on an equal footing in the stochastic theory, however, it seems that the standard treatment of spin is sufficient to explain experiments related to spin phenomena at this point. In some specific examples the considered stochastic model of a spinning top might reveal details on the spin orientations, which may include possible bound states for multiple particles with spin.

Results

With this at hand, the experiment by Stern-Gerlach may be recovered in the stochastic picture of a spinning particle by randomly choosing the incident spin projection δ_0 of each simulated particle. As shown in figure 6.4, the paths of the particles split into two channels independently of the initial spin expectation, and the spin expectations change accordingly. This contrasts with the classical prediction (dashed lines) in figure 6.4, where the deflection depends on the initial magnetic moment on the measurement axis only.

The averaged spins $\bar{s}(t)$ for each particle are represented as arrows in the same graph. The orientational average of the z component $\bar{s}_z(t)$ is shown in more detail in figure 6.5 during the numerical simulation. Finally, the spins will be fully aligned along the measurement axis. Thus, outside the magnet, the spins are subject to a torque that cannot be explained by a classical torque. In the stochastic picture, the osmotic velocity and osmotic spin angular momentum drive the change.

It should be noted that, in general, the averaged spins $\bar{s}_z(t)$ do not align within the magnetic field. Figure 6.5 reveals that some spins are not yet fully aligned when they enter the field free region (right of the dashed vertical line). Again, the osmotic contribution to the velocity and the spin are responsible for the change in the field-free region. This is similar to the discussion of the double-slit experiment. Given the boundary conditions, the osmotic velocity (and the current velocity) ensures that the diffusion is conservative. Under expectation, there is a quantum torque acting on the spins

$$d\bar{s} = (\gamma \bar{s} \times B + T_u) dt \quad (6.60)$$

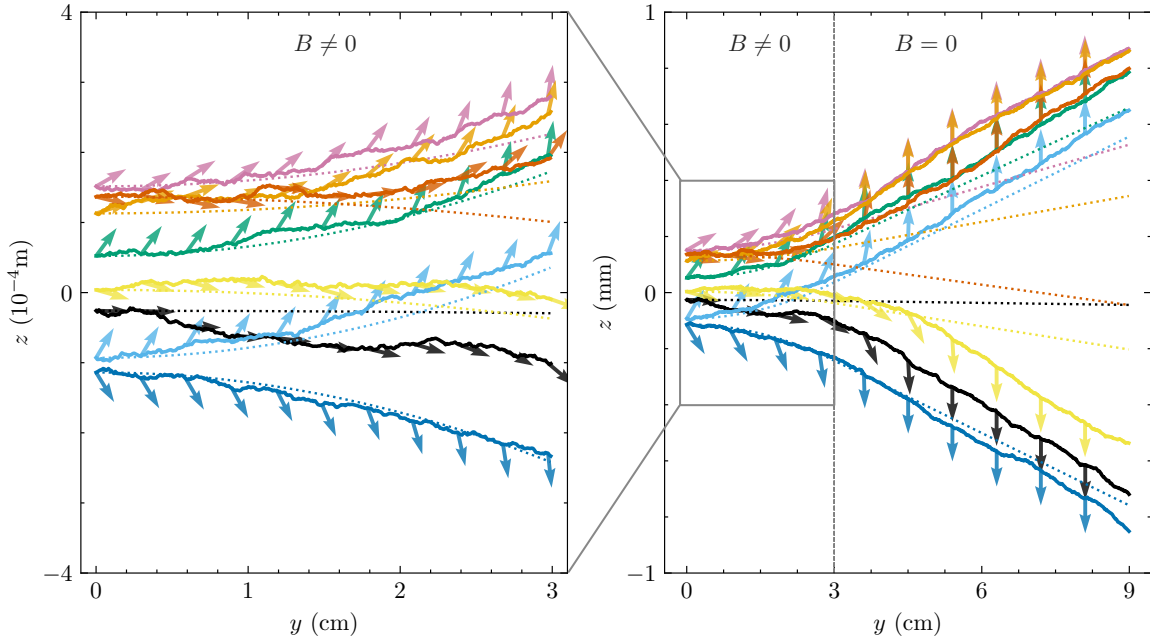


Figure 6.4: Spin- $\frac{1}{2}$ particles entering the magnet of length 3 cm with random spin expectation values are shown. The numerical solutions of 8 trajectories of the SG experiment in the stochastic approach are shown. The stochastic trajectories in the $y - z$ plane with arrows attached to selected positions of the realizations are shown as solid lines. The arrows represent the direction of the orientational mean of the spin vector \bar{s} . The dashed lines show the classically expected paths depending on the initial position and spin expectation. The right plot shows the paths and spins throughout the proposed SG device, where the vertical dashed line separates the field-free region from the magnet. The left plot depicts a zoomed-in version of the right plot, focusing only on the inside of the magnet.

where the averaged torque $T_u = \bar{s} \times (\hbar/2m\Delta\bar{s} + (\bar{u} \cdot \nabla)\bar{s})$ implies nontrivial changes of the expectation value of the spin, even in the absence of a magnetic field. Equation (6.60) follows again by comparing the drift terms of the complex Itô formula (4.25) applied to $\bar{s}(t, x)$ to the classically expected precession $\gamma\bar{s} \times Bdt$.³

As long as the beams are not separated, the stochastic particle has some reasonable probability of changing the beam it enters. Hence, as the assignment of a particle having a momentum pointing (anti-)parallel to the field in the experiment can only be made when the beams are disjoint, i.e., the distance to the recording screen is big enough, the same applies to the particle's spin expectation. Therefore, if the probability distributions are separated, so are the spin expectations. This can be seen in the left plot of figure 6.8 in the following subsection where \bar{s} is shown as a function of (t, z) for an initial spin $E[s(t=0)] = \frac{\hbar}{2}e_y$.

Polarization of the initial spin expectations

What happens in the Stern-Gerlach experiment if consecutive measurements are made, i.e., what if the spins have a certain polarization before entering the SG apparatus? The measurement outcome should depend on the position $z(t=0)$ and the spin orientation $\bar{s}_z(t=0)$. This is illustrated in figure 6.6 for three different incident angles δ_0 .

The initial spin expectation is crucial to the experiment's outcome, as illustrated by the plots in figure 6.6. If the spins are parallel to the measurement axis $\delta_0 = 0$, all particles will choose to go up, regardless of their initial position. For $\delta_0 \in (0, \pi)$, the dependence on the initial position seems to show some correlation with the outcome of the spin measurement. For example, consider the plots for $\delta_0 = \pi/4$. The only particle in the subensemble shown in

³In other causal theories of quantum mechanics such torque terms appear as well. E.g., in [dlPCVH15] the torque term follows from the stochastic derivative D_s from eq. (2.43) such that $T_u = \bar{s} \times D_s\bar{s}$. In Bohm's quantum mechanics, there is the so-called quantum torque [DHKV88, Hol95]. From the viewpoint of the quantum Madelung fluids, the quantum torque T_u results from the particle's interaction with the polarizable fluid [Tak52].

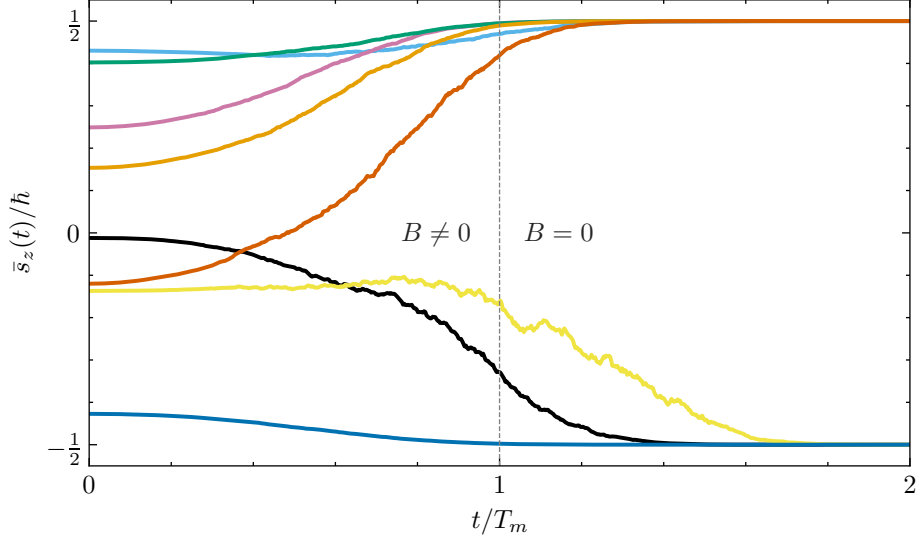


Figure 6.5: The graph depicts the same color-coded stochastic realizations as in figure 6.4 for $\bar{s}_z(t)$ as a function of the time. The vertical dashed line indicates the transition from the inhomogeneity of the field to a vanishing field. T_m is the time spent in the magnet.

the figure that is measured to be in a spin-down state is the one with the lowest $z(t = 0)$. A similar implication is drawn by looking at $\delta_0 = \pi/2$.⁴

The numerical results should give the same predictions as the standard approach with the Pauli spinor. In general, the two-component spinor in the basis $\Psi_{z'}$ of a z' axis tilted by the angle δ_0 w.r.t. the z axis, is given by

$$\Psi_{z'} = \begin{pmatrix} \cos \frac{\delta_0}{2} e^{-i\phi_0/2} \psi_+ \\ \sin \frac{\delta_0}{2} e^{i\phi_0/2} \psi_- \end{pmatrix}. \quad (6.61)$$

The probability for a spin to enter the up (down) channel is then $\rho_+^{QM} = \cos^2 \delta_0/2$ ($\rho_-^{QM} = \sin^2 \delta_0/2$). The comparison with the stochastic picture is shown in figure 6.7. The probabilities ρ_{\pm} were approximated by the share of particles going up/down N_{\pm}/N_{total} , so that $\rho_{\pm} \approx \frac{N_{\pm}}{N_{total}}$. For all measurement angles, the number of particles was $N_{total} = 10^6$. The stochastic model predicts the same results as in the Pauli theory. This will be used to discuss the Einstein-Podolsky-Rosen-Bohm “paradox” in the next section.

From the stochastic model we may infer that the inclusion of internal orientation coordinates points at a more detailed view on the phenomena considered around the concept of quantum spin. In this regard the description of Pauli is just like Occam’s razor; it is the minimal amount of structure added to the ordinary Schrödinger equation which is able to describe the statistical phenomena related to spin.

Spin expectations and the velocity fields

The figures 6.8 and 6.9 show the particle paths for two specific angles δ_0 associated with the initial spin expectations $E[\bar{s}(t = 0)]$ with a focus on spin expectation values and the role of the velocity fields.

Figure 6.8 shows 100 stochastic processes for $E[s_z(t = 0)] = 0$ (left, $\delta_0 = \frac{\pi}{2}$) and $E[s_z(t = 0)] = \frac{\hbar}{2\sqrt{2}}$ (right, $\delta_0 = \frac{\pi}{4}$). The black arrows indicate the averaged spin expectation values $\bar{s}(t, z)$ for the two initial settings. At the exit time $t = T_m$, it is visible that the spins are generally not aligned along the measurement axis. The spin average depends on the coordinate z , e.g., $s_z(T_m) \rightarrow \pm \hbar/2$ for $z(T_m) \rightarrow \pm \infty$. The plot on the right in figure 6.8 shows an upward bias due to the initial spin polarization.

⁴A larger ensemble of paths is shown in figure 6.8.

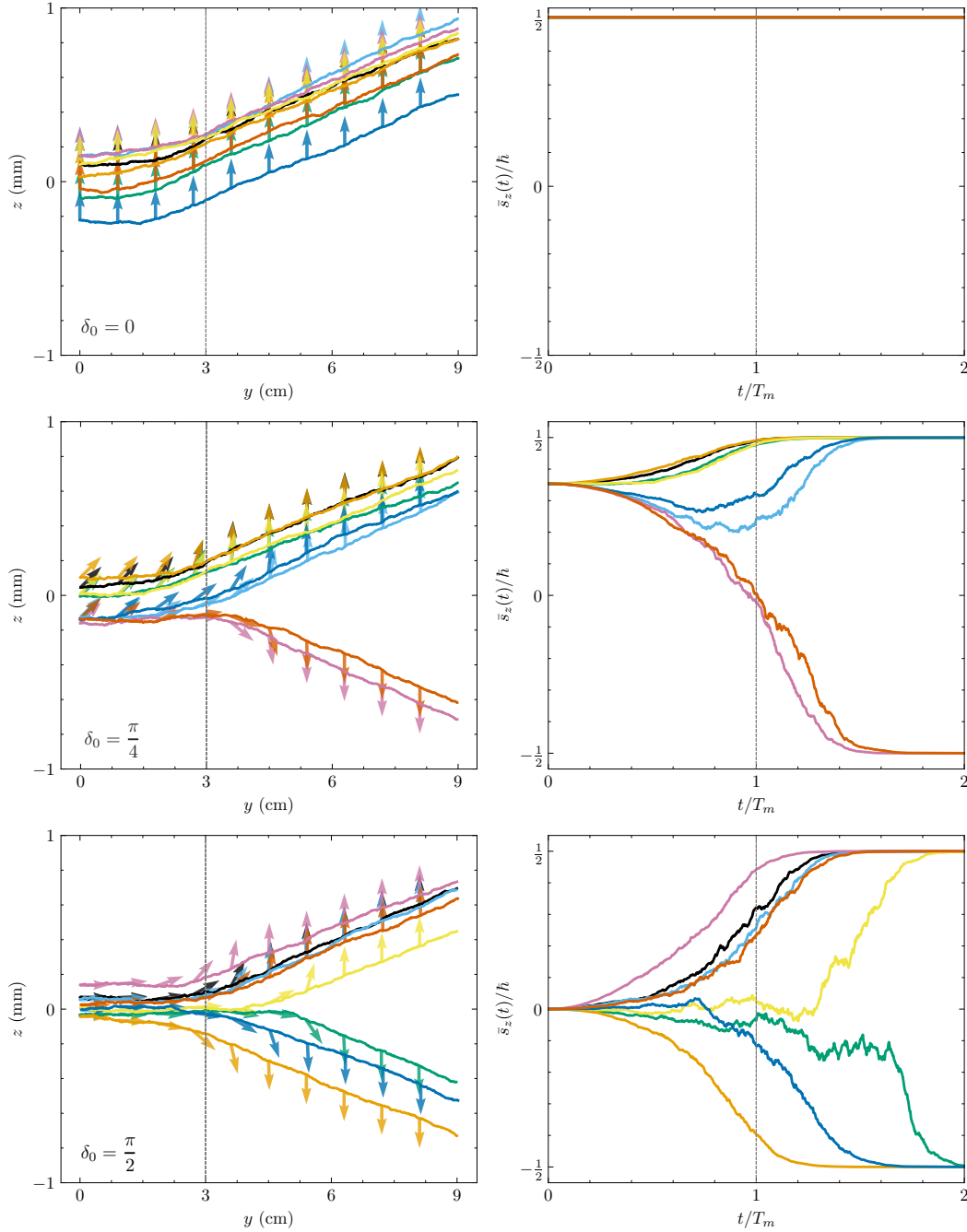


Figure 6.6: The figure shows stochastic paths of three different spin polarizations at the entrance of the SG magnet. The plots on the left depict the (z, y) -plane of 8 stochastic realizations entering the inhomogeneous magnetic field at $t = 0$ and leaving the magnetic field of length 0.03 m at $t = T_m$. The plots on the right show the associated spin averages $\bar{s}_z(t)$. The chosen incident angles are $\delta_0 = 0$ (top row), $\delta_0 = \pi/4$ (second row) and $\delta_0 = \pi/2$ (bottom row).

The role of the two velocity fields is shown in more detail in figure 6.9 with the same initial spin expectations as in 6.8. The realizations (blue) are shown together with vector plots for the averaged current velocity \bar{v} (black) and osmotic velocity \bar{u} (red). Note that due to simplicity this figure covers a magnetic field of length $d_1 = 0.09$ m as opposed to the usual $d_1 = 0.03$ m in the previous figures. Again the current velocity (black arrows) is the driving force for the propagation of the particle ensemble. In contrast, the osmotic velocity, shown in red, is responsible for the localization of the ensemble beam.

The discussion of the Stern-Gerlach experiment shows similarities to the explanations given in the pilot wave theory [Hol95]. In [DHKV88], the *deterministic* paths are analyzed for fixed initial spin expectations. There, the incident position $z_0 = z(t = 0)$ of the particle

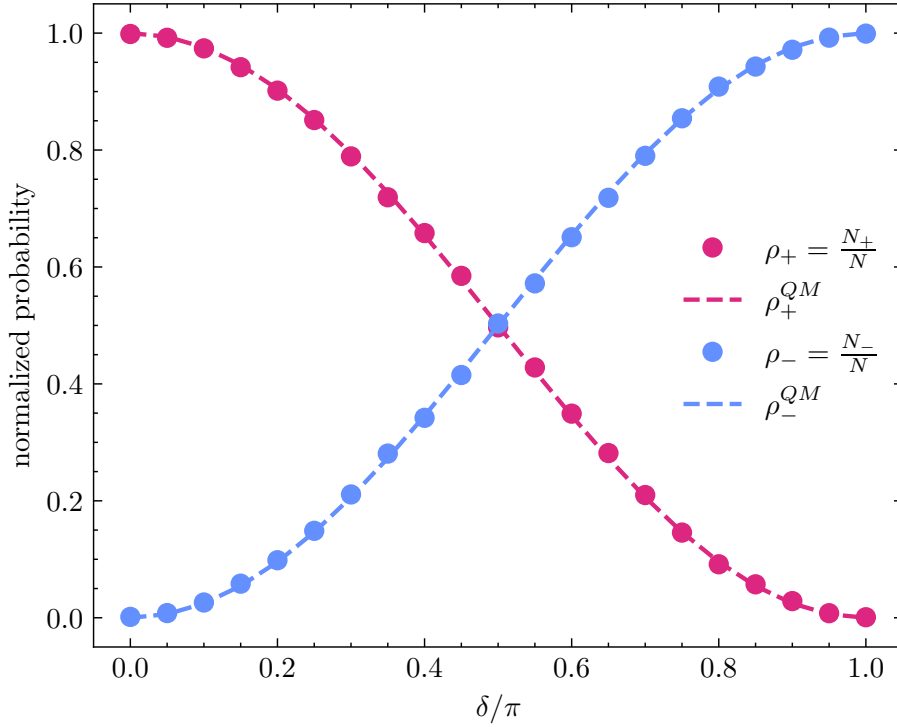


Figure 6.7: The plot shows the normalized probabilities for z polarized spin- $\frac{1}{2}$ particles entering a SG device to choose one of the two possible beams depending on the measurement angle δ_0 . The probabilities following from the Pauli-equation (dashed) are compared to the approximated probabilities from the numerical simulations based on the quantum Hamilton equations for the orientational average (dots).

determines the outcome of the individual particle, i.e., z_0 is the hidden variable. This led to a discussion about the possible reality of non-crossing paths when the beams are recombined because of singularities of the (current) velocity v , see e.g., [ESSW92, MRF⁺16, FDBS22]. In the stochastic picture, the velocity v has the same properties. The hidden variables, however, are *stochastic*. Hence, the initial position z_0 of the process does not predetermine the outcome but is rather an indicator of the probability of the measurement outcome. This is captured in figures 6.8 and 6.9 where it appears that the conditional probability of moving up depends - in the case of the spin averages - on the initial position. The particles with $\bar{Z}_{t=0} > 0$ are more likely to end up in the upper channel in figure 6.8 for spin expectation values perpendicular to the measurement axis, for example. From the plots in figure 6.6 on the other hand we know that the initial spin orientation in general has an impact on the movement of the particle, too. Hence, there is an interplay of the random initial positions and spins of the particle giving rise to the probabilities of ending up being measured as spin up or spin down particle.

Futher investigations

The further discussion of the SG experiment may be extended from here in the framework of stochastic mechanics. This includes the description of consecutive SG measurements. In the context of deterministic hidden variables where the particle's spins have a definite z projection before they enter the magnet, i.e., either up or down for a spin- $\frac{1}{2}$ particle, the outcome for each atom is predetermined for each particle. From that point of view, *one* Stern-Gerlach experiment may be explained, but not multiple consecutive ones in general. For example, consider three SG devices where the second measurement axis is perpendicular to the first, and the third measurement axis matches the first. If you only pass the *up* particles in the first two measurements, the third measurement shows a 50/50 splitting of the beam. In Heisenberg terms, this is described by the uncertainty principle where two spin projections,

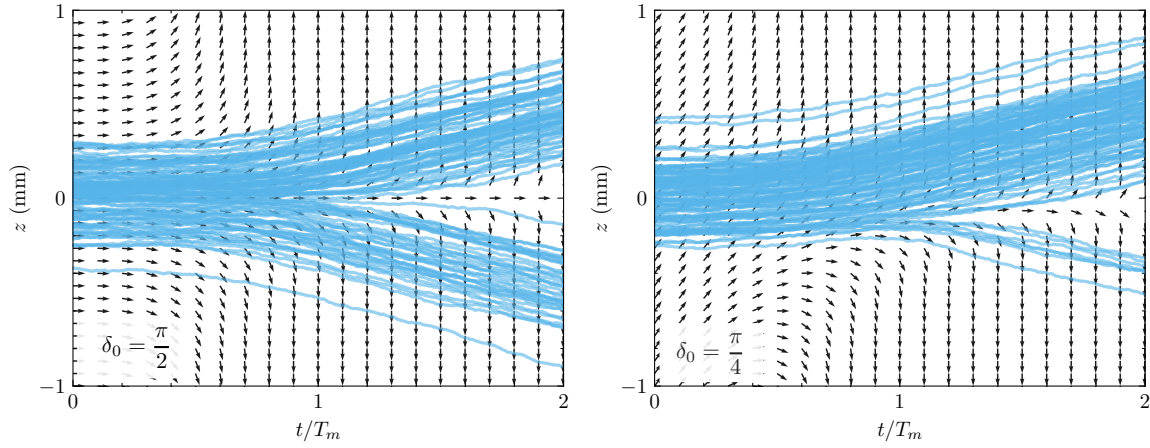


Figure 6.8: The graphs depict the (z, t) -dependency entering the inhomogeneous magnetic field at $t = 0$ and leaving the magnetic field of length 0.03 m at $t = T_m$. 100 Stochastic realizations are shown in blue for the initial spin expectations $E[s(t = 0)] = \frac{\hbar}{2}e_y$ (left) and $E[s(t = 0)] = \frac{\hbar}{2\sqrt{2}}(e_y + e_z)$ (right). The vector fields of the corresponding spin averages \bar{s} for the two initial spin expectations are shown in black arrows.

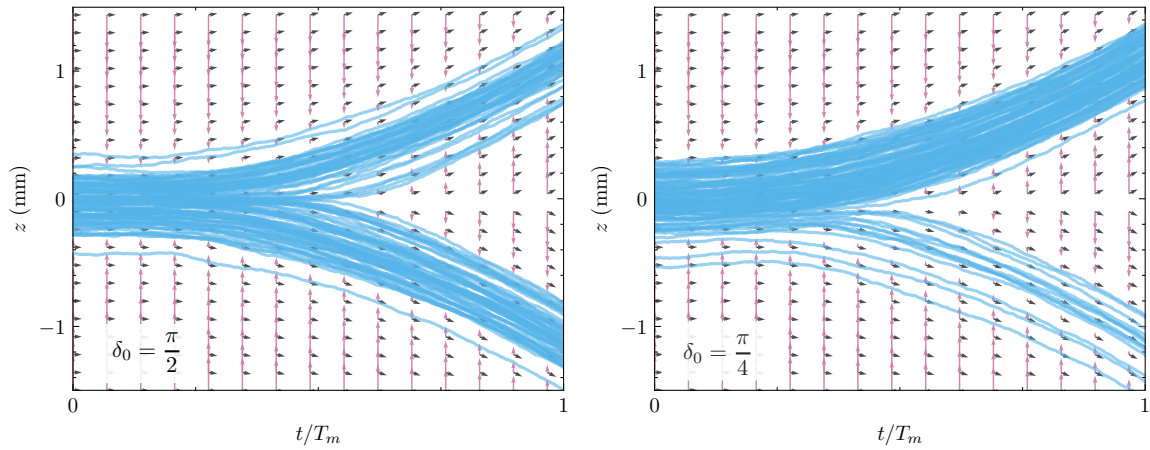


Figure 6.9: Both graphs show the vector fields of the current velocity \bar{v} (black arrows) and the osmotic velocity \bar{u} (red arrows) as functions of (t, z) in the magnet of length 0.09 m for two different initial spin expectations $E[s(t = 0)] = \frac{\hbar}{2}e_y$ (left) and $E[s(t = 0)] = \frac{\hbar}{2\sqrt{2}}(e_y + e_z)$ (right). 100 realizations of the stochastic process $z(t)$ as given in (6.58) are shown in blue on top of the vector mesh for the two different initial spin expectations.

e.g., s_x and s_z , cannot be known simultaneously. In terms of the two spinor in the Pauli theory, the selection of up beams leads to a collapse of the spinor after the first measurements. The ‘up’ particles in the first experiment, thus, do not always ‘choose’ the upward direction in the third experiment in general. Hence, the measurement apparatus alters the states. Therefore, the particle’s hidden variables must be adjusted to describe those experiments in a deterministic theory. For example, the theory should describe hidden variables which change with each measurement. The latter is related to the measurement in the stochastic picture, which leads to an update of the knowledge of the system. Hence, the probability distribution and v and u have to be adjusted after the measurement. The calculations are not carried out here, but they should be straightforward.

Another interesting example involves the recombination of a separated beam of atoms proposed in theory in [Boh51] and experimentally realized recently [MDZ⁺21]. Additionally, one could study the time of arrival as in the double slit experiment [NK08, KH23] depending on the initial settings. One may get similar effects in the time-of-arrival distributions as in the field free case for a spin- $\frac{1}{2}$ particle [DD19] where the velocity fields change with the measurement angles δ_0 . The following subsection, however, will focus on the Einstein-Podolsky-Rosen-Bohm Gedankenexperiment.

6.5 Einstein-Podolsky-Rosen-Bohm experiment

The theory of quantum mechanics allows for the description of a system of separated particles with interrelated, so-called *entangled*, properties in such a way that measuring the properties of one particle would instantaneously affect the properties of the other particle(s), regardless of the distance between them. This idea contradicts the classical understanding of physics, which suggests that any interaction cannot violate causality.⁵ This finding challenged the traditional view of reality and was a driving force in the search for different interpretations of quantum mechanics. These include the Copenhagen interpretation, the many-worlds interpretation, the pilot-wave theory, or Nelson's stochastic mechanics. For instance, within ordinary quantum interpretation, the superposition of states describing the wave function collapses instantaneously in the measurement.

The following section addresses the foundational aspects of entanglement exemplified by the model of two stochastic spins associated with the QHE derived in the previous sections. We derive feedback solutions for the QHE for both separable and entangled models using the usual construction using spin eigenstates. The corresponding trajectories and spins of the two particles are studied, including their treatment before and after interaction with the measurement devices. The essential point is that both particles act on each other's properties such as position and orientation, even though the two separated systems do not interact classically. The resulting correlations are analyzed in the context of Bell inequalities, which reveal that the stochastic model can describe correlations beyond any classical treatment. Some more background on the EPR paradox and the associated Bell tests is given beforehand.

6.5.1 The EPR, Bell's inequality, and Bell separability

In 1935, The New York Times turned the first impactful publication on the foundations of quantum mechanics [EPR35] into a headline "Einstein Attacks Quantum Theory", which, of course, was not intended by Einstein, Podolsky, and Rosen. The EPR paper raised fundamental questions about the theory developed to describe quantum mechanics at that time. It claimed to have found a paradox in quantum theory that suggested it might be incomplete, or simply put, that the wave function may not contain all the system's information. Hence, they asked: Can quantum mechanics be considered a complete theory?

In more detail, they introduced a gedankenexperiment involving a system of two particles "permit[ted] to interact" initially, before they are locally separated, such that "there is no longer any interaction between the two parts" [EPR35]. The system should be described by a unique quantum state, which is not a product but rather an entangled state. The wave function and the distribution are not factorizable. In the moment of a momentum measurement on particle A, the wave function will reduce so that the momentum of the second particle B is changed *depending on the measurement on A*. This occurs despite no interaction term in the system's Hamiltonian. That is, even in the case of large distances, where the particles cannot exchange information due to space-like separation, the measurement of particle A influences the state of particle B instantaneously. This contradicts the idea of locality, where objects are influenced by their local surroundings and seems to disagree with special relativity, which refers to causality since the speed of information transfer from A to B cannot exceed the speed of light.

The EPR paradox seems to arise when the position of B is measured instead of its momentum since the Heisenberg uncertainty states that two complementary properties cannot be known simultaneously. To resolve these conceptual problems, the authors of the EPR paper inferred that the "missing" information to the wave function should be added through hidden variables. However, another possible explanation, supported by Bohr and now widely accepted in quantum mechanics, is that a quantum system can be in multiple

⁵While the information stored in the entangled particle pairs can be utilized in various aspects, the information transfer between two space-like separated points cannot exceed the speed of light.

states simultaneously, where each specific outcome in a measurement appears with a certain probability. Hence, the wave function reduces to the observed state in measurement.

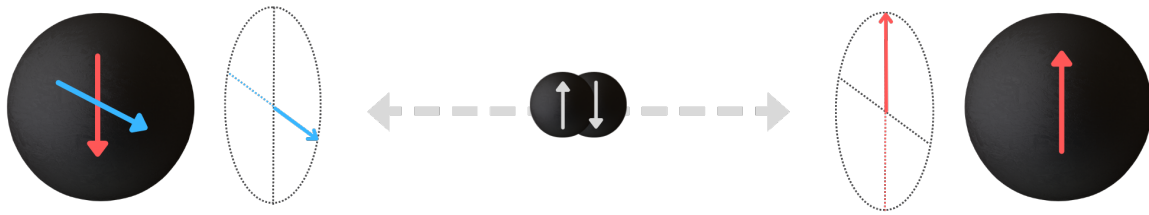


Figure 6.10: The figure shows a schematic of Bohm’s version of the EPR experiment. A pair of objects with antiparallel spins in an entangled state is space-like separated. The spin of particle A depicted on the right is measured along some axis a (red arrow), e.g., giving spin-up state for A. The measurement on A fixes spin B to be in a spin-down state without any measurement on B. The EPR “paradox” arises if the measurement axis b on B (blue arrow) is not parallel to A: the spin s^B seems to have two definite known spin projections due to the preparation of the two-particle state.

The EPR paradox describes characteristics of an entangled pair of objects when one applies measurements where the operators do not commute. To simplify the gedankenexperiment, Bohm restricted the variables to discrete measurements of spin. In his proposed experiment, depicted schematically in figure 6.10, he considered a system of two initially anti-correlated spins in a singlet state. The singlet state guarantees that measurements of the spin pair are always antiparallel, regardless of the measurement axis. When the particles are space-like separated, measuring the spin A, s_z^A , along the z -axis determines or “unveils” s_z^B immediately. The paradox arises when a different measurement axis for s^B is chosen when measuring s_z^A , for example, when measuring the x component of B, s_x^B , simultaneously with s_z^A . This scenario appears to violate Heisenberg’s uncertainty relation for non-commutative quantities, as s_z^B and s_x^B cannot be measured simultaneously.

Quantum theory describes the initially antiparallel spins of the entangled pair using the singlet ($-$) or triplet ($+$) state in Dirac notation

$$|\Psi_{\pm}\rangle = \frac{1}{\sqrt{2}} (|\uparrow\downarrow\rangle \pm |\downarrow\uparrow\rangle), \quad (6.62)$$

where the spatial part is usually not explicitly considered. Measuring the spin of particle A along some direction a causes the wave function to collapse to one of the two-state vectors in eq. (6.62). Figure 6.10 shows perfect anticorrelation for the spin expectation values if B measures the same axis $b = a$. However, if the second measurement axis is different, $b \neq a$, as shown in figure 6.11, the expected correlation yields

$$\frac{4}{\hbar^2} \langle (s^A \cdot a) (s^B \cdot b) \rangle_{\Psi_-} = -a \cdot b. \quad (6.63)$$



Figure 6.11: A schematic of Bohm’s version of the EPR experiment is shown, similar to figure 6.10. While the measurement axis on A to the right is parallel to a (red arrow), the measurement on B to the left is carried out along a different direction $b \neq a$ (blue arrow). Bell’s inequality is derived for three different measurement axes. The solid gray line symbolizes the entanglement before the measurement.

Bell's inequality

John Bell [Bel64] recognized the significance of the correlation (6.63) and derived an inequality for one of Bohm's versions of the EPR paradox. Starting from a singlet spin state, Bell added hidden parameters λ connected with a probability density function $\rho(\lambda)$ independent of the measurement axes. The measurement of $s^A(a, \lambda)$ and $s^B(b, \lambda)$ depends both on λ and on the measurement axes a and b . Each measurement, however, does not depend on the setting of the other measurement, which refers to *local* hidden variables. The possible normalized outcomes are $A(a, \lambda) = \pm 1$ and $B(b, \lambda) = \pm 1$. The expectation

$$P(a, b) = \int d\lambda \rho(\lambda) A(a, \lambda) B(b, \lambda). \quad (6.64)$$

gives the corresponding correlation in Bell's model of hidden variables, which leads to the inequality

$$|P(a, b) - P(a, c)| \leq 1 + P(b, c). \quad (6.65)$$

This inequality is violated by (6.63) for specific angles, e.g., for $a \perp b$ and $a \cdot c = b \cdot c = \frac{1}{\sqrt{2}}$ there is $\frac{1}{\sqrt{2}} \leq 1 - \frac{1}{\sqrt{2}}$.

As of today, numerous experiments conducted over the last few decades, such as those described in references [FC72, FT76, AGR81, AGR82, TRO94], have confirmed the existence of entangled states that defy local realism. Moreover, these experiments demonstrate that entangled states can produce stronger correlations than any local and realistic model, thus violating Bell's inequality (6.65) under specific circumstances.

Most of these experiments involve the use of photons and rely on the Clauser-Horne-Shimony-Holt (CHSH) inequality [CHSH69] or generalized versions, e.g., [CH74, Bel04]. The CHSH inequality is a redefinition of (6.65) that is easier to verify in experiment and, more importantly, does not rely on "Bell's experimentally unrealistic restriction that for some pair of parameters [b and c] there is perfect correlation" [CHSH69]. The CHSH inequality depends on four measurement settings a, a' at A and b, b' at B , such that Bell's inequality is transformed into

$$|P(a, b) + P(a, b') - P(a', b) + P(a', b')| \leq 2. \quad (6.66)$$

Most of these experiments rely on the entanglement of photons. Connected to that, there is a properly filled timeline of experiments searching for the resolution of so-called loopholes in Bell tests, e.g., those associated with detector efficiency [RKM⁺01] and/or locality of the measurements [HBD⁺15]. Another loophole is associated with the assumption that the measurement on A is always correlated to the measurement settings on B , which is supported by the theory of superdeterminism and variants thereof [Bra88, Hal10, Hal16, DH22]. The group of Zeilinger, for example, addressed this problem in an experiment [RHH⁺18].

The Nobel Prize Committee recently [nob22] emphasized the importance of the empirical verifications of Bell's inequalities over the last decades for the physics community as they added another checkmark to the validity of the current description of the quantum theory. The traditional view of reality is, thus, challenged by the experiments in combination with the standard theory regarding its foundations. This led to decades of controversy about how to understand the theory and its results. The entanglement phenomenon, for example, are often misinterpreted as "non-local" or "spooky action at a distance". This, however, depends on the interpretation of quantum mechanics. Another misconception is that there is no possibility of describing those effects with causal theories.

Nevertheless, quantum mechanics and Bell's inequality leaves room for realistic descriptions. The discussion of the EPRB gedankenexperiment and related to that, the search for alternative interpretations of quantum mechanics continues to be an active area of research even today since there is no decline in the number of papers referencing the papers by

EPR [EPR35] or Bell [Bel64] in the field of quantum foundations. In general, the fundamental discussion of possible quantum theories that violate Bell's inequality must include relaxations on the assumptions given in its derivation [Bel64]. Hence, the following question arises: What does it take to violate Bell's inequality?

Bell-separability

The use of non-locality to describe the EPRB is ambiguous, as noted by Hall [Hal16]. Instead, Hall suggests using the term *Bell-separability*. In this framework, an experiment is defined by a preparation procedure U , a measurement $m = (a, b)$ with submeasurements a and b , and corresponding outcomes $M = (A, B)$. The joint probability density $\rho(A, B|a, b, U)$ represents the statistical correlations of the outcomes of repeated measurement procedures. If there exist hidden variables λ , then the joint probability density can be written as the integral of the product of the conditional probability densities of A and B given λ , and the probability density of λ given a and b , as follows from Bayes' theorem

$$\rho(A, B|a, b, U) = \int d\lambda \rho(A, B|\lambda, a, b, U) \rho(\lambda|a, b, U). \quad (6.67)$$

Bell's inequality for the correlations between three measurement angles a, b, c (given by Equation (6.65)) can be expressed as a basic stochastic inequality for three subprocedures of the measurement settings a, b, c . For example, three different measurement axes a, b, c and their corresponding outcomes A, B, C . Specifically, the inequality relates the joint probability densities of measurement outcomes as follows

$$\rho(A, \bar{B}|a, b, U) + \rho(B, \bar{C}|b, c, U) \geq \rho(A, \bar{C}|a, c, U). \quad (6.68)$$

where \bar{B}, \bar{C} denotes the complement to the outcome B, C . In stochastic mechanics, the underlying variables are, e.g., the position in space, $\lambda = x$, with the associated probability distribution, $\rho(\lambda|a, b) = \rho(x|a, b)$, depending on the initial preparation and the measurement. We will omit the preparation procedure U from here on for brevity.

Given this, a probabilistic model must satisfy the following properties to obey Bell's inequality:

1) Statistical completeness:

The measurement outcomes are predetermined in the form of hidden variables λ in a way that the joint probability distribution factorizes as follows

$$\rho(A, B|\lambda, a, b) = \rho(A|\lambda, a, b) \rho(B|\lambda, a, b), \quad (6.69)$$

which is true for a deterministic model.

2) Statistical locality:

The two subprocedures a and b are not correlated with each other's outcome probability density,

$$\rho(A|\lambda, a, b) = \rho(A|\lambda, a) \quad \text{and} \quad \rho(B|\lambda, a, b) = \rho(B|\lambda, b). \quad (6.70)$$

This ensures that space-like separated measurements do not alter the outcome probability distributions. In other words, changing the measurement settings on A cannot affect anything outside its future light cone.

3) Measurement independence:

The hidden variable λ entails no information on the future measurements such that

$$\rho(\lambda|a, b) = \rho(\lambda). \quad (6.71)$$

This property ensures that the (stochastic) hidden variable is independent of the future measurement settings a, b .

It was known to Bell already [Bel76] that one of these properties must be violated in quantum mechanics. Standard quantum mechanics in the Hilbert space disobeys statistical completeness. A linear combination of solutions to the Schrödinger equation leads already to a non-factorizable probability density. The same holds, of course, for associated density matrices and entangled states. Hence, any theory with the same probability density associated with the wave function violates requirement 1), which is not directly connected to the locality but rather the separability of the probability. Suppose a quantum mechanical distribution is not separable. In that case, the Nelson processes derived from the associated wave functions do not fulfill statistical completeness. Nevertheless, the theory, in that case, is statistically local.

This type of locality, however, does not translate to local velocity fields, which are the physical entities in the trajectory pictures. Consider the quantum velocity fields $v_{(1)}^q, v_{(2)}^q$ of two particles 1, 2. Now assume that the system may be described by a non-factorizable probability distribution $\rho(t, x_{(1)}, x_{(2)})$, the osmotic velocity of particle 1 reads

$$u_{(1)}(t, x_{(1)}, x_{(2)}) = \frac{\hbar}{2m} \frac{\nabla_{(1)} \rho(t, x_{(1)}, x_{(2)})}{\rho(t, x_{(1)}, x_{(2)})}. \quad (6.72)$$

Hence, $u_{(1)}$ depends on the configuration of particle 2 independent of any local interaction between the particles. The non-locality follows in the sense that the Lagrangian in the cost function or the corresponding stochastic Hamiltonian do not contain any interaction terms to explain the correlation. Hence, the measurement of one particle can affect the velocity of a space-like separated other particle.⁶

Finally, note that there are other possible interpretations of quantum mechanics preserving reality. One of them is Everett's many worlds interpretation, accompanied by the branching of realities. I.e., local realism comes at the cost of multiple realities where all possible outcomes occur in different universes [DeW70]. Another local realistic and deterministic theory assumes that everything is predetermined by a common cause in the past, the so-called superdeterminism, e.g., see [Bra88, DH22]. The latter is related to the relaxation of the measurement independence 3) so that the measurement settings in an experiment cannot be chosen independently.

6.5.2 Stochastic description of a non-interacting particle pair

The discussion of the EPRB experiment schematically shown in figure 6.10 refers to massive and non-relativistic particles with spin, contrary to the common experiments using photons. For that the theory in section 6.2 is extended to two particles with positions $x_{(1)}, x_{(2)}$ including rotational degree of freedom denoted by $\theta_{(1)}, \theta_{(2)}$ as given in the appendix G. For simplicity, it is assumed that there are no external potentials until measurement, the two particles carry no net charge $q = 0$, and that their masses m and inertias I_m, I_c are identical. Generally, the interaction of the two magnetic moments related to their angular velocities may not be neglected at the experiment's preparation state, which from a purely classical point view, is dominant over the Coulombic interaction on short scales. The dipole interaction, however, is negligible on the distances considered in the EPRB gedankenexperiment due to their space-like separation later on.⁷

⁶Locality was also discussed in stochastic mechanics in more detail. On the one hand, the change of measurement settings on A cannot affect anything outside its future light cone, i.e., no instantaneous effect on the space like separated system B. This was labeled as *active* locality by Nelson [Nel86]. *Passive* locality, on the other hand, demands that the dependence between simultaneous and distant measurements must be explainable in the preparation state prior to the measurements. For a more detailed view of passive and active locality in terms of stochastic picture, see the appendix by Faris in [Wic12].

⁷A discussion of possible bound states of two interacting magnetic moments is an open question to the QHE. For one, the degrees of freedom for two diffusively rotating and interacting magnetic moments exceeds the

The quantum Hamilton equations for the canonical momenta $p_{(k)} = mv_{(k)}^q + q_{(k)}A_{(k)}$ and $s_{(k)} = I_{m(k)}\omega_{(k)}^q + I_{c(k)}B_{(k)}$ of particle k are then the momentum equations (6.34) and (6.35) given in the Stern-Gerlach chapter. Hence, we can write them as discussed in (G.3)-(G.4)

$$dp_{(k)} = -\gamma I_m \nabla_{(k)} \left(\omega_{q_{(k)}} \cdot B_{(k)} \right) dt + dA_{(k)} + \Pi_{(k)}^p dW_- \quad (6.73)$$

$$ds_{(k)} = \left[\gamma s_{(k)} \times B_{(k)} + \frac{\hbar}{I_m} T_{(k)} \right] dt + s_{(k)} \times \Pi_{(k)}^s dW_- \quad (6.74)$$

where $B_{(k)}$ are the magnetic fields generated by the Stern-Gerlach devices for each particle and $T_{(k)}$ is a purely quantum torque term which vanishes in the classical limit. The coupling of the particle's orientational degrees of freedom to their motion in space is apparent in equation (6.73), which includes an inhomogeneity in the magnetic field. In the absence of a magnetic field, i.e., before and after the particles interact with the Stern-Gerlach magnets, the classical force $\nabla_{(k)} (\omega_{q_{(k)}} \cdot B_{(k)})$ vanishes. The drift term in the momentum equations shows no sign of coupling between orientation and position. Thus, the rotational motion of the two particles moving in opposite directions can be treated separately from a classical point of view. Similarly, the orientational motions of the two particles are decoupled such that the evolution of the spins $s_{(1)}$ and $s_{(2)}$ are independent from a classical perspective. By adding uncorrelated random kicks to each particle's orientation, perfectly antiparallel spins will decorrelate rapidly. This does, however, not apply to the spin QHE (6.74) in general, where the spins may be correlated depending on the preparation of the initial state.

In general, the coupling depends on the initial (or final) settings in the formulation of the QHE for the momenta $p_{(k)}, s_{(k)}$. It can be explained by the current and osmotic velocity fields. They are feedback controls, i.e., in general $v_{(k)}^q(t, x_{(1)}, x_{(2)}, \theta_{(1)}, \theta_{(2)}) = v_{(k)} - iu_{(k)}$ and $\omega_{(k)}^q(t, x_{(1)}, x_{(2)}, \theta_{(1)}, \theta_{(2)}) = \omega_{(k),v} - i\omega_{(k),u}$. The canonical momenta $p_{(k)} = mv_{(k)}^q + qA_{(k)}$ and $s_{(k)} = I_m(\omega_{q_{(k)}} + \gamma_{(k)}B_{(k)})$ with $p_{(k)} = p_{(k),v} - ip_{(k),u}$ and $s_{(k)} = s_{(k),v} - is_{(k),u}$ can be viewed as feedback controls as well. E.g., the Itô formula for the momentum $p_{(k)}(t, x_{(1)}, x_{(2)}, \theta_{(1)}, \theta_{(2)})$ as feedback control depending on all configuration variables leads to a partial differential equation

$$\begin{aligned} \partial_t p_{(k)} + \sum_{k=1}^2 \left(v_{q_{(k)}} \cdot \nabla_{(k)} + \omega_{q_{(k)}} \cdot \nabla_{\theta_{(k)}} \right. \\ \left. - \frac{i\hbar}{4} \sum_{j=1}^2 \left(\frac{1}{m} \nabla_{(j)} \cdot \nabla_{(k)} + \frac{1}{I_m} \nabla_{\theta_{(j)}} \cdot \nabla_{\theta_{(k)}} + \frac{1}{\sqrt{mI_m}} \nabla_{(k)} \cdot \nabla_{\theta_{(j)}} \right) \right) p_{(k)} \\ = -\gamma I_m \nabla_{(k)} (\omega_{q_{(k)}} \cdot B_{(k)}) \end{aligned} \quad (6.75)$$

concerning the drift term in (6.73). Thus, even if the rhs of (6.75) is zero, there may be solutions to $p_{(k)}(t, x_{(1)}, x_{(2)}, \theta_{(1)}, \theta_{(2)})$ depending on all the configuration variables. Such cases arise especially when the joint probability distribution cannot be written in the form of a product.⁸ Furthermore, considering the stochastic integrals in (6.73), the matrix

$$\Pi_{(k)}^p = (\sigma_m \nabla_{(1)}, \sigma_m \nabla_{(2)}, \sigma_I \nabla_{\theta_{(1)}}, \sigma_I \nabla_{\theta_{(2)}}) P_{(k)} \quad (6.76)$$

is multiplied with a 12-dimensional Wiener process W_t^- . Hence, the stochastic contribu-

capabilities of the currently used numerical algorithms. Secondly, this system may need generalization to a relativistic stochastic theory following [Spo04].

⁸Consider, for example, the coupling of translation to spin in the Stern-Gerlach experiment, especially the case where the field setup leads to not yet fully aligned spins at the end of the magnet. The corresponding probability distribution is not spatially separated into two parts. Eventually, the spins align, and the probability distributions separate in the field-free part. This is due to the influence of the magnetic field so that at the end of the magnet, the probability distribution cannot be written as a product of probabilities w.r.t. position and orientation $\rho(x, \theta, t) \neq \rho_x(x, t)\rho_\theta(\theta, t)$. It follows that $u(x, \theta) = \frac{\hbar}{2m\rho} \nabla \rho(x, \theta)$ and $s_u(x, \theta) = \frac{\hbar}{2I_m\rho} \nabla \theta \rho(x, \theta)$ are fields depending on orientation and position. See appendix E for a discussion of these phenomena about the quantum potentials in the pilot-wave theory.

tion to the change of momentum, say $P_{(1)}$, is coupled to the position of particle 2 and the orientation of both particles in general.

Something similar holds for the spin fields. In the field free case, one may assume that $s_{(1)}$ and $s_{(2)}$ are decoupled from their positions before the measurement. Both can, however, depend on the other's orientational variable $s_{(1)}(t, \theta_{(1)}, \theta_{(2)})$ and $s_{(2)}(t, \theta_{(1)}, \theta_{(2)})$ due to the preparation of the particle pair. Assume, e.g., we have two feedback solutions $s_{(1),t} = s_{(1)}(t, \theta_{(1)}, \theta_{(2)})$ and $s_{(2),t} = s_{(2)}(t, \theta_{(1)}, \theta_{(2)})$ to the QHE. With the Itô formula the stochastic term in equation (6.74) may be written as gradients w.r.t. to $x_{(k)}$ and $\theta_{(k)}$, where $\sigma \nabla_{(1)} s_{(k)} = \sigma \nabla_{(2)} s_{(k)} = 0$ due to the assumption that $s_{(k)}$ does not depend on the positions. The gradients $\sigma_I \nabla_{\theta_{(1)}} s_{(2)}$ and $\sigma_I \nabla_{\theta_{(1)}} s_{(1)}$, however, do not vanish in general which leads to possible couplings in the two stochastic spin trajectories, even in the absence of drift terms.

The model of two decoupled particles with spin is considered first, where each particle's velocity field is independent of the other such that the probability distribution is separable. Using this classically motivated approach, we show that the stochastic picture of the EPRB paradox does not violate Bell's inequality, as this problem is Bell separable. After that, the *entangled* state of the gedankenexperiment is taken into account, leading to non-local drift fields that are necessary to explain the strongly correlated stochastic realizations.

6.5.3 Bell separable particle pairs

Consider two spin- $\frac{1}{2}$ particles, i.e., $E[s_{(1)}^2] = E[s_{(2)}^2] = \frac{3\hbar^2}{4}$, with Gaussian distributed starting positions. According to the EPRB experiment, both spins should be antiparallel at $t = 0$, i.e., under expectation

$$E[s_{(1)}(t = 0)] = -E[s_{(2)}(t = 0)]. \quad (6.77)$$

Here, $s_{(k)}(t) = s_{(k)}(t, y_{(1)}, y_{(2)})$ is shorthand for the spin field solutions to the QHE depending on the configuration variables $y_{(k)} = (x_{(k)}, \theta_{(k)})$. For $t > 0$ they move in opposite directions until they enter two space-like separated Stern-Gerlach-devices at $t = T$ with tilted measurement axes as shown in figure 6.11.⁹ The spin of particle 1 at magnet 1 is measured along $z_1 := z_1^{\delta_1}$, which is rotated by an angle δ_1 w.r.t. the z -axis around the y axis. The beam of particle 2 splits along the $z_2 := z_2^{\delta_2}$ -axis which is tilted by an angle δ_2 w.r.t. the z -axis.

In the separable model, it is assumed that the (angular) velocities for each particle $v_{q_{(1)}}(y_{(1)}, t)$ and $v_{q_{(2)}}(y_{(2)}, t)$ do not depend on the configuration variable of the other particle. This is associated with a factorizable probability distribution $\rho(y_{(1)}, y_{(2)}, t) = \rho_1(y_{(1)}, t)\rho_2(y_{(2)}, t)$ for all t . Before the measurement, it is also assumed that the orientation for each particle is not coupled to its position, so the discussion of the rotational diffusion follows the freely spinning top in section 5.4. The considered *uncorrelated* solutions to the QHE equations lead to spin fields $s_{(1)}(\theta_{(1)})$ and $s_{(2)}(\theta_{(2)})$ which are not explicitly time dependent. For a pair of spin- $\frac{1}{2}$ particle with antiparallel expectations along the z axis in particular, the feedback solutions $\Omega_{(1),\vartheta}^q = -\frac{\hbar}{2} \tan \frac{\vartheta_{(1)}}{2}$ and $\Omega_{(2),\vartheta}^q = -\frac{\hbar}{2} \cot \frac{\vartheta_{(2)}}{2}$ from section 5.3 to $\mu_{(1)} = -\mu_{(2)} = 1/2$ and $\nu_{(1)} = \nu_{(2)} = 1/2$ in the QHE (5.50) are used.

The measurement procedure leads then to a coupling of the particle's orientation to its position. This follows from the stochastic description of the Stern-Gerlach experiment in section 6.4 where the coupling of the rotation to the translation is analyzed with the orientational averages, e.g., $\bar{s}_{(k)}(t, z_{(k)})$. Repetitive measurements of the particle pairs will show a splitting into two Gaussian beams along the corresponding field axes at each magnet where the particle's spin expectation and position at the entrance slit of the inhomogeneous field $B = B_z(z)e_z$ are correlated with the outcome as seen in figure 6.4, for example.

⁹Note that this state is not an entangled state as demanded in the EPRB. We consider the entangled state later.

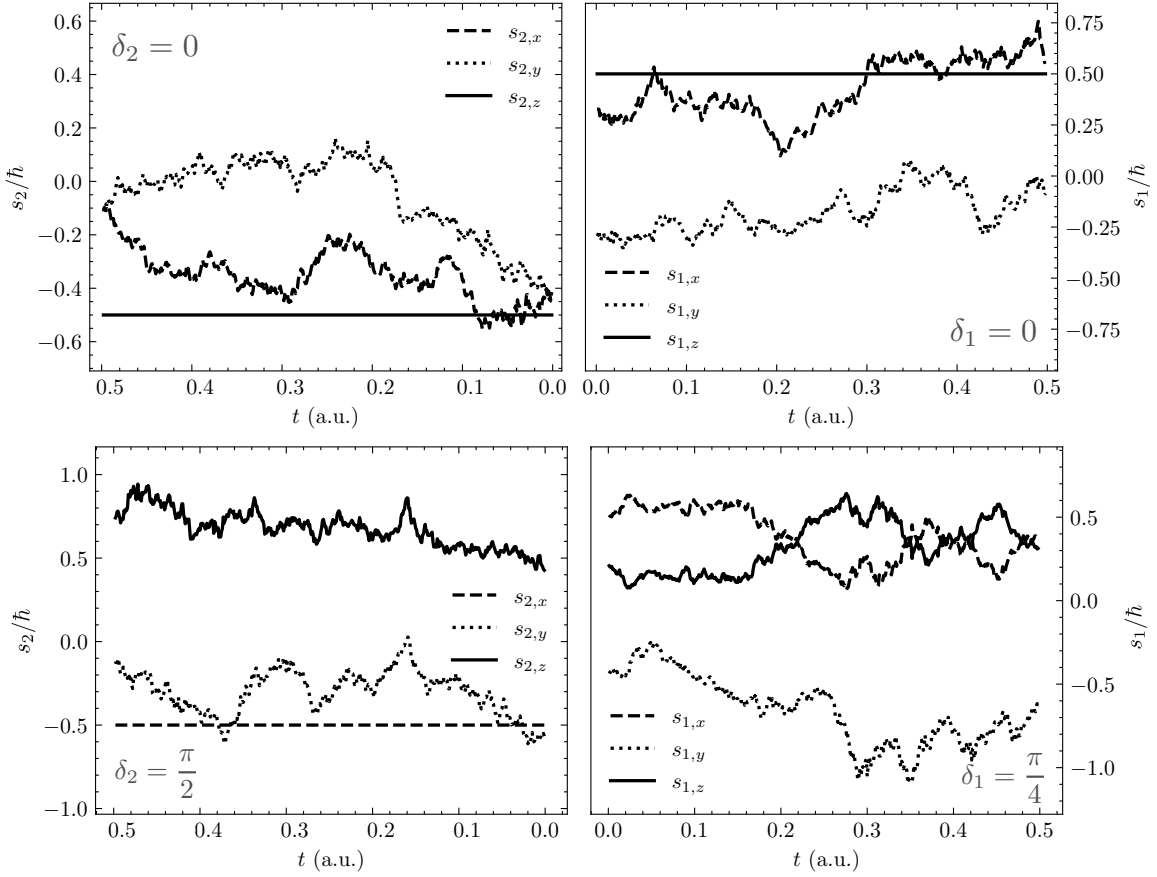


Figure 6.12: The figure displays the time evolution of the z component of the spin components of two antiparallel spin-pairs in each row. The spin components of particle 1 are denoted by $s_{(1)}(\theta_{(1)t})$ in the right column, while the spin components of particle 2 are denoted by $s_{(2)}(\theta_{(2)t})$ in the left column. The spins are initially prepared in a spin-up and a spin-down state. The figure shows the stochastic realizations of $\theta_{(i)t}$ in the field-free region before entering the Stern-Gerlach magnets. The top row of the figure displays the z components of the spins as measured by the Stern-Gerlach magnets along their $z_1 = z_2 = z$ axis ($\delta_1 = \delta_2 = 0$). The bottom row shows the spin components as viewed from a coordinate system defined by the measurement axes of the Stern-Gerlach devices. In the bottom right, the components of $s_{(1)}$ are shown for a rotation around the y axis by an angle $\delta_1 = \frac{\pi}{4}$. In the bottom left, a stochastic realization of $s_{(2)}$ for $\delta_2 = \frac{\pi}{2}$ is depicted. It is important to note that the time axis for the second particle (left column) is reversed.

Spin (de-)correlations

From the QHE for a freely spinning particle, it follows that the ensemble expectations $E[s_{(1)}] = E[s_{(1),v}]$ and $E[s_{(2)}] = E[s_{(2),v}]$ remain constant until measurement. The product of the spins

$$E[s_{(1)} \cdot s_{(2)}] = E_{(1)}[s_{(1),v} + s_{u(1)}] \cdot E_{(2)}[s_{(2),v} + s_{(2),u}] = E_{(1)}[s_{(1),v}] \cdot E_{(2)}[s_{(2),v}] = -\frac{\hbar^2}{4} \quad (6.78)$$

remains constant too. Here it is used that the expectations can be calculated separately for each particle

$$E[A(y_{(1)})] = \int A(y_{(1)})\rho_{(1)}(y_{(1)})dy_{(1)} \underbrace{\int \rho_{(2)}(y_{(2)})dy_{(2)}}_{=1} =: E_{(1)}[A(y_{(1)})], \quad (6.79)$$

since the probability distribution and the spin fields are separable. From this we can calculate $E[s_{\text{tot}}^2] = E[(s_{(1)} + s_{(2)})^2] = E[s_{(1)}^2] + E[s_{(2)}^2] + 2E[s_{(1)} \cdot s_{(2)}] = \hbar^2$. The stochastic correlation

$-1 \leq C(s_{(1)}, s_{(2)}) \leq 1$ of the two spin system

$$C(s_{(1)}, s_{(2)}) = \frac{\mathbb{E}[s_{(1)} \cdot s_{(2)}] - \mathbb{E}[s_{(1)}] \cdot \mathbb{E}[s_{(2)}]}{\sqrt{\mathbb{E}[s_{(1)}^2] - (\mathbb{E}[s_{(1)}])^2}} \quad (6.80)$$

vanishes for the separable model $C(s_{(1)}, s_{(2)}) = 0$. Although the particles are anti-correlated under expectation w.r.t. the chosen preparation axis according to equation (6.78), they are statistically uncorrelated according to equation (6.80).

As illustrated in figure 6.12, the stochastic spins are not anti-correlated. The plots show the particles' stochastic spin fields as functions of time of the separable model depending on the z -axes of Stern-Gerlach magnets tilted by δ_1, δ_2 . The two rows show particle 1 in the spin-up state and particle 2 in a spin-down state where the z -component for both particles is perfectly anti-correlated (top row) when viewed along the same z axis. The other spin components are not anti-correlated. The bottom row shows the spin components of a pair for two different measurement angles $\delta_1 = \pi/4$ and $\delta_2 = \pi/2$ with corresponding spin expectations

$$\mathbb{E}[s_{(1)}] = \frac{\hbar}{2}(\sin \delta_1 e_{x_1} + \cos \delta_1 e_{z_1}) = \frac{\hbar}{2\sqrt{2}}(e_{x_1} + e_{z_1}) \quad \text{and} \quad (6.81)$$

$$\mathbb{E}[s_{(2)}] = \frac{\hbar}{2}(\sin \delta_2 e_{x_2} + \cos \delta_2 e_{z_2}) = \frac{\hbar}{2}e_{x_2}, \quad (6.82)$$

respectively. Here e_{x_l} denotes the unit vector along the x direction in the δ_l tilted reference frame. From that, it can be assumed that the incident spin of the particles in the Stern-Gerlach experiments will not give perfect anticorrelations except for measuring along the preparation axis z , i.e., angles $\delta_1 = \delta_2 = 0$.

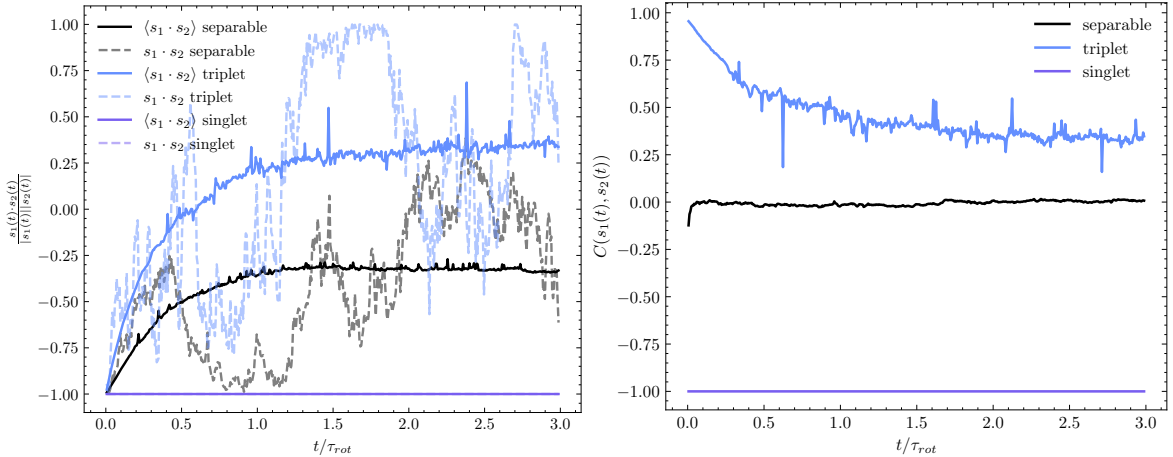


Figure 6.13: The spin fields as a function of the stochastic realizations of the orientation variables for independent spins (black) are analyzed. The plots include the spin fields for entangled spins in the triplet (blue) and singlet (purple) state, as considered in the next subsection. The left plot depicts the normalized dot product $-1 \leq s_{(1)}(t) \cdot s_{(2)}(t) / |s_{(1)}(t)| |s_{(2)}(t)| \leq 1$ of the two spin vector fields for a single path (dashed lines) and the ensemble average (solid lines) where the dashed purple line connected to the singlet state is hidden behind the solid purple line. The initial orientation variables for the two particles were chosen so that the stochastic spin fields $s_{(1)}(0) = -s_{(2)}(0)$ were initially antiparallel. The ensemble averages are calculated from 10^4 numerical realizations of the orientational process w.r.t. to a timescale $\tau_{rot} = \frac{I_m}{\hbar}$ depending on the inertia I_m . (Right plot) The numerical approximation of the stochastic correlation $C(s_{(1)}(t), s_{(2)}(t))$ as given in equation (6.80) is calculated from the same sample trajectories. The correlations for the separable and the triplet model have starting values that differ from their expectation due to the boundary condition of antiparallel spins.

The decorrelation of the spins is a natural consequence of the two uncoupled systems

in the stochastic theory, i.e., the two independently rotating tops. This is also true for $t > 0$ if the spin fields $s_{(1)}(0, \theta_{(1), t=0}) = -s_{(2)}(0, \theta_{(2), t=0})$ are chosen to be antiparallel at $t = 0$. They decorrelate exponentially due to the interaction with the background field as shown in figure 6.13. The black and gray graphs depict the correlation in terms of the normalized dot product $\frac{s_{(1)}(t) \cdot s_{(2)}(t)}{|s_{(1)}(t)| |s_{(2)}(t)|}$ ¹⁰ for a single trajectory (gray dashed) and an ensemble average (black solid) in the Bell separable model. The initially chosen perfect anticorrelation for a single pair is highly volatile. The ensemble average, on the other hand, decays to a value close to $-1/4$ since the z components of the spin pair are constant. Hence, the anticorrelation of the spins holds only under expectation in the considered model $E[s_{(1)}] = -E[s_{(2)}]$. The underlying uncorrelated randomness leads to spin states which cannot describe a total spin expectation $E[s_{\text{tot}}^2] < \hbar^2$ in the separable model. A perfectly anti-correlated spin pair is shown in purple in the same plot, and will be discussed in the following subsection for the entangled singlet spin. Only stochastically correlated states have a stochastic correlation $C(s_{(1)}(t), s_{(2)}(t)) \neq 0$ as shown in the right plot of figure 6.13 for the two entangled states. These stochastic processes are not independent, i.e., the spins are coupled. These states are discussed in subsection 6.5.4.

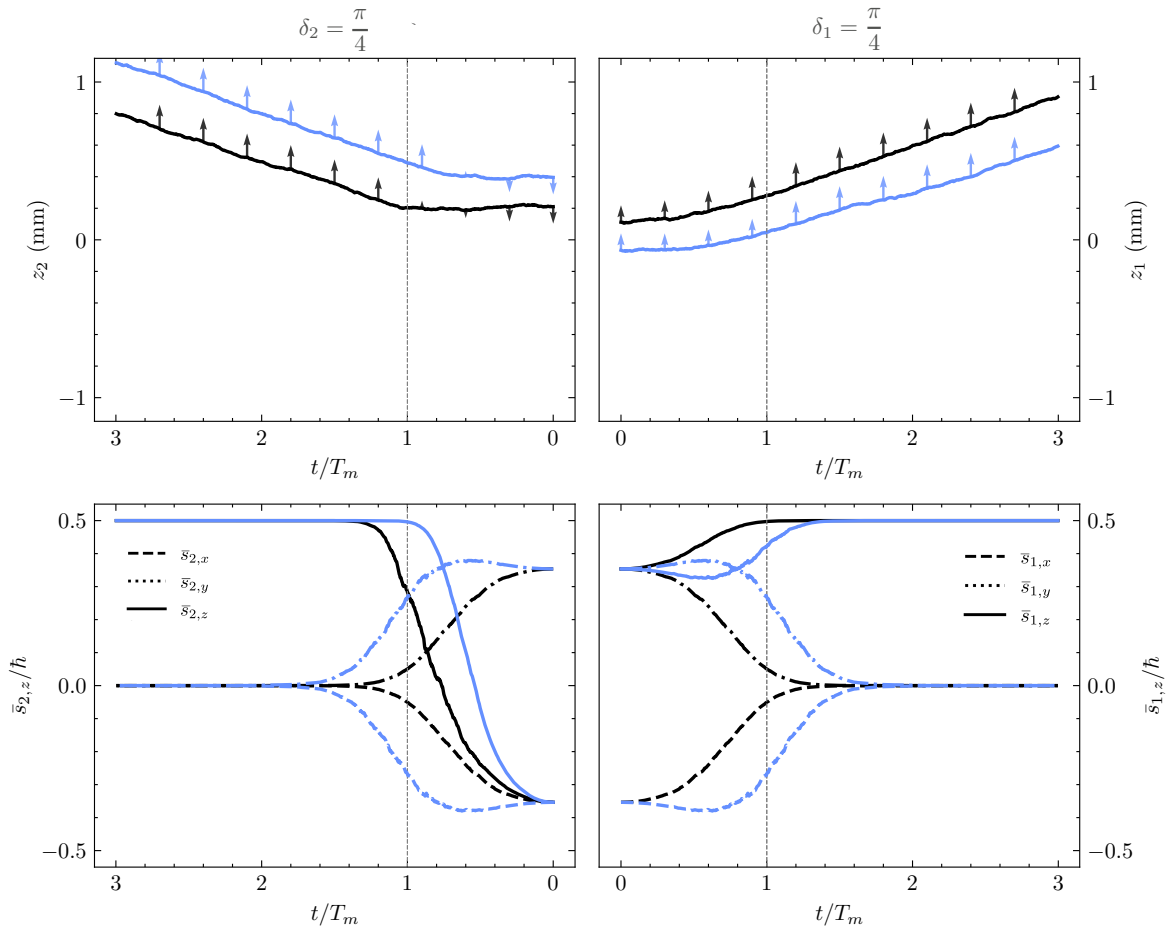


Figure 6.14: Two stochastic realizations (blue and black) of Bell separable antiparallel pairs entering the two identical Stern-Gerlach magnets at time $t = 0$ after being locally separated. The paths (top row) and spin averages (bottom row) of particle 1 (right column) and particle 2 (left column) are plotted as a function of time where T_m is the time spent in the magnet. The x (dashed) and y (dash-dotted) components of the spins are also depicted in the bottom plots. Particles 1 and 2 enter magnets tilted by an angle $\delta_1 = \delta_2 = \frac{\pi}{4}$ w.r.t. to the initial polarizations of the antiparallel spins along the z direction. The top row also shows the z_1 (z_2) projections of $\bar{s}_{(1)}$ ($\bar{s}_{(2)}$) indicated by arrows along the paths.

¹⁰Here we use shorthand $s_{(k)}(t) = s_{(k)}(t, \theta_{(k), t})$.

Measurement

Figure 6.13 reveals a timescale $\tau_{rot} = \frac{I_m}{\hbar}$ for the decorrelation in the Bell separable model. It is, again, much smaller than the timescale determined by the interaction with the measurement devices $\tau_{trans} = T_m$. Due to the particle's rapid rotational motion, the orientation averages are sufficient to study the motion of the particles in the measurement processes. Therefore, the averaged values for position and spin are sufficient to analyze the measurements as in section 6.4. When the particles are measured along the z axis they show perfect anticorrelation since the fully aligned spin expectation leads (almost surely) to a single deflection, as shown in the top plot of figure 6.6. The more interesting cases arise when the magnetic fields are not aligned with the spins at the preparation stage.

Two such stochastic realizations (blue and black) are shown in figure 6.14 for the measurement angles $\delta_1 = \delta_2 = \pi/4$ for particle 1 (right) and 2 (left) starting from the moment of entry into the magnets. The time $t = 0$ in the plots corresponds to the moment the particles simultaneously enter the two SG devices. The z_1 and z_2 averages of the spins at $t = 0$ comply with the spin expectation $E[s_{(1)}(t=0) \cdot e_{z_1}] = \hbar \cos \delta_1/2 = -E[s_{(2)}(t=0) \cdot e_{z_2}] = -\hbar \cos \delta_2/2 = \hbar/\sqrt{8}$ before the interaction with the magnets. The plots show that particles will be deflected and that the spins seem to align to the new z_k axes. It is also visible that the two selected particle pairs are correlated but not anti-correlated. The probability of correlated coincidences thus does not vanish for the different measurement angles in the separable model.

The correlation of the particles can be compared to the inequality for local hidden variable theories given by the Bell inequality (6.68)

$$\rho^{A\bar{B}}(0, \delta) + \rho^{B\bar{C}}(\delta, 2\delta) \geq \rho^{A\bar{C}}(0, 2\delta) \quad (6.83)$$

where the joint probabilities are defined as

$$\rho^{A\bar{B}}(\delta_1, \delta_2) := \rho \left(A = +, \bar{B} = - \mid a = z_1^{\delta_1}, b = z_2^{\delta_2} \right). \quad (6.84)$$

The probabilities $\rho^{A\bar{B}}(0, \delta) \approx \frac{N^{A\bar{B}}}{N_{total}}$ can be approximated by the coincidences of particle 1 ending up in the + channel and particle 2 in the – channel after the respective SG devices 1 and 2. In that specific case, the beams of particle 1 are split along the $z_1^{\delta_1=0} = z$ direction while the ensemble for particle 2 splits along the $z_2^{\delta_2=\delta}$ direction which is tilted by an angle δ w.r.t. z . Figure 6.15 reveals that the uncoupled model does not violate Bell's inequality since $\rho^{A\bar{B}} + \rho^{B\bar{C}} \geq \rho^{A\bar{C}}$ for all angles. The singlet state in quantum mechanics, however, yields $\rho_Q^{A\bar{B}} + \rho_Q^{B\bar{C}} \leq \rho_Q^{A\bar{C}}$ for $\delta < \pi/2$ and thus violates the inequality. In the stochastic model, the joint probability $\rho^{B\bar{C}} = \rho^{B\bar{C}}(\delta, 2\delta)$ (green circles) deviates heavily from the prediction of the singlet state $\rho_Q^{B\bar{C}}$ (green dashed). It shows a weaker anticorrelation than the entangled state since the measurements of the stochastic spins are only perfectly anti-correlated when the measurement axes of both Stern-Gerlach devices are aligned with the initial spin expectation, i.e., $\delta_1 = \delta_2 = 0$. In the singlet state, the same measurement angles $\delta_1 = \delta_2 \neq 0$ are sufficient to give perfectly anti-correlated results. Hence, it does not matter what measurement direction is used for a singlet state if the measurements are along the same axis.¹¹

The issue with the discussed local stochastic model is illustrated in figure 6.14 for $\delta_1 =$

¹¹Note that the direction of the initially antiparallel spins in (6.77)

$$E[s_{(1)}] = E[s_{(1),v}] = -E[s_{(2)}] = -E[s_{(2),v}] = \frac{\hbar}{2} e(\theta_0, \phi_0), \quad (6.85)$$

should depend on a chosen projection axis $e(\theta_0, \phi_0) = (\cos \phi_0 \sin \theta_0, \sin \phi_0 \sin \theta_0, \cos \theta_0)$ for each pair of particles in the preparation procedure in general. Since the expectation of the spins at the preparation stage over all simulated particle paths should be 0, an adjusted expectation, denoted by $\tilde{E}[\cdot]$, has to take into account the randomness of the initial projection, so that $\tilde{E}[s_{(k)}] = E_g[E[s_{(k)}]] = 0$. This is accomplished within this model via the random choice of θ_0, ϕ_0 according to a distribution $g(\theta_0, \phi_0)$ so that $E_g[s_{(k)}] = \hbar/2 \int e(\theta_0, \phi_0) g(\theta_0, \phi_0) d\theta_0 d\phi_0 = 0$. A uniform distribution of angles δ_0 with $\phi_0 = 0$, for example, leads to rescaled probabilities $E_g[\rho^{A\bar{B}}] = \frac{1}{2} \rho^{A\bar{B}}$ or $E_g[\rho^{B\bar{C}}] = \frac{1}{2} \rho^{B\bar{C}}$. Hence, it cannot describe statistically correlated processes needed to violate Bell's inequality.

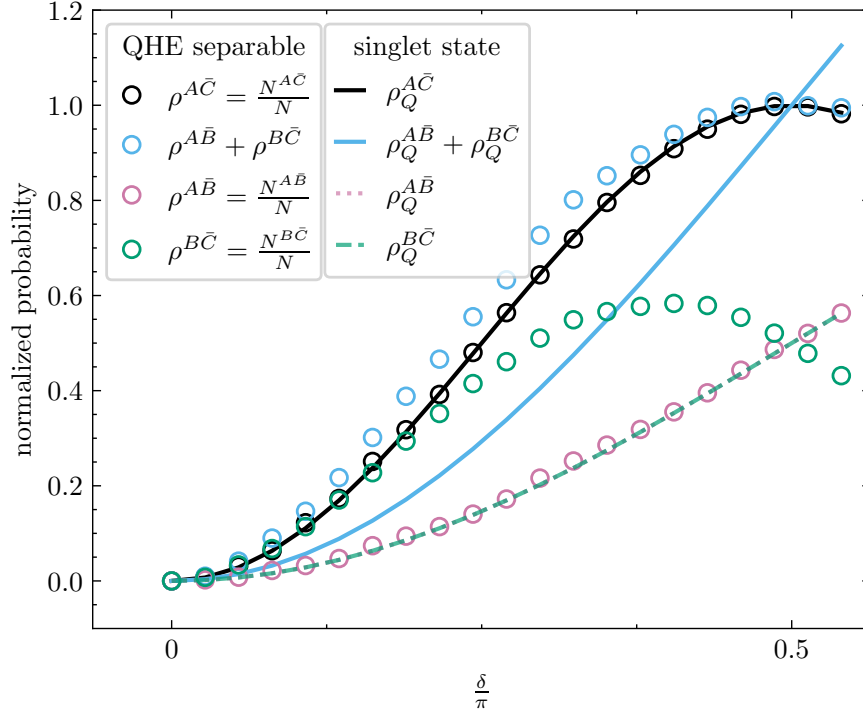


Figure 6.15: The plot compares the joint probability distributions from the singlet state wave function in quantum mechanics (solid) to the numerically calculated probabilities associated to the separable spin model (circles) as a function of angle δ as defined in equation (6.68). The uncoupled QHE model obeys Bell's inequality $\rho^{AB} + \rho^{BC} \geq \rho^{AC}$. Since $\rho_Q^{AB} = \rho_Q^{BC}$ the pink dotted line is not visible.

$\delta_2 = \pi/4$. The particles enter the magnets with spin expectations $|E[s_{(k)} \cdot e_{z_k}]| < \hbar/2$ and thus have probabilities of going up and down. As a result, neither of the two pairs shown in the figure 6.14 may be anti-correlated in the measurement, which would be impossible for a singlet state.

Speaking of separable states, it should be noted that perfect anticorrelations for any measurement axis in the stochastic picture can be achieved if the measurement angle δ_1 was known to particles 1 and 2 at the preparation stage. In this case, the spins could be arranged to be antiparallel w.r.t. the angle δ_1 initially. This relaxes the requirement for the Bell separability property 3) regarding measurement independence, thus enabling a violation of Bell's inequality. This idea is related to the superdeterministic interpretation of quantum mechanics, which posits that everything has a common cause in the past light cone [Hal16]. This, however, is not in line with the formalism in Nelson's stochastic mechanics.

The following subsection explains how non-local velocity fields in the stochastic picture enter the description of the quantum correlation as dependent stochastic processes.

6.5.4 Entangled spin states

An idealized antiparallel two-particle state in quantum mechanics, i.e., the quantum expectations $\langle \hat{s}_{(1)} \rangle = -\langle \hat{s}_{(2)} \rangle$, can be described by the superposition

$$|\psi\rangle_{\epsilon,\phi} = \frac{1}{\sqrt{2}} \left(\cos \frac{\epsilon}{2} |+\rangle_{(1)} |-\rangle_{(2)} - e^{i\phi} \sin \frac{\epsilon}{2} |-\rangle_{(1)} |+\rangle_{(2)} \right) \quad (6.86)$$

where $|\pm\rangle_{(k)}$ denotes the spin-up/down eigenstate of particle l in the z basis. For $\epsilon = 0$ and $\epsilon = \pi$ (6.86) reduces to the Bell separable two particles states $|+\rangle_{(1)} |-\rangle_{(2)}$ and $|-\rangle_{(1)} |+\rangle_{(2)}$.

For $\epsilon \in (0, \pi)$ the state $|\psi\rangle_{\epsilon,\phi}$ does not fulfill the properties of Bell separability anymore. These states are *entangled*, i.e., they cannot be written as a tensor product of single particle

states. Maximally entangled states are described for $\epsilon = \pi/2$. For example, Bell's original inequality [Bel64] addresses a singlet state ($\epsilon = \pi/2, \phi = 0$)

$$|\psi_s\rangle = |\psi\rangle_{\pi/2,0} = \frac{1}{\sqrt{2}} (|+\rangle_{(1)} |-\rangle_{(2)} - |-\rangle_{(1)} |+\rangle_{(2)}) , \quad (6.87)$$

which is one of the four so-called Bell states for a two-level system. Another Bell state is described by $|\psi\rangle_{\pi/2,\pi}$ which is the triplet state.¹²

The specific property of an entangled spin state is related to the fact that these states cannot be understood only from the viewpoint of individual particles. For example, the expectation values w.r.t. to the state (6.86) of the total spin operator $\hat{s} = \hat{s}_{(1)} + \hat{s}_{(2)}$ read

$$\langle \hat{s} \rangle = 0 \quad \langle \hat{s}^2 \rangle = \hbar^2(1 - \cos \phi) \quad (6.88)$$

while for the single spin operators

$$\langle \hat{s}_{(k)} \rangle = 0 \quad \langle \hat{s}_{(k)}^2 \rangle = \frac{3\hbar^2}{4} . \quad (6.89)$$

The expectation of the single particle spin is zero, although the magnitude of the single particle spin does not vanish. Hence, each spin- $\frac{1}{2}$ particle has an undefined quantization axis in these entangled states.

Consider the singlet state where $\phi = 0$ in more detail. The magnitude of the total spin in (6.88) is zero under expectation. In the stochastic picture this translates to the ensemble expectations $E[s_{\text{tot}}] = 0$ and $E[s_{\text{tot}}^2] = 0$ where

$$0 = E[s_{\text{tot}}^2] = E[s_{(1)}^2] + E[s_{(2)}^2] + 2E[s_{(1)} \cdot s_{(2)}] = \frac{3\hbar^2}{2} + 2E[s_{(1)} \cdot s_{(2)}] . \quad (6.90)$$

The dot product of the two spins thus has to fulfill $E[s_{(1)} \cdot s_{(2)}] = -\frac{3\hbar^2}{4}$, so that

$$E[s_{(1)} \cdot s_{(2)}] = E[s_{(1)}^v \cdot s_{(2)}^v] + E[s_{(1)}^u \cdot s_{(2)}^u] + E[s_{(1)}^v \cdot s_{(2)}^u] + E[s_{(1)}^u \cdot s_{(2)}^v] = -\frac{3\hbar^2}{4} \quad (6.91)$$

As mentioned in the discussion of the separable model, such a state is impossible to construct in stochastic mechanics if the angular velocity fields of the particles are independent of each other's orientation variables.

For example, take $E[s_{(1)} \cdot s_{(2)}] = -E[s_{(1)}^2] = -E[s_{(2)}^2]$. Then, $E[s_{\text{tot}}] = 0$ leads to $E[s_{(1)}^v] = -E[s_{(2)}^v]$ since $E[s_{(k)}^u] = 0$. These expectations state that the spins along all possible stochastic orientation trajectories have to be antiparallel $s_{(1)} = -s_{(2)}$ for $t > 0$ until one of them enters a measurement device. Hence, there is perfect anticorrelation without any decorrelation in the stochastic setting. This is also depicted in the correlation plots 6.13 for the singlet state. As shown in the following, such dependencies are also valid feedback solutions to the QHE in the field-free case, where the drift and the stochastic term vanish in the QHE for the total spin.

Considering the definition in (6.86), the singlet (and triplet state) in the field free regime can be derived by a combination of two solutions to a pair of spin- $\frac{1}{2}$ particles with antiparallel expectations along the z axis:

$$(\pm): \mu_{(1)} = -\mu_{(2)} = 1/2, \nu_{(1)} = \nu_{(2)} = 1/2, \text{ such that } E[s_{(1)}] = -E[s_{(2)}] = \frac{\hbar}{2}e_z \text{ and}$$

$$(\mp): \mu_{(2)} = -\mu_{(1)} = 1/2, \nu_{(2)} = \nu_{(1)} = 1/2, \text{ such that } E[s_{(2)}] = -E[s_{(1)}] = \frac{\hbar}{2}e_z.$$

As discussed in the previous subsection, both two-particle states address the Bell separable model. Thus they are product states of spin-up and spin-down particles with distributions $\rho_{(\pm)}(t, \theta_{(1)}, \theta_{(2)}) = \rho_+(\theta_{(1)})\rho_-(\theta_{(2)})$ and $\rho_{(\mp)}(t, \theta_{(1)}, \theta_{(2)}) = \rho_-(\theta_{(1)})\rho_+(\theta_{(2)})$ and can be seen as the stochastic analog to $|+\rangle_{(1)} |-\rangle_{(2)}$ and $|-\rangle_{(1)} |+\rangle_{(2)}$.

¹²There are two more maximally entangled states of a two-level system, which are not considered here.

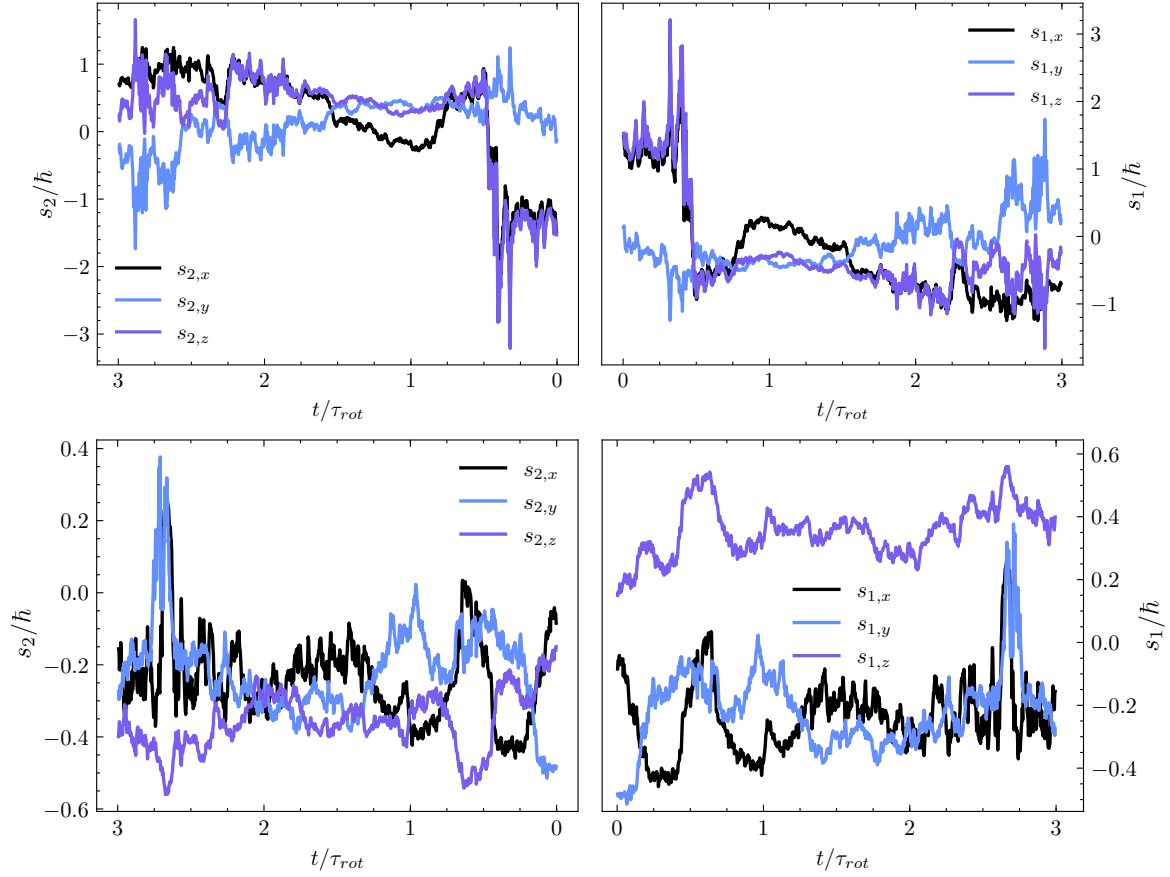


Figure 6.16: The spin components of each particle in a singlet (top row) and triplet state (bottom row) are shown w.r.t. time along a stochastic realization of the stochastic orientations $\theta_{(i),t}$ in the field free region before entering the magnets similar to figure 6.12.

The combination of the 2 two-particle solutions (\pm) and (\mp) then follows appendix F with the constants

$$c_1 = \frac{1}{\sqrt{2}} \cos \frac{\epsilon}{2} \quad \text{and} \quad c_2 = \frac{-e^{i\phi}}{\sqrt{2}} \sin \frac{\epsilon}{2} \quad (6.92)$$

in reference to equation (6.86). The procedure is similar to the one given in equation (6.45) for a rotation of a single spin. Carrying out the calculations yields a spin field of particle 1 for a maximally entangled state ($\epsilon = \pi/2$)

$$s_{(1)} = \frac{1}{\rho} \begin{pmatrix} -2iA \left(e^{i(\phi+\varphi_{(2)})} c \frac{\vartheta_{(1)}}{2} s \frac{\vartheta_{(2)}}{2} + e^{i\varphi_{(1)}} s \frac{\vartheta_{(1)}}{2} c \frac{\vartheta_{(2)}}{2} \right) \left(A^* c \frac{\vartheta_{(1)}}{2} c \frac{\vartheta_{(2)}}{2} - s \frac{\vartheta_{(1)}}{2} s \frac{\vartheta_{(2)}}{2} \right) \\ -s\vartheta_{(2)}(c(\phi + \varphi_{(2)}) + ic\vartheta_{(1)}s(\phi + \varphi_{(2)})) + s\vartheta_{(1)}(c\varphi_{(1)} + ic\vartheta_{(2)}s\varphi_{(1)}) \\ -is\vartheta_{(1)}s\vartheta_{(2)}s(\phi - \varphi_{(1)} + \varphi_{(2)}) + c\vartheta_{(1)} - c\vartheta_{(2)} \end{pmatrix} \quad (6.93)$$

with shorthand notations $c = \cos$ and $s = \sin$, zzz -Euler angles $(\vartheta_{(k)}, \varphi_{(k)}, \chi_{(k)})$ for the orientation of particle l , the definition of $A = e^{-i(\phi+\varphi_{(1)}+\varphi_{(2)})}$ and the probability distribution $\rho = \frac{1}{8}(2 \sin \vartheta_{(1)} \sin \vartheta_{(2)} \cos(\phi - \varphi_{(1)} + \varphi_{(2)}) - \cos(\vartheta_{(1)} - \vartheta_{(2)}) - \cos(\vartheta_{(1)} + \vartheta_{(2)}) + 2)$.

In the singlet state ($\phi = 0$) the spin fields $s_{(2)}(\theta_{(1)}, \theta_{(2)}) = -s_{(1)}(\theta_{(1)}, \theta_{(2)})$ are perfectly antiparallel. A sample trajectory of the spin fields as a function of the stochastic orientations is shown in the top row of figure 6.16, i.e., the spin field $s_{(k)}$ from equation (6.93) is used to numerically integrate the FSDE (5.9) for the orientation variable $\theta_{(k)}$ of particle k . Note that the stochastic process of the total spin $s_t = s_{(1),t} + s_{(2),t}$ as a critical feedback process to the spin QHE necessarily leads to $ds_t = 0$, i.e., the drift and the stochastic terms vanish in the SDE vanish. In terms of the single spin QHE we have $ds_{(1)} = -ds_{(2)}$.

For the triplet state ($\phi = \pi$) the x, y components of the feedback fields coincide and $s_{(1)z} = -s_{(2)z}$ as shown in the bottom row of figure 6.16. Note that these quantities are not ensemble expectations but the drift fields of the stochastic processes for each orientation. This is also manifested in the corresponding spin correlation matrix of the spin pair. The expected correlation depending on ϵ, ϕ reads

$$\mathbb{E} \left[s_{(1)i} s_{(2)j} \right] = \frac{\hbar^2}{4} \begin{pmatrix} -\sin \epsilon \cos \phi & \sin \epsilon \sin \phi & 0 \\ \sin \epsilon \sin \phi & -\sin \epsilon \cos \phi & 0 \\ 0 & 0 & -1 \end{pmatrix} \quad (6.94)$$

where $i, j \in \{x, y, z\}$. As expected, the uncoupled spins ($\epsilon = 0$) can be maximally (anti-)correlated for one axis, the z axis in the example. The entangled states ($0 < \epsilon < \pi$), on the other hand, show additional correlations between other components, e.g., the triplet (singlet) state shows perfect (anti-)correlation under expectation w.r.t. to the x, y components. Under this aspect, one can deduce that the stochastic spin fields for the singlet state violate Bell's inequality (before the measurement) but not a generalized Schwarz inequality

$$-\mathbb{E}[(a \cdot s_{(1)})(b \cdot s_{(2)})] - \mathbb{E}[(a \cdot s_{(1)})(c \cdot s_{(2)})] \leq \frac{3\hbar^2}{8} - \mathbb{E}[(b \cdot s_{(1)})(c \cdot s_{(2)})] \quad (6.95)$$

for continuous random variables. This follows the discussion in chapter 6 of [Far82], where it was pointed out that Bell's inequality only holds for discrete random variables. The treatment after the particles couple to the position in the measurement process is analyzed in the following subsection.

The spin fields for the separable ($\epsilon = 0$), the singlet, and the triplet state were used to numerically integrate the SDE for the orientations $\theta_{(1)}$ and $\theta_{(2)}$. Figure 6.13 in the previous subsection shows the corresponding numerical calculations of the spin correlation quantities as a function of time under the constraint $s_{(1)}(\theta_{(1)}, \theta_{(2)}) = -s_{(2)}(\theta_{(1)}, \theta_{(2)})$ at $t = 0$. Since the initial probability density in that specific case does not necessarily comply with the one associated with the spin fields, the spins' ensemble decay exponentially into the stationary distribution. For example, the left plot shows the decorrelation of the triplet and separable spin correlation to the values, which in approximation, agree with the trace of the matrix given in (6.94). Note that the numerically calculated values for separable and triplet state in the left plot of figure 6.13 are slightly off from the exact values $\pm 1/4$ following equation (6.94) due to the inaccuracy in the numerical integration related to regions where the orientational variables $\vartheta_{(k)}, \varphi_{(k)}$ are close to singularities of the drift fields.

Simultaneous measurement

The coupling of space-like particles also shows up in the description of the measurement procedures for the EPR pair. As discussed in the Bell separable model, the starting points are two uncoupled particles entering two space-like separated inhomogeneous magnets. The Bell separable (\pm) and (\mp) pairs are augmented to describe the coupling to the position with the corresponding (angular) velocities $v_{(1),q}^{\pm} = v_{(1),q}^{\pm}$, $v_{(2),q}^{\pm} = v_{(2),q}^{\pm}$ and $v_{(1),q}^{\mp} = v_{(1),q}^{\mp}$, $v_{(2),q}^{\mp} = v_{(2),q}^{\mp}$. Since these models are still product states, the velocity field of each particle can be described independently in analogy to the Stern-Gerlach description in section 6.4. To describe entangled states, the enhanced velocity fields for each particle (l), namely $v_{(k)}^{\pm}$ and $v_{(k)}^{\mp}$, are now combined with the same coefficients given in (6.92).

The equations (6.58) given in the Stern-Gerlach section were used for each particle l with the corresponding orientation averages of the forward drift fields

$$\bar{v}_{(l)}(t, z_1, z_2, \bar{\Omega}_{(l),\varphi}) + \bar{u}_{(l)}(t, z_1, z_2, \bar{\Omega}_{(l),\varphi})$$

depending on the φ component of the spin angular average. E.g., for particle 1 in the magnet,

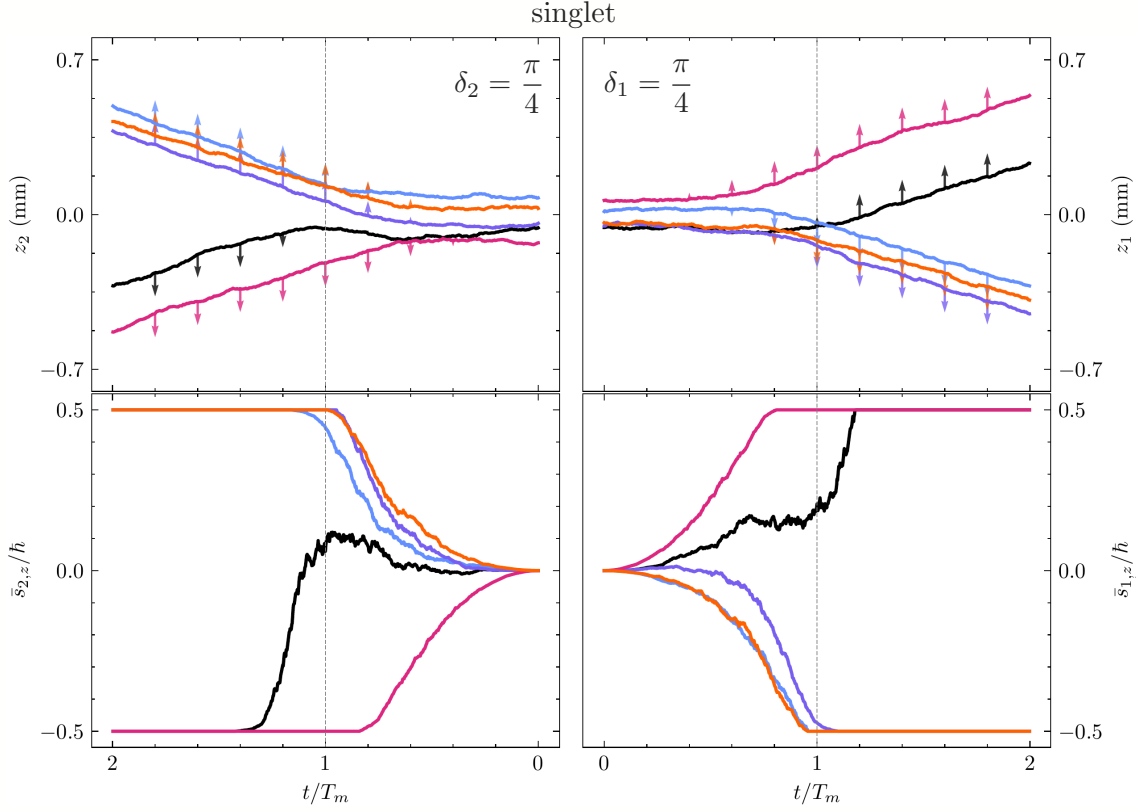


Figure 6.17: The plot depicts a sample of 5 numerically calculated particle pairs prepared in a singlet state entering the magnets simultaneously with measurement angles $\delta_1 = \delta_2 = \frac{\pi}{4}$.

denoted by the superscript m , the averaged spin along the measurement direction z^{δ_1} reads

$$\begin{aligned}
\bar{s}_{(1),z}^m &= \bar{\Omega}_{(1),\varphi}^m(t, z_1, z_2) \\
&= -\frac{\hbar}{2\bar{\rho}} \left(\cos^2 \frac{\epsilon}{2} (-\cos \delta_1 - (\cos \delta_1 + 1)A(z_1) + 1) (-\cos \delta_2 + (\cos \delta_2 - 1)A(z_2) - 1) \right. \\
&\quad - \sin^2 \frac{\epsilon}{2} (\cos \delta_1 + (\cos \delta_1 - 1)A(z_1) + 1) (-\cos \delta_2 + (\cos \delta_2 + 1)A(z_2) + 1) \\
&\quad \left. - \sin \epsilon \cos \phi \sin \delta_1 \sin \delta_2 (A(z_1) - 1)(A(z_2) - 1) \right) \quad (6.96)
\end{aligned}$$

where $A(z_l) = \exp\left(-\frac{4mz_l z_{cl}(t)}{\tau_0 \hbar}\right)$ and

$$\begin{aligned}
\bar{\rho}^m &= \cos^2 \frac{\epsilon}{2} (A(z_1)(\cos \delta_1 + 1) - \cos \delta_1 + 1)(A(z_2)(\cos \delta_2 - 1) - \cos \delta_2 - 1) \\
&\quad + \sin^2 \frac{\epsilon}{2} (A(z_1)(\cos \delta_1 - 1) - \cos \delta_1 - 1)(A(z_2)(\cos \delta_2 + 1) - \cos \delta_2 + 1) \\
&\quad + 2 \sin \delta_1 \sin \delta_2 \sin \epsilon \cos \phi (A(z_1) - 1)(A(z_2) - 1). \quad (6.97)
\end{aligned}$$

E.g., the SDE for the z component of particle l denoted by the stochastic process $\bar{Z}_{(l),t}$ in the magnet ($t < T_m$) read

$$d\bar{Z}_{(l),t} = \left[\frac{2}{\hbar} \left(v_{cl}(t) + \frac{z_{cl}(t)}{\tau_0} \right) \bar{\Omega}_{(l),\varphi}^m(t, \bar{Z}_{(1),t}, \bar{Z}_{(2),t}) - \frac{\bar{Z}_{(l),t}}{\tau_0} \right] dt + \sqrt{\frac{\hbar}{m}} dW_{(l),t} \quad (6.98)$$

where $v_{cl}(t) = \frac{\gamma \hbar b}{2m} t$ and a classical displacement $z_{cl}(t) = \frac{\gamma \hbar b}{4m} t^2$ are defined similar to equations (6.38)-(6.39). After the magnet the spin average $\bar{s}_{(1),z}^a$ is a copy of (6.96) with terms

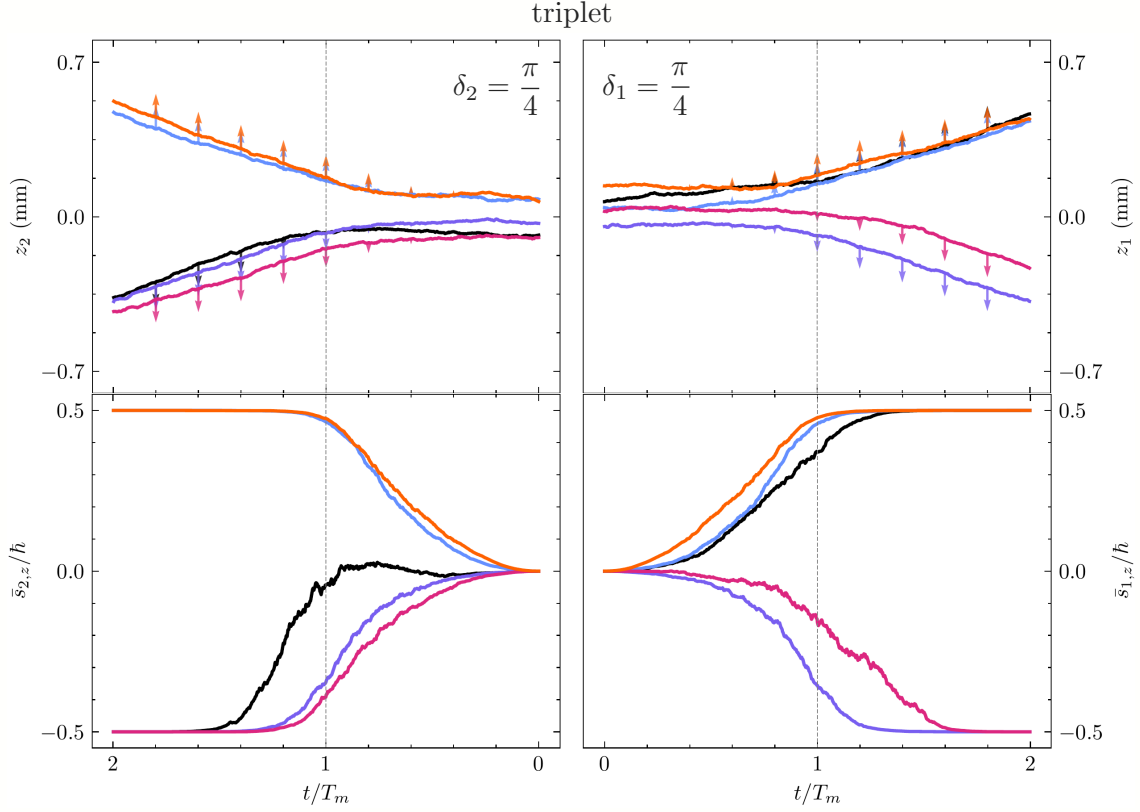


Figure 6.18: The plot depicts a sample of 5 numerically calculated particle pairs prepared in a triplet state entering the magnets simultaneously with measurement angles $\delta_1 = \delta_2 = \frac{\pi}{4}$.

including $z_{cl}(t)$ being replaced by $z_m + v_m t$. Note that the drift terms including $\mathcal{O}\left(\left(\frac{1}{\tau_0}\right)^2\right)$ have been neglected as in section 6.4.

For measurement angles $\delta_1 = \delta_2 = 0$, anti-correlated coincidences would be measured for the triplet and the singlet state similar to the separable model. The spin fields (6.96) in the magnet in z direction are independent of the phase ϕ . They simplify to

$$\bar{s}_{(z),1}^m = -\bar{s}_{(z),2}^m = \frac{\hbar}{2} \tanh\left(\frac{2m(z_1 - z_2)z_{cl}(t)}{\tau_0 \hbar}\right). \quad (6.99)$$

In contrast to the separable model, the averaged spin components are 0 before entering the magnet due to $z_{cl}(0) = 0$ and acquire z_l components for $t > 0$. If $\bar{Z}_{(1),t} > \bar{Z}_{(2),t}$, the first of the two drift terms in equation (6.98) are positive for particle 1 while negative for the other. Eventually, $\bar{s}_{(z),l}^m$ approaches $\pm\hbar/2$ for large times depending on the difference $\bar{Z}_{(1),t} - \bar{Z}_{(2),t}$ on *both* particle positions, which leads to an opposite deflection for the two-particle positions in the direction of measurement. Although the positions $\bar{Z}_{(1),t} \neq -\bar{Z}_{(2),t}$ for each particle pair are not exactly anti-correlated, the spin averages are, which is a feature of the entangled states considered here. The averaged x and y components of the spins remain 0 throughout the experiment.

A sample of trajectories for 5 particle pairs moving in opposite directions and entering a magnetic field is shown in figure 6.17 for the singlet pairs and in figure 6.18 for the triplet state. The measurement angles for the Stern-Gerlach devices are $\delta_1 = \delta_2 = \frac{\pi}{4}$ in these figures. The spin averages of the individual particles along the measured $z_l (\neq z)$ axes are also 0 at the entrance of the magnets according to (6.89), in contrast to the trajectories shown in figure 6.14 for the separable model where the spin averages depend on the measurement angles. Eventually, each particle chooses one of the two possible spin channels, and the spin aligns accordingly. In the moment of the measurement of a particle at a detector after

the magnet, one can assign a spin state for a single particle. Hence, the particles gradually disentangle in the stochastic picture until they choose one of the two distinct channels where the particle properties in terms of expectations can be described for uncoupled particles again. This mechanism is the counterpart to the collapse (or decoherence) of the state function in the Copenhagen interpretation given in (6.86) to one of the two states $|+_{(1)}\rangle|-_{(2)}\rangle$ or $|-_{(1)}\rangle|+_{(2)}\rangle$.

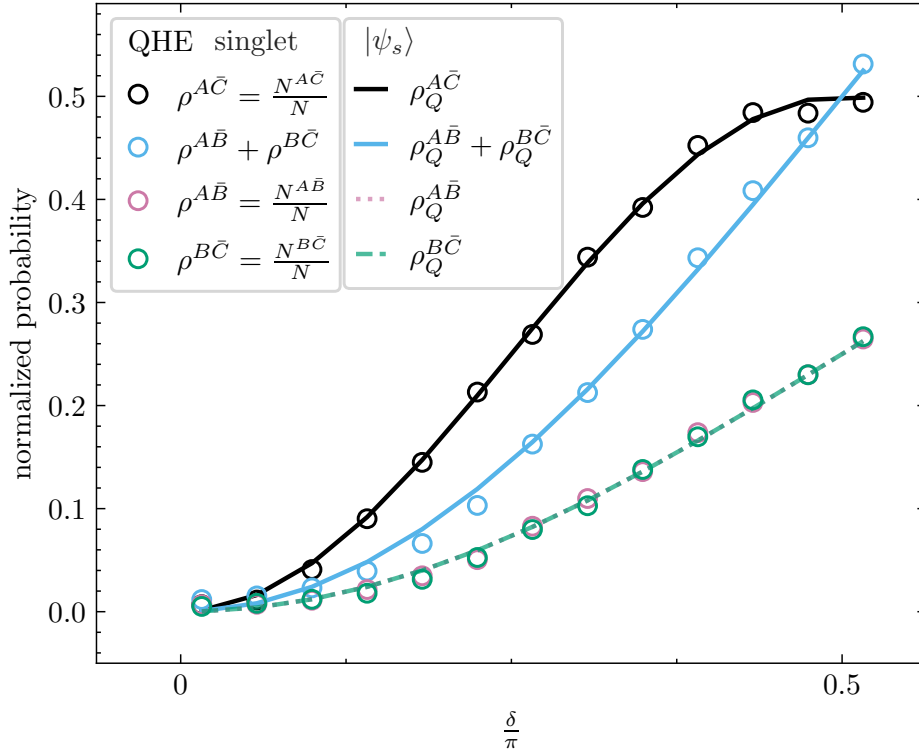


Figure 6.19: The plot compares the joint probability distributions from the singlet state wave function in quantum mechanics (solid) to the numerically calculated probabilities associated with the singlet spin model (circles) depending on the angle δ as defined in equation (6.68). The non-local velocity fields in the QHE model lead to the violation of Bell's inequality $\rho^{AB} + \rho^{BC} \geq \rho^{AC}$ for $\delta < \pi/2$. Since $\rho_Q^{AB} = \rho_Q^{BC}$ the pink dotted line is not visible.

For the singlet state, the spin pairs in figure 6.17 give anti-correlated outcomes since the measurement angles are the same $\delta_1 = \delta_2$. This agrees with the state's definition of perfect anticorrelation independent of the measurement axis where the probability of (positively) correlated outcomes, i.e., measuring $++$ or $--$ coincidences, only depends on the difference of the measurement angles $\delta_1 - \delta_2$. According to the Bell inequality (6.83) with the definition (6.84) figure 6.19 depicts the joint probabilities in magenta and green

$$\rho^{AB}(\delta_1 = 0, \delta_2 = \delta) \approx \rho^{BC}(\delta_1 = \delta, \delta_2 = 2\delta). \quad (6.100)$$

The plot shows that the stochastic model (circles) agrees with the predictions from quantum mechanics and, thus, violates Bell's inequality. This is not surprising since the model is based on the definition of the singlet wave function with the corresponding expected values. Moreover, the stochastic model's drift fields are non-local, allowing us to describe the strong correlations between the two particles. This is a result of the non-separability of the probability distribution, and thus relaxes argument 1) regarding Bell separability.

In the stochastic description, a local description of the measurement of entangled particles in a singlet state would need additional assumptions. As already suggested, one may constrain the averages of the continuous random spin variables of the two spin- $\frac{1}{2}$ particles to be opposite at all times, including the interaction with the measurement devices. Hence, in

order to violate Bell's inequalities, the constraint has to be extended so that the continuous spin random variables should be anti-correlated at all times *including* the measurements.

As pointed out by Faris [Far82], Bell's inequality for the stochastically spinning particle is violated, since, before the measurement, the components of the spins are not necessarily constant. After traversing the apparatus, the spin components in the direction of the field gradient can be considered as discrete random variables where the experimental settings are encoded in the probability distributions of the particles through the coupling of the spin and velocity fields of both particles.

Partial measurement

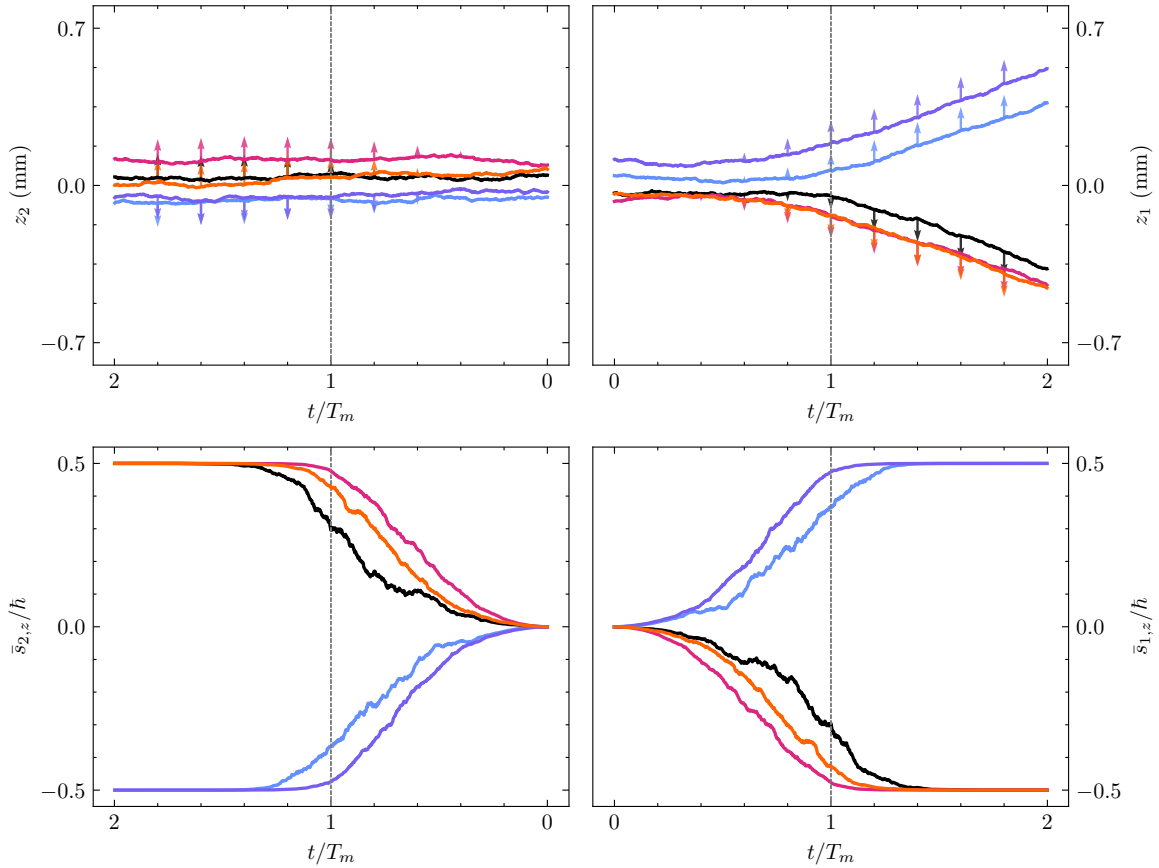


Figure 6.20: The plots show a singlet state where only particle 1 is measured while particle 2 does not enter a magnet for $\delta_1 = \delta_2 = 0$. The spin orientation average of particle 2 in the stochastic picture is changed in a non-local manner in accordance with the measurement of particle 1 and the corresponding change of the spin average $\bar{s}_{(1)}$. A torque acts on $\bar{s}_{(2)}$ while the momentum in z_2 direction is unchanged.

The apparently “non-local”¹³ Quantum phenomena become strongly visible when a measurement is made on one particle only. Example paths are shown in figure 6.20 where only particle 1 is deflected. With that, the spin average of particle 1 eventually aligns. Although the second particle is locally separated from the other particle, its spin is changed according to the measurement of particle 1. The position of particle 2 is unaffected, but its spin changes over the course of the measurement of particle 1 due to the non-local quantum

¹³The term non-local may be misleading since, in the case of entanglement, it does not state that information can be transferred between the two space-like separated observers. Statistically, one cannot gain information on the other particle by doing local measurements on one particle [GGRW88].

torque

$$T_{(k),u} = \bar{s}_{(k)} \times \sum_l \left(\frac{\hbar}{2m} \Delta_{(l)} \bar{s}_{(k)} + (\bar{u}_{(l)} \cdot \nabla_{(l)}) \bar{s}_{(k)} \right) \quad (6.101)$$

acting on the two-particle system.

This follows the treatment of a wave function, where the pair is said to be in a superposition of states. However, the physical intuition in the stochastic interpretation of this model crumbles due to the additional torque depending on the events in space-like separated regions, i.e., the measurement of particle 1. At this point, it seems reasonable to ask if that model of the spins actually describes the real changes of the spins or if it is a mathematically valid description for the empirical results.

If we shift the physically motivated picture of the drift fields of the processes to the case where they describe mean velocities only, the experiment could also be understood if one considers that a total spin state describes the system instead of two separate spins. The total spin is 0 before the measurement, and the individual particle properties in those cases cannot be described separately from the other particle. This changes if a measurement on at least 1 particle is taken where the changes of the one particle from zero average to $\pm\hbar/2$ leads to a complementary change in the spin average of 2 since the total spin state should be 0.¹⁴ Then, statistically, the measurement of particle 1 along z allows us to deduce the likelihood of outcomes on a possible measurement on the other subsystem. Empirically, the stochastic model cannot be distinguished from the ordinary quantum theory. The strange behavior of the individual spins in terms of instantaneous connections reflects the (mathematical) description of individual processes for a statistically correlated system of multiple particles. Thus, in the stochastic model, “non-local” means that the individual particles change their properties, although they are not necessarily interacting through classical fields.

CHSH inequalities

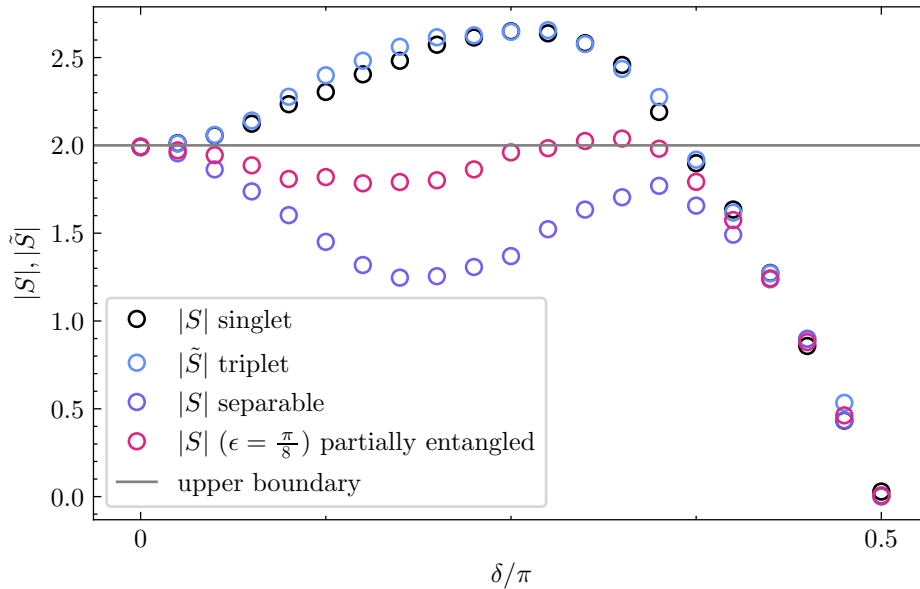


Figure 6.21: The plot shows the numerically calculated absolute values of the functions S and \tilde{S} from equations (6.66) and (6.103) from stochastic realizations as a function of the measurement angle δ . The CHSH inequality is violated for the singlet (black), triplet (blue), and partially entangled (magenta) where $|S(\delta)| > 2$ or $|\tilde{S}(\delta)| > 2$. The Bell separable model (purple) satisfies the inequality.

¹⁴For the individual spin pair this is only true if the measurement directions $z_1 = z_2$ are the same.

The triplet state is maximally entangled but cannot violate Bell's original inequality since it is not perfectly anti-correlated. For these cases, it is possible to use one of the generalized versions of Bell's inequality, which are usually subsumed as CHSH-inequalities [CHSH69]. E.g., consider the functions

$$S = C_{11} - C_{12} + C_{21} + C_{22} \quad (6.102)$$

$$\tilde{S} = C_{11} + C_{12} - C_{21} + C_{22} \quad (6.103)$$

for a system of two spins with correlations $C_{kl} = E[(a_k \cdot s_{(1)})(b_l \cdot s_{(2)})]$ along measurement directions a_k and b_l . Statistically, any locally realistic theory with independent measurement selections, see the subsection Bell-separability 6.5.3 for more details, with possible single particle outcomes ± 1 has to fulfill the inequalities

$$|S| \leq 2, \quad |\tilde{S}| \leq 2. \quad (6.104)$$

Quantum mechanics predicts a violation of these inequalities with a maximum upper bound of $2\sqrt{2} > 2$ [Cir80] for specific choices of measurement angles.

The inequalities (6.104) in the stochastic model for the singlet, the separable and the partially entangled model ($\epsilon = \pi/8, \phi = 0$) are analyzed for S from equation (6.102) with measurement angles $a_1 = 0, a_2 = 2\delta$ and $b_1 = \delta, b_2 = 3\delta$. The triplet state is analyzed for \tilde{S} (6.103) with measurement angles $a_1 = 0, a_2 = 2\delta$ and $b_1 = \delta, b_2 = -\delta$. The numerical correlations are approximated by counting the number of coincidences of the particle pairs

$$C_{kl} \approx \frac{1}{N_{\text{tot}}} (N_{++} + N_{--} - N_{+-} - N_{-+}) \quad (6.105)$$

where N_{tot} is the number of sample trajectories. Figure 6.21 shows the numerically calculated values of $|S|$ and $|\tilde{S}|$ as a function of the angle δ for $N_{\text{tot}} = 10^5$. The stochastic singlet and triplet model violate the CHSH boundary set by 2 for a range of angles δ , whereas the separable model cannot exceed the boundary. The plot also shows that partially entangled states, as exemplified by the circles in magenta, can violate the CHSH inequality. Again, this emphasizes that the velocity fields have to be non-local to describe violations of Bell or CHSH inequalities.

Concluding remarks

In summary, the stochastic model of a spinning top allows a consistent stochastic description of the EPRB with spins as continuous random variables contrary to the intrinsic property of a constant and discrete spin in standard quantum mechanics. Before the measurement, the spin fields of the particles may depend on the configuration of the two-particle system. The measurement leads to joint spin distributions, which depend on the chosen measurement axes and the configuration variables of both particles which lead to a clear violation of the Bell (CHSH) inequality. The spin components along the measured axes approach discrete values.

The drawback is that the underlying hidden variables, i.e., the stochastic positions and orientations of the particles, allow non-local changes due to the velocity fields. The origin in the stochastic formalism lies mainly in the postulate of a conservative Brownian motion which leads to specific dependencies between the forward and backward processes, i.e., the noise terms of the forward-backward processes are correlated to the osmotic velocity and its position. The physical explanation for such a specific correlation remains baffling. Gaeta [Gae93] suggested considering the system of particles being in permanent interaction with the "background noise field", which then produces the quantum phenomena. Hence, within the formalism of the QHE one needs the violation of statistical completeness, i.e., violation of statistical independence of the variables of the two particles. Although there is no physical interaction this leads to correlated changes on one of the particles depending on

the properties of the other due to the wonders of the osmotic velocity field associated to the background field interaction.

The findings in this section align with those discussed by Faris [Far82]. The study examined continuous random variables on $SU(2)$ derived from the covering's group representations, including spin measurements and correlations. However, the analysis at hand is focused on the underlying physical picture, especially on the changes of the spins and positions during the measurements. Thereby, it is noted that the analysis presented in this report also shares similarities with other causal descriptions of quantum mechanics, notably Dewdney's work in the 1980-90s, e.g., see [DHKV88, Hol95], on spin measurements, which served as inspiration for some of the plots. Notably, this discussion's unique aspect is using solutions to the QHE for spinning particles to deduce the velocity fields.

Chapter 7

Conclusion

The stochastic quantization associated with the Quantum Hamilton equations (QHE) can be summarized as follows: One begins by formulating the classical Lagrangian and subsequently replaces the velocity with the quantum velocity. Then, by searching for critical points of a stochastic Hamiltonian corresponding to the action function, we end up with kinematic and dynamic stochastic differential equations for the position and the momentum of the stochastic process.

The QHE are embedded into Nelson stochastic mechanics, sharing the fundamental quantities of stochastic mechanics. In that context, the role of the velocity fields, the connections to other similar interpretations of quantum mechanics, and the criticisms and controversies with them were addressed. The thesis discussed the variational principles of stochastic mechanics, including the quantum Hamilton principle. This is reformulated as a stochastic optimal control problem, ultimately resulting in the derivation of the QHE. These stochastic differential equations can be solved numerically, leading to results in perfect agreement with standard quantum mechanics.

The thesis extends the QHE to describe stochastic processes on manifolds, revealing the emergence of second-order terms in the drifts due to the stochastic nature of the system. The specific application of the hydrogen atom in curvilinear coordinates shows how these second-order terms explain the stability of the ground state, for example. Additionally, the QHE and the partner potentials in the SUSY approach determine the excited spectrum using symmetries analogous to classical mechanics.

Furthermore, the thesis discussed a model of a spinning object within the framework of the QHE, demonstrating the emergence of the familiar quantum spin states. This is verified through the calculation of expectation values. A key distinction between this model and standard quantum mechanics is the assumption that the quantum object has a randomly changing direction, leading to stochastic and continuous changes in the spin components over time, in contrast with the quantized values.

The thesis also investigated the measurement of spin. It showed that it is sufficient to consider orientational averages of the rotating particle for treating spin coupled to position, where, in this context, the Pauli equation is a suitable approximation. Moreover, the QHE allow for visualizing particle paths, where the resulting ensemble averages lead to predictions consistent with those of the Pauli theory. Additionally, the alignment of spin was discussed, revealing that individual spin expectation values are not predetermined before entering magnets. Instead, the spin expectations change due to an additional torque acting on the spins alongside the precession caused by the magnetic field.

Finally, the analysis of a single Stern-Gerlach experiment was extended to a pair of particles entering two devices. It is demonstrated that if the system is not Bell separable, the spin fields of the particles can not be described as independent of each other's configuration variables, leading to non-local velocity fields for entangled states in agreement with predictions from standard quantum mechanics. This leads to the violation of Bell's inequality within this model.

Outlook

Considering the Stern-Gerlach experiment, the study of detection times [DD19] could enhance the discussion for spin. Furthermore, the search for systems where detailed orientational dynamics play a significant role beyond orientational averages would be a valuable avenue of research. In that context, searching for bound states of a system of two spinning particles would be interesting, for example.

Further, studies of the quantum Hamilton equations could focus on multi-particle systems, particularly in the search for an algorithm similar to the treatment in density functional theory. It may be beneficial to approach quantum problems from a particle picture for high-dimensional systems once again. This problem is then related to the development of a reliable and fast algorithm for solving the QHE. Currently, the quantum Hamilton equations are an extension of the analytical tools available in quantum mechanics, mainly used to reproduce well-known quantum phenomena. However, they cannot be viewed as powerful tools for solving most state-of-the-art problems in quantum mechanics yet.

Additionally, extending the QHE to Lorentzian manifolds is one of the next natural steps to investigate relativistic phenomena like spin-orbit coupling in more detail. This could be conducted in line with the recent work by Kuipers [Kui21b] related to quantum gravity [Erl18]. It would also be valuable to investigate further the quantization in the variational principle, particularly the equivalence between an additional term in the stochastic Hamiltonian and the ad-hoc quantization condition proposed by Wallström as suggested in [Kui22].

Overall, this thesis hopefully contributes to a deeper understanding of the quantum Hamilton equations and, more generally, to Nelson's stochastic mechanics, its connection to quantum mechanics, and its applications in various scenarios. In addition, the future directions outlined here offer promising topics for further investigation and expansion of the field.

Appendix A

Basic definitions of probability theory

The following chapter is dedicated to a few basic definitions of probability theory needed in the thesis.

Definition A.1 *Sigma algebra*

A sigma algebra over a given set Ω is a set $\Sigma(\Omega) = \{A | A \subseteq \Omega\}$ with the following properties

- $\Omega \in \Sigma$
- $\forall A \in \Sigma : \Omega \setminus A \in \Sigma$
- $\bigcup_{i \in I} A_i \in \Sigma$ if $A_i \in \Sigma \forall i \in I$

Definition A.2 *Borel sigma algebra*

Given a topological space $(\mathcal{X}, \mathcal{S})$, a Borel set is a set that can be obtained by taking countable unions and intersections and complements of the sets in the topology \mathcal{S} . The collection of all Borel sets is the Borel sigma algebra $\mathcal{B}(\mathcal{X})$.

Definition A.3 *Measurable space*

Given a set Ω , a measurable space is a tuple (Ω, Σ) , where $\Sigma = \Sigma(\Omega)$ is a sigma algebra over Σ .

Definition A.4 *Probability measure*

Given a measurable space (Ω, Σ) , a probability measure is a function $P : \Sigma \rightarrow [0, 1]$, such that

- $P(\Omega) = 1$,
- $P(\bigcup_i A_i) = \sum_i P(A_i)$ for any countable collection $\{A_i \in \Sigma | i \in \mathbb{N}\}$ of pairwise disjoint sets.

Definition A.5 *Borel measurable function*

Given two topological spaces \mathcal{T} and \mathcal{R} , a function $f : \mathcal{S} \rightarrow \mathcal{R}$ is called Borel measurable, if $f^{-1}(U) := \{x \in \mathcal{T} | f(x) \in U\} \in \mathcal{B}(\mathcal{S}) \forall U \in \mathcal{B}(\mathcal{R})$.

Definition A.6 *Random variable*

A \mathcal{S} -valued random variable $X : (\Omega, \Sigma, P) \rightarrow (\mathcal{S}, \mathcal{B}(\mathcal{S}))$ is a measurable function on a given probability space (Ω, Σ, P) with a measurable space $(\mathcal{S}, \mathcal{B}(\mathcal{S}))$. $X(\omega)$ denotes a sample or an outcome for an event $\omega \in \Omega$.

Definition A.7 *Distribution*

A random variable $X : (\Omega, \Sigma, P) \rightarrow (\mathcal{S}, \mathcal{B}(\mathcal{S}))$ induces a probability measure $\mu_X = P \circ X^{-1}$ on $\mathcal{B}(\mathcal{T})$.

Definition A.8 *Expectation value*

For an integrable random variable $X : (\Omega, \Sigma, P) \rightarrow (\mathcal{S}, \mathcal{B}(\mathcal{S}))$, i.e., the Lebesgue integral

$$\int_{\Omega} |X(\omega)| dP(\omega)$$

converges, and a smooth function $f \in C^\infty(\mathcal{S})$, the expectation value of $f(X)$ is denoted by

$$\mathbb{E}[f(X)] = \int_{\Omega} f[X(\omega)] d\mathbb{P}(\omega). \quad (\text{A.1})$$

If the function f is Borel measurable and a scalar function $f : \mathcal{S} \rightarrow \mathbb{R}$, then the expectation is calculated as follows

$$\mathbb{E}[f(X)] = \int_{\mathcal{S}} f(x) d\mu_X(x), \quad (\text{A.2})$$

where $d\mu_X$ is the distribution of X on \mathcal{S} .

Definition A.9 Probability density on a manifold

Given a Manifold \mathcal{M} with a Riemannian metric g , a Borel-measurable function $\rho_X : \mathcal{S} \rightarrow \mathbb{R}_+$ is a probability density for an integrable random variable $X : \Omega \rightarrow \mathcal{S}$ as defined above, for all $B \in \mathcal{B}(\mathcal{S})$ there is

$$\mu_X(B) = \int_B \rho_X(x) \sqrt{|\det g(x)|} dx. \quad (\text{A.3})$$

Definition A.10 Independence

Two random variables X and Y defined on a probability space $(\Omega, \mathcal{F}, \mathbb{P})$ are said to be independent if for any Borel subsets A and B of Ω , we have

$$\mathbb{P}(X \in A, Y \in B) = \mathbb{P}(X \in A)\mathbb{P}(Y \in B).$$

Definition A.11 Filtration

A forward (backward) Filtration is family $\mathcal{F} = \{\mathcal{F}_t | t \in I\}$ on a measurable space $(\Omega, \Sigma, \mathbb{P})$ with an index set $I \subset \mathbb{R}$, where $\{\emptyset, \Omega\} \subset \mathcal{F}_s \subset \mathcal{F}_t \subset \Sigma$ for all $s > t \in I$ ($s < t \in I$).

Definition A.12 Adapted stochastic process

A stochastic process $(X_t) : I \times (\Omega, \Sigma, \mathbb{P}) \rightarrow (\mathcal{S}, \mathcal{B}(\mathcal{S}))$ is adapted to a Filtration \mathcal{F} on the given measurable space $(\Omega, \Sigma, \mathbb{P})$

Definition A.13 Markov Process

A stochastic process $(X_t) : I \times (\Omega, \Sigma, \mathbb{P}) \rightarrow (\mathcal{S}, \mathcal{B}(\mathcal{S}))$ is a Markov process, if it is adapted to the forward filtration \mathcal{F} such that

$$\mathbb{E}[X_t | \mathcal{F}_s] = \mathbb{E}[X_t | X_s] \quad \forall s < t \in I.$$

Appendix B

Numerical solution of stationary quantum Hamilton equations

The determination of stationary solutions to the QHE (3.52) requires a method for solving coupled FBSDEs with three unknown stochastic processes X_t, u_t, Π_t in $\mathbb{R}^d, \mathbb{R}^d,$ and $\mathbb{R}^{d \times d}$. The primary objective is to find the optimal feedback control $u(x)$ associated with these stochastic processes (X_t, u_t, Π_t) . Several approaches have been suggested in the literature [MY99, MT07, BS12], most of which are based on iterative schemes. Some of these methods are studied in detail in [Bey18], where the starting point is an initial estimate for the osmotic velocity $u^{(0)}(x) \approx u(x)$ and use it for the equation concerning X_t . The forward equation is then solved, and the new $u^{(1)}(x)$ is calculated. This cycle is repeated by replacing $u^{(0)}$ with $u^{(1)}$ until convergence criteria are met.

To solve a system of coupled FBSDEs, a two-step scheme is needed: (1) solution methods for the forward SDE and (2) solution methods for the backward SDE. The forward integration is achieved by discretizing the time axis $\pi = \{t_i | 0 < t_1 < \dots < t_m = T\}$. A variety of forward step schemes can be used, such as the Euler-Mayurama scheme with a convergence order of $1/2$, which is the simplest one. The approximated solution regarding the chosen time partition is denoted by $X_{t_i}^\pi$, with constant time step $t_{i+1} - t_i = \Delta t$. Here, π is used as an index to clarify that this is the approximated solution regarding the chosen time partition. Additionally, we denote $\Delta W_{t_i}^+ = W_{t_{i+1}}^+ - W_{t_i}^+$ as the Wiener increments.

On the other hand, the solution to the backward stochastic differential equation (BSDE) coupled to a forward stochastic differential equation (FSDE) in (3.52) is quite complicated. Evaluating the BSDE directly often involves a two-step process: first, a time discretization is performed, which includes a reformulation via conditional expectations, and second, an estimation of the conditional expectation is made [BT04]. Directly evaluating a BSDE using this two-step scheme requires the same partition, denoted by π . The Euler-Maruyama method for the backward equation in the j -th iteration is given by

$$\begin{aligned} u^{\pi,j}(X_T^{\pi,j}) &= u^{\pi,j-1}(X_T^{\pi,j}), \\ \Pi_T^{\pi,j} &= 0, \\ u(X_{t_i}^{\pi,j}) &\approx u_{t_i}^{\pi,j} = u_{t_{i+1}}^{\pi,j} - \frac{1}{\tilde{m}} \partial_x V(X_{t_i}^{\pi,j}) \Delta t - \frac{1}{\tilde{m}} \Pi_{t_i}^{\pi,j} \Delta W_{t_i}^-, \end{aligned} \quad (\text{B.1})$$

where $\Delta t > 0$ and the backward Wiener increments $\Delta W_{t_i}^- = W_{t_{i+1}}^- - W_{t_i}^-$. There are two unknown processes: Π_t and u_t . At this stage, we use the conditional expectation with respect to \mathcal{P}_{t_i} , where $(\mathcal{P}_{t_i})_{t_i \geq 0}$ is the filtration generated by the forward process $X_{t_i}^{\pi,j}$ up to time t_i . Then, if $(f_t)_{t \geq 0}, (g(X_t^\pi))_{t \geq 0} \subset \mathbb{R}^n$ are adapted to $(\mathcal{F}_t)_{t \geq 0}$, we can write

$$\mathbb{E} [f_{t_i} \Delta W_{t_i} | \mathcal{P}_{t_i}] = \mathbb{E} [f_{t_i} \Delta W_{t_i} | X_{t_i}] = 0, \quad (\text{B.2})$$

$$\mathbb{E} [g(X_{t_i}^\pi) | \mathcal{P}_{t_i}] = \mathbb{E} [g(X_{t_i}^\pi) | X_{t_i}^\pi] = g(X_{t_i}^\pi), \quad (\text{B.3})$$

where we used the Markov property of $X_{t_i}^\pi$. Since the stochastic process Π_t must be adapted to the stochastic process, it is possible to avoid the calculation of Π_t . Specifically, taking the conditional expectation in (B.1) with respect to \mathcal{P}_{t_i} yields

$$u_{t_i}^{\pi,j} = \mathbb{E} \left[u_{t_{i+1}}^{\pi,j} | X_{t_i}^{\pi,j} \right] - \partial_x V(X_{t_i}^{\pi,j}) \Delta t. \quad (\text{B.4})$$

An alternative method to calculate $\Pi_t^{\pi,j}$ is through conditional expectation. This allows for computing the matrix elements km of $\Pi_t^{\pi,j}$ using conditional expectation as follows

$$\Pi_{km,t_i}^{\pi,j} = \frac{1}{\Delta t} \mathbb{E} \left[u_{k,t_{i+1}}^{\pi,j} \Delta W_{m,t_i}^+ | X_{t_i}^{\pi,j} \right]. \quad (\text{B.5})$$

Equations (B.4) and (B.5) rely on numerical estimation of conditional expectations, which is often a critical aspect in solving coupled FBSDEs or BSDE directly. This issue has been widely discussed in mathematical finance over the years, as seen in the literature [BD07, JYC09]. In this work, the authors propose using a least-square Monte Carlo method, initially presented in [LS01] and later expanded upon in [GLW⁺05, BS12]. This method aims to provide the best estimate through least-square minimization. It is achieved by minimizing the expectation of the square of the difference between an admissible function and the considered stochastic variable over the set of admissible functions.

To numerically determine the conditional expectations, additional expansions and approximations are necessary. First, a number of forward paths, denoted by an index l , must be generated for each iteration step, typically N sample paths. For clarity, we will omit the indices for partition and iteration step in the following equations. In [LS01], it is demonstrated that the conditional expectation at time step t_i can be expressed as a linear combination of \mathcal{F}_{t_i} -measurable functions. Therefore, in the second step, a functional basis must be selected for numerical estimation. In this work, a multidimensional step-function $u(x)$ with L (hyper-)cubes or intervals I_j in space within the range $[a, b] = \bigcup_{i=1}^d [\alpha_i, \beta_i] = \bigcup_{j=1}^L I_j \subset \mathbb{R}^d$ was chosen as the functional basis [BS12]. This yields for the l -th generated sample path

$$\Pi_{km,t_i}^l \approx \frac{1}{\#(X_{t_{i+1}}^l)} \Delta t \sum_{n=1}^N \delta(X_{t_i}^l - X_{t_{i+1}}^n) u_{k,t_{i+1}}^n \Delta W_{m,t_i}^n \quad (\text{B.6})$$

where the first subscript k is the row number and the second m is the column number of the matrix Π . The function δ gives 1 if both positions $X_{t_i}^l, X_{t_{i+1}}^n$ are in the same interval and otherwise 0. The cardinality $\#(X_{t_{i+1}}^l)$ indicates the number of times all N sample paths visit the interval $I_j \ni X_{t_i}^l$ at step t_i . Therefore, this estimate is proportional to the average over all products of the velocity from the future time step t_{i+1} with the Wiener increment, where the position of the particle at t_{i+1} falls within a certain interval that overlaps with the position of particle l at t_i . Similarly, for (B.4) there is

$$\begin{aligned} u_{t_i}^l &= \mathbb{E} \left[u_{t_{i+1}}^l | X_{t_i}^l \right] - \partial_x V(X_{t_i}^l) \Delta t \\ &\approx \frac{1}{\#(X_{t_{i+1}}^l)} \Delta t \sum_{n=1}^N \left[\delta(X_{t_i}^l - X_{t_{i+1}}^n) u_{t_{i+1}}^n \right] - \partial_x V(X_{t_i}^l) \Delta t. \end{aligned} \quad (\text{B.7})$$

At each iteration step, the estimate of the conditional expectation is required as per (B.5) or (B.4). At the end of an iteration step, all $u_{t_i}^l$ in the same hyper-cube with respect to $X_{t_i}^l$ are averaged for all $l \in \{1, \dots, N\}$ and $i \in \{0, \dots, n_T - 1\}$, allowing the next iteration to start with the previously calculated step function $u(x)$. The choice of N , L , and n_T must be carefully considered, depending on the time partition Δt . For a detailed overview of the convergence criteria related to the numerical estimation of the conditional expectation, please refer to [BS12]. For the unidimensional case, typical values are $N \sim 10^4$, $50 \leq n_T \leq 500$, and $L \sim 1000$. In higher dimensions, the number of intervals L must be significantly

reduced due to the exponential increase in d . This requires higher values for N and n_T and, therefore, more computational effort.

In summary the iteration scheme including the initial and final values for the used approach to calculate the approximation of X^π and $u^\pi(X^\pi)$ concerning the partition π is given below.

Iteration method

0 Set $u_{\text{prev}}(x) \equiv 0$.

1 Set $u_{\text{prev}}^\pi = u_{\text{new}}^\pi$ and use u_{prev}^π to generate N paths (index l) with n_t time steps

$$\begin{aligned} X_0^{\pi,l} &= x_0 \\ X_{t_{i+1}}^{\pi,l} &= X_{t_i}^{\pi,l} + u_{\text{prev}}^\pi(X_{t_i}^{\pi,l})\Delta t + \sigma\Delta W_{t_i}. \quad (\text{Euler-Mayurama}) \end{aligned}$$

2 Integrate the BSDE numerically, e.g., with the help of conditional expectation according to (B.7)

$$\begin{aligned} u^{\pi,l}(T) &= u_{\text{prev}}^\pi(X^{\pi,l}(T)) \\ u_{t_i}^{\pi,l} &= \frac{1}{\#(X_{t_{i+1}}^{\pi,l})} \sum_{n=1}^N \left[\delta(X_{t_i}^{\pi,l} - X_{t_{i+1}}^{\pi,n}) u_{t_{i+1}}^{\pi,n} \right] - \partial_x V(X_{t_i}^{\pi,l}) \Delta t. \end{aligned}$$

3 Average over all values of $\{u_{t_i}^{\pi,l} | 1 \leq l \leq N, 0 \leq i \leq n_T - 1\}$ w. r. t. the positions $\{X_{t_i}^{\pi,l} | 1 \leq l \leq N, 0 \leq i \leq n_T - 1\}$ of the sample paths

$$u_{\text{new}}(x) = \langle u^{\pi,\cdot}(t.) \rangle_{\text{cube}}.$$

4 If $\sum_i |u_{\text{new}}(x_i) - u_{\text{prev}}(x_i)| > \varepsilon$ go to 1.

Appendix C

Basics of geometry

A vector in Cartesian coordinates $x \in \mathbb{R}^n$ can in general be parameterized by an array of parameters q_i denoted as $q \in \mathbb{R}^n$, where $x = \tilde{x}(q)$. Their curves are related by the metric tensor $G(q) = J^T(q)AJ(q) \in \mathbb{R}^{n \times n}$

$$\left(\frac{dx}{dt}\right)^2 = \frac{dq^T}{dt}G(q)\frac{dq}{dt} \quad (\text{C.1})$$

where J is the Jacobian matrix

$$J(q) = (\partial_1 x, \dots, \partial_n x) \quad (\text{C.2})$$

and A is a diagonal matrix that scales the distances for the different coordinates. In the coordinate formulation physicists often use the usual tensor notation g_{ij} for the metric $G(q)$ and use Einstein's sum convention. Then the inverse of the metric $G^{-1}(q) = g^{ij}$.

In the case of m -dimensional manifolds $M \subset \mathbb{R}^n$, the array of parameters denoted as a vector $q \in \mathbb{R}^m$ leads then to a metric tensor with m^2 entries. A m -dimensional manifold M is a subset of \mathbb{R}^n that can be covered in full by charts $\phi_i : \mathbb{R}^m \rightarrow M$, i. e. some lower dimensional generalized vector $q \in \mathbb{R}^m$ in the flat Euclidean space may represent the possible non-flat subset of \mathbb{R}^n . While distances on a surface are measured with the metric, the changes of direction of a curve on a surface in comparison to a straight (Euclidean) line are related to the curvature of a hyper-plane M . The curvature in general depends on the point of the surface as well as the direction and in general is given in the form of the Riemannian curvature tensor

$$R_{jkl}^i = -\partial_l \Gamma_{jk}^i + \partial_k \Gamma_{jl}^i - \Gamma_{kj}^m \Gamma_{ml}^i + \Gamma_{jl}^m \Gamma_{mk}^i. \quad (\text{C.3})$$

Here the Christoffel symbols of the second kind Γ_{ij}^k are introduced

$$\Gamma_{jk}^i = \frac{1}{2}g^{il}(\partial_k g_{lj} + \partial_j g_{lk} - \partial_l g_{jk}). \quad (\text{C.4})$$

Directly related to R_{jkl}^i is the Ricci curvature $R_{jl} = R_{jil}^i$ and the scalar curvature $R = g^{jl}R_{jl}$.

The basis vectors $e_i = \partial_i x$ form a tangent hyper-plane at each point $p \in M$, denoted by $T_p M$ and w. r. t. to the Euclidean inner product

$$e_i \cdot e_j = g_{ij}. \quad (\text{C.5})$$

The gradient ∇_q of a function f is calculated as

$$\nabla_q f = g^{ij} \frac{\partial f}{\partial q^j} e_i \quad (\text{C.6})$$

and the divergence of a vector field $F = F_i e^i$ on M

$$\nabla \cdot F = \frac{1}{\sqrt{\det g}} \frac{\partial}{\partial q^i} \left(\sqrt{\det g} F_i \right). \quad (\text{C.7})$$

The divergence and the gradient are connected via

$$(\nabla f, F) = -(f, \nabla \cdot F) \quad (\text{C.8})$$

where $(f, h) = \int_{\mathbb{R}^d} f(q)h(q) \det(g) dq$, F is a vector field on M and the scalar function f has compact support on M or is rapidly decaying to zero outside a compact region. Additionally, they define the Laplace-Beltrami operator Δ_M , often referred to as Laplacian,

$$\begin{aligned} \Delta_M f &= \nabla \cdot (\nabla f) = \frac{1}{\sqrt{\det g}} \partial_i \left(\sqrt{\det(g)} g^{ij} \partial^j f \right) \\ &= g^{ij} \left(\partial_{ij} f - \Gamma_{ij}^k \partial_k f \right). \end{aligned} \quad (\text{C.9})$$

In the case of the flat Cartesian coordinates in \mathbb{R}^n the metric is diagonal $g_{ij} = g^{ij} = \delta_{ij}$ and there is no curvature and thus $\Gamma_{ij}^k = 0$ for all i, j, k . For a vector field F , one usually considers the Laplace-Beltrami-de Rahm operator

$$(\tilde{\Delta}_M F)^j = \Delta_M F^j + R_i^j F^i \quad (\text{C.10})$$

which includes the Ricci curvature tensor R_j^i in local coordinates.

Appendix D

The rotation group $SO(3)$

D.1 Relation of $SO(3)$ to $SU(2)$

The classical description of rotation is connected to the group of rotations in \mathbb{R}^3

$$SO(3) = \{R \in \mathbb{R}^{3 \times 3} | R^T R = \mathbb{I}, \det R = 1\}.$$

$SO(3)$ is a Lie group, which is a closed subgroup of invertible linear transformations. The Lie algebra $\mathfrak{so}(3)$ is its associated vector space with the Lie Bracket $[\cdot, \cdot]$. $\mathfrak{so}(3)$ is the tangent space at the identity of the Lie group, and it is the structure that locally determines the Lie group. In this specific case, the elements of $\mathfrak{so}(3)$ consist of all skew-symmetric 3×3 Matrices and represent the angular velocities associated with the orientation of the body (just like velocity is related to the position of a body). By representing them as vectors $\omega = (\omega^1, \omega^2, \omega^3)^T$ via the right-hand rule, the Lie bracket is the cross product. The relation between a matrix $\Omega \in \mathfrak{so}(3)$ and $\omega \in \mathbb{R}^3$ is given by

$$[\omega]_{\times} = \begin{pmatrix} 0 & -\omega^3 & \omega^2 \\ \omega^3 & 0 & -\omega^1 \\ -\omega^2 & \omega^1 & 0 \end{pmatrix} = \Omega$$

with $\omega \times v = \Omega v$ for $v \in \mathbb{R}^3$. Since this representation in \mathbb{R}^3 is isomorphic to the skew-symmetric matrices, the Lie group $SO(3)$ is a three-dimensional manifold. Thus, the representation of $SO(3)$ needs at least three parameters. Euler was the first to show that any rotation in 3-space can be represented with three consecutive (intrinsic or extrinsic, or mixed) rotations along the axes. This is helpful for analytical reasons. In application, one often uses unit quaternions - having four parameters plus the additional unity constraint - because there are no singularities like when dealing with Euler angles. In addition, two different quaternions represent the same rotation in $SO(3)$, so one has to allow only one-half of it to have a 1-to-1 correspondence. As a third example, one may use an axis with unit vector e_{ϑ} and an angle ϑ . Then the vector ϑe_{ϑ} is the angle-axis representation of a rotation. In the latter case the corresponding rotation in $SO(3)$ is given by the exponential map $\exp(\vartheta e_{\vartheta}) = \mathbb{I} + \sin \vartheta [e_{\vartheta}]_{\times} + (1 - \cos \vartheta) [e_{\vartheta}]_{\times}^2$, were the mapping is not unique, cf. a π rotation around axes $\pm e_{\vartheta}$.

The symmetry group of a fermion in quantum mechanics is the Lie group of unitary transformations in \mathbb{C}^2

$$SU(2) = \{A \in \mathbb{C}^{2 \times 2} | A^* A = \mathbb{I}, \det A = 1\}.$$

Its Lie algebra $\mathfrak{su}(2)$ is isomorphic to $\mathfrak{so}(3)$, i.e., there is a one-to-one representation of elements of the algebras. That is the reason why there is the spinning ball analogy when describing a particle like the electron. On the other hand, $SU(2)$ is only *locally* isomorphic to $SO(3)$ - in the sense of infinitesimal rotations. Technically, $SU(2)$ is the universal covering

group of the rotation group, which simply states that the space $SU(2)$ is a simply connected space that covers $SO(3)$ with a covering map. This map is 2 to 1, because two elements of the unitary group can represent an element of the rotation group. Since we already had a 2-to-1 representation in the case of unit quaternions to rotation matrices in 3-space, the quaternions are actually a representation of $SU(2)$. In quantum mechanics, the irreducible, unique representations of $SO(3)$ are only able to describe bosons, whereas those of $SU(2)$ can describe fermions, see, for example, [KR27, BH50, Wal94].

To explain why the rotation group in \mathbb{R}^3 is not simply connected, recall the axis-angle representation ϑe_ϑ . The rotation angle can vary between $0 \leq \vartheta \leq \pi$. As already pointed out, for $\vartheta = \pi$, the unit vectors $\pm e_\vartheta$ give the same rotation. So $SO(3)$ can be pictured as a ball with radius π . Every point in the ball represents a rotation along the axis going through that point and the origin by the angle, which equals the distance of the point from the origin. The antipodal points on the ball's outer shell give the same rotations. If you go from one point from the shell to the antipodal point, the path forms a loop. It is not possible to shrink this path to one point without tearing the loop in parts.

Things change if the suggested loop fulfills a 4π rotation, i.e., two complete rotations. This path is contractable. In general, it follows that if there is a closed loop with even rotations, the loop can be shrunk to a point. Otherwise, it is not possible. Since $SO(3)$ is not simply connected, two distinct paths cannot be smoothly transformed into another in general, so one has to keep track if a path is in one of the angle classes of even or odd multiples of 2π . Hence, one could include the "full" topology associated with the orientational state in $SU(2)$ instead of using the geometric orientation $SO(3)$ only [DGR05].

To avoid this multi-valuedness in physics, a Spin group $spin(3)$ is defined such that it is the smallest simply connected space, including $SO(3)$. Here $spin(3) = SU(2)$ is the universal covering space of $SO(3)$ and $\mathbb{Z}_2 = \{-1, 1\}$ is the fundamental group of $SO(3)$. i.e., the kernel of the group homomorphism $\varphi : SU(2) \rightarrow SO(3)$ is $\text{Kern } \varphi = \{\pm 1_{SU(2)}\}$. This means that there is an isomorphism between $SU(2)$ and $SO(3)/\mathbb{Z}_2$, so a 2-to-1 correspondence. In a simply connected group, every path is only determined by its endpoints (when considering unitary transformations). An element A of $SU(2)$ can be represented by

$$A = a\mathbb{I}_{2 \times 2} + i(b, c, d)^T \cdot \sigma \quad a, b, c, d \in \mathbb{R}$$

where σ are the Pauli matrices. Thus, it can be seen as the sphere $S^3 = \{(a, b, c, d) \in \mathbb{R}^4 \mid a^2 + b^2 + c^2 + d^2 = 1\}$. Similar to the axis-angle representation, we can also write $A(\vartheta e_\vartheta) = \exp(-i\frac{\vartheta}{2} e_\vartheta \cdot \sigma) = \cos\frac{\vartheta}{2} - i e_\vartheta \cdot \sigma \sin\frac{\vartheta}{2}$. If we set $\vartheta = 2\pi$ then $A \rightarrow -A$ but the map elements corresponding to A and $-A$ in $SO(3)$ are the same.

D.2 Parametrizations of $SO(3)$

The choice of charts or parametrization of a group element of $SO(3)$ is huge, see for example [Chi00]. One can describe rotation around a certain axes in space which may change with the direction of translation (velocity). One may use the matrix exponential, which is useful in the limit of infinitesimal motions. Then the element in tangent space $(v, [\omega]_\times) \in TM = \mathbb{R}^3 \times \mathfrak{so}(3)$ may be represented by a vector $(v, \omega) \in \mathbb{R}^3 \times \mathbb{R}^3$ where the elements of the Lie algebra $\mathfrak{so}(3)$ are anti-symmetric matrices with vanishing diagonal, so it is common to use only 3 parameters for the rotation itself.

Consider a rotation $R(t)$ depending on time t describing the orientation of a rigid body. If x_0 is a fixed vector in the body frame the vector in the lab frame $x(t) = R(t)x_0$ and since $RR^T = \mathbb{I}$ there is $x_0 = R^T(t)x(t)$. The change of rate of x in the lab frame is

$$\dot{x} = \dot{R}x_0 = \dot{R}R^T x = \omega_L \times x. \quad (\text{D.1})$$

Here it is used that $\dot{R}R^T$ is antisymmetric and the definition of the instant angular velocity vector in the lab frame $\omega_L = [\dot{R}R^T]_\times$. The angular velocity in the rotating body fixed frame

is $\omega_R = R^T \omega_L$. L and R indicate the angular velocity where \dot{R} is multiplied from the left (L) or right (R) w. r. t. R^T . In terms of the parameterization $x(t)$ used for the rotation $R(t) = \tilde{R}(x(t))$

$$\omega_L = \left([(\partial_1 \tilde{R}) R^T]_\times, [(\partial_2 \tilde{R}) R^T]_\times, \dots \right) \dot{q} = J_L(\tilde{R}(x)) \dot{q}. \quad (\text{D.2})$$

In the same way the body fixed angular velocity is written $\omega_R = J_R(\tilde{R}(x)) \dot{x}$ with the Jacobi matrix defined for the right multiplication.

Euler angles

The thesis will mainly use Euler angles in the $z x z$ -convention, i.e., the rotation is carried around body fixed axes z' then x' and z' again consecutively. Written in terms of the rotation matrix $\tilde{R}(\vartheta, \varphi, \chi) = R_z(\varphi) R_x(\vartheta) R_z(\chi)$, the Jacobians are

$$J_L(\vartheta, \varphi, \chi) = (R_z(\varphi) e_x, e_z, R_z(\varphi) R_x(\vartheta) e_z) = \begin{pmatrix} \cos \varphi & 0 & \sin \varphi \sin \vartheta \\ \sin \varphi & 0 & -\cos \varphi \sin \vartheta \\ 0 & 1 & \cos \vartheta \end{pmatrix} \quad (\text{D.3})$$

and

$$J_R(\vartheta, \varphi, \chi) = \tilde{R}^T J_L = (R_z(\varphi) e_x, R_z(\varphi) R_x(\vartheta) e_z, e_z) = \begin{pmatrix} \cos \chi & \sin \vartheta \sin \chi & 0 \\ \sin \chi & \sin \vartheta \cos \chi & 0 \\ 0 & \cos \vartheta & 1 \end{pmatrix}. \quad (\text{D.4})$$

The inverse matrices read

$$J_L^{-1} = \begin{pmatrix} \cos \varphi & \sin \varphi & 0 \\ -\cot \vartheta \sin \varphi & \cos \varphi \cot \vartheta & 1 \\ \frac{\sin \varphi}{\sin \vartheta} & -\frac{\cos \varphi}{\sin \vartheta} & 0 \end{pmatrix} \quad \text{and} \\ J_R^{-1} = \begin{pmatrix} \cos \chi & -\sin \chi & 0 \\ -\frac{\sin \chi}{\sin \vartheta} & \frac{\cos \chi}{\sin \vartheta} & 0 \\ -\cot \vartheta \sin \chi & -\cos \chi \cot \vartheta & 1 \end{pmatrix}. \quad (\text{D.5})$$

In general, the angular velocity of a rigid body can be calculated via the rate of change of the local coordinates (or parameters) [Chi00] $\omega^i = \mathbb{J}_j^i(R(x)) \dot{x}^j$ with the help of the Jacobian \mathbb{J} . $R(x)$ is the rotation matrix in terms of the parameters x^i . The integral over $\text{SO}(3)$ is then

$$\int_{\text{SO}(3)} f(R) dR = \frac{1}{\int_Q |\det(J(R(x)))| dq} \int_Q f(R(x)) |\det(J(R(x)))| dq \quad (\text{D.6})$$

with the parameter space Q . In the case of the euler angles used within the thesis this leads to

$$\int_{\text{SO}(3)} f(R) dR = \frac{1}{8\pi^2} \int_0^{2\pi} \int_0^\pi \int_0^{2\pi} f(\vartheta, \varphi, \chi) \sin \vartheta d\varphi d\vartheta d\chi. \quad (\text{D.7})$$

The thesis uses a prime for body fixed quantities, i. e. $\omega' = \omega_R$, and unprimed for the lab frame if not further specified.

Quaternions

Due to the singularity problems with 3-parameter representations of rotations, i. e. also the Euler angles, quaternions may be numerically superior. William R. Hamilton generalized the concept of complex numbers to a higher dimension in the sense that the imaginary part

is has a basis of three $\{i, j, k\}$ with $i^2 = jk = -1$. They are often denoted as $q = q_0 + iq_1 + jq_2 + kq_3 = (q_0, \mathbf{q})$ where $\mathbf{q} = iq_1 + jq_2 + kq_3$ is subsumed as a vector and is a so called pure quaternion. For two quaternions q and p the multiplication gives

$$qp = (q_0, \mathbf{q})(p_0, \mathbf{p}) = (q_0p_0 - \mathbf{q}^T \mathbf{p}, q_0\mathbf{p} + p_0\mathbf{q} + \mathbf{q} \times \mathbf{p}). \quad (\text{D.8})$$

Due to the cross product it is apparent that $qp \neq pq$. The inverse of a quaternion is defined as $q^{-1} = \frac{q^*}{qq^*}$. The constraint of a unit norm $|q|^2 = qq^* = (q_0, \mathbf{q})(q_0, -\mathbf{q}) = \sum_{l=0}^3 q_l^2 = 1$ leads to the S^3 manifold, the quaternion sphere in \mathbb{R}^4 . Then for a pure quaternion $v = (0, \mathbf{v})$ the multiplication

$$v' = (0, \mathbf{v}') = qvq^* \quad (\text{D.9})$$

leads to a new vector \mathbf{v}' with $|\mathbf{v}'| = |\mathbf{v}|$ that has been rotated. The corresponding rotation about an axis with unit vector \mathbf{n} by an angle ϑ is $q = (\cos \vartheta/2, \mathbf{n} \sin \vartheta/2)$. Considering rotations in \mathbb{R}^3 with quaternions in (D.9) we see that q and $-q$ lead to the same outcome \mathbf{v}' . Thus there is a 2-to-1 representation in the case of rotation by unit quaternions. In physics one usually encounters the Pauli matrices $\hat{\sigma}_i \in SU(2) \subset \mathbb{C}^{2 \times 2}$ where each Pauli matrix can be related to one basis of the imaginary part $\{i, j, k\}$. In the same manner a rotation of a position vector, represented as $X = x_1\sigma_1 + x_2\sigma_2 + x_3\sigma_3$, by a unitary matrix $U \in SU(2)$ is described as

$$X' = UXU^\dagger. \quad (\text{D.10})$$

Here U^\dagger is the complex conjugate and transpose of U . Again to each rotation $R \in SO(3)$ correspond two unitary matrices $\pm U \in SU(2)$.

The Jacobian matrices read (q_0, q_1, q_2, q_3)

$$\begin{pmatrix} 0 \\ \omega_L \end{pmatrix} = 2 \begin{pmatrix} q_0 & q_1 & q_2 & q_3 \\ -q_1 & q_0 & q_3 & -q_2 \\ -q_2 & -q_3 & q_0 & q_1 \\ -q_3 & q_2 & -q_1 & q_0 \end{pmatrix} \dot{\mathbf{q}} \quad \text{and} \quad J_L^{-1} = \frac{1}{4} J_L^T. \quad (\text{D.11})$$

Appendix E

The role of the osmotic kinetic energy terms

In the absence of a magnetic field, the osmotic velocity occurs in the kinetic part of the quantum Lagrangian $\mathcal{L} = T - V$

$$\mathcal{L} = \frac{m}{2}v_q^2 + -V = \frac{m}{2}(v^2 - u^2) + \frac{I_m}{2}(\omega_v^2 - \omega_u^2) - i(mv \cdot u + I_m\omega_v \cdot \omega_u) - V. \quad (\text{E.1})$$

Let us neglect the angular velocity at first and focus on the translation only. The minus sign in the osmotic kinetic energy term is often interpreted as an additional contribution to the potential. In fact, this term can be related to the quantum potential $V_Q = -\frac{\hbar^2}{4m} \frac{\Delta\rho}{\rho}$, as used in fluid dynamics and the Pilot-wave theory [Tak52, Boh51]. The quantum potential may be written in terms of the osmotic velocity

$$V_Q = -\frac{m}{2}u^2 - \frac{\hbar}{2}\nabla \cdot u, \quad (\text{E.2})$$

which arises in the corresponding stochastic Hamiltonian (4.20) to the quantum Lagrangian when the costate momentum process in the flat space is replaced by the maximum principle $P = m(v - iu)$ and the costate matrix by the Jacobian of the momentum $\Pi = \sigma\nabla(v - iu)$. The latter follows from the comparison of the SDE of the costate (4.22) to the SDE for the feedback field $m(v - iu)$ by applying the complex Itô formula. The real part of the stochastic Hamiltonian then reads

$$\Re\{\mathcal{H}\} = \frac{m}{2}v^2 - \frac{m}{2}u^2 - \frac{\hbar}{2}\nabla \cdot u + V = \frac{m}{2}v^2 + V_Q + V \quad (\text{E.3})$$

The inclusion of the spin to this problem goes by analogy. An additional spin quantum potential

$$V_{Q_s} = -\frac{I_m}{2}\omega_u^2 - \frac{\hbar}{2}\nabla_\theta \cdot \omega_u \quad (\text{E.4})$$

appears in the stochastic Hamiltonian. These two terms in the Hamiltonian are thus relevant to the time evolution of the stochastic process. The osmotic velocity takes the role of the quantum potential. This leads to the partial differential equations for the momentum

$$\begin{aligned} & \partial_t v + (v \cdot \nabla)v + (\omega_v \cdot \nabla_\theta)v \\ & - (u \cdot \nabla)u - \frac{\hbar}{2m}\Delta u - (\omega_u \cdot \nabla_\theta)u - \frac{\hbar}{2m}\Delta u - \frac{\hbar}{2I_m}\Delta_\theta u \\ & = -\frac{\gamma I_m}{m}\nabla(\omega_v \cdot B) \end{aligned} \quad (\text{E.5})$$

which can be related to classical time derivative $\frac{d_{cl}}{dt} = \partial_t + (v \cdot \nabla) + (\omega_v \cdot \nabla_\theta)$ of the current velocity as

$$\frac{d_{cl}v}{dt} = -\frac{\gamma I_m}{m} \nabla(\omega_v \cdot B) - \frac{1}{m} \nabla V_Q(u) - \frac{1}{m} \nabla V_{Q_s}(\omega_u) \quad (E.6)$$

where it can be shown that

$$\frac{1}{m} \nabla V_Q(u) = (u \cdot \nabla)u + \frac{\hbar}{2m} \Delta u, \quad (E.7)$$

$$\frac{1}{m} \nabla V_{Q_s}(\omega_u) = (\omega_u \cdot \nabla_\theta)u + \frac{\hbar}{2I_m} \Delta_\theta u. \quad (E.8)$$

This equivalence of the PDE associated with the QHE for the spinning particles to the description in fluid mechanics with the quantum potentials, see, e.g., chapter 10.3 in [Hol95], is given if the velocity fields are gradients of a scalar function S (for the current velocity) and of the logarithm of the probability distribution $\ln \rho$ (for the osmotic velocity). In the book of Pena [dlPCVH15] they use similar definitions for a classical derivative $D_c = \frac{d_{cl}}{dt}$ and an additional stochastic derivative $D_s u = -\frac{1}{m} \nabla V_Q(u)$.

In more detail, one may consider the Hamilton-Jacobi-like equation only, which is the real part of (6.75). The quantities V_Q and V_{Q_s} arise herein from the osmotic part of the kinetic energy $E[\frac{m}{2}u^2] = E[V_Q]$ and $E[\frac{I_m}{2}\omega_u^2] = E[V_{Q_s}]$ and are the so-called quantum (spin) potentials. In the Pilot-wave theory, they lead to the quantum phenomena and are also present without any external field. Hence, in the stochastic theory, all of this information is stored in the contributions associated with the osmotic velocity. Something similar holds for the angular velocities ω_v and ω_u , where in the Hamilton-Jacobi-Bellmann equation of the angular momentum

$$\frac{d_{cl}\omega_v}{dt} = \gamma \omega_v \times B - \gamma \dot{B} - \frac{1}{I_m} \nabla_\theta (V_Q(u) + V_{Q_s}(\omega_u)) \quad (E.9)$$

the additional quantities corresponding to the osmotic velocity appear. Therefore, it is vital to note that the equations (6.73) and (6.74) are strongly influenced by the general configuration of the system, which also includes the preparation of the experiment and thus the initial velocities.

Appendix F

Superposition of solutions

This section addresses the combination of possibly multiple solutions in the theory of the Quantum Hamilton equations. It differs from the linear superposition when dealing with solutions to the Schrödinger equation. *E.g.*, suppose that ψ_1 and ψ_2 are solutions to the Schrödinger equation, then $\psi = \psi_1 + \psi_2$ is also a solution to the Schrödinger equation. Suppose now that the quantum velocity fields $v_1^q(t, x)$ and $v_2^q(t, x)$ with associated probability distributions $\rho_1(t, x)$ and $\rho_2(t, x)$ are two solutions to the QHE equation. Both velocities solve the associated partial differential equation by applying the complex Itô formula (4.25) to $v_j^q(t, x)$. Comparing the drift terms yields the Nelson-Madelung-equations in complex form

$$\left(\partial_t + (v_j^q \cdot \nabla) - i\sigma^2 \frac{\Delta}{2} \right) v_j^q(t, x) = -\frac{\nabla V}{m} \quad (\text{F.1})$$

where ∇ is the nabla and Δ the Laplace-Beltrami(-deRham) [DG79] operator acting on scalars and vector fields associated to the chosen metric. Note that the coupling to a vector field is omitted here for simplicity, but can be extended straight-forwardly to include the coupling to an electromagnetic field, for example. A simple superposition of

$$\rho_{\text{new}} v_{\text{new}}^q = \rho_1 v_1^q + \rho_2 v_2^q \quad (\text{F.2})$$

with $\rho = \rho_1 + \rho_2$ does not solve the QHE in general since (F.1) is not linear. An example is the double slit experiment, where the velocities for each slit may be solved independently at first and combined afterwards. With the simple addition of the two processes the quantum interference pattern does not appear. The sum (F.2) is only approximately valid in cases where the probability distributions ρ_1 and ρ_2 are well separated, i.e., $\rho_1(t, x) \approx 0$ for $x \in M$ where $\rho_2(t, x) \neq 0$. Hence, the combination of two known solutions requires additional terms. In general the newly generated velocity v_{new}^q has to fulfil $\rho_{\text{new}} v_{\text{new}}^q = \sum_j C_j v_j^q$ where

$$C_j = |c_j|^2 \rho_j + \sum_{k \neq j} c_j c_k^* \sqrt{\rho_k \rho_j} e^{-i(S_j - S_k)/\hbar}. \quad (\text{F.3})$$

Here c_j are complex constants with $\sum_j |c_j|^2 = 1$ and the scalar fields $S_j(t, x)$ are the potentials of the current velocity $v_j = \Im \left(v_j^q \right) = \frac{1}{m} \nabla S_j$.¹ The validity of summation with coefficients given in (F.3) may be verified by the superposition of wave functions $\psi_j = \sqrt{\rho_j} e^{iS_j/\hbar}$ corresponding to v_j^q , e.g., see equations (7) and (8) in [NK08].

¹Note that the latter equation does not define the function S_j uniquely.

Appendix G

Extension to multiple spins

Extending the quantum Hamilton theory of stochastic rigid bodies to multiple particles is straightforward. We can start again with the classical Lagrangian for n particles with masses $m_{(k)}$, charges $q_{(k)}$, inertias $I_{m(k)}$, $I_{c(k)}$ and velocities $v_{(k)}$, $\omega_{(k)}$

$$\mathcal{L} = \sum_{k=1}^n \left(\frac{1}{2} m_{(k)} v_{(k)}^2 + \frac{1}{2} I_{m(k)} \omega_{(k)}^2 + q_{(k)} v_{(k)} \cdot A_{(k)} - \gamma I_{c(k)} \omega_{(k)} \cdot B_{(k)} \right) - V, \quad (\text{G.1})$$

where V is the sum of the external and all Coulombic interaction potentials of the particles. In the model of rotating charged rotors, each particle k is subject to the fields $A_{(k)}$ and $B_{(k)}$ depending on external fields and the fields generated by the dynamics of the other particles in the system. The magnetic moment $\gamma I_{m(k)} \omega_{(k)}$ generated by particle k at position $x_{(k)} \in \mathbb{R}$ interacts with the spinning particle $j \neq k$ at position $x_{(j)}$ via

$$\mathcal{V}_{\text{SI}}^{kj} = -\gamma I_{m(k)} \omega_{(k)} \cdot B_{(j)} \quad (\text{G.2})$$

where the field $B_{(j)}$, and the associated vector field $A_{(j)}$, is due to the magnetic moment of particle j . The sum over $j \neq k$ in (G.2) leads to the effective field $B_{(k)}$ acting on particle k .

Setting up the stochastic Lagrangian associated to (G.1) with quantum (angular) velocities $v_{q_{(k)}} (\omega_{q_{(k)}})$ in the quantum Hamilton principle leads to the corresponding QHE. Consider, for example, the canonical momenta of particle k

$$dp_{(k)} = \left[-\nabla_{(k)} V + F_{(k)}^{\text{Lor}} - \gamma I_{m(k)} \nabla_{(k)} \left(\sum_j \omega_{q_{(k)}} \cdot B_{(j)} \right) \right] dt + dA_{(k)} + \Pi_{(k)}^p dW_- \quad (\text{G.3})$$

$$ds_{(k)} = \left[\gamma s_{(k)} \times B_{(k)} + \frac{\hbar}{I_{m(k)}} T_{(k)} \right] dt + s_{(k)} \times \Pi_{(k)}^s dW_- \quad (\text{G.4})$$

where W_- is a $6n$ -dimensional stochastic process, $\Pi_{(k)}^p, \Pi_{(k)}^s \in \mathbb{C}^{6n \times 3}$, $F_{(k)}^{\text{Lor}}$ denotes the Lorenz force depending on the quantum velocity $v_{q_{(k)}}$ and $T_{(k)}$ is the additional torque term acting introduced in equation (5.32) acting on particle k . The momentum equation (G.3), as well as the spin dynamics (G.4), contains the classically expected coupling terms to other particles. However, the coupling of the angular velocities, and with that, the particles' spins, is not only due to the classical coupling terms. This is studied in section 6.5 regarding the EPRB paradox where the classical coupling terms are neglected. That spins system is highly coupled due to the preparation of the entangled states where the probability distribution w.r.t. to the orientation variables of the two particles is not factorizable, which leads to non-local dependencies of the angular velocity fields.

Due to the complexity, a detailed discussion of these terms is not given here. However, a remark on the dipole interaction is given in the following.

Dipole-dipole interaction

The magnetic field generated by a magnetic moment M follows Ampère's law for the corresponding vector field $\nabla^2 A = -\mu_0 J$ where μ_0 is the vacuum magnetic permeability, and J is the current of the rotating charge. For large distances compared to the size of the object, the dominant term in the multipole expansion is the dipole vector field

$$A_{\text{dip}} = \frac{\mu_0}{4\pi} \frac{M \times x}{|x|^3} \quad (\text{G.5})$$

with magnetic field

$$B_{\text{dip}} = \frac{\mu_0}{4\pi|x|^5} [3(M \cdot x)x - Mx^2]. \quad (\text{G.6})$$

Given (G.6), the spin-spin interaction in the limit of two separated magnetic dipoles modeled as point particles enters the corresponding Lagrangian

$$\mathcal{V}_{\text{SI}}^{kj} = \frac{\mu_0 \gamma^{(k)} \gamma^{(j)}}{4\pi|x_{kj}|^3} (\omega_{(k)} \cdot \omega_{(j)} - 3(\omega_{(i)} \cdot e_{x_{kj}})(\omega_{(j)} \cdot e_{x_{kj}})) \quad (\text{G.7})$$

where $x_{kj} = x_{(k)} - x_{(j)}$. The magnetic moment interaction generally leads to a coupling of position and spin, which is not trivial to solve in classical mechanics. If the distances are large enough, the dipole interaction is small compared to the Coulomb interaction. The magnetic interaction, however, dominates on short scales comparable to the size of nuclei. Hence, it would be worthwhile to study if there are stable states in the stochastic theory of two rotating charges in the non-relativistic limit. Unfortunately, this is beyond the current scope of the numerical treatment regarding the QHE due to the dimensions of the problem. Additionally, it is unclear if that would need an extension to relativistic theory.

Appendix H

Spin orbit coupling in the hydrogen atom

We consider the interaction between an electron's spin and orbital angular momentum in a central potential $\phi(|r|)$. This spin-orbit interaction is significant in relativistic equations of quantum mechanics, such as the Dirac equation for a spin- $\frac{1}{2}$ particle and the Pauli equation. To model this interaction in a semi-relativistic limit, we consider the nucleus moving relative to the electron's rest frame [Tho26, Fre26]. By applying a Lorentz transformation to the electric field of the nucleus, denoted as $E = -\nabla\phi(|r|)e_r$ we obtain an effective magnetic field at the electron's position, given by $B_{\text{eff}} = \frac{1}{c^2}v \times E$, up to first order in terms of $\frac{v}{c}$. It is important to note that this approximation assumes the electron's rest frame is non-inertial. We also neglect a possible spin of the nucleus in the following. In principle, formulating a Lagrangian for the particles interacting with the electromagnetic fields generated by their motion, as demonstrated in [IKS15], would be necessary. However, such considerations lie beyond the scope of this thesis.

The Lagrangian for this system may be chosen as

$$\mathcal{L} = \frac{m}{2}v^2 + e\phi(|r|) + \frac{I_m}{2}\omega^2 + \frac{a_{\text{SOC}}(|r|)}{m}\omega \cdot l \quad (\text{H.1})$$

where the vector field $A = 0$, $a_{\text{SOC}}(|r|) = \frac{I_c\phi'(|r|)}{c^2|r|}$ and the orbital angular momentum is defined as $l = (r \times mv)$. The last term in (H.1) is the spin-orbit interaction. The transition to the variational approach discussed in section 3.1 requires the replacement of the classical velocities v, ω by the quantum velocities $v_q = v - iu, \omega_q = \omega_v - i\omega_u$. The corresponding stochastic momenta follow from the maximum principle of the Hamiltonian defined in (4.20)

$$\begin{aligned} P &= mv_q + a_{\text{SOC}}(|r|)(\omega_q \times r) \\ S &= I_m\omega_q + a_{\text{SOC}}(|r|)(r \times v_q), \end{aligned} \quad (\text{H.2})$$

with shorthand $P = P_t, S = S_t, \dots$. The canonical angular momentum S above thus is the sum of the dynamical eigenrotation and the orbital angular momentum.

The QHE concerning the canonical momenta read

$$\begin{aligned} dP &= [(-e\phi'(|r|) + a'_{\text{SOC}}(|r|)\omega_q \cdot (r \times v_q))e_r + a_{\text{SOC}}(|r|)(v_q \times \omega_q)]dt + \tilde{P}dW_- \\ dS &= a_{\text{SOC}}(|r|)[S \times (r \times v_q)]dt + S \times \tilde{S}dW_- \end{aligned} \quad (\text{H.3})$$

where $dW_- \in \mathbb{R}^6$ is the backward Wiener process and \tilde{P}, \tilde{S} are stochastic processes in $\mathbb{R}^{3 \times 6}$. Due to the coupling of translation and rotation, the SDEs at hand are not easily solvable. However, the following quantity is conserved in the limit $|v| \ll c$, i.e., it has a

time-independent expectation value:

$$\mathbb{E}[dS + d(r \times P)] = \mathcal{O}\left(\frac{1}{c^4}\right). \quad (\text{H.4})$$

Here $r \times P$ is the canonical angular momentum $L = r \times [mv_q + a_{\text{SOC}}(\omega_q \times r)]$. Thus, these equations describe the conservation of the sum of the canonical orbital momentum and the spin. This corresponds to the conservation of the total angular momentum operator $\hat{j} = \hat{l} + \hat{s}$ in the operator based formulation of quantum mechanics.

Bibliography

- [ADG92] E. Aldrovandi, D. Dohrn, and F. Guerra. The Lagrangian approach to stochastic variational principles on curved manifolds. *Acta Applicandae Mathematica*, 26(3):219–236, doi:10.1007/BF00047204.
- [Adl21] E. Adlam. *Foundations of Quantum mechanics*. Cambridge University Press, doi:10.1017/9781108885515.
- [AGR81] A. Aspect, P. Grangier, and G. Roger. Experimental tests of realistic local theories via Bell’s theorem. *Physical Review letters*, 47(7):460, doi:10.1103/PhysRevLett.47.460.
- [AGR82] A. Aspect, P. Grangier, and G. Roger. Experimental realization of Einstein-Podolsky-Rosen-Bohm Gedankenexperiment: a new violation of Bell’s inequalities. *Physical Review letters*, 49(2):91, doi:10.1103/PhysRevLett.49.91.
- [Ans22] Q. Ansel. Loop quantum gravity with optimal control path integral, and application to black hole tunneling. *General Relativity and Gravitation*, 54(5):42, doi:10.1007/s10714-022-02923-6.
- [Baz66] A. I. Baz. Lifetime of intermediate states. *Yadern. Fiz.*, 4, 1966.
- [BBM92] A. O. Barut, M. Božić, and Z. Marić. The magnetic top as a model of quantum spin. *Annals of Physics*, 214(1):53–83, doi:10.1016/0003-4916(92)90061-P.
- [BD07] C. Bender and R. Denk. A forward scheme for backward SDEs. *Stochastic Processes and their applications*, 117(12):1793–1812, doi:10.1016/j.spa.2007.03.005.
- [Bel64] J. S. Bell. On the Einstein Podolsky Rosen paradox. *Physics Physique Fizika*, 1(3):195, doi:10.1017/CBO9780511815676.004.
- [Bel76] J. S. Bell. A Theory of Local Beables. *Epistemological Letters*, 9:11–24, doi:10.1017/CBO9780511815676.009.
- [Bel04] J. S. Bell. *Speakable and unspeakable in quantum mechanics: Collected papers on quantum philosophy*. Cambridge university press, doi:10.1017/CBO9780511815676.
- [Bey18] M. Beyer. Derivation of Quantum Hamilton Equations of Motion for Multi-Dimensional Systems. Master’s thesis, Martin-Luther Universität Halle-Wittenberg, 2018.
- [BG10] S. Bahlali and B. Gherbal. Optimality conditions of controlled backward doubly stochastic differential equations. *Random Operators and Stochastic Equations*, 18(3):247–265, doi:10.1515/rose.2010.014.
- [BGS86] P. Blanchard, S. Golin, and M. Serva. Repeated measurements in stochastic mechanics. *Physical Review D*, 34(12):3732, doi:10.1103/PhysRevD.34.3732.

- [BH50] F. Bopp and R. Haag. Über die Möglichkeit von Spinmodellen. *Zeitschrift für Naturforschung A*, 5(12):644–653, doi:10.1515/zna-1950-1203.
- [BH89] D. Bohm and B. Hiley. Non-locality and locality in the stochastic interpretation of quantum mechanics. *Physics Reports*, 172(3):93–122, doi:10.1016/0370-1573(89)90160-9.
- [Bis78] J.-M. Bismut. An introductory approach to duality in optimal stochastic control. *SIAM review*, 20(1):62–78, doi:10.1137/1020004.
- [BL82] M. Büttiker and R. Landauer. Traversal time for tunneling. *Physical Review Letters*, 49(23):1739, doi:10.1007/BFb0108208.
- [Boh51] D. Bohm. *Quantum Theory*. Prentice-Hall, Englewood Cliffs, NJ, doi:10.1119/1.1933314.
- [Boh52a] D. Bohm. A Suggested Interpretation of the Quantum Theory in Terms of “Hidden” Variables. I. *Physical Review*, 85:166–179, doi:10.1103/PhysRev.85.166.
- [Boh52b] D. Bohm. A Suggested Interpretation of the Quantum Theory in Terms of “Hidden” Variables. II. *Physical Review*, 85:180–193, doi:10.1103/PhysRev.85.180.
- [BP21] M. Beyer and W. Paul. On the Stochastic Mechanics Foundation of Quantum Mechanics. *Universe*, 7(6):166, doi:10.3390/universe7060166.
- [BPGP19] M. Beyer, M. Patzold, W. Grecksch, and W. Paul. Quantum Hamilton equations for multidimensional systems. *Journal of Physics A: Mathematical and Theoretical*, 52(16):165301, doi:10.1088/1751-8121/ab0bcf.
- [Bra88] C. H. Brans. Bell’s theorem does not eliminate fully causal hidden variables. *International Journal of Theoretical Physics*, 27:219–226, doi:10.1007/BF00670750.
- [BS12] C. Bender and J. Steiner. *Least-Squares Monte Carlo for Backward SDEs*, pages 257–289. Springer Berlin Heidelberg, Berlin, Heidelberg, doi:10.1007/978-3-642-25746-9.
- [BSS21] U. Boscain, M. Sigalotti, and D. Sugny. Introduction to the Pontryagin maximum principle for quantum optimal control. *PRX Quantum*, 2(3):030203, doi:10.1103/PRXQuantum.2.030203.
- [BST55] D. Bohm, R. Schiller, and J. Tiomno. A causal interpretation of the Pauli equation (A). *Il Nuovo Cimento (1955-1965)*, 1:48–66, doi:10.1007/BF02743528.
- [BT04] B. Bouchard and N. Touzi. Discrete-time approximation and Monte-Carlo simulation of backward stochastic differential equations. *Stochastic Processes and their applications*, 111(2):175–206, doi:10.1016/j.spa.2004.01.001.
- [BV09] G. Bacciagaluppi and A. Valentini. *Quantum theory at the crossroads: reconsidering the 1927 Solvay conference*. Cambridge University Press, doi:10.1017/CBO9781139194983.
- [Car84] E. A. Carlen. Conservative diffusions. *Communications in Mathematical Physics*, 94(3):293–315, doi:10.1007/BF01224827.
- [Cas32] H. B. G. Casimir. Rotation of a Rigid Body in Quantum-mechanics. *Nature*, 129:780–780, 1932.

- [CdlPA71] A. M. Cetto and L. de la Peña-Auerbach. The anomalous magnetic moment of the electron in stochastic quantum mechanics. *Revista Mexicana de Física*, 20(3):191–201, 1971.
- [CGP16] Y. Chen, T. T. Georgiou, and M. Pavon. On the relation between optimal transport and Schrödinger bridges: A stochastic control viewpoint. *Journal of Optimization Theory and Applications*, 169:671–691, doi:10.1007/s10957-015-0803-z.
- [CH74] J. F. Clauser and M. A. Horne. Experimental consequences of objective local theories. *Physical Review D*, 10(2):526, doi:10.1103/PhysRevD.10.526.
- [Chi00] G. S. Chirikjian. *Engineering applications of noncommutative harmonic analysis: with emphasis on rotation and motion groups*. CRC press, doi:10.1201/9781420041767.
- [CHSH69] J. F. Clauser, M. A. Horne, A. Shimony, and R. A. Holt. Proposed experiment to test local hidden-variable theories. *Physical Review letters*, 23(15):880, doi:10.1103/PhysRevLett.23.880.
- [Cir80] B. S. Cirel’son. Quantum generalizations of Bell’s inequality. *Letters in Mathematical Physics*, 4:93–100, doi:10.1007/BF00417500.
- [CP18] G. Conforti and M. Pavon. Extremal flows in Wasserstein space. *Journal of Mathematical Physics*, 59(6):063502, doi:10.1063/1.5018402.
- [CPV17] M. Contreras, R. Pellicer, and M. Villena. Dynamic optimization and its relation to classical and quantum constrained systems. *Physica A: Statistical Mechanics and its Applications*, 479:12–25, doi:10.1016/j.physa.2017.02.075.
- [DAJL82] G. De Angelis and G. Jona-Lasinio. A stochastic description of a spin-1/2 particle in a magnetic field. *Journal of Physics A: Mathematical and General*, 15(7):2053, doi:10.1088/0305-4470/15/7/016.
- [Dan70] T. G. Dankel. Mechanics on manifolds and the incorporation of spin into Nelson’s stochastic mechanics. *Archive for Rational Mechanics and Analysis*, 37(3):192–221, doi:10.1007/BF00281477.
- [Dan77] T. G. Dankel. Higher spin states in the stochastic mechanics of the Bopp–Haag spin model. *Journal of Mathematical Physics*, 18(2):253–255, doi:10.1063/1.523266.
- [Dav79] M. Davidson. A generalization of the Fényes—Nelson stochastic model of quantum mechanics. *Letters in Mathematical Physics*, 3(4):271–277, doi:10.1007/BF01821846.
- [DB27] L. De Broglie. La mécanique ondulatoire et la structure atomique de la matière et du rayonnement. *Journal de Physique et Le Radium*, 8(5):225–241, 1927.
- [DD19] S. Das and D. Dürr. Arrival time distributions of spin-1/2 particles. *Scientific reports*, 9(1):2242, doi:10.1038/s41598-018-38261-4.
- [DDKS22] S. Das, D.-A. Deckert, L. Kellers, and W. Struyve. Double-slit experiment remastered. *arXiv preprint arXiv:2211.13362*, doi:10.48550/arXiv.2211.13362.
- [Der17] M. Derakhshani. *Stochastic Mechanics Without Ad Hoc Quantization: Theory And Applications To Semiclassical Gravity*. PhD thesis, Universiteit Utrecht, 2017.
- [DeW70] B. S. DeWitt. Quantum mechanics and reality. *Physics today*, 23(9):30–35, doi:10.1515/9781400868056-005.

- [DG79] D. Dohrn and F. Guerra. Geodesic correction to stochastic parallel displacement of tensors. In *Stochastic Behavior in Classical and Quantum Hamiltonian Systems*, pages 241–249. Springer, doi:10.1007/BFb0021748.
- [DG85] D. Dohrn and F. Guerra. Compatibility between the Brownian metric and the kinetic metric in Nelson stochastic quantization. *Physical Review D*, 31(10):2521, doi:10.1103/PhysRevD.31.2521.
- [DGR05] D. Dohrn, F. Guerra, and P. Ruggiero. Spinning particles and relativistic particles in the framework of Nelson’s stochastic mechanics. In *Feynman Path Integrals: Proceedings of the International Colloquium Held in Marseille, May 1978*, pages 165–181. Springer, doi:10.1007/3-540-09532-2.
- [DH09] J. Dunkel and P. Hänggi. Relativistic brownian motion. *Physics Reports*, 471(1):1–73, doi:10.1016/j.physrep.2008.12.001.
- [DH22] S. Donadi and S. Hossenfelder. Toy model for local and deterministic wave-function collapse. *Physical Review A*, 106(2):022212, doi:10.1103/PhysRevA.106.022212.
- [DHKV88] C. Dewdney, P. R. Holland, A. Kyprianidis, and J.-P. Vigiér. Spin and non-locality in quantum mechanics. *Nature*, 336(6199):536–544, doi:10.1038/336536a0.
- [Dir26] P. A. M. Dirac. On the theory of quantum mechanics. *Proceedings of the Royal Society of London. Series A, Containing Papers of a Mathematical and Physical Character*, 112(762):661–677, 1926.
- [Dir51] P. A. M. Dirac. The relation of Classical to Quantum mechanics. In *Proceedings of the Second Canadian Mathematical Congress, Vancouver 1949*, pages 10–31. Toronto University Press, 1951.
- [Dir81] P. A. M. Dirac. *The principles of quantum mechanics*. Oxford university press, doi:10.1063/1.3062610.
- [dIPA71] L. de la Peña-Auerbach. Stochastic theory of quantum mechanics for particles with spin. *Journal of Mathematical Physics*, 12(3):453–461, doi:10.1063/1.1665609.
- [dlPCVH15] L. de la Peña, A. M. Cetto, and A. Valdés-Hernández. The Emerging Quantum. *The Physics Behind Quantum Mechanics*. Cham: Springer International Publishing, doi:10.1007/978-3-319-07893-9.
- [DM89] N. David Mermin. What’s wrong with this pillow? *Physics Today*, 42(4):9, doi:10.1063/1.2810963.
- [Doo53] J. Doob. *Stochastic Processes*, volume 7. Wiley New York, 1953.
- [Dud66] R. M. Dudley. Lorentz-invariant Markov processes in relativistic phase space. *Arkiv för Matematik*, 6(3):241–268, doi:10.1007/978-1-4419-5821-1.
- [Ein05] A. Einstein. Über die von der molekularkinetischen Theorie der Wärme geforderte Bewegung von in ruhenden Flüssigkeiten suspendierten Teilchen. *Annalen der Physik*, 4, 1905.
- [Elw82] K. D. Elworthy. *Stochastic differential equations on manifolds*, volume 70. Cambridge University Press, doi:10.1017/CBO9781107325609.009.
- [Éme12] M. Émery. *Stochastic calculus in manifolds*. Springer Science & Business Media, doi:10.1007/978-3-642-75051-9.

- [EPR35] A. Einstein, B. Podolsky, and N. Rosen. Can quantum-mechanical description of physical reality be considered complete? *Physical Review*, 47(10):777, doi:10.1007/978-3-322-91080-6.
- [Erl18] J. Erlich. Stochastic emergent quantum gravity. *Classical and Quantum Gravity*, 35(24):245005, doi:10.1088/1361-6382/aaeb55.
- [ESSW92] B.-G. Englert, M. O. Scully, G. Süssmann, and H. Walther. Surrealistic bohm trajectories. *Zeitschrift für Naturforschung A*, 47(12):1175–1186, doi:10.1515/zna-1992-1201.
- [Far82] W. G. Faris. Spin correlation in stochastic mechanics. *Foundations of Physics*, 12(1):1–26, doi:10.1007/BF00726872.
- [FC72] S. J. Freedman and J. F. Clauser. Experimental test of local hidden-variable theories. *Physical Review Letters*, 28(14):938, doi:10.1103/PhysRevLett.28.938.
- [FDBS22] V. Frumkin, D. Darrow, J. W. Bush, and W. Struyve. Real surreal trajectories in pilot-wave hydrodynamics. *Physical Review A*, 106(1):L010203, doi:10.1103/PhysRevA.106.L010203.
- [Fén52] I. Fényes. Eine wahrscheinlichkeits-theoretische Begründung und Interpretation der Quantenmechanik. *Zeitschrift für Physik*, 132(1):81–106, doi:10.1007/BF01338578.
- [Fre26] J. Frenkel. Die Elektrodynamik des rotierenden Elektrons. *Zeitschrift für Physik*, 37(4):243–262, doi:10.1007/BF01397099.
- [FT76] E. S. Fry and R. C. Thompson. Experimental test of local hidden-variable theories. *Physical Review Letters*, 37(8):465, doi:10.1103/PhysRevLett.37.465.
- [Für33] R. Fürth. Über einige Beziehungen zwischen klassischer Statistik und Quantenmechanik. *Zeitschrift für Physik*, 81(3):143–162, 1933.
- [Gae93] G. Gaeta. EPR and stochastic mechanics. *Physics Letters A*, 175(5):267–268, doi:10.1016/0375-9601(93)90618-A.
- [Gar90] P. Garbaczewski. Randomness in the quantum description of neutral spin 1/2 particles. *Fortschritte der Physik/Progress of Physics*, 38(6):447–475, doi:10.1002/prop.2190380604.
- [GGRW88] G. C. Ghirardi, R. Grassi, A. Rimini, and T. Weber. Experiments of the EPR type involving CP-violation do not allow faster-than-light communication between distant observers. *Europhysics Letters*, 6(2):95, doi:10.1209/0295-5075/6/2/001.
- [GHT79] H. Grabert, P. Hänggi, and P. Talkner. Is quantum mechanics equivalent to a classical stochastic process? *Physical Review A*, 19(6):2440, doi:10.1103/PhysRevA.19.2440.
- [GJKS84] B. Gaveau, T. Jacobson, M. Kac, and L. Schulman. Relativistic extension of the analogy between quantum mechanics and Brownian motion. *Physical Review Letters*, 53(5):419, doi:10.1103/PhysRevLett.53.419.
- [GL81] F. Guerra and M. Loffeedo. Thermal mixtures in stochastic mechanics. *Lettere al Nuovo Cimento (1971-1985)*, 30(3):81–87, doi:10.1007/BF02817316.
- [GLW⁺05] E. Gobet, J.-P. Lemor, X. Warin, et al. A regression-based Monte Carlo method to solve backward stochastic differential equations. *The Annals of Applied Probability*, 15(3):2172–2202, doi:10.1214/105051605000000412.

- [GM83] F. Guerra and L. M. Morato. Quantization of dynamical systems and stochastic control theory. *Physical Review D*, 27:1774–1786, doi:10.1103/PhysRevD.27.1774.
- [GM84] F. Guerra and R. Marra. Stochastic mechanics of spin-1/2 particles. *Physical Review D*, 30(12):2579, doi:10.1103/PhysRevD.30.2579.
- [Gol85] S. Golin. Uncertainty relations in stochastic mechanics. *Journal of Mathematical Physics*, 26(11):2781–2783, doi:10.1063/1.526700.
- [GR73] F. Guerra and P. Ruggiero. New interpretation of the Euclidean-Markov field in the framework of physical Minkowski space-time. *Physical Review Letters*, 31(16):1022, doi:10.1103/PhysRevLett.31.1022.
- [GR78] F. Guerra and P. Ruggiero. A note on relativistic Markov processes. *Lettere al Nuovo Cimento*, 23(15):529–534, doi:10.1007/BF02770538.
- [Gri91] A. Grigorenko. Excited states in stochastic mechanics. *Physics Letters A*, 155(6-7):348–350, doi:10.1016/0375-9601(91)91037-E.
- [GS22a] W. Gerlach and O. Stern. Das magnetische Moment des Silberatoms. *Zeitschrift für Physik*, 9(1):353–355, doi:10.1007/978-3-642-74813-4.
- [GS22b] W. Gerlach and O. Stern. Der experimentelle Nachweis der Richtungsquantelung im Magnetfeld. *Zeitschrift für Physik*, 9(1):349–352, doi:10.1007/978-3-642-74813-4.
- [GS69] I. Gikhman and A. Skorokhod. Introduction to the theory of random processes. *Saunders Company*, 1969.
- [Gue81] F. Guerra. Structural aspects of stochastic mechanics and stochastic field theory. *Physics Reports*, 77(3):263–312, doi:10.1016/0370-1573(81)90078-8.
- [Hal10] M. J. Hall. Local deterministic model of singlet state correlations based on relaxing measurement independence. *Physical Review letters*, 105(25):250404, doi:10.1103/PhysRevLett.105.250404.
- [Hal16] M. J. Hall. The significance of measurement independence for Bell inequalities and locality. In *At the frontier of spacetime*, pages 189–204. Springer, doi:10.1007/978-3-319-31299-6.
- [HBD⁺15] B. Hensen, H. Bernien, A. E. Dréau, A. Reiserer, N. Kalb, M. S. Blok, J. Ruitenberg, R. F. Vermeulen, R. N. Schouten, C. Abellán, et al. Loophole-free Bell inequality violation using electron spins separated by 1.3 kilometres. *Nature*, 526(7575):682–686, doi:10.1038/nature15759.
- [Hei25] W. Heisenberg. Über quantentheoretische Umdeutung kinematischer und mechanischer Beziehungen. *Zeitschrift für Physik*, 33(1):879–893, doi:10.1007/BF01328377.
- [Hol95] P. R. Holland. *The quantum theory of motion: an account of the de Broglie-Bohm causal interpretation of quantum mechanics*. Cambridge university press, 1995.
- [Hos18] S. Hossenfelder. *Lost in math: How beauty leads physics astray*. Hachette UK, 2018.
- [Hsu02] E. P. Hsu. *Stochastic analysis on manifolds*. American Mathematical Soc., doi:10.1090/gsm/038.

- [HZ23] Q. Huang and J.-C. Zambrini. Stochastic geometric mechanics in nonequilibrium thermodynamics: Schrödinger meets Onsager. *Journal of Physics A: Mathematical and Theoretical*, 56(13):134003, doi:10.1088/1751-8121/acbf8d.
- [IKS15] V. Imaykin, A. Komech, and H. Spohn. On the Lagrangian theory for rotating charge in the Maxwell field. *Physics Letters A*, 379(1-2):5–10, doi:10.1016/j.physleta.2014.10.038.
- [IOY95] K. Imafuku, I. Ohba, and Y. Yamanaka. Tunneling time based on the quantum diffusion process approach. *Physics Letters A*, 204(5-6):329–335, doi:10.1016/0375-9601(95)00507-Y.
- [Itô51] K. Itô. *On stochastic differential equations*. American Mathematical Soc., doi:10.1007/978-1-4612-5370-9.
- [Ito62] K. Ito. The Brownian motion and tensor fields on Riemannian manifold. *Proceedings of the International Congress of Mathematicians, Stockholm, 2, 1962*.
- [IZ12] C. Itzykson and J.-B. Zuber. *Quantum field theory*. Courier Corporation, doi:10.1063/1.2916419.
- [JP84] M. Jaekel and D. Pignon. Stochastic mechanics of mixed states. *Journal of Physics A: Mathematical and General*, 17(1):131, doi:10.1088/0305-4470/17/1/015.
- [JYC09] M. Jeanblanc, M. Yor, and M. Chesney. *Mathematical methods for financial markets*. Springer Science & Business Media, doi:10.1007/978-1-84628-737-4.
- [Kac74] M. Kac. A stochastic model related to the telegrapher's equation. *The Rocky Mountain Journal of Mathematics*, 4(3):497–509, doi:10.1216/RMJ-1974-4-3-497.
- [KGP17] J. Köppe, W. Grecksch, and W. Paul. Derivation and application of quantum Hamilton equations of motion. *Annalen Der Physik*, 529(3):1600251, doi:10.1002/andp.201600251.
- [KH23] M. Kazemi and V. Hosseinzadeh. Detection statistics in a double-double-slit experiment. *Physical Review A*, 107(1):012223, doi:10.1103/PhysRevA.107.012223.
- [KN13] T. Kudo and H. Nitta. Tunneling time and stochastic-mechanical trajectories for the double-barrier potential. *Physics Letters A*, 377(5):357–361, doi:10.1016/j.physleta.2012.12.008.
- [Köp18] J. Köppe. *Derivation and application of quantum Hamilton equations of motion*. PhD thesis, Martin-Luther Universität Halle-Wittenberg, doi:10.25673/2172.
- [KPB⁺20] J. Köppe, M. Patzold, M. Beyer, W. Grecksch, and W. Paul. Quantum Hamilton Equations from Stochastic Optimal Control Theory. In *Infinite Dimensional and Finite Dimensional Stochastic Equations and Applications in Physics*, pages 213–250. World Scientific, doi:10.1142/9789811209796.
- [KPGP18] J. Köppe, M. Patzold, W. Grecksch, and W. Paul. Quantum Hamilton equations of motion for bound states of one-dimensional quantum systems. *Journal of Mathematical Physics*, 59(6):062102, doi:10.1063/1.5026377.
- [KR27] R. d. L. Kronig and I. Rabi. The symmetrical top in the undulatory mechanics. *Physical Review*, 29(2):262, doi:10.1103/PhysRev.29.262.
- [Kui21a] F. Kuipers. Stochastic quantization of relativistic theories. *Journal of Mathematical Physics*, 62(12):122301, doi:10.1063/5.0057720.

- [Kui21b] F. Kuipers. Stochastic quantization on Lorentzian manifolds. *Journal of High Energy Physics*, 2021(5):1–51, doi:10.1007/JHEP05(2021)028.
- [Kui22] F. Kuipers. Analytic continuation of stochastic mechanics. *Journal of Mathematical Physics*, 63(4):042301, doi:10.1063/5.0073096.
- [Kui23] F. Kuipers. *Stochastic Mechanics: The Unification of Quantum Mechanics with Brownian Motion*. Springer Cham, doi:10.1007/978-3-031-31448-3.
- [LL67] J.-M. Lévy-Leblond. Nonrelativistic particles and wave equations. *Communications in Mathematical Physics*, 6(4):286–311, doi:10.1007/BF01646020.
- [LL19] J. Lindgren and J. Liukkonen. Quantum Mechanics can be understood through stochastic optimization on spacetimes. *Scientific reports*, 9(1):19984, doi:10.1038/s41598-019-56357-3.
- [Lop53] J. Lopuszanski. Relativisierung der Theorie der Stochastischen Prozesse. *Acta Physica Polonica*, 12:87–99, 1953.
- [LS01] F. Longstaff and E. Schwartz. Valuing American options by simulation: a simple least-squares approach. *The Review of Financial Studies*, 14(1):113–147, doi:10.1093/rfs/14.1.113.
- [Mac32] L. MacColl. Note on the transmission and reflection of wave packets by potential barriers. *Physical Review*, 40(4):621, doi:10.1103/PhysRev.40.621.
- [Mad27] E. Madelung. Quantentheorie in hydrodynamischer Form. *Zeitschrift für Physik*, 40(3):322–326, doi:10.1007/BF01400372.
- [MDZ⁺21] Y. Margalit, O. Dobkowski, Z. Zhou, O. Amit, Y. Japha, S. Moukouri, D. Rohrlich, A. Mazumdar, S. Bose, C. Henkel, and R. Folman. Realization of a complete Stern-Gerlach interferometer: Toward a test of quantum gravity. *Science Advances*, 7(22):eabg2879, doi:10.1126/sciadv.abg2879.
- [Mor22] L. M. Morato. Free time evolution of the quantum wave function and optimal transportation. *Journal of Mathematical Physics*, 63(10):103508, doi:10.1063/5.0105914.
- [MR88] M. McClendon and H. Rabitz. Numerical simulations in stochastic mechanics. *Physical Review A*, 37(9):3479, doi:10.1103/PhysRevA.37.3479.
- [MRF⁺16] D. H. Mahler, L. Rozema, K. Fisher, L. Vermeyden, K. J. Resch, H. M. Wiseman, and A. Steinberg. Experimental nonlocal and surreal Bohmian trajectories. *Science advances*, 2(2):e1501466, doi:10.1126/sciadv.1501466.
- [MT07] G. Milstein and M. Tretyakov. Discretization of forward–backward stochastic differential equations and related quasi-linear parabolic equations. *IMA Journal of Numerical Analysis*, 27(1):24–44, doi:10.1093/imanum/drl019.
- [MV95] L. M. Morato and L. Viola. Markov diffusions in comoving coordinates and stochastic quantization of the free relativistic spinless particle. *Journal of Mathematical Physics*, 36(9):4691–4710, doi:10.1063/1.531333.
- [MY99] J. Ma and J. Yong. *Forward-backward stochastic differential equations and their applications*. Springer Science & Business Media, doi:10.1007/978-3-540-48831-6.
- [Nel66] E. Nelson. Derivation of the Schrödinger equation from Newtonian mechanics. *Physical review*, 150(4):1079, doi:10.1103/PhysRev.150.1079.

- [Nel73] E. Nelson. Construction of quantum fields from Markoff fields. *Journal of Functional Analysis*, 12(1):97–112, doi:10.1016/0022-1236(73)90091-8.
- [Nel85] E. Nelson. *Quantum fluctuations*. Princeton University Press, doi:10.1515/9780691218021.
- [Nel86] E. Nelson. The locality problem in stochastic mechanics. *Annals of the New York Academy of Sciences*, 480(1):533–538, doi:10.1111/j.1749-6632.1986.tb12456.x.
- [Nel12] E. Nelson. Review of stochastic mechanics. In *Journal of Physics: Conference Series*, page 012011. IOP Publishing, doi:10.1088/1742-6596/361/1/012011.
- [NK07] H. Nitta and T. Kudo. Time of arrival in the Aharonov–Bohm effect. *Physica E: Low-dimensional Systems and Nanostructures*, 40(2):390–393, doi:10.1016/j.physe.2007.06.049.
- [NK08] H. Nitta and T. Kudo. Time of arrival of electrons in the double-slit experiment. *Physical Review A*, 77(1):014102, doi:10.1103/PhysRevA.77.014102.
- [nob22] The Nobel Prize in Physics 2022. NobelPrize.org. Nobel Media AB 2022., 2022.
- [Ohs19] A. Ohsumi. An interpretation of the Schrödinger equation in quantum mechanics from the control-theoretic point of view. *Automatica*, 99:181–187, doi:10.1016/j.automatica.2018.10.033.
- [Øks03] B. Øksendal. *Stochastic differential equations*. Springer, Berlin, Heidelberg, 3. edition, doi:10.1007/978-3-662-03620-4.
- [ØS14] B. Øksendal and A. Sulem. Forward–backward stochastic differential games and stochastic control under model uncertainty. *Journal of Optimization Theory and Applications*, 161(1):22–55, doi:10.1007/s10957-012-0166-7.
- [Pau25] W. Pauli. Über den Zusammenhang des Abschlusses der Elektronengruppen im Atom mit der Komplexstruktur der Spektren. *Einführ. Orig*, 229:765–783, 1925.
- [Pau12] W. Paul. Harmonically confined Tonks-Girardeau gas: A simulation study based on Nelson’s stochastic mechanics. *Physical Review A*, 86(1):013607, doi:10.1103/PhysRevA.86.013607.
- [Pav95a] M. Pavon. A new formulation of stochastic mechanics. *Physics Letters A*, 209(3-4):143–149, doi:10.1016/0375-9601(95)00847-4.
- [Pav95b] M. Pavon. Hamilton’s principle in stochastic mechanics. *Journal of Mathematical Physics*, 36(12):6774–6800, doi:10.1063/1.531187.
- [Pav00] M. Pavon. Stochastic mechanics and the Feynman integral. *Journal of Mathematical Physics*, 41(9):6060–6078, doi:10.1063/1.1286880.
- [Pav01] M. Pavon. On the stochastic mechanics of the free relativistic particle. *Journal of Mathematical Physics*, 42(10):4846–4856, doi:10.1063/1.1401135.
- [Pav14] G. A. Pavliotis. *Stochastic processes and applications: diffusion processes, the Fokker-Planck and Langevin equations*, volume 60. Springer, New York, NY, doi:10.1007/978-1-4939-1323-7.
- [PB13] W. Paul and J. Baschnagel. *Stochastic processes*. Springer, doi:10.1007/978-3-319-00327-6.

- [Pen90] S. Peng. A general stochastic maximum principle for optimal control problems. *SIAM Journal on Control and Optimization*, 28(4):966–979, doi:10.1137/0328054.
- [Pla92] D. E. Platt. A modern analysis of the Stern–Gerlach experiment. *American Journal of Physics*, 60(4):306–308, doi:10.1119/1.17136.
- [PM00] N. C. Petroni and L. M. Morato. Entangled states in stochastic mechanics. *Journal of Physics A: Mathematical and General*, 33(33):5833, doi:10.1088/0305-4470/33/33/304.
- [PT27] T. Phipps and J. Taylor. The magnetic moment of the hydrogen atom. *Physical Review*, 29(2):309, doi:10.1103/PhysRev.29.309.
- [PW27] F. Peter and H. Weyl. Die Vollständigkeit der primitiven Darstellungen einer geschlossenen kontinuierlichen Gruppe. *Mathematische Annalen*, 97(1):737–755, doi:10.1007/BF01447892.
- [PW81] G. Parisi and Y. S. Wu. Perturbation theory without gauge fixing. *Sci. Sin*, 24(4):483–496, 1981.
- [Rei26] F. Reiche. Die Quantelung des symmetrischen Kreisels nach Schrödingers Undulationsmechanik. *Zeitschrift für Physik*, 39(5-6):444–464, doi:10.1007/BF01322053.
- [RHH⁺18] D. Rauch, J. Handsteiner, A. Hochrainer, J. Gallicchio, A. S. Friedman, C. Leung, B. Liu, L. Bulla, S. Ecker, F. Steinlechner, et al. Cosmic Bell test using random measurement settings from high-redshift quasars. *Physical Review letters*, 121(8):080403, doi:10.1103/PhysRevLett.121.080403.
- [RKM⁺01] M. A. Rowe, D. Kielpinski, V. Meyer, C. A. Sackett, W. M. Itano, C. Monroe, and D. J. Wineland. Experimental violation of a Bell’s inequality with efficient detection. *Nature*, 409(6822):791–794, doi:10.1038/35057215.
- [Ros51] N. Rosen. Particle spin and rotation. *Physical Review*, 82(5):621, doi:10.1103/PhysRev.82.621.
- [RSRS20] R. Ramos, D. Spierings, I. Racicot, and A. M. Steinberg. Measurement of the time spent by a tunnelling atom within the barrier region. *Nature*, 583(7817):529–532, doi:10.1038/s41586-020-2490-7.
- [Sch26a] E. Schrödinger. Der stetige Übergang von der Mikro-zur Makromechanik. *Naturwissenschaften*, 14(28):664–666, 1926.
- [Sch26b] E. Schrödinger. Quantisierung als Eigenwertproblem. *Annalen der Physik*, 385(13):437–490, doi:10.1515/9783112596647-007.
- [Sch26c] E. Schrödinger. Über das Verhältnis der Heisenberg-Born-Jordanschen Quantenmechanik zu der meinem. *Annalen der Physik*, 384(8):734–756, 1926.
- [Sch31] E. Schrödinger. *Über die Umkehrung der Naturgesetze*. Sonderausgabe aus den Sitzungsberichten der Preußischen Akademie der Wissenschaften, doi:10.1002/ange.19310443014.
- [Smo86] L. Smolin. Quantum fluctuations and inertia. *Physics Letters A*, 113(8):408–412, doi:10.1016/0375-9601(86)90661-4.
- [Spo04] H. Spohn. *Dynamics of charged particles and their radiation field*. Cambridge university press, doi:10.1017/CBO9780511535178.

- [SSE88] J. Schwinger, M. O. Scully, and B.-G. Englert. Is spin coherence like Humpty-Dumpty? *Zeitschrift für Physik D Atoms, Molecules and Clusters*, 10(2):135–144, doi:10.1007/BF01384847.
- [SXW⁺19] U. S. Sainadh, H. Xu, X. Wang, A. Atia-Tul-Noor, W. C. Wallace, N. Douguet, A. Bray, I. Ivanov, K. Bartschat, A. Kheifets, et al. Attosecond angular streaking and tunnelling time in atomic hydrogen. *Nature*, 568(7750):75–77, doi:10.1038/s41586-019-1028-3.
- [Tak52] T. Takabayashi. On the Formulation of Quantum Mechanics associated with Classical Pictures. *Progress of Theoretical Physics*, 8:143, doi:10.1143/ptp/8.2.143.
- [Tak55] T. Takabayashi. The vector representation of spinning particle in the quantum theory, I. *Progress of Theoretical Physics*, 14(4):283–302, doi:10.1143/PTP.14.283.
- [tH20] G. 't Hooft. Deterministic quantum mechanics: the mathematical equations. *Frontiers in Physics*, 8:253, doi:10.3389/fphy.2020.00253.
- [Tho26] L. H. Thomas. The motion of the spinning electron. *Nature*, 117(2945):514–514, doi:10.1038/117514a0.
- [TRO94] P. R. Tapster, J. G. Rarity, and P. Owens. Violation of Bell's inequality over 4 km of optical fiber. *Physical Review Letters*, 73(14):1923, doi:10.1103/PhysRevLett.73.1923.
- [UG25] G. Uhlenbeck and S. Goudsmit. Ersetzung der Hypothese vom unmechanischen Zwang durch eine Forderung bezüglich des inneren Verhaltens jedes einzelnen Elektrons. *Naturwiss*, 47:953, doi:10.1007/BF01558878.
- [VMB90] A. Valance, T. Morgan, and H. Bergeron. Eigensolution of the Coulomb Hamiltonian via supersymmetry. *American Journal of Physics*, 58(5):487–491, doi:10.1119/1.16452.
- [vR12] M. von Renesse. An optimal transport view of Schrödinger's equation. *Canadian mathematical bulletin*, 55(4):858–869, doi:10.4153/CMB-2011-121-9.
- [VS06] M. Von Smoluchowski. Zur kinetischen Theorie der Brownschen Molekularbewegung und der Suspensionen. *Annalen der Physik*, 326(14):756–780, doi:10.1002/andp.19063261405.
- [VZNS82] A. Vainshtein, V. I. Zakharov, V. A. Novikov, and M. A. Shifman. ABC of instantons. *Soviet Physics Uspekhi*, 25(4):195, doi:10.1142/9789812798961.
- [Wal89] T. C. Wallstrom. On the derivation of the Schrödinger equation from stochastic mechanics. *Foundations of Physics Letters*, 2(2):113–126, doi:10.1007/BF00696108.
- [Wal90] T. C. Wallstrom. The stochastic mechanics of the Pauli equation. *Transactions of the American Mathematical Society*, 318(2):749–762, doi:10.1090/S0002-9947-1990-0986033-3.
- [Wal94] T. C. Wallstrom. Inequivalence between the Schrödinger equation and the Madelung hydrodynamic equations. *Physical Review A*, 49(3):1613, doi:10.1103/PhysRevA.49.1613.
- [Wic12] D. Wick. *The Infamous Boundary: Seven decades of heresy in quantum physics*. Springer Science & Business Media, 2012.

- [Wie23] N. Wiener. Differential-space. *Journal of Mathematics and Physics*, 2(1-4):131–174, doi:10.1002/sapm192321131.
- [Wig31] E. P. Wigner. *Gruppentheorie und ihre Anwendung auf die Quantenmechanik der Atomspektren*. Vieweg Verlag, doi:10.1007/978-3-663-02555-9.
- [Wig55] E. P. Wigner. Lower limit for the energy derivative of the scattering phase shift. *Physical Review*, 98(1):145, doi:10.1103/PhysRev.98.145.
- [Yas80] K. Yasue. Schrödinger's variational method of quantization revisited. *Letters in Mathematical Physics*, 4(2):143–146, doi:10.1007/BF00417507.
- [Yas81a] K. Yasue. Quantum mechanics and stochastic control theory. *Journal of Mathematical Physics*, 22(5):1010–1020, doi:10.1063/1.525006.
- [Yas81b] K. Yasue. Stochastic calculus of variations. *Journal of functional Analysis*, 41(3):327–340, doi:10.1007/BF00402586.
- [Yas83] K. Yasue. A variational principle for the Navier-Stokes equation. *Journal of Functional Analysis*, 51(2):133–141, doi:10.1016/0022-1236(83)90021-6.
- [Zam85] J.-C. Zambrini. Stochastic dynamics: A review of stochastic calculus of variations. *International Journal of Theoretical Physics*, 24(3):277–327, doi:10.1007/BF00669792.

List of publications

Michael Beyer, Markus Patzold, Wilfried Grecksch, and Wolfgang Paul.
Quantum Hamilton equations for multidimensional systems.

Journal of Physics A: Mathematical and Theoretical, 52(16):165301, 2019. doi:10.1088/1751-8121/ab0bcf.

Jeanette Köppe, Markus Patzold, Michael Beyer, Wilfried Grecksch, and Wolfgang Paul.
Quantum Hamilton Equations from Stochastic Optimal Control Theory.

In *Infinite Dimensional and Finite Dimensional Stochastic Equations and Applications in Physics*, pages 213–250. World Scientific, 2020. doi:10.1142/9789811209796_0005.

Michael Beyer and Wolfgang Paul.

On the Stochastic Mechanics Foundation of Quantum Mechanics.

Universe, 7(6):166, 2021. doi:10.3390/universe7060166.

Michael Beyer and Wolfgang Paul.

Particle Spin Described by Quantum Hamilton Equations.

Annalen der Physik, 535(1):2200433, 2023. doi:10.1002/andp.202200433.

Declaration under Oath

I declare under oath that this thesis is my own work entirely and has been written without any help from other people. I used only the sources mentioned and included all the citations correctly both in word or content.

I declare that all information given is accurate and complete. The thesis has not been used previously at this or any other university in order to achieve an academic degree.

I certify that no criminal or investigative proceedings are pending against me. I affirm that I have no criminal record.

December 12, 2023, Michael Beyer

Curriculum Vitae

Personal data

Name: Michael Beyer

Orcid-ID: 0000-0002-2234-4774

Education

09/04-05/11: **Abitur**, general qualification for university entrance, Bertolt-Brecht-Gymnasium
Schwarzenberg

10/12-09/15: **Bachelor of Science**, Physics, Martin-Luther-Universität Halle-Wittenberg, Score: 1.2

10/15-02/18: **Master of Science**, Physics, Martin-Luther-Universität Halle-Wittenberg, Score: 1.2

05/18-12/23: **PhD student**, (Theoretical) Physics, Martin-Luther-Universität Halle-Wittenberg
Supervisor: Prof. Wolfgang Paul

Acknowledgement

The completion of this thesis would've never been possible without the help of the people around me.

First and foremost, I would like to express my deep gratitude to Prof Wolfgang Paul for providing me with the opportunity to work on this project. His support and willingness to engage in any kind of discussion, both technical and personal, have contributed significantly to my understanding and provided invaluable insights. His knowledge and guidance proved immensely beneficial to me throughout my time in the research group. I am also grateful for his patience and mentorship, which helped steering me back on track whenever necessary.

Overall, I've always felt comfortable working in the group over the last years. The restriction imposed by the pandemic showed how valuable the discussion in the group was to me. I'd like to thank Jeanette, Benno, Arne, Eunsang, Timur for the warm welcome into the group. Additionally, I'd like to extend my gratitude to Lama, Christian, Kai, Viktor, Evgeniia and many more for keeping the group discussions interesting and funny, making the time I had in the group very enjoyable.

I would also like to acknowledge Prof. Steffen Trimper for his collaboration in teaching, which further enhanced my academic experience. His expertise and insightful contributions have been invaluable.

Furthermore, I am grateful to Prof. Wilfried Grecksch and Prof. Jörg-Uwe Löbus for their guidance on the mathematical aspects. Both always had an open ear for my questions and took their time to explain complex concepts in detail, even providing special mini-lectures when needed.

I'd like to extend my gratitude to the individuals that were exposed to me most of the time, especially Denise and Hedi. I am also grateful to Yara for constantly cheering me up, which has kept me motivated and energized.

Finally, I would like to acknowledge all the other individuals who have impacted my academic and personal growth but may not be mentioned here. Your influence and contributions have been significant, and I am sincerely grateful for your presence in my life.